(12) INTERNATIONAL APPLICATION PUBLISHED UNDER THE PATENT COOPERATION TREATY (PCT)

(19) World Intellectual Property Organization
International Bureau

(43) International Publication Date
19 January 2017 (19.01.2017)

WIPO | PCT

(10) International Publication Number
WO 2017/011705 A1

(51) International Patent Classification:
C07K 14/00 (2006.01)

(21) International Application Number:
PCT/US2016/042361

(22) International Filing Date:
14 July 2016 (14.07.2016)

(25) Filing Language: English

(26) Publication Language: English

(30) Priority Data:
62/193,459 16 July 2015 (16.07.2015) US
62/220,157 17 September 2015 (17.09.2015) US

(71) Applicant: **THE REGENTS OF THE UNIVERSITY OF CALIFORNIA** [US/US]; 1111 Franklin Street, 5th Floor, Oakland, CA 94607-5200 (US).

(72) Inventors: **TEZCAN, Faik, Akif**; 8975 Cliffridge Ave., La Jolla, CA 92037 (US). **SUZUKI, Yuta**; 2-5-10 Takarada, Saburina Garden A201, Tsuruoka City, Yamagata Prefecture, 997-0011 (JP).

(74) Agent: **HART, Daniel**; Knobbe, Martens, Olson & Bear LLP, 2040 Main Street 14th Floor, Irvine, CA 92614 (US).

(81) Designated States *(unless otherwise indicated, for every kind of national protection available)*: AE, AG, AL, AM, AO, AT, AU, AZ, BA, BB, BG, BH, BN, BR, BW, BY, BZ, CA, CH, CL, CN, CO, CR, CU, CZ, DE, DK, DM, DO, DZ, EC, EE, EG, ES, FI, GB, GD, GE, GH, GM, GT, HN, HR, HU, ID, IL, IN, IR, IS, JP, KE, KG, KN, KP, KR, KZ, LA, LC, LK, LR, LS, LU, LY, MA, MD, ME, MG, MK, MN, MW, MX, MY, MZ, NA, NG, NI, NO, NZ, OM, PA, PE, PG, PH, PL, PT, QA, RO, RS, RU, RW, SA, SC, SD, SE, SG, SK, SL, SM, ST, SV, SY, TH, TJ, TM, TN, TR, TT, TZ, UA, UG, US, UZ, VC, VN, ZA, ZM, ZW.

(84) Designated States *(unless otherwise indicated, for every kind of regional protection available)*: ARIPO (BW, GH, GM, KE, LR, LS, MW, MZ, NA, RW, SD, SL, ST, SZ, TZ, UG, ZM, ZW), Eurasian (AM, AZ, BY, KG, KZ, RU, TJ, TM), European (AL, AT, BE, BG, CH, CY, CZ, DE, DK, EE, ES, FI, FR, GB, GR, HR, HU, IE, IS, IT, LT, LU, LV, MC, MK, MT, NL, NO, PL, PT, RO, RS, SE, SI, SK, SM, TR), OAPI (BF, BJ, CF, CG, CI, CM, GA, GN, GQ, GW, KM, ML, MR, NE, SN, TD, TG).

Declarations under Rule 4.17:

— *as to applicant's entitlement to apply for and be granted a patent (Rule 4.17(ii))*

— *as to the applicant's entitlement to claim the priority of the earlier application (Rule 4.17(iii))*

Published:

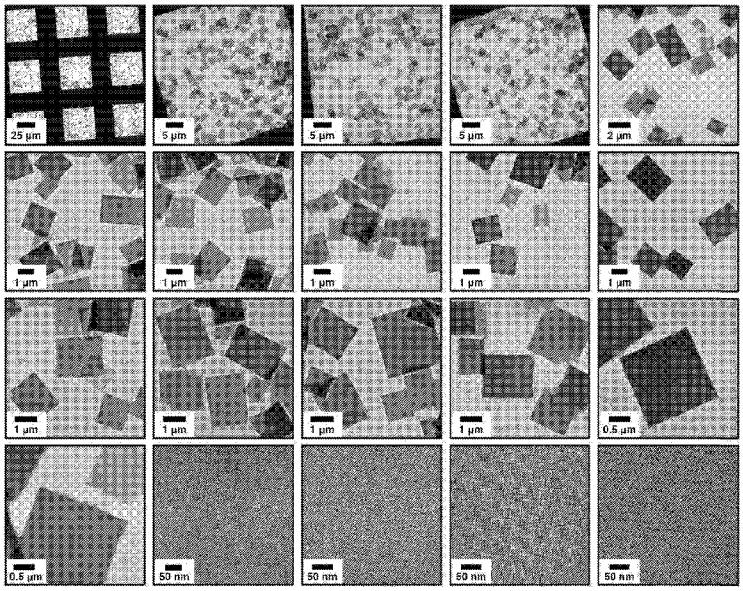
— *with international search report (Art. 21(3))*

— *before the expiration of the time limit for amending the claims and to be republished in the event of receipt of amendments (Rule 48.2(h))*

— *with sequence listing part of description (Rule 5.2(a))*

(54) Title: METHOD FOR FABRICATING TWO-DIMENSIONAL PROTEIN CRYSTALS

FIG. 11E



(57) Abstract: Polypeptide assemblies and building blocks and methods for making them are provided.

WO 2017/011705 A1

METHOD FOR FABRICATING TWO-DIMENSIONAL PROTEIN CRYSTALS

INCORPORATION BY REFERENCE TO ANY PRIORITY APPLICATIONS

[0001] Any and all applications for which a foreign or domestic priority claim is identified in the Application Data Sheet as filed with the present application are hereby incorporated by reference under 37 CFR 1.57 in their entireties. The disclosures of U.S. Provisional Application Serial No. 62/193459, entitled METHOD FOR FABRICATING TWO-DIMENSIONAL PROTEIN CRYSTALS, filed July 16, 2015, and U.S. Provisional Application Serial No. 62/220157, entitled METHOD FOR FABRICATING TWO-DIMENSIONAL PROTEIN CRYSTALS, filed September 17, 2015 are incorporated herein by reference in their entireties.

STATEMENT REGARDING FEDERALLY SPONSORED R&D

[0002] This invention was made with government support under U.S. Department of Energy Grant/Contract Number DE-FG02-10ER46677. The government has certain rights in the invention.

REFERENCE TO SEQUENCE LISTING, TABLE, OR COMPUTER PROGRAM LISTING

[0003] The present application is being filed along with a Sequence Listing in electronic format. The Sequence Listing is provided as a file entitled UCSD093-001WO_Sequence_Listing.TXT, created July 11, 2016, which is 29 Kb in size. The information in the electronic format of the Sequence Listing is incorporated herein by reference in its entirety.

BACKGROUND OF THE INVENTION

Field of the Invention

[0004] Some embodiments described herein relate to 2D crystalline structures and to polypeptide building blocks for making such structures.

Description of the Related Art

[0005] Existing approaches for designed protein assembly may be too design-intensive and involve sophisticated, but not sure-fire computational methods or protein fusion strategies that do not always give the desired product, and the desired products are not scalable and do not always possess superior materials properties.

[0006] Accordingly, there is a need for improved polypeptide assemblies and building blocks and methods for making them.

SUMMARY OF THE INVENTION

[0007] In a first aspect, a non-naturally occurring symmetrical polypeptide building block is provided. The non-naturally occurring symmetrical polypeptide building block can comprise a plurality of cysteine residues positioned such that formation of disulfide bonds between some or all of said plurality of cysteine residues facilitates formation of 2D crystals. In some embodiments, said polypeptide building block comprises a symmetrical polypeptide comprising a single set of surface cysteine residues in the corner positions. In some embodiments, said polypeptide has inherent C3, C4, C6, D3, D4 or D6 symmetry. In some embodiments, at least one of said cysteine residues has been introduced into said polypeptide building block through genetic engineering. In some embodiments, said polypeptide is generated via solid phase synthesis. In some embodiments, said polypeptide is genetically engineered. In some embodiments, said polypeptide comprises the RhuA protein. In some embodiments, said polypeptide further comprises an additional polypeptide modification. In some embodiments, said additional modification is selected from the group consisting of a chemical modification, a modification made via an enzymatic reaction, and a modification made via genetic engineering. In some embodiments, said additional modification is selected from the group consisting of functional groups, tags, other polypeptides, peptide tags, detectable labels, fluorophores, and nanoparticles. In some embodiments, the peptide tag comprises a His tag. In some embodiments, the His tag comprises a sequence set forth in SEQ ID NO: 22. In some embodiments, the peptide tag comprises a Pd4 peptide. In some embodiments, the Pd4 peptide comprises a sequence set forth in SEQ ID NO: 23. In some embodiments, the peptide tag comprises an ACP protein. In some embodiments, the ACP protein comprises a sequence set forth in SEQ ID NO: 24. In

some embodiments, the polypeptide building block can be chemically modified. In some embodiments, the polypeptide is chemically modified with inorganic nanoparticles. In some embodiments, the polypeptide building block is modified with one or more organic functional groups. In some embodiments, the polypeptide building block is modified for different modes of controllable self-assembly. In some embodiments, the organic functional group is a fluorophore, metal chelating group or a host complex. In some embodiments, the polypeptide building block can be genetically modified/fused with functional proteins and peptides.

[0008] In a second aspect, a 2D crystalline material comprising a polypeptide building block as described in the embodiments of the first aspect is provided. The non-naturally occurring symmetrical polypeptide building block can comprise a plurality of cysteine residues positioned such that formation of disulfide bonds between some or all of said plurality of cysteine residues facilitates formation of 2D crystals. In some embodiments, said polypeptide building block comprises a symmetrical polypeptide comprising a single set of surface cysteine residues in the corner positions. In some embodiments, said polypeptide has inherent C3, C4, C6, D3, D4 or D6 symmetry. In some embodiments, at least one of said cysteine residues has been introduced into said polypeptide building block through genetic engineering. In some embodiments, said polypeptide is generated via solid phase synthesis. In some embodiments, said polypeptide is genetically engineered. In some embodiments, said polypeptide comprises the RhuA protein. In some embodiments, said polypeptide further comprises an additional polypeptide modification. In some embodiments, said additional modification is selected from the group consisting of a chemical modification, a modification made via an enzymatic reaction, and a modification made via genetic engineering. In some embodiments, said additional modification is selected from the group consisting of functional groups, tags, other polypeptides, peptide tags, detectable labels, fluorophores, and nanoparticles. In some embodiments, the peptide tag comprises a His tag. In some embodiments, the His tag comprises a sequence set forth in SEQ ID NO: 22. In some embodiments, the peptide tag comprises a Pd4 peptide. In some embodiments, the Pd4 peptide comprises a sequence set forth in SEQ ID NO: 23. In some embodiments, the peptide tag comprises an ACP protein. In some embodiments, the ACP protein comprises a sequence

set forth in SEQ ID NO: 24. In some embodiments, the polypeptide building block can be chemically modified. In some embodiments, the polypeptide is chemically modified with inorganic nanoparticles. In some embodiments, the polypeptide building block is modified with one or more organic functional groups. In some embodiments, the polypeptide building block is modified for different modes of controllable self-assembly. In some embodiments, the organic functional group is a fluorophore, metal chelating group or a host complex. In some embodiments, the polypeptide building block can be genetically modified/fused with functional proteins and peptides. In some embodiments, said 2D crystalline material is auxetic. In some embodiments, the 2D crystalline material comprises a Poisson's ratio of at least -1. In some embodiments, the 2D crystalline material comprises a Poisson's ratio of -1. In some embodiments, the 2D crystalline material can be chemically modified. In some embodiments, the 2D crystalline material is chemically modified with inorganic nanoparticles. In some embodiments, the 2D crystalline material is modified with one or more organic functional groups. In some embodiments, the 2D crystalline material is modified for different modes of controllable self-assembly. In some embodiments, the organic functional group is a fluorophore, metal chelating group or a host complex. In some embodiments, the 2D crystalline material can be genetically modified/fused with functional proteins and peptides. In some embodiments, the 2D crystalline material can be assembled by visible light and dissembled by UV light.

[0009] In a third aspect, a lab-on-a-chip comprising the 2D crystalline material as described in the embodiments of the second aspect is provided. The 2D crystalline material can comprise the polypeptide building block as described in the first aspect. The non-naturally occurring symmetrical polypeptide building block can comprise a plurality of cysteine residues positioned such that formation of disulfide bonds between some or all of said plurality of cysteine residues facilitates formation of 2D crystals. In some embodiments, said polypeptide building block comprises a symmetrical polypeptide comprising a single set of surface cysteine residues in the corner positions. In some embodiments, said polypeptide has inherent C3, C4, C6, D3, D4 or D6 symmetry. In some embodiments, at least one of said cysteine residues has been introduced into said polypeptide building block through genetic engineering. In some embodiments, said polypeptide is generated via solid phase synthesis. In

some embodiments, said polypeptide is genetically engineered. In some embodiments, said polypeptide comprises the RhuA protein. In some embodiments, said polypeptide further comprises an additional polypeptide modification. In some embodiments, said additional modification is selected from the group consisting of a chemical modification, a modification made via an enzymatic reaction, and a modification made via genetic engineering. In some embodiments, said additional modification is selected from the group consisting of functional groups, tags, other polypeptides, peptide tags, detectable labels, fluorophores, and nanoparticles. In some embodiments, the peptide tag comprises a His tag. In some embodiments, the His tag comprises a sequence set forth in SEQ ID NO: 22. In some embodiments, the peptide tag comprises a Pd4 peptide. In some embodiments, the Pd4 peptide comprises a sequence set forth in SEQ ID NO: 23. In some embodiments, the peptide tag comprises an ACP protein. In some embodiments, the ACP protein comprises a sequence set forth in SEQ ID NO: 24. In some embodiments, the polypeptide building block can be chemically modified. In some embodiments, the polypeptide is chemically modified with inorganic nanoparticles. In some embodiments, the polypeptide building block is modified with one or more organic functional groups. In some embodiments, the polypeptide building block is modified for different modes of controllable self-assembly. In some embodiments, the organic functional group is a fluorophore, metal chelating group or a host complex. In some embodiments, the polypeptide building block can be genetically modified/fused with functional proteins and peptides. In some embodiments, said 2D crystalline material is auxetic. In some embodiments, the 2D crystalline material comprises a Poisson's ratio of at least -1. In some embodiments, the 2D crystalline material comprises a Poisson's ratio of -1. In some embodiments, the 2D crystalline material can be chemically modified. In some embodiments, the 2D crystalline material is chemically modified with inorganic nanoparticles. In some embodiments, the 2D crystalline material is modified with one or more organic functional groups. In some embodiments, the 2D crystalline material is modified for different modes of controllable self-assembly. In some embodiments, the organic functional group is a fluorophore, metal chelating group or a host complex. In some embodiments, the 2D crystalline material can be genetically modified/fused with functional

proteins and peptides. In some embodiments, the 2D crystalline material can be assembled by visible light and dissembled by UV light.

[0010] In a fourth aspect, a molecular membrane comprising the 2D crystalline material as described in the embodiments of the second aspect is provided. The 2D crystalline material can comprise the polypeptide building block as described in the embodiments of the first aspect. The non-naturally occurring symmetrical polypeptide building block can comprise a plurality of cysteine residues positioned such that formation of disulfide bonds between some or all of said plurality of cysteine residues facilitates formation of 2D crystals. In some embodiments, said polypeptide building block comprises a symmetrical polypeptide comprising a single set of surface cysteine residues in the corner positions. In some embodiments, said polypeptide has inherent C3, C4, C6, D3, D4 or D6 symmetry. In some embodiments, at least one of said cysteine residues has been introduced into said polypeptide building block through genetic engineering. In some embodiments, said polypeptide is generated via solid phase synthesis. In some embodiments, said polypeptide is genetically engineered. In some embodiments, said polypeptide comprises the RhuA protein. In some embodiments, said polypeptide further comprises an additional polypeptide modification. In some embodiments, said additional modification is selected from the group consisting of a chemical modification, a modification made via an enzymatic reaction, and a modification made via genetic engineering. In some embodiments, said additional modification is selected from the group consisting of functional groups, tags, other polypeptides, peptide tags, detectable labels, fluorophores, and nanoparticles. In some embodiments, the peptide tag comprises a His tag. In some embodiments, the His tag comprises a sequence set forth in SEQ ID NO: 22. In some embodiments, the peptide tag comprises a Pd4 peptide. In some embodiments, the Pd4 peptide comprises a sequence set forth in SEQ ID NO: 23. In some embodiments, the peptide tag comprises an ACP protein. In some embodiments, the ACP protein comprises a sequence set forth in SEQ ID NO: 24. In some embodiments, the polypeptide building block can be chemically modified. In some embodiments, the polypeptide is chemically modified with inorganic nanoparticles. In some embodiments, the polypeptide building block is modified with one or more organic functional groups. In some embodiments, the polypeptide building block is modified for different modes of controllable

self-assembly. In some embodiments, the organic functional group is a fluorophore, metal chelating group or a host complex. In some embodiments, the polypeptide building block can be genetically modified/fused with functional proteins and peptides. In some embodiments, said 2D crystalline material is auxetic. In some embodiments, the 2D crystalline material comprises a Poisson's ratio of at least -1. In some embodiments, the 2D crystalline material comprises a Poisson's ratio of -1. In some embodiments, the 2D crystalline material can be chemically modified. In some embodiments, the 2D crystalline material is chemically modified with inorganic nanoparticles. In some embodiments, the 2D crystalline material is modified with one or more organic functional groups. In some embodiments, the 2D crystalline material is modified for different modes of controllable self-assembly. In some embodiments, the organic functional group is a fluorophore, metal chelating group or a host complex. In some embodiments, the 2D crystalline material can be genetically modified/fused with functional proteins and peptides. In some embodiments, the 2D crystalline material can be assembled by visible light and dissembled by UV light.

[0011] In a fifth aspect, a molecular template comprising the 2D crystalline material as described in the embodiments of the second aspect is provided. The 2D crystalline material can comprise the polypeptide building block as described in the embodiments of the first aspect. The non-naturally occurring symmetrical polypeptide building block can comprise a plurality of cysteine residues positioned such that formation of disulfide bonds between some or all of said plurality of cysteine residues facilitates formation of 2D crystals. In some embodiments, said polypeptide building block comprises a symmetrical polypeptide comprising a single set of surface cysteine residues in the corner positions. In some embodiments, said polypeptide has inherent C3, C4, C6, D3, D4 or D6 symmetry. In some embodiments, at least one of said cysteine residues has been introduced into said polypeptide building block through genetic engineering. In some embodiments, said polypeptide is generated via solid phase synthesis. In some embodiments, said polypeptide is genetically engineered. In some embodiments, said polypeptide comprises the RhuA protein. In some embodiments, said polypeptide further comprises an additional polypeptide modification. In some embodiments, said additional modification is selected from the group consisting of a chemical modification, a modification made via an enzymatic reaction, and a modification

made via genetic engineering. In some embodiments, said additional modification is selected from the group consisting of functional groups, tags, other polypeptides, peptide tags, detectable labels, fluorophores, and nanoparticles. In some embodiments, the peptide tag comprises a His tag. In some embodiments, the His tag comprises a sequence set forth in SEQ ID NO: 22. In some embodiments, the peptide tag comprises a Pd4 peptide. In some embodiments, the Pd4 peptide comprises a sequence set forth in SEQ ID NO: 23. In some embodiments, the peptide tag comprises an ACP protein. In some embodiments, the ACP protein comprises a sequence set forth in SEQ ID NO: 24. In some embodiments, the polypeptide building block can be chemically modified. In some embodiments, the polypeptide is chemically modified with inorganic nanoparticles. In some embodiments, the polypeptide building block is modified with one or more organic functional groups. In some embodiments, the polypeptide building block is modified for different modes of controllable self-assembly. In some embodiments, the organic functional group is a fluorophore, metal chelating group or a host complex. In some embodiments, the polypeptide building block can be genetically modified/fused with functional proteins and peptides. In some embodiments, said 2D crystalline material is auxetic. In some embodiments, the 2D crystalline material comprises a Poisson's ratio of at least -1. In some embodiments, the 2D crystalline material comprises a Poisson's ratio of -1. In some embodiments, the 2D crystalline material can be chemically modified. In some embodiments, the 2D crystalline material is chemically modified with inorganic nanoparticles. In some embodiments, the 2D crystalline material is modified with one or more organic functional groups. In some embodiments, the 2D crystalline material is modified for different modes of controllable self-assembly. In some embodiments, the organic functional group is a fluorophore, metal chelating group or a host complex. In some embodiments, the 2D crystalline material can be genetically modified/fused with functional proteins and peptides. In some embodiments, the 2D crystalline material can be assembled by visible light and dissembled by UV light.

[0012] In a sixth aspect a stabilized polypeptide formulation comprising the 2D crystalline material as described in the embodiments of the second aspect is provided. The 2D crystalline material can comprise the polypeptide building block as described in the embodiments of the first aspect. The non-naturally occurring symmetrical polypeptide

building block can comprise a plurality of cysteine residues positioned such that formation of disulfide bonds between some or all of said plurality of cysteine residues facilitates formation of 2D crystals. In some embodiments, said polypeptide building block comprises a symmetrical polypeptide comprising a single set of surface cysteine residues in the corner positions. In some embodiments, said polypeptide has inherent C3, C4, C6, D3, D4 or D6 symmetry. In some embodiments, at least one of said cysteine residues has been introduced into said polypeptide building block through genetic engineering. In some embodiments, said polypeptide is generated via solid phase synthesis. In some embodiments, said polypeptide is genetically engineered. In some embodiments, said polypeptide comprises the RhuA protein. In some embodiments, said polypeptide further comprises an additional polypeptide modification. In some embodiments, said additional modification is selected from the group consisting of a chemical modification, a modification made via an enzymatic reaction, and a modification made via genetic engineering. In some embodiments, said additional modification is selected from the group consisting of functional groups, tags, other polypeptides, peptide tags, detectable labels, fluorophores, and nanoparticles. In some embodiments, the peptide tag comprises a His tag. In some embodiments, the His tag comprises a sequence set forth in SEQ ID NO: 22. In some embodiments, the peptide tag comprises a Pd4 peptide. In some embodiments, the Pd4 peptide comprises a sequence set forth in SEQ ID NO: 23. In some embodiments, the peptide tag comprises an ACP protein. In some embodiments, the ACP protein comprises a sequence set forth in SEQ ID NO: 24. In some embodiments, the polypeptide building block can be chemically modified. In some embodiments, the polypeptide is chemically modified with inorganic nanoparticles. In some embodiments, the polypeptide building block is modified with one or more organic functional groups. In some embodiments, the polypeptide building block is modified for different modes of controllable self-assembly. In some embodiments, the organic functional group is a fluorophore, metal chelating group or a host complex. In some embodiments, the polypeptide building block can be genetically modified/fused with functional proteins and peptides. In some embodiments, said 2D crystalline material is auxetic. In some embodiments, the 2D crystalline material comprises a Poisson's ratio of at least -1. In some embodiments, the 2D crystalline material comprises a Poisson's ratio of -1. In some

embodiments, the 2D crystalline material can be chemically modified. In some embodiments, the 2D crystalline material is chemically modified with inorganic nanoparticles. In some embodiments, the 2D crystalline material is modified with one or more organic functional groups. In some embodiments, the 2D crystalline material is modified for different modes of controllable self-assembly. In some embodiments, the organic functional group is a fluorophore, metal chelating group or a host complex. In some embodiments, the 2D crystalline material can be genetically modified/fused with functional proteins and peptides. In some embodiments, the 2D crystalline material can be assembled by visible light and dissembled by UV light.

[0013] In a seventh aspect, a molecular scaffold comprising the 2D crystalline material as described in the embodiments of the second aspect is provided. The 2D crystalline material can comprise the polypeptide building block as described in the embodiments of the first aspect. The non-naturally occurring symmetrical polypeptide building block can comprise a plurality of cysteine residues positioned such that formation of disulfide bonds between some or all of said plurality of cysteine residues facilitates formation of 2D crystals. In some embodiments, said polypeptide building block comprises a symmetrical polypeptide comprising a single set of surface cysteine residues in the corner positions. In some embodiments, said polypeptide has inherent C3, C4, C6, D3, D4 or D6 symmetry. In some embodiments, at least one of said cysteine residues has been introduced into said polypeptide building block through genetic engineering. In some embodiments, said polypeptide is generated via solid phase synthesis. In some embodiments, said polypeptide is genetically engineered. In some embodiments, said polypeptide comprises the RhuA protein. In some embodiments, said polypeptide further comprises an additional polypeptide modification. In some embodiments, said additional modification is selected from the group consisting of a chemical modification, a modification made via an enzymatic reaction, and a modification made via genetic engineering. In some embodiments, said additional modification is selected from the group consisting of functional groups, tags, other polypeptides, peptide tags, detectable labels, fluorophores, and nanoparticles. In some embodiments, the peptide tag comprises a His tag. In some embodiments, the His tag comprises a sequence set forth in SEQ ID NO: 22. In some embodiments, the peptide tag comprises a Pd4 peptide. In some

embodiments, the Pd4 peptide comprises a sequence set forth in SEQ ID NO: 23. In some embodiments, the peptide tag comprises an ACP protein. In some embodiments, the ACP protein comprises a sequence set forth in SEQ ID NO: 24. In some embodiments, the polypeptide building block can be chemically modified. In some embodiments, the polypeptide is chemically modified with inorganic nanoparticles. In some embodiments, the polypeptide building block is modified with one or more organic functional groups. In some embodiments, the polypeptide building block is modified for different modes of controllable self-assembly. In some embodiments, the organic functional group is a fluorophore, metal chelating group or a host complex. In some embodiments, the polypeptide building block can be genetically modified/fused with functional proteins and peptides. In some embodiments, said 2D crystalline material is auxetic. In some embodiments, the 2D crystalline material comprises a Poisson's ratio of at least -1. In some embodiments, the 2D crystalline material comprises a Poisson's ratio of -1. In some embodiments, the 2D crystalline material can be chemically modified. In some embodiments, the 2D crystalline material is chemically modified with inorganic nanoparticles. In some embodiments, the 2D crystalline material is modified with one or more organic functional groups. In some embodiments, the 2D crystalline material is modified for different modes of controllable self-assembly. In some embodiments, the organic functional group is a fluorophore, metal chelating group or a host complex. In some embodiments, the 2D crystalline material can be genetically modified/fused with functional proteins and peptides. In some embodiments, the 2D crystalline material can be assembled by visible light and dissembled by UV light.

[0014] In an eighth aspect, a protective armor comprising the 2D crystalline material as described in the embodiments of the second aspect is provided. The 2D crystalline material can comprise the polypeptide building block as described in the embodiments of first aspect. The non-naturally occurring symmetrical polypeptide building block can comprise a plurality of cysteine residues positioned such that formation of disulfide bonds between some or all of said plurality of cysteine residues facilitates formation of 2D crystals. In some embodiments, said polypeptide building block comprises a symmetrical polypeptide comprising a single set of surface cysteine residues in the corner positions. In some embodiments, said polypeptide has inherent C3, C4, C6, D3, D4 or D6 symmetry. In some

embodiments, at least one of said cysteine residues has been introduced into said polypeptide building block through genetic engineering. In some embodiments, said polypeptide is generated via solid phase synthesis. In some embodiments, said polypeptide is genetically engineered. In some embodiments, said polypeptide comprises the RhuA protein. In some embodiments, said polypeptide further comprises an additional polypeptide modification. In some embodiments, said additional modification is selected from the group consisting of a chemical modification, a modification made via an enzymatic reaction, and a modification made via genetic engineering. In some embodiments, said additional modification is selected from the group consisting of functional groups, tags, other polypeptides, peptide tags, detectable labels, fluorophores, and nanoparticles. In some embodiments, the peptide tag comprises a His tag. In some embodiments, the His tag comprises a sequence set forth in SEQ ID NO: 22. In some embodiments, the peptide tag comprises a Pd4 peptide. In some embodiments, the Pd4 peptide comprises a sequence set forth in SEQ ID NO: 23. In some embodiments, the peptide tag comprises an ACP protein. In some embodiments, the ACP protein comprises a sequence set forth in SEQ ID NO: 24. In some embodiments, the polypeptide building block can be chemically modified. In some embodiments, the polypeptide is chemically modified with inorganic nanoparticles. In some embodiments, the polypeptide building block is modified with one or more organic functional groups. In some embodiments, the polypeptide building block is modified for different modes of controllable self-assembly. In some embodiments, the organic functional group is a fluorophore, metal chelating group or a host complex. In some embodiments, the polypeptide building block can be genetically modified/fused with functional proteins and peptides. In some embodiments, said 2D crystalline material is auxetic. In some embodiments, the 2D crystalline material comprises a Poisson's ratio of at least -1. In some embodiments, the 2D crystalline material comprises a Poisson's ratio of -1. In some embodiments, the 2D crystalline material can be chemically modified. In some embodiments, the 2D crystalline material is chemically modified with inorganic nanoparticles. In some embodiments, the 2D crystalline material is modified with one or more organic functional groups. In some embodiments, the 2D crystalline material is modified for different modes of controllable self-assembly. In some embodiments, the organic functional group is a fluorophore, metal chelating group or a host

complex. In some embodiments, the 2D crystalline material can be genetically modified/fused with functional proteins and peptides. In some embodiments, the 2D crystalline material can be assembled by visible light and dissembled by UV light.

[0015] In a ninth aspect, a smart textile comprising the 2D crystalline material as described in the embodiments of the second aspect is provided. The 2D crystalline material can comprise the polypeptide building block as described in the embodiments of the first aspect. The non-naturally occurring symmetrical polypeptide building block can comprise a plurality of cysteine residues positioned such that formation of disulfide bonds between some or all of said plurality of cysteine residues facilitates formation of 2D crystals. In some embodiments, said polypeptide building block comprises a symmetrical polypeptide comprising a single set of surface cysteine residues in the corner positions. In some embodiments, said polypeptide has inherent C3, C4, C6, D3, D4 or D6 symmetry. In some embodiments, at least one of said cysteine residues has been introduced into said polypeptide building block through genetic engineering. In some embodiments, said polypeptide is generated via solid phase synthesis. In some embodiments, said polypeptide is genetically engineered. In some embodiments, said polypeptide comprises the RhuA protein. In some embodiments, said polypeptide further comprises an additional polypeptide modification. In some embodiments, said additional modification is selected from the group consisting of a chemical modification, a modification made via an enzymatic reaction, and a modification made via genetic engineering. In some embodiments, said additional modification is selected from the group consisting of functional groups, tags, other polypeptides, peptide tags, detectable labels, fluorophores, and nanoparticles. In some embodiments, the peptide tag comprises a His tag. In some embodiments, the His tag comprises a sequence set forth in SEQ ID NO: 22. In some embodiments, the peptide tag comprises a Pd4 peptide. In some embodiments, the Pd4 peptide comprises a sequence set forth in SEQ ID NO: 23. In some embodiments, the peptide tag comprises an ACP protein. In some embodiments, the ACP protein comprises a sequence set forth in SEQ ID NO: 24. In some embodiments, the polypeptide building block can be chemically modified. In some embodiments, the polypeptide is chemically modified with inorganic nanoparticles. In some embodiments, the polypeptide building block is modified with one or more organic functional groups. In some

embodiments, the polypeptide building block is modified for different modes of controllable self-assembly. In some embodiments, the organic functional group is a fluorophore, metal chelating group or a host complex. In some embodiments, the polypeptide building block can be genetically modified/fused with functional proteins and peptides. In some embodiments, said 2D crystalline material is auxetic. In some embodiments, the 2D crystalline material comprises a Poisson's ratio of at least -1. In some embodiments, the 2D crystalline material comprises a Poisson's ratio of -1. In some embodiments, the 2D crystalline material can be chemically modified. In some embodiments, the 2D crystalline material is chemically modified with inorganic nanoparticles. In some embodiments, the 2D crystalline material is modified with one or more organic functional groups. In some embodiments, the 2D crystalline material is modified for different modes of controllable self-assembly. In some embodiments, the organic functional group is a fluorophore, metal chelating group or a host complex. In some embodiments, the 2D crystalline material can be genetically modified/fused with functional proteins and peptides. In some embodiments, the 2D crystalline material can be assembled by visible light and dissembled by UV light.

[0016] In a tenth aspect, a piezo electronic component comprising the 2D crystalline material as described in the embodiments of the second aspect is provided. The 2D crystalline material can comprise the polypeptide building block as described in the embodiments of the first aspect. The non-naturally occurring symmetrical polypeptide building block can comprise a plurality of cysteine residues positioned such that formation of disulfide bonds between some or all of said plurality of cysteine residues facilitates formation of 2D crystals. In some embodiments, said polypeptide building block comprises a symmetrical polypeptide comprising a single set of surface cysteine residues in the corner positions. In some embodiments, said polypeptide has inherent C3, C4, C6, D3, D4 or D6 symmetry. In some embodiments, at least one of said cysteine residues has been introduced into said polypeptide building block through genetic engineering. In some embodiments, said polypeptide is generated via solid phase synthesis. In some embodiments, said polypeptide is genetically engineered. In some embodiments, said polypeptide comprises the RhuA protein. In some embodiments, said polypeptide further comprises an additional polypeptide modification. In some embodiments, said additional modification is selected from the group

consisting of a chemical modification, a modification made via an enzymatic reaction, and a modification made via genetic engineering. In some embodiments, said additional modification is selected from the group consisting of functional groups, tags, other polypeptides, peptide tags, detectable labels, fluorophores, and nanoparticles. In some embodiments, the peptide tag comprises a His tag. In some embodiments, the His tag comprises a sequence set forth in SEQ ID NO: 22. In some embodiments, the peptide tag comprises a Pd4 peptide. In some embodiments, the Pd4 peptide comprises a sequence set forth in SEQ ID NO: 23. In some embodiments, the peptide tag comprises an ACP protein. In some embodiments, the ACP protein comprises a sequence set forth in SEQ ID NO: 24. In some embodiments, the polypeptide building block can be chemically modified. In some embodiments, the polypeptide is chemically modified with inorganic nanoparticles. In some embodiments, the polypeptide building block is modified with one or more organic functional groups. In some embodiments, the polypeptide building block is modified for different modes of controllable self-assembly. In some embodiments, the organic functional group is a fluorophore, metal chelating group or a host complex. In some embodiments, the polypeptide building block can be genetically modified/fused with functional proteins and peptides. In some embodiments, said 2D crystalline material is auxetic. In some embodiments, the 2D crystalline material comprises a Poisson's ratio of at least -1. In some embodiments, the 2D crystalline material comprises a Poisson's ratio of -1. In some embodiments, the 2D crystalline material can be chemically modified. In some embodiments, the 2D crystalline material is chemically modified with inorganic nanoparticles. In some embodiments, the 2D crystalline material is modified with one or more organic functional groups. In some embodiments, the 2D crystalline material is modified for different modes of controllable self-assembly. In some embodiments, the organic functional group is a fluorophore, metal chelating group or a host complex. In some embodiments, the 2D crystalline material can be genetically modified/fused with functional proteins and peptides. In some embodiments, the 2D crystalline material can be assembled by visible light and dissembled by UV light.

[0017] In an eleventh aspect, an adaptive membrane or sieve comprising the 2D crystalline material as described in the embodiments of the second aspect is provided. The 2D

crystalline material can comprise the polypeptide building block as described in the embodiments of the first aspect. The non-naturally occurring symmetrical polypeptide building block can comprise a plurality of cysteine residues positioned such that formation of disulfide bonds between some or all of said plurality of cysteine residues facilitates formation of 2D crystals. In some embodiments, said polypeptide building block comprises a symmetrical polypeptide comprising a single set of surface cysteine residues in the corner positions. In some embodiments, said polypeptide has inherent C3, C4, C6, D3, D4 or D6 symmetry. In some embodiments, at least one of said cysteine residues has been introduced into said polypeptide building block through genetic engineering. In some embodiments, said polypeptide is generated via solid phase synthesis. In some embodiments, said polypeptide is genetically engineered. In some embodiments, said polypeptide comprises the RhuA protein. In some embodiments, said polypeptide further comprises an additional polypeptide modification. In some embodiments, said additional modification is selected from the group consisting of a chemical modification, a modification made via an enzymatic reaction, and a modification made via genetic engineering. In some embodiments, said additional modification is selected from the group consisting of functional groups, tags, other polypeptides, peptide tags, detectable labels, fluorophores, and nanoparticles. In some embodiments, the peptide tag comprises a His tag. In some embodiments, the His tag comprises a sequence set forth in SEQ ID NO: 22. In some embodiments, the peptide tag comprises a Pd4 peptide. In some embodiments, the Pd4 peptide comprises a sequence set forth in SEQ ID NO: 23. In some embodiments, the peptide tag comprises an ACP protein. In some embodiments, the ACP protein comprises a sequence set forth in SEQ ID NO: 24. In some embodiments, the polypeptide building block can be chemically modified. In some embodiments, the polypeptide is chemically modified with inorganic nanoparticles. In some embodiments, the polypeptide building block is modified with one or more organic functional groups. In some embodiments, the polypeptide building block is modified for different modes of controllable self-assembly. In some embodiments, the organic functional group is a fluorophore, metal chelating group or a host complex. In some embodiments, the polypeptide building block can be genetically modified/fused with functional proteins and peptides. In some embodiments, said 2D crystalline material is auxetic. In some

embodiments, the 2D crystalline material comprises a Poisson's ratio of at least -1. In some embodiments, the 2D crystalline material comprises a Poisson's ratio of -1. In some embodiments, the 2D crystalline material can be chemically modified. In some embodiments, the 2D crystalline material is chemically modified with inorganic nanoparticles. In some embodiments, the 2D crystalline material is modified with one or more organic functional groups. In some embodiments, the 2D crystalline material is modified for different modes of controllable self-assembly. In some embodiments, the organic functional group is a fluorophore, metal chelating group or a host complex. In some embodiments, the 2D crystalline material can be genetically modified/fused with functional proteins and peptides. In some embodiments, the 2D crystalline material can be assembled by visible light and dissembled by UV light.

[0018] In a twelfth aspect a controlled drug release formulation comprising the 2D crystalline material as described in the embodiments of the second aspect is provided. The 2D crystalline material can comprise the polypeptide building block as described in embodiments of the first aspect. The non-naturally occurring symmetrical polypeptide building block can comprise a plurality of cysteine residues positioned such that formation of disulfide bonds between some or all of said plurality of cysteine residues facilitates formation of 2D crystals. In some embodiments, said polypeptide building block comprises a symmetrical polypeptide comprising a single set of surface cysteine residues in the corner positions. In some embodiments, said polypeptide has inherent C3, C4, C6, D3, D4 or D6 symmetry. In some embodiments, at least one of said cysteine residues has been introduced into said polypeptide building block through genetic engineering. In some embodiments, said polypeptide is generated via solid phase synthesis. In some embodiments, said polypeptide is genetically engineered. In some embodiments, said polypeptide comprises the RhuA protein. In some embodiments, said polypeptide further comprises an additional polypeptide modification. In some embodiments, said additional modification is selected from the group consisting of a chemical modification, a modification made via an enzymatic reaction, and a modification made via genetic engineering. In some embodiments, said additional modification is selected from the group consisting of functional groups, tags, other polypeptides, peptide tags, detectable labels, fluorophores, and nanoparticles. In some

embodiments, the peptide tag comprises a His tag. In some embodiments, the His tag comprises a sequence set forth in SEQ ID NO: 22. In some embodiments, the peptide tag comprises a Pd4 peptide. In some embodiments, the Pd4 peptide comprises a sequence set forth in SEQ ID NO: 23. In some embodiments, the peptide tag comprises an ACP protein. In some embodiments, the ACP protein comprises a sequence set forth in SEQ ID NO: 24. In some embodiments, the polypeptide building block can be chemically modified. In some embodiments, the polypeptide is chemically modified with inorganic nanoparticles. In some embodiments, the polypeptide building block is modified with one or more organic functional groups. In some embodiments, the polypeptide building block is modified for different modes of controllable self-assembly. In some embodiments, the organic functional group is a fluorophore, metal chelating group or a host complex. In some embodiments, the polypeptide building block can be genetically modified/fused with functional proteins and peptides. In some embodiments, said 2D crystalline material is auxetic. In some embodiments, the 2D crystalline material comprises a Poisson's ratio of at least -1. In some embodiments, the 2D crystalline material comprises a Poisson's ratio of -1. In some embodiments, the 2D crystalline material can be chemically modified. In some embodiments, the 2D crystalline material is chemically modified with inorganic nanoparticles. In some embodiments, the 2D crystalline material is modified with one or more organic functional groups. In some embodiments, the 2D crystalline material is modified for different modes of controllable self-assembly. In some embodiments, the organic functional group is a fluorophore, metal chelating group or a host complex. In some embodiments, the 2D crystalline material can be genetically modified/fused with functional proteins and peptides. In some embodiments, the 2D crystalline material can be assembled by visible light and dissembled by UV light.

[0019] In a thirteenth aspect, a run-flat tire comprising the 2D crystalline material as described in the embodiments of the second aspect is provided. The 2D crystalline material can comprise the polypeptide building block as described in the embodiments of the first aspect. The non-naturally occurring symmetrical polypeptide building block can comprise a plurality of cysteine residues positioned such that formation of disulfide bonds between some or all of said plurality of cysteine residues facilitates formation of 2D crystals. In some

embodiments, said polypeptide building block comprises a symmetrical polypeptide comprising a single set of surface cysteine residues in the corner positions. In some embodiments, said polypeptide has inherent C3, C4, C6, D3, D4 or D6 symmetry. In some embodiments, at least one of said cysteine residues has been introduced into said polypeptide building block through genetic engineering. In some embodiments, said polypeptide is generated via solid phase synthesis. In some embodiments, said polypeptide is genetically engineered. In some embodiments, said polypeptide comprises the RhuA protein. In some embodiments, said polypeptide further comprises an additional polypeptide modification. In some embodiments, said additional modification is selected from the group consisting of a chemical modification, a modification made via an enzymatic reaction, and a modification made via genetic engineering. In some embodiments, said additional modification is selected from the group consisting of functional groups, tags, other polypeptides, peptide tags, detectable labels, fluorophores, and nanoparticles. In some embodiments, the peptide tag comprises a His tag. In some embodiments, the His tag comprises a sequence set forth in SEQ ID NO: 22. In some embodiments, the peptide tag comprises a Pd4 peptide. In some embodiments, the Pd4 peptide comprises a sequence set forth in SEQ ID NO: 23. In some embodiments, the peptide tag comprises an ACP protein. In some embodiments, the ACP protein comprises a sequence set forth in SEQ ID NO: 24. In some embodiments, the polypeptide building block can be chemically modified. In some embodiments, the polypeptide is chemically modified with inorganic nanoparticles. In some embodiments, the polypeptide building block is modified with one or more organic functional groups. In some embodiments, the polypeptide building block is modified for different modes of controllable self-assembly. In some embodiments, the organic functional group is a fluorophore, metal chelating group or a host complex. In some embodiments, the polypeptide building block can be genetically modified/fused with functional proteins and peptides. In some embodiments, said 2D crystalline material is auxetic. In some embodiments, the 2D crystalline material comprises a Poisson's ratio of at least -1. In some embodiments, the 2D crystalline material comprises a Poisson's ratio of -1. In some embodiments, the 2D crystalline material can be chemically modified. In some embodiments, the 2D crystalline material is chemically modified with inorganic nanoparticles. In some embodiments, the 2D crystalline material is

modified with one or more organic functional groups. In some embodiments, the 2D crystalline material is modified for different modes of controllable self-assembly. In some embodiments, the organic functional group is a fluorophore, metal chelating group or a host complex. In some embodiments, the 2D crystalline material can be genetically modified/fused with functional proteins and peptides. In some embodiments, the 2D crystalline material can be assembled by visible light and dissembled by UV light.

[0020] In a fourteenth aspect a method of making a crystalline material is provided. The method can comprise placing a plurality of polypeptide building blocks as described in the embodiments of the first aspect under oxidizing conditions and allowing said plurality of polypeptide building blocks to self-assemble into said crystalline material. The non-naturally occurring symmetrical polypeptide building block can comprise a plurality of cysteine residues positioned such that formation of disulfide bonds between some or all of said plurality of cysteine residues facilitates formation of 2D crystals. In some embodiments, said polypeptide building block comprises a symmetrical polypeptide comprising a single set of surface cysteine residues in the corner positions. In some embodiments, said polypeptide has inherent C3, C4, C6, D3, D4 or D6 symmetry. In some embodiments, at least one of said cysteine residues has been introduced into said polypeptide building block through genetic engineering. In some embodiments, said polypeptide is generated via solid phase synthesis. In some embodiments, said polypeptide is genetically engineered. In some embodiments, said polypeptide comprises the RhuA protein. In some embodiments, said polypeptide further comprises an additional polypeptide modification. In some embodiments, said additional modification is selected from the group consisting of a chemical modification, a modification made via an enzymatic reaction, and a modification made via genetic engineering. In some embodiments, said additional modification is selected from the group consisting of functional groups, tags, other polypeptides, peptide tags, detectable labels, fluorophores, and nanoparticles. In some embodiments, the peptide tag comprises a His tag. In some embodiments, the His tag comprises a sequence set forth in SEQ ID NO: 22. In some embodiments, the peptide tag comprises a Pd4 peptide. In some embodiments, the Pd4 peptide comprises a sequence set forth in SEQ ID NO: 23. In some embodiments, the peptide tag comprises an ACP protein. In some embodiments, the ACP protein comprises a sequence

set forth in SEQ ID NO: 24. In some embodiments, the polypeptide building block can be chemically modified. In some embodiments, the polypeptide is chemically modified with inorganic nanoparticles. In some embodiments, the polypeptide building block is modified with one or more organic functional groups. In some embodiments, the polypeptide building block is modified for different modes of controllable self-assembly. In some embodiments, the organic functional group is a fluorophore, metal chelating group or a host complex. In some embodiments, the polypeptide building block can be genetically modified/fused with functional proteins and peptides. In some embodiments, oxidizing conditions are controllable. In some embodiments, said plurality of polypeptide building blocks are incubated in solution under said oxidizing conditions.

[0021] In a fifteenth aspect, a non-naturally occurring symmetrical polypeptide building block is provided. The non-naturally occurring symmetrical polypeptide building block can comprise a plurality of histidine residues positioned such that coordination of some or all of said plurality of histidine residues with one or more metal ions facilitates formation of 2D crystals. In some embodiments, said polypeptide building block comprises a symmetrical polypeptide comprising surface histidine residues in the corner positions. In some embodiments, said polypeptide has inherent C3, C4, C6, D3, D4 or D6 symmetry. In some embodiments, at least one of said histidine residues has been introduced into said polypeptide building block through genetic engineering. In some embodiments, said polypeptide is generated via solid phase synthesis. In some embodiments, said polypeptide is genetically engineered. In some embodiments, the polypeptide further comprises an additional modification. In some embodiments, said additional modification is selected from the group consisting of a chemical modification, a modification made via an enzymatic reaction, and a modification made via genetic engineering. In some embodiments, said additional modification is selected from the group consisting of functional groups, tags, other polypeptides, peptide tags, detectable labels, fluorophores, and nanoparticles. In some embodiments, said symmetrical polypeptide comprises the RhuA protein. In some embodiments, the peptide tag comprises a His tag. In some embodiments, the His tag comprises a sequence set forth in SEQ ID NO: 22. In some embodiments, the peptide tag comprises a Pd4 peptide. In some embodiments, the Pd4 peptide comprises a sequence set

forth in SEQ ID NO: 23. In some embodiments, the peptide tag comprises an ACP protein. In some embodiments, the ACP protein comprises a sequence set forth in SEQ ID NO: 24. In some embodiments, the polypeptide building block can be chemically modified. In some embodiments, the polypeptide is chemically modified with inorganic nanoparticles. In some embodiments, the polypeptide building block is modified with one or more organic functional groups. In some embodiments, the polypeptide building block is modified for different modes of controllable self-assembly. In some embodiments, the organic functional group is a fluorophore, metal chelating group or a host complex. In some embodiments, the polypeptide building block can be genetically modified/fused with functional proteins and peptides. In some embodiments, the 2D crystalline material can be assembled by visible light and dissembled by UV light.

[0022] In a sixteenth aspect, a 2D crystalline material is provided. The 2D crystalline material can comprise the polypeptide building block as described in the embodiments of the fifteenth aspect. The polypeptide building block is a non-naturally occurring symmetrical polypeptide building block. The non-naturally occurring symmetrical polypeptide building block can comprise a plurality of histidine residues positioned such that coordination of some or all of said plurality of histidine residues with one or more metal ions facilitates formation of 2D crystals. In some embodiments, said polypeptide building block comprises a symmetrical polypeptide comprising surface histidine residues in the corner positions. In some embodiments, said polypeptide has inherent C3, C4, C6, D3, D4 or D6 symmetry. In some embodiments, at least one of said histidine residues has been introduced into said polypeptide building block through genetic engineering. In some embodiments, said polypeptide is generated via solid phase synthesis. In some embodiments, said polypeptide is genetically engineered. In some embodiments, the polypeptide further comprises an additional modification. In some embodiments, said additional modification is selected from the group consisting of a chemical modification, a modification made via an enzymatic reaction, and a modification made via genetic engineering. In some embodiments, said additional modification is selected from the group consisting of functional groups, tags, other polypeptides, peptide tags, detectable labels, fluorophores, and nanoparticles. In some embodiments, said symmetrical polypeptide comprises the RhuA protein. In some

embodiments, the peptide tag comprises a His tag. In some embodiments, the His tag comprises a sequence set forth in SEQ ID NO: 22. In some embodiments, the peptide tag comprises a Pd4 peptide. In some embodiments, the Pd4 peptide comprises a sequence set forth in SEQ ID NO: 23. In some embodiments, the peptide tag comprises an ACP protein. In some embodiments, the ACP protein comprises a sequence set forth in SEQ ID NO: 24. In some embodiments, the polypeptide building block can be chemically modified. In some embodiments, the polypeptide is chemically modified with inorganic nanoparticles. In some embodiments, the polypeptide building block is modified with one or more organic functional groups. In some embodiments, the polypeptide building block is modified for different modes of controllable self-assembly. In some embodiments, the organic functional group is a fluorophore, metal chelating group or a host complex. In some embodiments, the polypeptide building block can be genetically modified/fused with functional proteins and peptides. In some embodiments, said 2D crystalline material is auxetic. In some embodiments, the 2D crystalline material comprises a Poisson's ratio of at least -1. In some embodiments, the 2D crystalline material comprises a Poisson's ratio of -1. In some embodiments, the 2D crystalline material can be chemically modified. In some embodiments, the 2D crystalline material is chemically modified with inorganic nanoparticles. In some embodiments, the 2D crystalline material is modified with one or more organic functional groups. In some embodiments, the 2D crystalline material is modified for different modes of controllable self-assembly. In some embodiments, organic functional group is a fluorophore, metal chelating group or a host complex. In some embodiments, the 2D crystalline material can be genetically modified/fused with functional proteins and peptides. In some embodiments, the 2D crystalline material can be assembled by visible light and dissembled by UV light.

[0023] In a seventeenth aspect, a lab-on-a-chip comprising the 2D crystalline material of the embodiments described in the sixteenth aspect is provided. The 2D crystalline material can comprise the polypeptide building block as described in the embodiments of the fifteenth aspect. The polypeptide building block is a non-naturally occurring symmetrical polypeptide building block. The non-naturally occurring symmetrical polypeptide building block can comprise a plurality of histidine residues positioned such that coordination of some

or all of said plurality of histidine residues with one or more metal ions facilitates formation of 2D crystals. In some embodiments, said polypeptide building block comprises a symmetrical polypeptide comprising surface histidine residues in the corner positions. In some embodiments, said polypeptide has inherent C3, C4, C6, D3, D4 or D6 symmetry. In some embodiments, at least one of said histidine residues has been introduced into said polypeptide building block through genetic engineering. In some embodiments, said polypeptide is generated via solid phase synthesis. In some embodiments, said polypeptide is genetically engineered. In some embodiments, the polypeptide further comprises an additional modification. In some embodiments, said additional modification is selected from the group consisting of a chemical modification, a modification made via an enzymatic reaction, and a modification made via genetic engineering. In some embodiments, said additional modification is selected from the group consisting of functional groups, tags, other polypeptides, peptide tags, detectable labels, fluorophores, and nanoparticles. In some embodiments, said symmetrical polypeptide comprises the RhuA protein. In some embodiments, the peptide tag comprises a His tag. In some embodiments, the His tag comprises a sequence set forth in SEQ ID NO: 22. In some embodiments, the peptide tag comprises a Pd4 peptide. In some embodiments, the Pd4 peptide comprises a sequence set forth in SEQ ID NO: 23. In some embodiments, the peptide tag comprises an ACP protein. In some embodiments, the ACP protein comprises a sequence set forth in SEQ ID NO: 24. In some embodiments, the polypeptide building block can be chemically modified. In some embodiments, the polypeptide is chemically modified with inorganic nanoparticles. In some embodiments, the polypeptide building block is modified with one or more organic functional groups. In some embodiments, the polypeptide building block is modified for different modes of controllable self-assembly. In some embodiments, the organic functional group is a fluorophore, metal chelating group or a host complex. In some embodiments, the polypeptide building block can be genetically modified/fused with functional proteins and peptides. In some embodiments, said 2D crystalline material is auxetic. In some embodiments, the 2D crystalline material comprises a Poisson's ratio of at least -1. In some embodiments, the 2D crystalline material comprises a Poisson's ratio of -1. In some embodiments, the 2D crystalline material can be chemically modified. In some embodiments,

the 2D crystalline material is chemically modified with inorganic nanoparticles. In some embodiments, the 2D crystalline material is modified with one or more organic functional groups. In some embodiments, the 2D crystalline material is modified for different modes of controllable self-assembly. In some embodiments, organic functional group is a fluorophore, metal chelating group or a host complex. In some embodiments, the 2D crystalline material can be genetically modified/fused with functional proteins and peptides. In some embodiments, the 2D crystalline material can be assembled by visible light and dissembled by UV light.

[0024] In an eighteenth aspect, a molecular membrane comprising the 2D crystalline material as described in the sixteenth aspect is provided. The 2D crystalline material can comprise the polypeptide building block as described in the embodiments of the fifteenth aspect. The polypeptide building block is a non-naturally occurring symmetrical polypeptide building block. The non-naturally occurring symmetrical polypeptide building block can comprise a plurality of histidine residues positioned such that coordination of some or all of said plurality of histidine residues with one or more metal ions facilitates formation of 2D crystals. In some embodiments, said polypeptide building block comprises a symmetrical polypeptide comprising surface histidine residues in the corner positions. In some embodiments, said polypeptide has inherent C3, C4, C6, D3, D4 or D6 symmetry. In some embodiments, at least one of said histidine residues has been introduced into said polypeptide building block through genetic engineering. In some embodiments, said polypeptide is generated via solid phase synthesis. In some embodiments, said polypeptide is genetically engineered. In some embodiments, the polypeptide further comprises an additional modification. In some embodiments, said additional modification is selected from the group consisting of a chemical modification, a modification made via an enzymatic reaction, and a modification made via genetic engineering. In some embodiments, said additional modification is selected from the group consisting of functional groups, tags, other polypeptides, peptide tags, detectable labels, fluorophores, and nanoparticles. In some embodiments, said symmetrical polypeptide comprises the RhuA protein. In some embodiments, the peptide tag comprises a His tag. In some embodiments, the His tag comprises a sequence set forth in SEQ ID NO: 22. In some embodiments, the peptide tag

comprises a Pd4 peptide. In some embodiments, the Pd4 peptide comprises a sequence set forth in SEQ ID NO: 23. In some embodiments, the peptide tag comprises an ACP protein. In some embodiments, the ACP protein comprises a sequence set forth in SEQ ID NO: 24. In some embodiments, the polypeptide building block can be chemically modified. In some embodiments, the polypeptide is chemically modified with inorganic nanoparticles. In some embodiments, the polypeptide building block is modified with one or more organic functional groups. In some embodiments, the polypeptide building block is modified for different modes of controllable self-assembly. In some embodiments, the organic functional group is a fluorophore, metal chelating group or a host complex. In some embodiments, the polypeptide building block can be genetically modified/fused with functional proteins and peptides. In some embodiments, said 2D crystalline material is auxetic. In some embodiments, the 2D crystalline material comprises a Poisson's ratio of at least -1. In some embodiments, the 2D crystalline material comprises a Poisson's ratio of -1. In some embodiments, the 2D crystalline material can be chemically modified. In some embodiments, the 2D crystalline material is chemically modified with inorganic nanoparticles. In some embodiments, the 2D crystalline material is modified with one or more organic functional groups. In some embodiments, the 2D crystalline material is modified for different modes of controllable self-assembly. In some embodiments, organic functional group is a fluorophore, metal chelating group or a host complex. In some embodiments, the 2D crystalline material can be genetically modified/fused with functional proteins and peptides. In some embodiments, the 2D crystalline material can be assembled by visible light and dissembled by UV light.

[0025] In a nineteenth aspect, a molecular template comprising the 2D crystalline material as described in the embodiments of the sixteenth aspect is provided. The 2D crystalline material can comprise the polypeptide building block as described in the embodiments of the fifteenth aspect. The polypeptide building block is a non-naturally occurring symmetrical polypeptide building block. The non-naturally occurring symmetrical polypeptide building block can comprise a plurality of histidine residues positioned such that coordination of some or all of said plurality of histidine residues with one or more metal ions facilitates formation of 2D crystals. In some embodiments, said polypeptide building block

comprises a symmetrical polypeptide comprising surface histidine residues in the corner positions. In some embodiments, said polypeptide has inherent C3, C4, C6, D3, D4 or D6 symmetry. In some embodiments, at least one of said histidine residues has been introduced into said polypeptide building block through genetic engineering. In some embodiments, said polypeptide is generated via solid phase synthesis. In some embodiments, said polypeptide is genetically engineered. In some embodiments, the polypeptide further comprises an additional modification. In some embodiments, said additional modification is selected from the group consisting of a chemical modification, a modification made via an enzymatic reaction, and a modification made via genetic engineering. In some embodiments, said additional modification is selected from the group consisting of functional groups, tags, other polypeptides, peptide tags, detectable labels, fluorophores, and nanoparticles. In some embodiments, said symmetrical polypeptide comprises the RhuA protein. In some embodiments, the peptide tag comprises a His tag. In some embodiments, the His tag comprises a sequence set forth in SEQ ID NO: 22. In some embodiments, the peptide tag comprises a Pd4 peptide. In some embodiments, the Pd4 peptide comprises a sequence set forth in SEQ ID NO: 23. In some embodiments, the peptide tag comprises an ACP protein. In some embodiments, the ACP protein comprises a sequence set forth in SEQ ID NO: 24. In some embodiments, the polypeptide building block can be chemically modified. In some embodiments, the polypeptide is chemically modified with inorganic nanoparticles. In some embodiments, the polypeptide building block is modified with one or more organic functional groups. In some embodiments, the polypeptide building block is modified for different modes of controllable self-assembly. In some embodiments, the organic functional group is a fluorophore, metal chelating group or a host complex. In some embodiments, the polypeptide building block can be genetically modified/fused with functional proteins and peptides. In some embodiments, said 2D crystalline material is auxetic. In some embodiments, the 2D crystalline material comprises a Poisson's ratio of at least -1. In some embodiments, the 2D crystalline material comprises a Poisson's ratio of -1. In some embodiments, the 2D crystalline material can be chemically modified. In some embodiments, the 2D crystalline material is chemically modified with inorganic nanoparticles. In some embodiments, the 2D crystalline material is modified with one or more organic functional

groups. In some embodiments, the 2D crystalline material is modified for different modes of controllable self-assembly. In some embodiments, organic functional group is a fluorophore, metal chelating group or a host complex. In some embodiments, the 2D crystalline material can be genetically modified/fused with functional proteins and peptides. In some embodiments, the 2D crystalline material can be assembled by visible light and dissembled by UV light.

[0026] In a twentieth aspect, a stabilized polypeptide formulation comprising the 2D crystalline material as described in the embodiments of the sixteenth aspect is provided. The 2D crystalline material can comprise the polypeptide building block as described in the embodiments of the fifteenth aspect. The polypeptide building block is a non-naturally occurring symmetrical polypeptide building block. The non-naturally occurring symmetrical polypeptide building block can comprise a plurality of histidine residues positioned such that coordination of some or all of said plurality of histidine residues with one or more metal ions facilitates formation of 2D crystals. In some embodiments, said polypeptide building block comprises a symmetrical polypeptide comprising surface histidine residues in the corner positions. In some embodiments, said polypeptide has inherent C3, C4, C6, D3, D4 or D6 symmetry. In some embodiments, at least one of said histidine residues has been introduced into said polypeptide building block through genetic engineering. In some embodiments, said polypeptide is generated via solid phase synthesis. In some embodiments, said polypeptide is genetically engineered. In some embodiments, the polypeptide further comprises an additional modification. In some embodiments, said additional modification is selected from the group consisting of a chemical modification, a modification made via an enzymatic reaction, and a modification made via genetic engineering. In some embodiments, said additional modification is selected from the group consisting of functional groups, tags, other polypeptides, peptide tags, detectable labels, fluorophores, and nanoparticles. In some embodiments, said symmetrical polypeptide comprises the RhuA protein. In some embodiments, the peptide tag comprises a His tag. In some embodiments, the His tag comprises a sequence set forth in SEQ ID NO: 22. In some embodiments, the peptide tag comprises a Pd4 peptide. In some embodiments, the Pd4 peptide comprises a sequence set forth in SEQ ID NO: 23. In some embodiments, the peptide tag comprises an ACP protein.

In some embodiments, the ACP protein comprises a sequence set forth in SEQ ID NO: 24. In some embodiments, the polypeptide building block can be chemically modified. In some embodiments, the polypeptide is chemically modified with inorganic nanoparticles. In some embodiments, the polypeptide building block is modified with one or more organic functional groups. In some embodiments, the polypeptide building block is modified for different modes of controllable self-assembly. In some embodiments, the organic functional group is a fluorophore, metal chelating group or a host complex. In some embodiments, the polypeptide building block can be genetically modified/fused with functional proteins and peptides. In some embodiments, said 2D crystalline material is auxetic. In some embodiments, the 2D crystalline material comprises a Poisson's ratio of at least -1. In some embodiments, the 2D crystalline material comprises a Poisson's ratio of -1. In some embodiments, the 2D crystalline material can be chemically modified. In some embodiments, the 2D crystalline material is chemically modified with inorganic nanoparticles. In some embodiments, the 2D crystalline material is modified with one or more organic functional groups. In some embodiments, the 2D crystalline material is modified for different modes of controllable self-assembly. In some embodiments, organic functional group is a fluorophore, metal chelating group or a host complex. In some embodiments, the 2D crystalline material can be genetically modified/fused with functional proteins and peptides. In some embodiments, the 2D crystalline material can be assembled by visible light and dissembled by UV light. In some embodiments, the stabilized polypeptide comprises an enzyme or protein.

[0027] In a twenty-second aspect, a molecular scaffold comprising the 2D crystalline material as described in the embodiments of the sixteenth aspect is provided. The 2D crystalline material can comprise the polypeptide building block as described in the embodiments of the fifteenth aspect. The polypeptide building block is a non-naturally occurring symmetrical polypeptide building block. The non-naturally occurring symmetrical polypeptide building block can comprise a plurality of histidine residues positioned such that coordination of some or all of said plurality of histidine residues with one or more metal ions facilitates formation of 2D crystals. In some embodiments, said polypeptide building block comprises a symmetrical polypeptide comprising surface histidine residues in the corner

positions. In some embodiments, said polypeptide has inherent C3, C4, C6, D3, D4 or D6 symmetry. In some embodiments, at least one of said histidine residues has been introduced into said polypeptide building block through genetic engineering. In some embodiments, said polypeptide is generated via solid phase synthesis. In some embodiments, said polypeptide is genetically engineered. In some embodiments, the polypeptide further comprises an additional modification. In some embodiments, said additional modification is selected from the group consisting of a chemical modification, a modification made via an enzymatic reaction, and a modification made via genetic engineering. In some embodiments, said additional modification is selected from the group consisting of functional groups, tags, other polypeptides, peptide tags, detectable labels, fluorophores, and nanoparticles. In some embodiments, said symmetrical polypeptide comprises the RhuA protein. In some embodiments, the peptide tag comprises a His tag. In some embodiments, the His tag comprises a sequence set forth in SEQ ID NO: 22. In some embodiments, the peptide tag comprises a Pd4 peptide. In some embodiments, the Pd4 peptide comprises a sequence set forth in SEQ ID NO: 23. In some embodiments, the peptide tag comprises an ACP protein. In some embodiments, the ACP protein comprises a sequence set forth in SEQ ID NO: 24. In some embodiments, the polypeptide building block can be chemically modified. In some embodiments, the polypeptide is chemically modified with inorganic nanoparticles. In some embodiments, the polypeptide building block is modified with one or more organic functional groups. In some embodiments, the polypeptide building block is modified for different modes of controllable self-assembly. In some embodiments, the organic functional group is a fluorophore, metal chelating group or a host complex. In some embodiments, the polypeptide building block can be genetically modified/fused with functional proteins and peptides. In some embodiments, said 2D crystalline material is auxetic. In some embodiments, the 2D crystalline material comprises a Poisson's ratio of at least -1. In some embodiments, the 2D crystalline material comprises a Poisson's ratio of -1. In some embodiments, the 2D crystalline material can be chemically modified. In some embodiments, the 2D crystalline material is chemically modified with inorganic nanoparticles. In some embodiments, the 2D crystalline material is modified with one or more organic functional groups. In some embodiments, the 2D crystalline material is modified for different modes of

controllable self-assembly. In some embodiments, organic functional group is a fluorophore, metal chelating group or a host complex. In some embodiments, the 2D crystalline material can be genetically modified/fused with functional proteins and peptides. In some embodiments, the 2D crystalline material can be assembled by visible light and dissembled by UV light.

[0028] In a twenty-third aspect, a protective armor comprising the 2D crystalline material as described in the embodiments of the sixteenth aspect is provided. The 2D crystalline material can comprise the polypeptide building block as described in the embodiments of the fifteenth aspect. The polypeptide building block is a non-naturally occurring symmetrical polypeptide building block. The non-naturally occurring symmetrical polypeptide building block can comprise a plurality of histidine residues positioned such that coordination of some or all of said plurality of histidine residues with one or more metal ions facilitates formation of 2D crystals. In some embodiments, said polypeptide building block comprises a symmetrical polypeptide comprising surface histidine residues in the corner positions. In some embodiments, said polypeptide has inherent C3, C4, C6, D3, D4 or D6 symmetry. In some embodiments, at least one of said histidine residues has been introduced into said polypeptide building block through genetic engineering. In some embodiments, said polypeptide is generated via solid phase synthesis. In some embodiments, said polypeptide is genetically engineered. In some embodiments, the polypeptide further comprises an additional modification. In some embodiments, said additional modification is selected from the group consisting of a chemical modification, a modification made via an enzymatic reaction, and a modification made via genetic engineering. In some embodiments, said additional modification is selected from the group consisting of functional groups, tags, other polypeptides, peptide tags, detectable labels, fluorophores, and nanoparticles. In some embodiments, said symmetrical polypeptide comprises the RhuA protein. In some embodiments, the peptide tag comprises a His tag. In some embodiments, the His tag comprises a sequence set forth in SEQ ID NO: 22. In some embodiments, the peptide tag comprises a Pd4 peptide. In some embodiments, the Pd4 peptide comprises a sequence set forth in SEQ ID NO: 23. In some embodiments, the peptide tag comprises an ACP protein. In some embodiments, the ACP protein comprises a sequence set forth in SEQ ID NO: 24. In

some embodiments, the polypeptide building block can be chemically modified. In some embodiments, the polypeptide is chemically modified with inorganic nanoparticles. In some embodiments, the polypeptide building block is modified with one or more organic functional groups. In some embodiments, the polypeptide building block is modified for different modes of controllable self-assembly. In some embodiments, the organic functional group is a fluorophore, metal chelating group or a host complex. In some embodiments, the polypeptide building block can be genetically modified/fused with functional proteins and peptides. In some embodiments, said 2D crystalline material is auxetic. In some embodiments, the 2D crystalline material comprises a Poisson's ratio of at least -1. In some embodiments, the 2D crystalline material comprises a Poisson's ratio of -1. In some embodiments, the 2D crystalline material can be chemically modified. In some embodiments, the 2D crystalline material is chemically modified with inorganic nanoparticles. In some embodiments, the 2D crystalline material is modified with one or more organic functional groups. In some embodiments, the 2D crystalline material is modified for different modes of controllable self-assembly. In some embodiments, organic functional group is a fluorophore, metal chelating group or a host complex. In some embodiments, the 2D crystalline material can be genetically modified/fused with functional proteins and peptides. In some embodiments, the 2D crystalline material can be assembled by visible light and dissembled by UV light.

[0029] In a twenty-fourth aspect, a smart textile comprising the 2D crystalline material of any one of the embodiments as described in the sixteenth aspect is provided. The 2D crystalline material can comprise the polypeptide building block as described in the embodiments of the fifteenth aspect. The polypeptide building block is a non-naturally occurring symmetrical polypeptide building block. The non-naturally occurring symmetrical polypeptide building block can comprise a plurality of histidine residues positioned such that coordination of some or all of said plurality of histidine residues with one or more metal ions facilitates formation of 2D crystals. In some embodiments, said polypeptide building block comprises a symmetrical polypeptide comprising surface histidine residues in the corner positions. In some embodiments, said polypeptide has inherent C3, C4, C6, D3, D4 or D6 symmetry. In some embodiments, at least one of said histidine residues has been introduced

into said polypeptide building block through genetic engineering. In some embodiments, said polypeptide is generated via solid phase synthesis. In some embodiments, said polypeptide is genetically engineered. In some embodiments, the polypeptide further comprises an additional modification. In some embodiments, said additional modification is selected from the group consisting of a chemical modification, a modification made via an enzymatic reaction, and a modification made via genetic engineering. In some embodiments, said additional modification is selected from the group consisting of functional groups, tags, other polypeptides, peptide tags, detectable labels, fluorophores, and nanoparticles. In some embodiments, said symmetrical polypeptide comprises the RhuA protein. In some embodiments, the peptide tag comprises a His tag. In some embodiments, the His tag comprises a sequence set forth in SEQ ID NO: 22. In some embodiments, the peptide tag comprises a Pd4 peptide. In some embodiments, the Pd4 peptide comprises a sequence set forth in SEQ ID NO: 23. In some embodiments, the peptide tag comprises an ACP protein. In some embodiments, the ACP protein comprises a sequence set forth in SEQ ID NO: 24. In some embodiments, the polypeptide building block can be chemically modified. In some embodiments, the polypeptide is chemically modified with inorganic nanoparticles. In some embodiments, the polypeptide building block is modified with one or more organic functional groups. In some embodiments, the polypeptide building block is modified for different modes of controllable self-assembly. In some embodiments, the organic functional group is a fluorophore, metal chelating group or a host complex. In some embodiments, the polypeptide building block can be genetically modified/fused with functional proteins and peptides. In some embodiments, said 2D crystalline material is auxetic. In some embodiments, the 2D crystalline material comprises a Poisson's ratio of at least -1. In some embodiments, the 2D crystalline material comprises a Poisson's ratio of -1. In some embodiments, the 2D crystalline material can be chemically modified. In some embodiments, the 2D crystalline material is chemically modified with inorganic nanoparticles. In some embodiments, the 2D crystalline material is modified with one or more organic functional groups. In some embodiments, the 2D crystalline material is modified for different modes of controllable self-assembly. In some embodiments, organic functional group is a fluorophore, metal chelating group or a host complex. In some embodiments, the 2D crystalline material

can be genetically modified/fused with functional proteins and peptides. In some embodiments, the 2D crystalline material can be assembled by visible light and dissembled by UV light.

[0030] In a twenty- fifth aspect, a piezo electronic component comprising the 2D crystalline material as described in the embodiments of the sixteenth aspect are provided. The 2D crystalline material can comprise the polypeptide building block as described in the embodiments of the fifteenth aspect. The polypeptide building block is a non-naturally occurring symmetrical polypeptide building block. The non-naturally occurring symmetrical polypeptide building block can comprise a plurality of histidine residues positioned such that coordination of some or all of said plurality of histidine residues with one or more metal ions facilitates formation of 2D crystals. In some embodiments, said polypeptide building block comprises a symmetrical polypeptide comprising surface histidine residues in the corner positions. In some embodiments, said polypeptide has inherent C3, C4, C6, D3, D4 or D6 symmetry. In some embodiments, at least one of said histidine residues has been introduced into said polypeptide building block through genetic engineering. In some embodiments, said polypeptide is generated via solid phase synthesis. In some embodiments, said polypeptide is genetically engineered. In some embodiments, the polypeptide further comprises an additional modification. In some embodiments, said additional modification is selected from the group consisting of a chemical modification, a modification made via an enzymatic reaction, and a modification made via genetic engineering. In some embodiments, said additional modification is selected from the group consisting of functional groups, tags, other polypeptides, peptide tags, detectable labels, fluorophores, and nanoparticles. In some embodiments, said symmetrical polypeptide comprises the RhuA protein. In some embodiments, the peptide tag comprises a His tag. In some embodiments, the His tag comprises a sequence set forth in SEQ ID NO: 22. In some embodiments, the peptide tag comprises a Pd4 peptide. In some embodiments, the Pd4 peptide comprises a sequence set forth in SEQ ID NO: 23. In some embodiments, the peptide tag comprises an ACP protein. In some embodiments, the ACP protein comprises a sequence set forth in SEQ ID NO: 24. In some embodiments, the polypeptide building block can be chemically modified. In some embodiments, the polypeptide is chemically modified with inorganic nanoparticles. In some

embodiments, the polypeptide building block is modified with one or more organic functional groups. In some embodiments, the polypeptide building block is modified for different modes of controllable self-assembly. In some embodiments, the organic functional group is a fluorophore, metal chelating group or a host complex. In some embodiments, the polypeptide building block can be genetically modified/fused with functional proteins and peptides. In some embodiments, said 2D crystalline material is auxetic. In some embodiments, the 2D crystalline material comprises a Poisson's ratio of at least -1. In some embodiments, the 2D crystalline material comprises a Poisson's ratio of -1. In some embodiments, the 2D crystalline material can be chemically modified. In some embodiments, the 2D crystalline material is chemically modified with inorganic nanoparticles. In some embodiments, the 2D crystalline material is modified with one or more organic functional groups. In some embodiments, the 2D crystalline material is modified for different modes of controllable self-assembly. In some embodiments, organic functional group is a fluorophore, metal chelating group or a host complex. In some embodiments, the 2D crystalline material can be genetically modified/fused with functional proteins and peptides. In some embodiments, the 2D crystalline material can be assembled by visible light and dissembled by UV light.

[0031] In a twenty-sixth aspect, an adaptive membrane or sieve comprising the 2D crystalline material as described in the embodiments of the sixteenth aspect is provided. The 2D crystalline material can comprise the polypeptide building block as described in the embodiments of the fifteenth aspect. The polypeptide building block is a non-naturally occurring symmetrical polypeptide building block. The non-naturally occurring symmetrical polypeptide building block can comprise a plurality of histidine residues positioned such that coordination of some or all of said plurality of histidine residues with one or more metal ions facilitates formation of 2D crystals. In some embodiments, said polypeptide building block comprises a symmetrical polypeptide comprising surface histidine residues in the corner positions. In some embodiments, said polypeptide has inherent C3, C4, C6, D3, D4 or D6 symmetry. In some embodiments, at least one of said histidine residues has been introduced into said polypeptide building block through genetic engineering. In some embodiments, said polypeptide is generated via solid phase synthesis. In some embodiments, said polypeptide is

genetically engineered. In some embodiments, the polypeptide further comprises an additional modification. In some embodiments, said additional modification is selected from the group consisting of a chemical modification, a modification made via an enzymatic reaction, and a modification made via genetic engineering. In some embodiments, said additional modification is selected from the group consisting of functional groups, tags, other polypeptides, peptide tags, detectable labels, fluorophores, and nanoparticles. In some embodiments, said symmetrical polypeptide comprises the RhuA protein. In some embodiments, the peptide tag comprises a His tag. In some embodiments, the His tag comprises a sequence set forth in SEQ ID NO: 22. In some embodiments, the peptide tag comprises a Pd4 peptide. In some embodiments, the Pd4 peptide comprises a sequence set forth in SEQ ID NO: 23. In some embodiments, the peptide tag comprises an ACP protein. In some embodiments, the ACP protein comprises a sequence set forth in SEQ ID NO: 24. In some embodiments, the polypeptide building block can be chemically modified. In some embodiments, the polypeptide is chemically modified with inorganic nanoparticles. In some embodiments, the polypeptide building block is modified with one or more organic functional groups. In some embodiments, the polypeptide building block is modified for different modes of controllable self-assembly. In some embodiments, the organic functional group is a fluorophore, metal chelating group or a host complex. In some embodiments, the polypeptide building block can be genetically modified/fused with functional proteins and peptides. In some embodiments, said 2D crystalline material is auxetic. In some embodiments, the 2D crystalline material comprises a Poisson's ratio of at least -1. In some embodiments, the 2D crystalline material comprises a Poisson's ratio of -1. In some embodiments, the 2D crystalline material can be chemically modified. In some embodiments, the 2D crystalline material is chemically modified with inorganic nanoparticles. In some embodiments, the 2D crystalline material is modified with one or more organic functional groups. In some embodiments, the 2D crystalline material is modified for different modes of controllable self-assembly. In some embodiments, organic functional group is a fluorophore, metal chelating group or a host complex. In some embodiments, the 2D crystalline material can be genetically modified/fused with functional proteins and peptides. In some

embodiments, the 2D crystalline material can be assembled by visible light and dissembled by UV light.

[0032] In a twenty-seventh aspect, a controlled drug release formulation comprising the 2D crystalline material as described in the embodiments of the sixteenth aspect is provided. The 2D crystalline material can comprise the polypeptide building block as described in the embodiments of the fifteenth aspect. The polypeptide building block is a non-naturally occurring symmetrical polypeptide building block. The non-naturally occurring symmetrical polypeptide building block can comprise a plurality of histidine residues positioned such that coordination of some or all of said plurality of histidine residues with one or more metal ions facilitates formation of 2D crystals. In some embodiments, said polypeptide building block comprises a symmetrical polypeptide comprising surface histidine residues in the corner positions. In some embodiments, said polypeptide has inherent C3, C4, C6, D3, D4 or D6 symmetry. In some embodiments, at least one of said histidine residues has been introduced into said polypeptide building block through genetic engineering. In some embodiments, said polypeptide is generated via solid phase synthesis. In some embodiments, said polypeptide is genetically engineered. In some embodiments, the polypeptide further comprises an additional modification. In some embodiments, said additional modification is selected from the group consisting of a chemical modification, a modification made via an enzymatic reaction, and a modification made via genetic engineering. In some embodiments, said additional modification is selected from the group consisting of functional groups, tags, other polypeptides, peptide tags, detectable labels, fluorophores, and nanoparticles. In some embodiments, said symmetrical polypeptide comprises the RhuA protein. In some embodiments, the peptide tag comprises a His tag. In some embodiments, the His tag comprises a sequence set forth in SEQ ID NO: 22. In some embodiments, the peptide tag comprises a Pd4 peptide. In some embodiments, the Pd4 peptide comprises a sequence set forth in SEQ ID NO: 23. In some embodiments, the peptide tag comprises an ACP protein. In some embodiments, the ACP protein comprises a sequence set forth in SEQ ID NO: 24. In some embodiments, the polypeptide building block can be chemically modified. In some embodiments, the polypeptide is chemically modified with inorganic nanoparticles. In some embodiments, the polypeptide building block is modified with one or more organic

functional groups. In some embodiments, the polypeptide building block is modified for different modes of controllable self-assembly. In some embodiments, the organic functional group is a fluorophore, metal chelating group or a host complex. In some embodiments, the polypeptide building block can be genetically modified/fused with functional proteins and peptides. In some embodiments, said 2D crystalline material is auxetic. In some embodiments, the 2D crystalline material comprises a Poisson's ratio of at least -1. In some embodiments, the 2D crystalline material comprises a Poisson's ratio of -1. In some embodiments, the 2D crystalline material can be chemically modified. In some embodiments, the 2D crystalline material is chemically modified with inorganic nanoparticles. In some embodiments, the 2D crystalline material is modified with one or more organic functional groups. In some embodiments, the 2D crystalline material is modified for different modes of controllable self-assembly. In some embodiments, organic functional group is a fluorophore, metal chelating group or a host complex. In some embodiments, the 2D crystalline material can be genetically modified/fused with functional proteins and peptides. In some embodiments, the 2D crystalline material can be assembled by visible light and dissembled by UV light.

[0033] In a twenty-eighth aspect, a run-flat tire comprising the 2D crystalline material of any as described in the embodiments of the sixteenth aspect is provided. The 2D crystalline material can comprise the polypeptide building block as described in the embodiments of the fifteenth aspect. The polypeptide building block is a non-naturally occurring symmetrical polypeptide building block. The non-naturally occurring symmetrical polypeptide building block can comprise a plurality of histidine residues positioned such that coordination of some or all of said plurality of histidine residues with one or more metal ions facilitates formation of 2D crystals. In some embodiments, said polypeptide building block comprises a symmetrical polypeptide comprising surface histidine residues in the corner positions. In some embodiments, said polypeptide has inherent C3, C4, C6, D3, D4 or D6 symmetry. In some embodiments, at least one of said histidine residues has been introduced into said polypeptide building block through genetic engineering. In some embodiments, said polypeptide is generated via solid phase synthesis. In some embodiments, said polypeptide is genetically engineered. In some embodiments, the polypeptide further comprises an

additional modification. In some embodiments, said additional modification is selected from the group consisting of a chemical modification, a modification made via an enzymatic reaction, and a modification made via genetic engineering. In some embodiments, said additional modification is selected from the group consisting of functional groups, tags, other polypeptides, peptide tags, detectable labels, fluorophores, and nanoparticles. In some embodiments, said symmetrical polypeptide comprises the RhuA protein. In some embodiments, the peptide tag comprises a His tag. In some embodiments, the His tag comprises a sequence set forth in SEQ ID NO: 22. In some embodiments, the peptide tag comprises a Pd4 peptide. In some embodiments, the Pd4 peptide comprises a sequence set forth in SEQ ID NO: 23. In some embodiments, the peptide tag comprises an ACP protein. In some embodiments, the ACP protein comprises a sequence set forth in SEQ ID NO: 24. In some embodiments, the polypeptide building block can be chemically modified. In some embodiments, the polypeptide is chemically modified with inorganic nanoparticles. In some embodiments, the polypeptide building block is modified with one or more organic functional groups. In some embodiments, the polypeptide building block is modified for different modes of controllable self-assembly. In some embodiments, the organic functional group is a fluorophore, metal chelating group or a host complex. In some embodiments, the polypeptide building block can be genetically modified/fused with functional proteins and peptides. In some embodiments, said 2D crystalline material is auxetic. In some embodiments, the 2D crystalline material comprises a Poisson's ratio of at least -1. In some embodiments, the 2D crystalline material comprises a Poisson's ratio of -1. In some embodiments, the 2D crystalline material can be chemically modified. In some embodiments, the 2D crystalline material is chemically modified with inorganic nanoparticles. In some embodiments, the 2D crystalline material is modified with one or more organic functional groups. In some embodiments, the 2D crystalline material is modified for different modes of controllable self-assembly. In some embodiments, organic functional group is a fluorophore, metal chelating group or a host complex. In some embodiments, the 2D crystalline material can be genetically modified/fused with functional proteins and peptides. In some embodiments, the 2D crystalline material can be assembled by visible light and dissembled by UV light.

[0034] In a twenty-ninth aspect, a method of making a crystalline material is provided. The method can comprise placing a plurality of the polypeptide building blocks as described in the embodiments of the fifteenth aspect under conditions in which said histidine residues form metal coordinates and allowing said plurality of polypeptide building blocks to self-assemble into said crystalline material. The non-naturally occurring symmetrical polypeptide building block can comprise a plurality of histidine residues positioned such that coordination of some or all of said plurality of histidine residues with one or more metal ions facilitates formation of 2D crystals. In some embodiments, said polypeptide building block comprises a symmetrical polypeptide comprising surface histidine residues in the corner positions. In some embodiments, said polypeptide has inherent C3, C4, C6, D3, D4 or D6 symmetry. In some embodiments, at least one of said histidine residues has been introduced into said polypeptide building block through genetic engineering. In some embodiments, said polypeptide is generated via solid phase synthesis. In some embodiments, said polypeptide is genetically engineered. In some embodiments, the polypeptide further comprises an additional modification. In some embodiments, said additional modification is selected from the group consisting of a chemical modification, a modification made via an enzymatic reaction, and a modification made via genetic engineering. In some embodiments, said additional modification is selected from the group consisting of functional groups, tags, other polypeptides, peptide tags, detectable labels, fluorophores, and nanoparticles. In some embodiments, said symmetrical polypeptide comprises the RhuA protein. In some embodiments, the peptide tag comprises a His tag. In some embodiments, the His tag comprises a sequence set forth in SEQ ID NO: 22. In some embodiments, the peptide tag comprises a Pd4 peptide. In some embodiments, the Pd4 peptide comprises a sequence set forth in SEQ ID NO: 23. In some embodiments, the peptide tag comprises an ACP protein. In some embodiments, the ACP protein comprises a sequence set forth in SEQ ID NO: 24. In some embodiments, the polypeptide building block can be chemically modified. In some embodiments, the polypeptide is chemically modified with inorganic nanoparticles. In some embodiments, the polypeptide building block is modified with one or more organic functional groups. In some embodiments, the polypeptide building block is modified for different modes of controllable self-assembly. In some embodiments, the organic functional

group is a fluorophore, metal chelating group or a host complex. In some embodiments, the polypeptide building block can be genetically modified/fused with functional proteins and peptides. In some embodiments, the 2D crystalline material can be assembled by visible light and dissembled by UV light. In some embodiments, said conditions in which said histidine residues form metal coordinates are controllable. In some embodiments, said metal coordinates comprise a metal selected from the group consisting of Zn2+ and Cu2+.

[0035] In a thirtieth aspect, a polypeptide comprising an amino acid sequence selected from the group consisting of SEQ ID NO: 3, SEQ ID NO: 4 and SEQ ID NO: 5 is provided. In some embodiments, the polypeptide further comprises an additional modification. In some embodiments, said additional modification is selected from the group consisting of a chemical modification, a modification made via an enzymatic reaction, and a modification made via genetic engineering. In some embodiments, said additional modification is selected from the group consisting of functional groups, tags, other polypeptides, peptide tags, detectable labels, fluorophores, and nanoparticles. In some embodiments, the peptide tag comprises a His tag. In some embodiments, the His tag comprises a sequence set forth in SEQ ID NO: 22. In some embodiments, the peptide tag comprises a Pd4 peptide. In some embodiments, the Pd4 peptide comprises a sequence set forth in SEQ ID NO: 23. In some embodiments, the peptide tag comprises an ACP protein. In some embodiments, the ACP protein comprises a sequence set forth in SEQ ID NO: 24. In some embodiments, the polypeptide building block can be chemically modified. In some embodiments, the polypeptide is chemically modified with inorganic nanoparticles. In some embodiments, the polypeptide building block is modified with one or more organic functional groups. In some embodiments, the polypeptide building block is modified for different modes of controllable self-assembly. In some embodiments, the organic functional group is a fluorophore, metal chelating group or a host complex. In some embodiments, the polypeptide building block can be genetically modified/fused with functional proteins and peptides.

[0036] In a thirty first aspect, a 2D crystalline material comprising the polypeptide of the embodiments described in the thirtieth aspect is provided. The polypeptide can comprise an amino acid sequence selected from the group consisting of SEQ ID NO: 3, SEQ

ID NO: 4 and SEQ ID NO: 5. a polypeptide comprising an amino acid sequence selected from the group consisting of SEQ ID NO: 3, SEQ ID NO: 4 and SEQ ID NO: 5 are provided. In some embodiments, the polypeptide further comprises an additional modification. In some embodiments, said additional modification is selected from the group consisting of a chemical modification, a modification made via an enzymatic reaction, and a modification made via genetic engineering. In some embodiments, said additional modification is selected from the group consisting of functional groups, tags, other polypeptides, peptide tags, detectable labels, fluorophores, and nanoparticles. In some embodiments, the peptide tag comprises a His tag. In some embodiments, the His tag comprises a sequence set forth in SEQ ID NO: 22. In some embodiments, the peptide tag comprises a Pd4 peptide. In some embodiments, the Pd4 peptide comprises a sequence set forth in SEQ ID NO: 23. In some embodiments, the peptide tag comprises an ACP protein. In some embodiments, the ACP protein comprises a sequence set forth in SEQ ID NO: 24. In some embodiments, the polypeptide building block can be chemically modified. In some embodiments, the polypeptide is chemically modified with inorganic nanoparticles. In some embodiments, the polypeptide building block is modified with one or more organic functional groups. In some embodiments, the polypeptide building block is modified for different modes of controllable self-assembly. In some embodiments, the organic functional group is a fluorophore, metal chelating group or a host complex. In some embodiments, the polypeptide building block can be genetically modified/fused with functional proteins and peptides. In some embodiments, said 2D crystalline material is auxetic. In some embodiments, the 2D crystalline material comprises a Poisson's ratio of at least -1. In some embodiments, the 2D crystalline material comprises a Poisson's ratio of -1. In some embodiments, the 2D crystalline material can be chemically modified. In some embodiments, the 2D crystalline material is chemically modified with inorganic nanoparticles. In some embodiments, the 2D crystalline material is modified with one or more organic functional groups. In some embodiments, the 2D crystalline material is modified for different modes of controllable self-assembly. In some embodiments, the organic functional group is a fluorophore, metal chelating group or a host complex. In some embodiments, the 2D crystalline material can be genetically modified/fused with functional proteins and peptides.

[0037] In a thirty-second aspect, a polypeptide comprising the amino acid sequence of SEQ ID NO: 2, 19, 20, 21 or 24 is provided. In some embodiments, the further comprises an additional modification. In some embodiments, said additional modification is selected from the group consisting of a chemical modification, a modification made via an enzymatic reaction, and a modification made via genetic engineering. In some embodiments, said additional modification is selected from the group consisting of functional groups, tags, other polypeptides, peptide tags, detectable labels, fluorophores, and nanoparticles. In some embodiments, the peptide tag comprises a His tag. In some embodiments, the His tag comprises a sequence set forth in SEQ ID NO: 22. In some embodiments, the peptide tag comprises a Pd4 peptide. In some embodiments, the Pd4 peptide comprises a sequence set forth in SEQ ID NO: 23. In some embodiments, the peptide tag comprises an ACP protein. In some embodiments, the ACP protein comprises a sequence set forth in SEQ ID NO: 24. In some embodiments, the polypeptide can be chemically modified. In some embodiments, the polypeptide is chemically modified with inorganic nanoparticles. In some embodiments, the polypeptide is modified with one or more organic functional groups. In some embodiments, the polypeptide is modified for different modes of controllable self-assembly. In some embodiments, the organic functional group is a fluorophore, metal chelating group or a host complex. In some embodiments, the polypeptide can be genetically modified/fused with functional proteins and peptides.

[0038] In a thirty-third aspect, 2D crystalline material comprising the polypeptide as described in the embodiments of the thirty-second aspect is provided. The polypeptide can comprise the amino acid sequence of SEQ ID NO: 2, 19, 20, 21 or 24. In some embodiments, the further comprises an additional modification. In some embodiments, said additional modification is selected from the group consisting of a chemical modification, a modification made via an enzymatic reaction, and a modification made via genetic engineering. In some embodiments, said additional modification is selected from the group consisting of functional groups, tags, other polypeptides, peptide tags, detectable labels, fluorophores, and nanoparticles. In some embodiments, the peptide tag comprises a His tag. In some embodiments, the His tag comprises a sequence set forth in SEQ ID NO: 22. In some embodiments, the peptide tag comprises a Pd4 peptide. In some embodiments, the Pd4

peptide comprises a sequence set forth in SEQ ID NO: 23. In some embodiments, the peptide tag comprises an ACP protein. In some embodiments, the ACP protein comprises a sequence set forth in SEQ ID NO: 24. In some embodiments, the polypeptide can be chemically modified. In some embodiments, the polypeptide is chemically modified with inorganic nanoparticles. In some embodiments, the polypeptide is modified with one or more organic functional groups. In some embodiments, the polypeptide is modified for different modes of controllable self-assembly. In some embodiments, the organic functional group is a fluorophore, metal chelating group or a host complex. In some embodiments, the polypeptide can be genetically modified/fused with functional proteins and peptides. In some embodiments, said 2D crystalline material is auxetic. In some embodiments, the 2D crystalline material comprises a Poisson's ratio of at least -1. In some embodiments, the 2D crystalline material comprises a Poisson's ratio of -1. In some embodiments, the 2D crystalline material can be chemically modified. In some embodiments, the 2D crystalline material is chemically modified with inorganic nanoparticles. In some embodiments, the 2D crystalline material is modified with one or more organic functional groups. In some embodiments, the 2D crystalline material is modified for different modes of controllable self-assembly. In some embodiments, organic functional group is a fluorophore, metal chelating group or a host complex. In some embodiments, the 2D crystalline material can be genetically modified/fused with functional proteins and peptides. In some embodiments, the 2D crystalline material can be assembled by visible light and dissembled by UV light.

BRIEF DESCRIPTION OF THE DRAWINGS

[0039] **Figure 1** shows that a majority of biological machines and materials are self assembled and have dynamic/responsive multiprotein architecture.

[0040] **Figure 2** shows hierarchically assembled protein materials.

[0041] **Figure 3** shows proteins as building blocks for functional nanomaterials.

[0042] **Figure 4** shows the advantages of fabricating 20 supramolecular protein assemblies.

[0043] **Figure 5** shows the existing approaches for designed protein assembly.

[0044] **Figure 6** shows the existing approaches for designed protein assembly, in particular

[0045] covalent fusion of homooligomeric proteins or self-assembling protein monomers.

[0046] **Figure 7** shows an outline of preparing disulfide-mediated assembly of 2D protein materials and the advantages.

[0047] **Figure 8** shows the proof of principle of preparing the assembly of 2D protein materials.

[0048] **Figure 9** shows disulfide-linker 20 C98-RhuA crystals.

Figure 10 shows RhuA constructs and their disulfide- and metal-mediated self-assembly modes. **10A)** schematic representations of the C98RhuA, H63/H98RhuA and F88/C98RhuA structures. The top and bottom halves of RhuA have different relative molecular orientations as shown in 10A, in which a horizontal line splits the molecule in to the top portion and bottom portion. As shown for the F88/C98 RhuA protein, the top portion and bottom portion are equivalent to one another and the two portions in the middle are equivalent to one anoter. **Figure 10B**. Cys and His residues inserted into positions 98 and 63 are shown by the numbering on the figure (98 and 63). As shown in **Figure 10B** are expected 2D molecular arrangements of ^{C98}RhuA, $^{H63/H98}$RhuA and $^{F88/C98}$RhuA lattices. In the top row showing the oxidation-reduction reaction, the corners are bound by disulfide bonds (curvy lines in between the square structures). The structure can be the lattice on the left or the lattice structure on the right which is to assume a checkered pattern in which the middle square structure in the top row is equivalent to the first and third square structure in the second row and the middle structure in the third row. As shown for the $^{H63/H98}$RhuA, the Self-assembly was initiated by addition of 4–40 molar equivalents of Zn2+ and Cu2+ (1–10 equiv. per bis-His motif), both of which can accommodate the desired four-coordinate geometries to link H63/H98RhuA building blocks at their corners. It is envisioned that the *C*4-symmetric C98RhuA and H63/H98RhuA variants could yield square lattices with two distinct patterns in terms of the orientation of the building blocks with respect to the 2D plane. For the $^{H63/H98}$RhuA lattice, the structure can be the lattice on the left or the lattice structure on the right which is to assume a checkered pattern in which the middle square structure in the top

row is equivalent to the first and third square structure in the second row and the middle structure in the third row. In the bottom row showing the reaction with the F88/C98RhuA, the square structure as shown has angled lines representing the cysteines. Figure 10C shows 25 μM C98RhuA was incubated at 4 °C under air exposure for 1 day; the solution contained 20 mM Tris (pH 8) and no reductants or oxidants. **10D**, 25 μM H63/H98RhuA was incubated in the presence of 1 mM ZnCl2 at 4 °C for 1 day; the solution contained 20 mM MOPS (pH 7).

Figure 11 shows ns-TEM characterization of the 2D crystals of ^{C98}RhuA (**11A**), $^{H63/H98}$RhuA (Zn^{2+} coordination) (**11B**) and $^{F88/C98}$RhuA (**11C**). (i) Low-magnification views, (ii) high-magnification views, (iii) Fourier transforms of ii, (iv) reconstructed 2D images, (v) structural models based on the 2D reconstructions. The high resolution limits in panels iii are ~14 Å. For a comparison of experimental and computed 2D reconstructions, see **Figure 20.** Unit cells are shown as black squares (with corners placed at two-fold symmetry axes); unit cell constants (α=β, γ) are: ^{C98}RhuA (114 Å, 90°); $^{H63/H98}$RhuA (91 Å, 90°); $^{F88/C98}$RhuA (115 Å, 90°). TEM characterization of optimized 2D C98RhuA crystals**: 11D**: 125 μM C98RhuA was incubated in the presence of 10 mM βME at 4 °C in a standing solution for 3 days. **11E:** 125 μM C98RhuA was incubated in the presence of 10 mM βME at 4 °C with gentle shaking for 3 days, followed by 2 days at rest, during which a dense precipitate of crystals formed.

Figure 12 shows: (**12A**) Reconstructed 2D images of seven distinct conformational states (I–VII) of 2D C98RhuA crystals. **12B**, High-magnification views and derived structural models of conformations II, V and VII. Unit cells and hinge angles (α) between C98RhuA units are highlighted by the black square and the hinge angle shown, respectively. The four corners of the square in the figure (bottom panel) represent the top half of the structure shown in 10A (structure on the left), while the structure in the middle of the square in the second row of **12B** is in a checkboard confirmation with the structures in the corner and is also represented by the bottom half of the structure shown in **Figure 10A** (left structure). **12C**, Population distributions of C98RhuA crystals in different conformational states during repeated resuspension/sedimentation cycles. *n* refers to the total number of individual lattices analyzed in each panel. **12D**, Schematic representation of the rotating, rigid-square model that describes the 2D C98RhuA lattice dynamics (as in **Figure 10**; the building blocks are

numbered for clarity) As shown, numbers 9, 11, 23, 1, 13, 7, 3, 21, 5, 15, 19 and 17 are equivalent to one another. Numbers 24, 10, 12, 8, 2, 22, 0, 14, 6, 4, 20, 18 and 16 are equivalent to one another. Thus there is a check patterning. Δx and Δy denote changes in the transverse- and longitudinal-dimension lengths upon lattice opening and closing. **12E**, Digital image-correlation analysis of reconstructed TEM images of C98RhuA crystals for determining auxetic behavior. Representative volume elements (RVEs) in the lattices of the two extreme states (I and VII) are indicated with squares, with the vertices of the RVEs numbered 1–4 , and the vectors ***M***, ***N*** (in state I) and ***m***, ***n*** (in state VII) used to calculate local engineering strains are shown with the arrows. The edges of the lattice pores, used for determining the positions of the RVE vertices, are shown as lines that are tracing around the edges of the lattice pores in state I and VII. **12F**, Calculated Poisson's ratios (v) of lattice conformational states with respect to state I. The error bars correspond to the uncertainties in pixel selection during digital image processing (see Methods for details). Additional structural characterization of 2D C98RhuA crystals is shown in **12G-12I. 12G**, AFM; **12H**, SEM; **12I**, Cryo-TEM. The middle column in **12G** shows the profiles along the arrows in the left column.

[0049] **Figure 13** shows the SDS-PAGE characterization of RhuA mutants.

[0050] **Figure 14** shows the positive ESI-MS characterization of RhuA mutants. Top spectrum displays the raw data showing the cluster ions. The bottom spectrum is the deconvoluted spectrum after software transformation.

[0051] **Figure 15** shows ns-TEM images of 2D ^{C98}RhuA crystals. 125 μM ^{C98}RhuA was incubated in the presence of 10 mM βME at 4 °C in a standing solution for 3 days.

[0052] **Figure 16** shows ns-TEM images of 2D ^{C98}RhuA crystals. 125 μM ^{C98}RhuA was incubated in the presence of 10 mM βME at 4 °C with gentle shaking for 3 days, followed by 2 days at rest, during which a dense precipitate of crystals formed.

[0053] **Figure 17** shows ns-TEM images of 2D $^{H63/H98}$RhuA crystals. 25 μM ^{H63H98}RhuA was incubated with 200 μM $ZnCl_2$ (**17A**) or $CuCl_2$ (**17B**) in a 20 mM MOPS buffer solution (pH 7.0) at 4 °C for 1 day.

[0054] **Figure 18** shows: (**18A**) ns-TEM images for $^{F88/C98}$RhuA 2D crystals. 125 μM $^{F88/C98}$RhuA was incubated in the presence of 10 mM βME at 4 °C with gentle shaking for 2 days. (**18B**) Cartoon representations of various types of defects observed in $^{F88/C98}$RhuA crystals, corresponding to boxed areas (I – IV) in Figure 18A.

[0055] **Figure 19** shows the reversibility of oxidative or metal-mediated self-assembly of RhuA variants. **19A and 19B**: C98RhuA (**19a**) and F88/C98RhuA (**19B**) crystals. Left panels, the crystals were incubated in the presence of 20 mM or 30 mM βME (as indicated) and imaged by TEM at the indicated times after addition of βME. Right panels, 125 μM C98RhuA (**19A**) or F88/C98RhuA (**19B**) were incubated under oxidative self-assembly conditions (in the presence of 10 mM βME at 4 °C with gentle shaking) and self-assembly was monitored by DLS at t = 0 (top), t = 3 days (center) and upon addition of 100 mM βME after self-assembly (bottom). Dh refers to the hydrodynamic diameter. **19C,** Left panel, H63/H98RhuA crystals were incubated in the presence of 10 mM EDTA and imaged by TEM at 2 h after addition of EDTA. Right panels, 25 μM H63/H98RhuA was incubated under metal mediated self-assembly conditions (in the presence of 200 μM ZnCl2 at 4 °C) and self-assembly was monitored by DLS at t = 0 (top), t = 3 days (center) and upon addition of 10 mM EDTA (bottom). Scale bars are 5 μm in all panels.

[0056] **Figure 20** shows the 2D TEM reconstruction and structural modelling of the 2D lattices of RhuA variants. Comparison of the observed (experimental) and simulated projection maps of the 2D lattices of RhuA variants.

[0057] **Figure 21** shows molecular arrangements in ^{C98}RhuA, $^{H63/H98}$RhuA and $^{F88/C98}$RhuA lattices viewed from different angles. As shown for C98-RhuA, the first and second panel corresponds to the panels on the left column of Figure 10. The top and bottom of the protein structure shown in figure 10 that is separated by the dashed line is shown in the lattice structure of in the panels of the first row. In the first panel of the first row, the structures are arranged side by side but in contrasting orientations. In a repeated unit, the protein structure is arranged in a checkered pattern such that for each row, the protein are side by side, but alternating units are flipped such that in every other unit, the bottom portion of the protein as shown in Figure 10 is right side up. In the first and second row, the proteins that make up the lattice structure are all in the same orientation in which the tops of the

proteins as shown in **Figure 10** are right side up. However in the third row, the protein unist of F88/C98 RhuA, are stacked as shown in **Figure 10,** and these stacked units make up the lattices as shown in the third row.

[0059] **Figure 22** shows representative images of 2D C98RhuA crystals containing no defects. Representative images 2D ^{C98}RhuA crystals contain no defects (**Figure 22A**) or one lattice vacancy (**Figure 22B**). The stain artifacts images are shown to highlighted areas that may appear to contain lattice vacancies in low-magnification images but in actuality do not.

[0060] **Figure 23** shows conformational analysis of C98RhuA lattices. **23A**, Photographs of sedimented and resuspended C98RhuA crystals (alternative views with different backgrounds are shown for clarity). **23B**, Representative TEM images for different conformational states (I–VII) of the C98RhuA crystals shown in Figure 12. Scale bars are 25 nm in all panels. **23C**, Digital image processing of reconstructed images of each conformational state. Lines represent the border of the pores in the lattice structure which outline the pores, in which the pores represent the black circular or oval structures. Selected RVEs are shown with drawn in squares which enclose points 1, 2, 3 and 4, with the vertices of the RVEs numbered 1–4. Lines that show the circles are circumscribed to the square RhuA building block. Values of the scaling between these and the TEM images (with conformational state I as a reference) are shown below each image. **23D**, Changes in the dimensions of a C98RhuA lattice of arbitrary size assuming a rotating-rigid-squares model.

[0061] **Figure 24** shows Rhu-C98 sheet on Grid followed by the addition of Maleimido-Au for two hours.

[0062] **Figure 25** shows another example of Rhu-C98 Rhu-C98 sheet on Grid followed by the addition of Maleimido-Au for two hours.

[0063] **Figure 26** shows Rhu-C98 sheet on Grid followed by the addition of Maleimido-Au for overnight experiment.

[0064] **Figure 27** shows Rhu-C98 sheet on Grid followed by the addition of Maleimido-Au for three hours.

[0065] **Figure 28** shows Rhu-C98 sheet stock sample with $HauCl_4$.

[0066] **Figure 29** shows Rhu-C98 (4μL) added into 0.5 mM $HauCl_4$ in 5mM NaPi pH 7.2 for 6 days then an addition of 5mM βME for one day.

[0067] **Figure 30** shows Rhu-C98 (4μL) added into 100 μL of Au(I) ($HauCl_4$ plus 2eq thiodiethanol) in 5mM NaPi pH 7.2 for 4 days.

[0068] **Figure 31** shows Rhu-C98 on Grids followed by the addition of $HauCl_4/K_2CO_3/NaBH_4$ for one hour then in 10% formaldehyde for 2 hours.

[0069] **Figure 32** shows Rhu-C98 sheet/ $HauCl_4$ on grids followed by $HauCl_4/K_2CO_3/NaBH_4$ in NaPi pH 7.2 for two hours.

[0070] **Figure 33** shows Rhu-C98 sheet/ $HauCl_4$ on grids followed by $HauCl_4/K_2CO_3$/formaldehyde in NaPi pH 7.2 for two hours.

[0071] **Figure 34** shows Rhu-C98 sheet with addition of 200μM Iodo-Fl.

[0072] **Figure 35** shows another example of Rhu-C98 sheet with addition of 200μM Iodo-Fl.

[0073] **Figure 36** shows synthesis of Rhu-Cys-iPhen.

[0074] **Figure 37** shows Rhu-Cys-iPhen (100μM) with 2eq $NiCl_2$ in 20mM Mes at pH 5.5 after day 1.

[0075] **Figure 38** shows Rhu-Cys-iPhen (100μM) with 2eq $CuCl_2$ in 20mM Mes at pH 5.5 after day 1 and Rhu-Cys-iPhen (100μM) with 2eq $ZnCl_2$ in 20mM Mes at pH 5.5 after day 1.

[0076] **Figure 39** shows CD-iPhen with 2eq Ni in at pH 5.5 after day 2.

[0077] **Figure 40** shows Rhu-Cys-iPhen (100μM) with 2eq $NiCl_2$ in 20mM Mes at pH 5.5 after day 12 and with the addition of 4 eq imidazole.

[0078] **Figure 41** shows Rhu-Cys-iPhen (100μM) with 2eq $NiCl_2$ in 20mM Mes at pH 5.5 after day 12 and with the addition of 2 eq zinc.

[0079] **Figure 42** shows photoswitchable protein assembly by Azo-CD.

[0080] **Figure 43** shows protein assembly by small molecules.

[0081] **Figure 44** shows protein assembly by small molecules, 1mM Curcumin after one hour.

[0082] **Figure 45** shows protein assembly by small molecules, 5mM Curcumin after one hour.

[0083] **Figure 46** shows protein assembly by small molecules, with Biz-azobenzene and then using Curcumin as a binding partner.

[0084] **Figure 47** shows protein assembly by small molecules, 100μM Curcumin after one hour.

[0085] **Figure 48** shows another example of protein assembly by small molecules, 1mM Curcumin after one hour.

[0086] **Figure 49** shows another example of protein assembly by small molecules, 1mM Curcumin after three days.

[0087] **Figure 50** shows another example of protein assembly by small molecules, 1mM Curcumin after one hour. The results are repeatable.

[0088] **Figure 51** shows another example of protein assembly by small molecules, 5mM Curcumin after one hour.

[0089] **Figure 52** shows another example of protein assembly by small molecules, 5mM Curcumin after three days.

[0090] **Figure 53** shows another example of protein assembly by small molecules, 5mM Curcumin after one hour.

[0091] **Figure 54** shows crystals of C98C18 RhuA and 198C22 RhuA mutants.

[0092] **Figure 55** shows crystals of C98-His tagged RhuA mutant (100μM) in 20mM MOPS at pH 7 in reduced conditions after 5 days.

[0093] **Figure 56** shows crystals of C98-His tagged RhuA mutant (100μM) in 20mM MOPS at pH 7 in redoxed conditions after 1 day.

[0094] **Figure 57** shows assembly of C98- RhuA-Pd4 mutant (125μM) under various conditions after 1 day with shaking conditions (20mM Mes pH 5.5 10mM βME, no ZnCl2; and 10mM Tris pH 7.5, 10mM βME, no ZnCl2).

[0095] **Figure 58** shows assembly of C98- RhuA-Pd4 mutant (125μM) under various conditions after 1 day with shaking conditions (20mM Tris pH 7.5 10mM βME, 1mM ZnCl2; 10mM Tris pH 7.5, 5mM βME, no ZnCl2; and 10mM Tris pH 7.5, 10mM βME, no ZnCl2).

[0096] **Figure 59** shows fusion protein 2D assemblies: RhuA-ACP

[0097] **Figure 60** shows the characterization of the self-assembly of D98RhuA, C133RhuA and C266RhuA variants by TEM and DLS. **60A**, TEM (right panels) and DLS (left panels) characterization of D98RhuA self-assembly under oxidative or metal-mediated self-assembly conditions that were optimized for C98RhuA; Figures **11D and 11E** and **Figure 17** for details. **60B**: Possible mode of disulfide-mediated self-assembly of C133RhuA (top panels) and TEM characterization of the self-assembly products obtained under conditions that were optimized for C98RhuA (bottom panels). **60C**, Possible mode of disulfide-mediated self-assembly of C266RhuA (top panels) and TEM characterization of the self-assembly products obtained under conditions that were optimized for C98RhuA (bottom panels). No crystalline assemblies were detected under these conditions for any of these three variants (or other conditions that were used for screening C98RhuA self-assembly). In the top panels of **60B** and **60C** as in **Figure 10**.

[0098] **Figure 61** shows the crystallographic analysis of the 2D lattices of RhuA variants. **61A**, (i) Representative Fourier transforms calculated from the full field of view of crystal images, displayed up to 10 Å. Reciprocal lattice axes are indicated with H and K. The reflections are consistent with the plane group symmetries estimated from the analysis of the phase residuals (**Table 8**). (ii) Integer quality (IQ) plots calculated from the spectra in column (i). The size of the boxes around the reflections reflects their IQ value, defined as the ratio of the reflectionpeak amplitude and the amplitude of the background signal around each peak[42]. The most significant reflections are labelled with their IQ values, 1–4. Rings are displayed at resolutions of 30 Å, 15 Å and 10 Å. (iii) Overlap of fast Fourier transform and IQ plots. **61B**, Crystallographic data for the 2D lattices of RhuA variants. Reported are the numbers of TEM images used for the analysis of plane group symmetry. The numbers in parentheses are the number of images used for determining the statistics for the unit-cell dimensions of each lattice. The plane group symmetry was determined by consensus from all the available images. **61C**, Electron diffraction patterns of C98RhuA and H63/H98RhuA lattices.

[0099] **Figure 62 (62A, 62B, 62C, 62D, 62E)** shows the thermal and organic-solvent stability of ^{C98}RhuA crystals. **Figures 62A-E**, ^{C98}RhuA crystals were incubated at 50 °C, 75 °C, 50% DMF/H_2O and 100% DMF for indicated periods and characterized by TEM. The lattices were found to be stable at 50 °C for prolonged periods and retained their

crystallinity, whereas at 75 °C, both the lattice morphology and the crystallinity were lost due likely to the denaturation of ^{C98}RhuA building blocks. Likewise, in 50 50% DMF/H_2O solutions, the lattices were indefinitely stable and crystalline, but appear to gradually lose both properties in 100% DMF. Interestingly, the lattice morphologies were retained, suggesting that the ^{C98}RhuA building blocks likely denatured but still remained tightly associated with one another within the framework. **62E**, The crystallinity of the samples in 100% DMF could not be recovered upon exchange into aqueous buffer, indicating that protein denaturation is irreversible.

[0100] **Figure 63** shows the Metal directed self-assembly of $^{iPhen\text{-}C98}$RhuA (and $^{iPhen\text{-}C133}$RhuA) 2 eq of $ZnCl_2$, $CuCl_2$, or $NiSO_4$ was mixed with 100 μM ^{iPhenC98}RhuA at pH 5.5 in 20 mM MES for 1 day (or as indicated) to assemble 2D crystals. Sample was deposited onto negatively glow-discharged carbon-coated Cu grids, washed with Milli-Q water at 4 °C, and stained with 1% uranyl acetate at 4 °C. ^{C133}RhuA (control) was also tested in this experiment. Even though ^{C133}RhuA could not form ordered array via disulfide bonds, $^{iPhen\text{-}C133}$RhuA (modification of cysteines) was able to form crystals via metal directed assembly due to additional space between protein-protein interactions.

[0101] **Figure 64** shows additional Cys residues onto ^{C98}RhuA: ^{C18C98}RhuA and ^{C22C98}RhuA Several solution conditions were screened for optimizing the formation of 2D protein crystals of fusion proteins and best condition so far was indicated in the figure.

Definitions

[0102] Unless defined otherwise, all technical and scientific terms used herein have the same meaning as commonly understood by one of ordinary skill in the art to which the invention pertains.

[0103] "About" as used herein when referring to a measurable value is meant to encompass variations of ±20% or ±10%, more preferably ±5%, even more preferably ±l%, and still more preferably ±0.1 % from the specified value.

[0104] As described herein, a linear chain of amino acid residues is called a "polypeptide." A protein contains at least one long polypeptide. Short polypeptides, can have less than 20-30 residues, although they can be considered to be proteins, they are commonly called peptides, or sometimes oligopeptides. The individual amino acid residues are bonded together by peptide bonds and adjacent amino acid residues. The sequence of amino acid

residues in a protein is defined by the sequence of a gene, which is encoded in the genetic code. In general, the genetic code specifies 20 standard amino acids, such as alanine, arginine, asparagine, aspartic acid, cysteine, glutamic acid, glutamine, glycine, histidine, isoleucine, leucine, lysine, methionine, phenylalanine, proline, serine, threonine, tryptophan, tyrosine and valine. Shortly after or even during synthesis, the residues in a protein can also be chemically modified by posttranslational modification, which can alter the physical and chemical properties, folding, stability, activity, and ultimately, the function of the proteins. Sometimes proteins have non-peptide groups attached, which can be called prosthetic groups or cofactors. Proteins can also work together to achieve a particular function, and they can often associate to form stable protein complexes.

[0105] "Proteins" as described herein, are large biomolecules, or macromolecules, that can consist of one or more long chains of amino acid residues. Proteins can perform a vast array of functions within living organisms, including catalyzing metabolic reactions, DNA replication, responding to stimuli, and transporting molecules from one location to another. Proteins differ from one another primarily in their sequence of amino acids, which is dictated by the nucleotide sequence of their genes, and which usually results in protein folding into a specific three-dimensional structure that determines its activity. As described herein "enzymes" are proteins that can accelerate, or catalyze, chemical reactions. The molecules at the beginning of the process are called substrates and the enzyme converts these into different molecules, called products. In some embodiments described herein, a stabilized polypeptide formulation comprising the 2D crystalline material of any one of the embodiments described herein is provided. In some embodiments , the stabilized polypeptide comprises an enzyme or protein.

[0106] "Disulfide bonds" can also be called an S-S bond, or disulfide bridge, and is a covalent bond derived from two thiol groups. In some embodiments described herein, cysteine residues can be positioned such that formation of disulfide bonds between two cysteine residues can occur.

[0107] "Protein crystallization," as described herein, is a process or method of forming a protein crystal. Protein crystals can been observed in nature, however the protein crystallization method can also be used for scientific or industrial purposes, such as, for

example, study by X-ray crystallography. Proteins can be prompted to form crystals when the solution in which they are dissolved becomes supersaturated. Under these conditions, individual protein molecules can pack in a repeating array, held together by noncovalent interactions. These crystals can then be used in structural biology to study the molecular structure of the protein, or for various industrial or biotechnological purposes. Some embodiments described herein relate to a non-naturally occurring symmetrical polypeptide building block comprising a plurality of cysteine residues positioned such that formation of disulfide bonds between some or all of said plurality of cysteine residues facilitates formation of 2D crystals. In some embodiments described herein, a 2D crystalline material comprising a polypeptide building block of any one of the embodiments described herein is provided. The 2D crystalline material can reside on a lab-on-a-chip, a molecular membrane, a molecular template, stabilized polypeptide formulation, molecular scaffold, protective armor, smart textile, piezo electronic component, controlled drug release formulation or a run-flat tire.

[0108] Proteins are biological macromolecules and function in an aqueous environment. As such protein crystallization, for example, can be carried out in water. However, protein crystallization is challenging due to restrictions of the aqueous environment, difficulties in obtaining high-quality protein samples, as well as sensitivity of protein samples to temperature, pH, ionic strength, and other factors. Proteins can greatly in their physicochemical characteristics, and so crystallization of a particular protein is rarely predictable. Determination of appropriate crystallization conditions for a given protein often requires empirical testing of many conditions before a successful crystallization condition is found.

[0109] In crystallography, a crystallographic point group is a set of symmetry operations, like rotations or reflections that leave a central point fixed while moving other directions and faces of the crystal to the positions of features of the same kind. This symmetry can be described as C_n (for cyclic) which indicates that the group has an n-fold rotation axis. C_{nh} is C_n with the addition of a mirror (reflection) plane perpendicular to the axis of rotation. C_{nv} is Cn with the addition of n mirror planes parallel to the axis of rotation.

[0110] S_{2n} (for Spiegel, German for mirror) denotes a group that contains only a 2n-fold rotation-reflection axis.

[0111] D_n (for dihedral, or two-sided) indicates that the group has an n-fold rotation axis plus n twofold axes perpendicular to that axis. D_{nh} has, in addition, a mirror plane perpendicular to the n-fold axis. Dnd has, in addition to the elements of D_n, mirror planes parallel to the n-fold axis.

[0112] The letter T (for tetrahedron) indicates that the group has the symmetry of a tetrahedron. T_d includes improper rotation operations, T excludes improper rotation operations, and T_h is T with the addition of an inversion.

[0113] The letter O (for octahedron) indicates that the group has the symmetry of an octahedron (or cube), with (O_h) or without (O) improper operations (those that change handedness). Due to the crystallographic restriction theorem, n = 1, 2, 3, 4, or 6 in 2- or 3-dimensional space. In some embodiments described herein, a polypeptide is provided wherein the polypeptide has inherent C3, C4, C6, D3, D4 or D6 symmetry.

[0114] "Genetic engineering," as described herein, is the direct manipulation of an organism's genome using biotechnology. One skilled in the art would appreciate the variety of technologies that can be used to change the genetic makeup of nucleic acid in order to make mutations, insertions or deletions. Without being limiting, this can also include transfer of genes within and across species boundaries to produce improved or novel organisms. New DNA may be inserted in the host genome by first isolating and copying the genetic material of interest using molecular cloning methods to generate a DNA sequence, or by synthesizing the DNA, and then inserting this construct into the host organism. Genes can also be mutated at certain points in order to make introduction of polypeptide segments into a protein, create a deletion mutant or make protein mutants with point mutations, for example. In some embodiments described herein, the polypeptide described comprises at least one cysteine residue that has been introduced into said polypeptide building block through genetic engineering. In some embodiments, polypeptide is genetically engineered.

[0115] "Solid phase synthesis" as described herein refers to a method in which molecules are bound on a bead and synthesized step-by-step in a reactant solution.. In this method, building blocks can be protected at all reactive functional groups. The two functional groups that are able to participate in the desired reaction between building blocks in the solution and on the bead can be controlled by the order of deprotection. This method can be

used, for example, for the synthesis of peptides, deoxyribonucleic acid (DNA), and other molecules that need to be synthesized in a certain alignment. In some embodiments described herein, polypeptide is generated via solid phase synthesis.

[0116] "Chemical Modification," as described herein, refers to addition or removal, through chemical reaction, of any of a variety of macromolecules, without being limiting, this can include proteins, polypeptides and nucleic acids, and are known to those skilled in the art.

[0117] "Modification by enzymatic reaction," refers to modification of macromolecules, without being limiting, this can include proteins, polypeptides and nucleic acids, in which the macromolecule is modified in a reaction using an enzyme. As there are a variety of commercially available enzymes for modification, techniques for enzymatic modification can be appreciated by those skilled in the art.

[0118] "Peptide tags" as described herein, are known to those skilled in the art and can be used as an affinity tag or can be a small organic molecule, such as biotin or a short peptide sequence. Tags can be attached at the N-terminus, or C terminus, but in principle can be positioned anywhere in a molecule and can be separated from the molecule by a spacer. There are a variety of spacers of varying length and polarity. Additionally, peptide tags can be attached by a cleavable linker. In some embodiments, a polypeptide building block is provided, wherein the polypeptide building block comprises a peptide tag.

[0119] "Functional groups" as described herein are specific moieties within a molecule that are responsible for a chemical reaction or a characteristic of a molecule. Common functional groups can include but are not limited to alkyls, alkenyl, alkynyl, phenyls, haloalkanes, fluoroalkanes, chloroalkanes, bromoalkanes, iodoalkanes, alcohols (hydroxyl), ketones (cabonyls), aldehydes, Acyl halides, carbonates (carbonate ester), carboxylate, carboyxlic acids (carboxyl), esters, methoxy, hydroperoxide (hydroperoxy), peroxide (peroxy), ethers, hemiacetals, hemiketals, acetals, ketals, orthoester, heterocycles (methylenedioxy), orthocarbonate esters, amides (carboxyamides), primary amines, secondary amines, tertiary amines, quaternary amines, primary ketimines, secondary ketimines, primary aldimine, secondary almidine, imides, axides, azo compounds, cyanate, isocyanta, nitrate, nitriles, isonitriles, nitosooxy, nitro compounds, nitroso compounds,

oxime, pyridines, sulfhydril, sulfides, disulfides, sulfinyls, sulfonyl, sulfino, sulfo, tiocyanate, isothiocyanate, carbonotyioyl, carbonothioyl, phosphine, phosphonic acids, phosphate, boronic acids, boronic esters borinic acids and borinic esters. In some embodiments, a polypeptide building block is provided, wherein the polypeptide building block comprises a functional group.

[0120] "Fluorophores" as described herein are flourescent chemical compound that can re-emit light upon light excitation. Without being limiting, fluorophores can include, for example, Xanthene derivatives (fluorescein, rhodamine, Oregon green, eosin, and Texas red), Cyanine derivatives (cyanine, indocarbocyanine, oxacarbocyanine, thiacarbocyanine, and merocyanine), Squaraine derivatives and ring-substituted squaraines (Seta, SeTau, and Square dyes), Naphthalene derivatives (dansyl and prodan derivatives) Coumarin derivatives, oxadiazole derivatives (pyridyloxazole, nitrobenzoxadiazole and benzoxadiazole), Anthracene derivatives (anthraquinones, including DRAQ5, DRAQ7 and CyTRAK Orange), Pyrene derivatives (cascade blue), Oxazine derivatives (Nile red, Nile blue, cresyl violet, oxazine 170), Acridine derivatives (proflavin, acridine orange, acridine yellow), Arylmethine derivatives (auramine, crystal violet, malachite green, and Tetrapyrrole derivatives (porphin, phthalocyanine, bilirubin). In some embodiments, a polypeptide building block is provided, wherein the polypeptide building block comprises a fluorophore.

[0121] "Nanoparticles" as described herein, refers to particles between 1 and 100 nanometers in size. In nanotechnology, a particle is defined as a small object that behaves as a whole unit with respect to its transport and properties. In some embodiments, a polypeptide building block is provided, wherein the polypeptide building block comprises a nanoparticle.

[0122] As used herein, "nucleic acid" or "nucleic acid molecule" refers to polynucleotides or oligonucleotides such as deoxyribonucleic acid (DNA) or ribonucleic acid (RNA), oligonucleotides, fragments generated by the polymerase chain reaction (PCR), and fragments generated by any of ligation, scission, endonuclease action, exonuclease action, and by synthetic generation. Nucleic acid molecules can be composed of monomers that are naturally-occurring nucleotides (such as DNA and RNA), or analogs of naturally-occurring nucleotides (e.g., enantiomeric forms of naturally-occurring nucleotides), or a combination of both. Modified nucleotides can have alterations in sugar moieties and/or in pyrimidine or

purine base moieties. Sugar modifications include, for example, replacement of one or more hydroxyl groups with halogens, alkyl groups, amines, and azido groups, or sugars can be functionalized as ethers or esters. Moreover, the entire sugar moiety can be replaced with sterically and electronically similar structures, such as aza-sugars and carbocyclic sugar analogs. Examples of modifications in a base moiety include alkylated purines and pyrimidines, acylated purines or pyrimidines, or other well-known heterocyclic substitutes. Nucleic acid monomers can be linked by phosphodiester bonds or analogs of such linkages. Analogs of phosphodiester linkages include phosphorothioate, phosphorodithioate, phosphoroselenoate, phosphorodiselenoate, phosphoroanilothioate, phosphoranilidate, phosphoramidate, and the like. The term "nucleic acid molecule" also includes so-called "peptide nucleic acids," which comprise naturally-occurring or modified nucleic acid bases attached to a polyamide backbone. Nucleic acids can be either single stranded or double stranded."

[0123] "Rhamnulose-1-phosphate aldolase," or RhuA, is an enzyme belonging to the lyase family. In some embodiments described herein, a polypeptide building block is provided. In some embodiments, the polypeptide comprises the RhuA protein.

[0124] A "2D crystalline material" as described herein are atoms or molecules are arranged in a regular, periodic manner, in which they are in two dimensions. In some embodiments, the 2D crystalline material is auxetic.

[0125] "Auxetic" as described herein, refers to structures or materials that have a negative "Poisson's ratio." When a material that is auxetic is stretched, it becomes thicker perpendicular to the applied force. This occurs due to their particular internal structure and the way this deforms when the sample is uniaxially loaded. Auxetics can be single molecules, crystals, or a particular structure of macroscopic matter. Such materials and structures are expected to have mechanical properties such as high energy absorption and fracture resistance. In some embodiments described herein, a 2D crystalline material is provided, wherein the 2D crystalline material is auxetic.

[0126] A lab-on-a-chip (LOC), as described herein, can be a device that integrates one or several laboratory functions on a single chip of only millimeters to a few square centimeters to achieve automation and high-throughput screening, for example. Lab-on-a-

chip are used for the handling of extremely small fluid volumes down to less than pico liters. Lab-on-a-chip devices are can also be a subset of Micro-electro-mechanical systems (MEMS) devices, for example and can be indicated by "Micro Total Analysis Systems" (μTAS) as well. Lab-on-a-chip is closely related to, and overlaps with, microfluidics which describes primarily the physics, the manipulation and study of minute amounts of fluids. Lab-on-a-Chip can also indicate the scaling of single or multiple lab processes down to chip-format, whereas "μTAS" is dedicated to the integration of the total sequence of lab processes to perform chemical analysis.

[0127] "Molecular membrane" can refer to the two dimensional membrane comprising molecules with polar and nonpolar regions, such as for example, a lipid, polypeptides and/or proteins.

[0128] A "molecular template" as described herein, can comprise a molecule, such as, for example, DNA that serves as a pattern for the synthesis of a macromolecule. In some embodiments described herein, a molecular template is provided, wherein the molecular template comprises a 2D crystalline material of any one of the embodiments described herein.

[0129] "Protective armor" as described herein is refers to armor that can protect a body from high heat, cold temperature, strong force or impact. Without being limiting, protective armor can be a scuba suit, a lab coat, work boots material, motorcycle vest, motorcycle pants, motorcycle protective clothing, race protective gear, bullet proof vest, bulletproof gear, cryoprotecting gloves, cryoprotecting material and heat resistant clothing or gear.

[0130] "Smart textile" as described herein is a passive textile structure capable of responding to external stimulation i.e. from pressure, temperature, light, low voltage current etc. The definition generally means that SMART textiles is a form of textiles that utilizes materials which aids it purpose, and can 'sense' what is around it. For example, a textiles company explains it as : Smart materials respond to differences in temperature or light and change in some way. They are called smart because they sense conditions in their environment and respond to those conditions. Smart materials appear to 'think' and some have a 'memory' as they revert back to their original state. In some embodiments, a smart

textile comprising any one of the 2D crystalline material of any one of the embodiments described herein is provided.

[0131] "Piezo electronic component" as described herein can be a material that can convert mechanical signals, such as force, pressure, strain or acceleration, into electrical voltage, or, vice versa, an electrical voltage into mechanical motion or oscillations. In some embodiments, a Piezoelectronic component comprising any one of the 2D crystalline material of any one of the embodiments described herein is provided.

[0132] "Adaptive membrane or sieve" as described herein, can be a filter made of the materials described herein for preventing the passage of certain molecules, particles or substances. In some embodiments, the adaptive membrane or sieve is a passive and kinetic system that allows expansion of geometry in response to heat, temperature and other changes in its environment. In some embodiments, an adaptive membrane or sieve comprising any one of the 2D crystalline material of any one of the embodiments described herein is provided.

[0133] A "controlled drug release formulation" as described herein, refers to a drug which can be gradually released at a constant set dosage for a specific amount of time. In some embodiments herein, the polypeptide building block is attached to a drug for delivery. In some embodiments herein the polypeptide building block attached to a drug for delivery

[0134] A "run-flat tire" as described herein is pneumatic vehicle tire that is designed to resist the effects of deflation when punctured, and to enable the vehicle to continue to be driven at reduced speeds (under 55 mph (89 km/h)), and for limited distances (up to 10 mi (16 km), depending on the type of tire). In some embodiments described herein, a run-flat tire comprising the 2D crystalline material of any one of the embodiments described herein is provided. The run-flat tire can resist the effects of deflation when punctured. In some embodiments the tire can be used in a vehicle wherein the vehicle is driven at a speed of 30, 35, 40, 45, 50 or 55 mph or any speed in between any two aforementioned values, when the tire is punctured. In some embodiments, a run flat tire comprising any one of the 2D crystalline material of any one of the embodiments described herein is provided.

[0135] "Poisson's ratio" as described herein, is the coefficient of expansion on the transverse axial, and is the negative ratio of transverse to axial strain. When a material is compressed in one direction, it can tend to expand in the other two directions perpendicular to the direction of compression. This phenomenon is called the Poisson effect. Poisson's ratio, υ (nu) is a measure of this effect. The Poisson ratio is the fraction (or percent) of expansion divided by the fraction (or percent) of compression, for small values of these changes. The Poisson's ratio of a stable, isotropic, linear elastic material cannot be less than -1.0 or greater than 0.5 because of the requirement for Young's modulus, the shear modulus and bulk modulus to have positive values. In some embodiments described herein, the 2D crystalline material of any of the embodiments herein comprises a Poisson's ratio of -1.

DETAILED DESCRIPTION OF THE PREFERRED EMBODIMENT

[0136] A majority of biological machines and materials are self-assembled, dynamic/responsive multiprotein architectures. For example, biological machines such as Photosystem II, nitrogenase and hydrogenase involve discrete oligomers (**Figure 1**). Some systems involve periodic polymers. For example, spherical viruses, ferritin, and carboxysome are 0-D, tubular viruses, actin, microtubules, and flagella are 1-D, S-layers are 2D and collagen superstructures are 3-D.

[0137] Some protein materials are assembled hierarchically. For example, going from the macro scale to the nano scale, a spider web may comprise a silk fibril, which can further comprise a hetero-nano-composite, which can further comprise beta-sheet nano-crystal, which can also further comprise H-bonded beta-strands. Via supramolecular assembly, weakly held, unstable building blocks may give rise to strong, functional, dynamic, stimuli-responsive materials. (See **Figure 2).**

[0138] 2D crystalline materials exhibit unique mechanical and electronic attributes, possess high surface area-to-volume ratios, offer a uniform display of atomic/molecular entities as well as pores, and provide structural access to materials with all other dimensionalities: to 0- and 1D materials through folding and to 3D materials through stacking. These properties have rendered synthetic 2D materials immensely attractive in applications including electronics, sensing, coating, filtration and catalysis. Nevertheless, the

rational design of self-assembling 2D crystals remains a considerable challenge and a very active area of development.

[0139] Currently, the fabrication of non-biological 2-D crystalline materials is not generalizable and scalable. Other protein design strategies require extensive computational work and protein engineering, have low success rates, contain large defects, are not single-layered, and often require the presence of lipids for supported assembly. Some embodiments of the 2D crystalline materials described herein are essentially defect-free and self-assemble in an unsupported fashion in solution. They also offer a better strategy because of their simplicity, low cost nature, effectiveness, and potential generalizability. These new 2D crystalline materials as described herein led to a surprising effect of providing a mechanism for making these 2D crystalline materials that had a higher success rate, no large defects and little to no need for the presence of lipids for supported assembly.

[0140] Proteins provide certain advantages as building blocks for functional nanomaterials. For example, they involve 20 distinct components (i.e., amino acids) which allow nearly infinite structural and functional diversity. They are inherently nanoscale. In addition, they are genetically encoded and are producible and evolvable in living systems. However, their utilization of 20 distinct components may render their structure, self-assembly and function difficult to program (See **Figure 3)**.

[0141] Fabrication of 2D supramolecular protein assemblies may provide one or more of the following advantageous features: 1) high surface area/volume ratio; 2) dense display of a diverse set of chemical functionalities in a highly ordered, yet dynamic fashion; 3) innately functional building blocks (e.g., functional enzymes); and 4) potential for smart materials, lab-on-a-chip technologies, heterogeneous catalyst platforms (**Figure 4)**. As described herein, some embodiments of the 2D crystalline structures are advantageous over previous crystalline materials as they are designed to have a high surface area/volume ratio. As such the 2D crystalline materials as described herein can be used for a variety of materials as well as functions.

[0142] However, some existing approaches for designed protein assembly may be too design-intensive and involve sophisticated, but not sure-fire computational methods or protein fusion strategies that do not always give the desired product, and the desired products

are not scalable and do not always possess superior materials properties (e.g, perfect structural order, stimuli-responsiveness, etc.)(**Figure 5**). (See, for example, Baker/King et al., Nature 510, 103–108 (2014)).

[0143] Other approaches are also too design-intensive, involve sophisticated and but not sure-fire computational methods or protein fusion strategies that do not always give the desired product and the desired products are not scalable, and do not always possess superior materials properties (e.g, perfect structural order, stimuli-responsiveness, etc.)(**Figure 6**). (See, for example, Sinclair, Yeates etc. Nat. Nanotech. 6, 558–562 (2011)).

[0144] Other approaches have been described in Colson, J. W.; Dichtel, W. R. Rationally synthesized two-dimensional polymers. *Nat. Chem.* 2013, *5*, 453-465" and Butler, S. Z.; Hollen, S. M.; Cao, L.; Cui, Y.; Gupta, J. A.; Gutiérrez, H. R.; Heinz, T. F.; Hong, S. S.; Huang, J.; Ismach, A. F.; Johnston-Halperin, E.; Kuno, M.; Plashnitsa, V. V.; Robinson, R. D.; Ruoff, R. S.; Salahuddin, S.; Shan, J.; Shi, L.; Spencer, M. G.; Terrones, M.; Windl, W.; Goldberger, J. E. Progress, Challenges, and Opportunities in Two-Dimensional Materials Beyond Graphene. *ACS Nano* 2013, *7*, 2898-2926; Sinclair, J. C.; Davies, K. M.; Venien-Bryan, C.; Noble, M. E. M. Generation of protein lattices by fusing proteins with matching rotational symmetry. *Nat. Nanotechnol.* 2011, *6*, 558-562; Lanci, C. J.; MacDermaid, C. M.; Kang, S.-g.; Acharya, R.; North, B.; Yang, X.; Qiu, X. J.; DeGrado, W. F.; Saven, J. G. Computational design of a protein crystal. *Proc. Natl. Acad. Sci. USA* 2012, *109*, 7304-7309; King, N. P.; Sheffler, W.; Sawaya, M. R.; Vollmar, B. S.; Sumida, J. P.; Andro, I.; Gonen, T.; Yeates, T. O.; Baker, D. Computational Design of Self-Assembling Protein Nanomaterials with Atomic Level Accuracy. *Science* 2012, *336*, 1171-1174; Lai, Y.-T.; Cascio, D.; Yeates, T. O. Structure of a 16-nm Cage Designed by Using Protein Oligomers. *Science* 2012, *336*, 1129; Lebeau, L. *et al.*, Two-dimensional crystallization of a membrane protein on a detergent- resistant lipid monolayer. (2001). *J. Mol. Biol*, 306, 639-647; Uzgiris, E. & Kornberg, R. Two-dimensional crystallization technique for imaging macromolecules with application to antigen-antibody-complement complexes. (1983). *Nature*, 301, 125-129. (All incorporated by reference in their entireties herein).

[0145] Some embodiments provided herein relate to a highly efficient/expeditious design strategy for the fabrication of single layered, ultra-low defect 2D crystalline materials

out of protein building blocks. Such 2D crystalline materials exhibit unique mechanical and electronic attributes, possess high surface area-to-volume ratios, offer a uniform display of atomic/molecular entities as well as pores, and provide structural access to materials with all other dimensionalities: to 0- and 1D materials through folding and to 3D materials through stacking.

[0146] In some embodiments, an inherently symmetrical or an artificially "symmetrized" protein is modified with Cys residues in appropriate locations. The selective and easily tunable nature of Cys-Cys disulfide bonding is then utilized to assemble these protein building blocks into crystalline, 2D materials that 1) exhibit very low frequency of defects, 2) exhibit coherent dynamicity (i.e., lattices that open up and close in a cooperative fashion without loss of crystallinity), 3) are scalable, and 4) are readily modified chemically or genetically. The 2D crystalline materials produced by the methods of the embodiments described herein, are coherently dynamic and show large flexibility.

[0147] In some embodiments, the 2D crystalline protein materials described herein may be used in applications including the following: 1) Fabrication of self-assembled, chemically dense, lab-on-a-chip platforms for sensing, diagnostics, vaccine development, and drug delivery; 2) Fabrication of molecular membranes for sieving and filtration; 3) Fabrication of molecular templates that provide 5-100 nm spatial resolution for patterning and deposition (which is a length scale that is hard to attain with diffraction-based methods); 4) Stabilization of enzymes and proteins of commercial value; and 5) Fabrication of crystalline molecular scaffolds for macromolecular structure determination by 2D crystallography and electron microscopy.

[0148] In some embodiments, an inherently symmetrical or an artificially "symmetrized" protein is very simply modified with Cys residues in appropriate locations. The selective and easily tunable nature of Cys-Cys disulfide bonding is then utilized to assemble these protein building blocks into crystalline, 2D materials that 1) exhibit very low frequency of defects; 2) exhibit coherent dynamicity (i.e., lattices that open up and close in a cooperative fashion without loss of crystallinity); 3) are scalable; and 4) are readily modified chemically or genetically.

[0149] Some embodiments of the methods and compositions described herein provide advantages over prior approaches due to their simplicity, low cost nature, effectiveness and potential generalizability. For example, some embodiments require a simple visual inspection of the protein building block that possesses the proper symmetry (C3, C4, C6, D3, D4 or D6), and incorporation of single Cys residues into appropriate positions for self-assembly. This contrasts with other protein design strategies that require extensive computational work and protein engineering, and have low success rates. It also contrasts with the fabrication of non-biological 2-D crystalline materials, which are not generalizable and scalable.

[0150] Some embodiments of the 2D crystalline materials described herein are essentially defect-free and self-assemble in an unsupported fashion in solution. These contrasts with other 2D protein crystalline materials previously designed or produced that contain large defects, are not single-layered and often require the presence of lipids for supported assembly. In some embodiments, the 2D crystalline materials described herein are coherently dynamic. Other previous examples of dynamic 2D materials (based on proteins or other building blocks) do not show large flexibility. As such, the methods of some of the embodiments described herein, produce 2D crystals that are surprisingly flexible and dynamic and do not require the presence of lipids for supported assembly.

[0151] In some embodiments described herein, a protein building block with inherent C3, C4, C6, D3, D4 or D6 symmetry is appropriately engineered to contain a single set of surface cysteine residues in the corner positions. The resulting variant may be incubated in solution under controllable oxidizing conditions (such as controlled atmosphere, a redox buffer consisting of reduced and oxidized glutathione, or a slowly degrading reducing agent like beta-mercaptoethanol) to self-assemble into suspended crystalline materials. The quality of the material may be readily validated by routine transmission electron microscopy or atomic force microscopy measurements. When/if desired, the protein building blocks may be genetically or chemically modified prior to self-assembly with functional groups and tags, including other proteins, peptide tags, fluorophores, nanoparticles.

[0152] The strategy described here can be readily implemented on other protein systems that possess the appropriate inherent symmetry.

[0153] As described herein, the 2D crystalline protein materials generated by the embodiments have diverse potential applications: 1) Fabrication of self-assembled, chemically dense, lab-on-a-chip platforms for sensing, diagnostics, vaccine development, drug delivery; 2) Fabrication of molecular membranes for sieving and filtration; 3) Fabrication of molecular templates that provide 5-100 nm spatial resolution for patterning and deposition (which is a length scale that is hard to attain with diffraction-based methods; 4) Stabilization of enzymes and proteins of commercial value; 5) Fabrication of crystalline molecular scaffolds for macromolecular structure determination by 2D crystallography and electron microscopy. In some embodiments, the 2D crystalline protein materials can be used in lab-on-a-chip platforms for sensing, diagnostics, vaccine development, drug delivery, fabrication of molecular membranes for sieving and filtration, fabrication of molecular templates that provide 5-100 nm spatial resolution for patterning and deposition (which is a length scale that is hard to attain with diffraction-based methods), stabilization of enzymes and proteins of commercial value and fabrication of crystalline molecular scaffolds for macromolecular structure determination by 2D crystallography and electron microscopy.

[0154] Some embodiments described herein involve disulfide-mediated assembly of 2D protein materials. Some embodiments bypass the need for time-/cost-intensive computational design or protein-fusion. For example, in some embodiments the only step is the engineering of cysteine residues at proper positions on a protein building block of choice. In some embodiments, the cysteine residues are in appropriate positions in a C3, C4 or C6-symmetric protein that is expressible in bacteria or other desired organism, cell, or system. In some embodiments, the experimental flow/feasibility testing is highly streamlined, involving protein expression/purification, testing of different oxidative conditions for self-assembly (such as air oxidation or redox buffer systems), and characterization by electron microscopy) (**Figure 7**).

[0155] In an exemplary embodiment, the RhuA protein was engineered to have cysteines at the corners of the protein. In particular, the wild type RhuA protein of SEQ ID NO: 1 (RCSB Protein Data Bank accession number 1OJR, the disclosure of which is incorporated herein by reference in its entirety) was modified to replace the Asp at position 98 with Cys and to replace the Cys at position 126 with a Ser (SEQ ID NO: 2). In addition, to

replacing the Asp at position 98 with Cys and to replacing the Cys at position 126, the modified protein RhuA protein had the E192A mutation such that the modified RhuA protein had the sequence of SEQ ID NO: 3. Oxidation was performed via gradual degradation of the reducing agent β-mercaptoethanol (10 mM) at 4 °C under constant shaking to allow formation of disulfide bonds. This approach was simple to design, (only took 10 min to find proper locations for Cys incorporation) and readily tested. In particular, visual inspection of the RhuA crystal structure indicated four protrusions from the surface (since it is C4 symmetry protein, cysteines will be exact same location) which were identified as ideal locations for incorporating single cysteine residues (**Figures 8-10)**.

[0156] In addition, it provided robust, reproducible self-assembly, crystalline order over large length-scales (up to several microns), and single-layered structures which were essentially defect-free and dynamic.

[0157] In some embodiments, new potential for smart/stimuli-responsive nano- and bio-materials or mechanical Nano devices are provided.

[0158] Additional embodiments are provided in the figures submitted herewith.

[0159] Fabrication of crystalline materials with distinct dimensionalities and tailorable structural, physical and chemical properties represents a major goal in fundamental and applied sciences. As reported herein, the bottom-up self-assembly of unsupported, two-dimensional protein lattices with precise spatial arrangements and patterns through a readily accessible design strategy, are provided. Three single- or double-point mutants of the soluble, C4 symmetric protein RhuA were designed to assemble via different modes of intermolecular interactions (single disulfide, double disulfide and metal coordination) into crystalline, two-dimensional arrays in a chemically tunable fashion. Owing to the flexibility of the single disulfide interactions, the lattices of one of the variants (C98RhuA) are essentially defect-free and undergo substantial but highly correlated changes in molecular arrangement and porosity, yielding a Poisson's ratio of –1, the lowest thermodynamically possible value for an isotropic material. In some embodiments described herein, the polypeptide building block can be designed to have one, two, three, four or more point mutations to allow assembly of intermolecular interactions into crystalline, two-dimensional arrays. In some embodiments,

the sites for the point mutations that allow the protein-protein interactions are selected by structure prediction programs, which are known to those skilled in the art.

[0160] Some embodiments relate to a self-assembled, protein-based molecular material that is auxetic. In some embodiments, this material displays the thermodynamically lowest possible Poisson's ratio of -1 for an isotropic material. Some embodiments relate to a general method to fabricate such auxetic materials from protein building blocks. In some embodiments, the self-assembled, protein-based molecular material comprises 2D crystals of a protein termed C98-RhuA. The method to fabricate auxetic self-assembled protein-based molecular material, such as, for example, 2D C98-RhuA crystals, is highly expeditious and can be readily utilized with a wide variety of protein building blocks. In some embodiments of this methodology, an inherently symmetrical or an artificially "symmetrized" protein is very simply modified with cysteine (Cys) residues in appropriate, "corner" locations. In some embodiments, the inherently symmetrical or an artificially "symmetrized" protein is selected to have cysteine mutations that allow the proteins to self assemble, wherein the cysteine mutation sites selected by studying the predicted protein structures from protein structure prediction databases. Alternatively, if there is a wild-type cysteine, these can also be mutated into an amino acid whose functional group will not interfere with self-assembly. These Cys-containing protein building blocks self-assemble selectively through the formation of disulfide bonds between Cys side chains. The simultaneous flexibility and short linker-length of Cys-Cys disulfide bonding allows the formation of highly ordered (crystalline) lattices that undergo dramatic conformational changes in a coherent manner. The "rotary" motion of each protein building block results in auxetic behavior.

[0161] Poisson's ratio is a fundamental parameter that describes the response of a material to uniaxial strain. Most materials have positive Poisson's ratios, meaning that when they are stretched in one direction, they become thinner in the lateral direction (for example, a rubber band). Materials with negative Poisson's ratios (auxetic materials), on the other hand, display the counterintuitive behavior of lateral expansion upon transverse stretching. This property endows them with enhanced toughness, resistance to indentation, and shear stiffness, among many other advantageous. Though several auxetic materials have been identified or fabricated at the macroscopic level (most of them having Poisson's ratios

between -0.3 and 0), in some embodiments the auxetic self-assembled, protein-based molecular material, such as for example, the 2D C98-RhuA crystals described herein, display the minimum allowed value of -1, which is not only significant because of its unprecedented magnitude, but also because it was achieved through bottom-up molecular design (which is extremely rare-if not unprecedented-among auxetic materials).As such the material processed by the methods described in some of the embodiments herein led to a material with surprising characteristics. In some embodiments the auxetic self-assembled, protein-based molecular material, such as for example, the C98-RhuA crystals, can be used as feedstocks for macroscopic auxetic and adaptive materials. This in turn permits tailoring of the macroscopic auxetic properties of resulting materials through molecular engineering. Several functionalized 2D crystalline protein arrays have been prepared using the procedures provided herein.

[0162] Due to their superior/advantageous physical properties (toughness, high resistance to indentation, high shear stiffness while being lightweight, adaptiveness), auxetic materials have numerous potential applications, including, for example, as structural and functional components of: 1) protective armors; 2) smart textiles; 3) piezo electronics; 4) adaptive membranes, sieves; 5) controlled drug release; 6) run-flat tires.

[0163] Some embodiments relate to a self-assembled, protein-based molecular material that is auxetic. In some embodiments, this material displays the thermodynamically lowest possible Poisson's ratio (-1; minus one) for an isotropic material. In some embodiments, the auxetic material comprises 2D crystals of a protein termed C98-RhuA. Other embodiments relate to a general method to fabricate such auxetic materials from protein building blocks.

[0164] Poisson's ratio is a fundamental parameter that describes the response of a material to uniaxial strain. Most materials have positive Poisson' ratios, meaning that when they are stretched in one direction, they become thinner in the lateral direction (for example, a rubber band). Materials with negative Poisson' ratios (auxetic materials), on the other hand, display the counterintuitive behavior of lateral expansion upon transverse stretching. This property endows them with enhanced toughness, resistance to indentation, and shear stiffness, among many other advantageous.

[0165] Though several auxetic materials have been identified or fabricated at the macroscopic level (most of them having Poisson's ratios between $\nu = 0.5$ to -0.85), 2D C98-RhuA crystals that were disclosed here displays the minimum allowed value of –1, which is not only significant because of its unprecedented magnitude, but also because it was achieved through bottom-up molecular design (which is extremely rare-if not unprecedented-among auxetic materials). In some embodiments, the auxetic materials, such as, for example, the C98-RhuA crystals, can be used as feedstocks for macroscopic auxetic and adaptive materials. This in turn allows tailoring of the macroscopic auxetic properties of resulting materials through molecular engineering.

[0166] The method to fabricate auxetic self-assembled protein-based molecular material, such as, for example, 2D C98-RhuA crystals, is highly expeditious and can be readily utilized with a wide variety of protein building blocks. In some embodiments, an inherently symmetrical or an artificially "symmetrized" protein is very simply modified with cysteine (Cys) residues in appropriate, "corner" locations. These Cys-containing protein building blocks self-assemble selectively through the formation of disulfide bonds between Cys side chains. The simultaneous flexibility and short linker-length of Cys-Cys disulfide bonding allows the formation of highly ordered (crystalline) lattices that undergo dramatic conformational changes in a coherent manner. The "rotary" motion of each protein building block results in auxetic behavior.

[0167] Some embodiments relate to a designed/synthetic, molecular material that has a Poisson's ratio of –1 (minus one). Other embodiments relate to a designed biological material that has a negative Poisson's ratio. Some embodiments provide a general method to fabricate molecular auxetic materials.

[0168] Auxetic materials have been described recently in G. N. Greaves, A. Greer, R. Lakes, T. Rouxel, Nat. Mater. 10, 823 (2011) as well as existing patents but these predominantly involve macroscopic materials obtained through physical fabrication methods (and not by molecular self-assembly).

[0169] In some embodiments, a protein building block (such as, for example, RhuA) with inherent C3, C4, C6 symmetry is appropriately engineered to contain a single set of surface cysteine residues in the corner positions. The resulting variant is incubated in

solution under controllable oxidizing conditions (such as, for example, controlled atmosphere, a redox buffer consisting of reduced and oxidized glutathione, or a slowly degrading reducing agent like beta-mercaptoethanol) to self-assemble into suspended crystalline materials. If desired, the quality of the material may readily be validated by routine transmission electron microscopy or atomic force microscopy measurements. In some embodiments, the resulting 2D crystalline materials show dynamic/adaptive/auxetic behavior.

[0170] Due to their superior/advantageous physical properties (toughness, high resistance to indentation, high shear stiffness while being lightweight, adaptiveness), auxetic materials have numerous potential applications, including, for example, as structural and functional components of 1) protective armors; 2) smart textiles; 3) piezo electronics; 4) adaptive membranes, sieves; 5) controlled drug release; 6) run-flat tires. In some embodiments described herein, the 2D crystalline material can be utilized in aerospace applications, materials in aircraft gas turbine engines, prosthetic materials, surgical implants, suture/muscle/ligament anchors, electrodes, piezoelectric sensors, filters and actuators.

[0171] A summary of some applications for these materials is provided on the internet at www.azom.com/article.aspx?ArticleID=168.

[0172] In some embodiments, coherently dynamic 2D protein crystals are obtained by design and exhibit the lowest possible Poisson's ratio for an isotropic material.

[0173] Two-dimensional (2D) crystalline materials possess unique structural, mechanical, and electronic properties (R. Mas-Balleste, C. Gomez-Navarro, J. Gomez-Herrero, F. Zamora, *Nanoscale* 3, 20 (2011); S. Z. Butler *et al.*, *ACS Nano* 7, 2898 (2013)), which has rendered them highly attractive in applications including electronics, sensing, coating, filtration and catalysis (S. Z. Butler *et al.*, *ACS Nano* **7**, 2898 (2013); F. Schedin *et al.*, *Nat. Mater.* 6, 652 (2007); A. K. Geim, K. S. Novoselov, *Nat. Mater.* 6, 183 (2007); C.-H. Lu, H.-H. Yang, C.-L. Zhu, X. Chen, G.-N. Chen, *Angew. Chem. Int. Ed. Engl.* 121, 4879 (2009); R. K. Joshi *et al.*, *Science* 343, 752 (2014); M. A. Lukowski *et al.*, *J. Am. Chem. Soc.* 135, 10274 (2013)). Although there have been considerable advances in the preparation of 2D materials that consist of one or few atomic/molecular layers (V. Nicolosi, M. Chhowalla, M. G. Kanatzidis, M. S. Strano, J. N. Coleman, *Science* 340, 1226419 (2013); D. Li, M. B. Muller, S. Gilje, R. B. Kaner, G. G. Wallace, *Nat. Nano.* 3, 101 (2008)), bottom-up design

and assembly of 2D crystalline materials remains a considerable challenge and a highly active area of development (J. W. Colson *et al.*, *Science* 332, 228 (2011); P. Kissel, D. J. Murray, W. J. Wulftange, V. J. Catalano, B. T. King, *Nat. Chem.* 6, 774 (2014); M. J. Kory *et al.*, *Nat. Chem.* 6, 779 (2014)). Even more challenging is the design of dynamic 2D lattices that can undergo large-scale coherent motions in the 2D plane without loss of crystallinity. Dynamicity in porous 3D crystalline solids has been exploited for stimuli-responsive functions and adaptive behavior (S. Shimomura *et al.*, *Nat. Chem.* 2, 633 (2010); J. Rabone *et al.*, *Science* 329, 1053 (2010); C. Serre *et al.*, *Science* 315, 1828 (2007)). As in the case of such 3D materials, integrating flexibility into crystalline 2D lattices would greatly broaden the functional scope of 2D materials.

[0174] Proteins are attractive building blocks for 2D materials because of their structural and chemical diversity, genetic tailorability and inherent functions. Prominent examples for natural, protein-based 2D materials are bacterial surface-layer (S-layer) proteins and purple-membrane bacteriorhodopsin assemblies, which form crystalline arrays in association with cell walls and membranes, respectively, and have been employed in diverse technological applications (F. Baneyx, J. F. Matthaei, *Curr. Opin. Biotech.* 28, 39 (2014); U. B. Sleytr, B. Schuster, E. M. Egelseer, D. Pum, *FEMS Microbiol. Rev.*, (2014); N. Hampp, *Chem. Rev.* 100, 1755 (2000)). On the synthetic front, methods for 2D protein crystallization have been developed for the structural characterization of membrane proteins (A. Engel *et al.*, *J. Struct. Biol.* 109, 219 (1992); H. Stahlberg *et al.*, *FEBS Lett.* 504, 166 (2001)) or functional applications (P. O. Saboe *et al.*, *Adv. Mater.* 26, 7064 (2014)), generally relying on the presence of lipid layers as supports. Recently, there has been progress in the rational, *de novo* design of 2- or 3D supramolecular protein arrays (J. C. Sinclair, K. M. Davies, C. Venien-Bryan, M. E. M. Noble, *Nat. Nanotechnol.* 6, 558 (2011); J. D. Brodin *et al.*, *Nat. Chem.* 4, 375 (2012); N. P. King *et al.*, *Science* 336, 1171 (2012); S. Gonen, F. DiMaio, T. Gonen, D. Baker, *Science* 348, 1365 (2015); C. J. Lanci *et al.*, *Proc. Natl. Acad. Sci. USA* 109, 7304 (2012)), which has entailed the symmetric polymerization of protein building blocks through computationally designed protein-protein interactions or through genetic fusion of protein components. While elegant, these approaches are design-intensive, and the integration of dynamic/adaptive behavior has not been explored.

[0175] To address these issues, a simple chemical bonding strategy to control protein self-assembly was used. It was reasoned that both cysteine (Cys)-mediated disulfide bonds and metal coordination interactions between protein building blocks could produce crystalline and dynamic protein arrays with minimal design, because these bonds are: 1) strong but reversible (to minimize the surface area to be designed and ensure self-healing), 2) short yet sufficiently flexible (to simultaneously afford crystallinity and adaptiveness), and 3) chemically tunable (to exert external control over self-assembly and enable stimuli-responsiveness), and 4) easily designed and engineered. As such, the embodiments described herein, the 2D crystalline material comprise polypeptides, wherein the polypeptides can form bond that are: 1) strong but reversible (to minimize the surface area to be designed and ensure self-healing), 2) short yet sufficiently flexible (to simultaneously afford crystallinity and adaptiveness), and 3) chemically tunable (to exert external control over self-assembly and enable stimuli-responsiveness), and 4) easily designed and engineered.

[0176] The most straightforward route to obtaining 2D lattices is the tesselation of C_3, C_4 or C_6 symmetric building blocks through appropriately positioned C_2 symmetric linkages such as disulfide bonds or many metal coordination interactions. As a model building block, the L-rhamnulose-1-phosphate aldolase (RhuA) protein, was chosen, which is a stable, C_4 symmetric homotetramer (4 × 274 residues) that was previously used as a synthon for engineering supramolecular assemblies (P. Ringler, G. E. Schulz, *Science* 302, 106 (2003)). RhuA roughly resembles a four-legged stool with dimensions of 7 × 7 × 5 nm (**Figure 10A**). A quick inspection of the RhuA structure indicated protrusions in the four corner positions that would be ideal locations to incorporate single cysteine or two histidine residues for disulfide-mediated or metal-directed self-assembly, respectively. Two variants, ^{C98}RhuA (SEQ ID NO: 3) and $^{H63/H98}$RhuA (SEQ ID NO: 4), were generated with four conditionally self-associating corners for forming square lattices (**Figure 10A** and 10B, top and middle rows). The relative positions of residues 63 and 98 were deemed to be conducive to forming a bis-histidine metal coordination motif to afford a tetrahedral or square planar coordination geometry for metal-mediated RhuA pairing interactions. Additionally, it was noted that RhuA could be converted into a stable D_4 symmetric octamer through a single point mutation (A88F) (D. Grueninger *et al.*, *Science* 319, 206 (2008)). Thus, a third variant,

$^{F88/C98}$RhuA (SEQ ID NO: 5) was prepared, which presents eight symmetry-related cysteine residues at roughly 45° angles in a 2D projection (**Figure 10A**, bottom row). It was envisioned that the C_4 symmetric ^{C98}RhuA and $^{H63/H98}$RhuA variants could potentially yield different square lattices with two distinct patterns in terms of the up/down orientation of the building blocks with respect to the 2D plane (**Figure 10B**, top and middle rows). On the other hand, the D_4 symmetry of $^{F88/C98}$RhuA would necessarily dictate a 2D lattice with equivalent faces (**Figure 10B**, bottom row). These RhuA building blocks would also provide three distinct modes of inter-building-block interactions, whose effects on self-assembly were to be investigated, such as, for example, single disulfide, double disulfide and bis-His-anchored metal coordination.

[0177] For the oxidation-driven self-assembly of the Cys-bearing variants ^{C98}RhuA and $^{F88/C98}$RhuA, various strategies were tested, including air oxidation, redox buffer systems containing reduced and oxidized glutathione (GSH and GSSG) or low concentrations of the reductant β-mercaptoethanol βME (≤10 mM), which slowly decomposes in aqueous solution and results in gradually more oxidizing conditions. For the metal-coordination driven self-assembly of $^{H63/H98}$RhuA, two different divalent metal ions (Zn^{2+} and Cu^{2+}) that can accommodate the desired four-coordinate geometries and various buffering agents were screened, which can influence metal coordination by regulating both the solution pH and effective metal ion concentration. It was found that the self-assembly of all three variants was robust and occurred under a broad range of conditions (protein concentrations ranging from 25 to 175 μM, all methods of oxidation, metal identity, and 6<pH<8) at 4° C. The following solution conditions yielded 2D assemblies that were optimized in terms of size, crystallinity, yield and reproducibility: ^{C98}RhuA and $^{F88/C98}$RhuA (≥125 μM protein, 10 mM βME, pH 7.5, 10 mM TRIS); $^{H63/H98}$RhuA (25 μM protein, 200 μM $ZnCl_2$, pH 7, 20 mM MOPS). Under these conditions, ^{C98}RhuA reproducibly and in high yield assembled into straight-edged, single- or few-layered 2D crystals that grew to several μm's over several days (**Figure 11A, 11D and 11E**). Transmission electron microscopy (TEM) measurements revealed that the ^{C98}RhuA crystals were highly ordered and possessed uniform, square shapes with molecularly sharp boundaries, which has not been previously observed in designed 2D protein crystals ((J. C. Sinclair, K. M. Davies, C. Venien-Bryan, M. E. M. Noble, *Nat. Nanotechnol.* 6, 558

(2011); J. D. Brodin *et al.*, *Nat. Chem.* 4, 375 (2012); N. P. King *et al.*, *Science* 336, 1171 (2012); S. Gonen, F. DiMaio, T. Gonen, D. Baker, *Science* 348, 1365 (2015))). In many instances, the growing lattice edges and the surface attachment points of individual ^{C98}RhuA molecules could be clearly visualized (**Figure 15**), suggesting that further growth of ^{C98}RhuA crystals was limited by the depletion of ^{C98}RhuA molecules from solution. 2D crystals of $^{H63/H98}$RhuA (**Figures 11B and 17**) and $^{F88/C98}$RhuA (**Figures 11C and 18**) were several hundred nm's to 1 μm in size, but typically displayed irregular morphologies. $^{H63/H98}$RhuA lattices were monocrystalline but tended to grow in 3D over time, whereas $^{F88/C98}$RhuA crystals consisted of aggregates of smaller, single-layered poly-crystalline domains. Self-assembly of all three variants was reversible upon addition of high concentrations of βME (>20 mM) or the metal chelator ethylene-diaminetetraacetic acid (EDTA, >10 mM) as judged by the disappearance of the cloudiness of the suspensions and by TEM measurements (**Figure 19**).

[0178] The computed diffraction patterns from negative stain (ns) TEM images are consistent with $P42_12$ plane group symmetry for ^{C98}RhuA and $^{F88/C98}$RhuA, and $P4$ symmetry for $^{H63/H98}$RhuA crystals (**Figures 11 and 20**). There is excellent agreement between experimental 2D EM projection maps and those calculated from structural models (Fig 20). The square shape of the RhuA building blocks combined with the small footprints of the disulfide- and metal-mediated interactions makes the molecular arrangements in the 2D reconstructions unambiguous (**Figure 11**, columns iv and v) and confirms the expected protein-protein interaction geometries: corner-attached ^{C98}RhuA and $^{H63/H98}$RhuA, and side-attached $^{F88/C98}$RhuA. There are small but clearly distinguishable differences between the relative orientations of RhuA tetramers in the ^{C98}RhuA and $^{H63/H98}$RhuA lattices, owing to the geometric differences between disulfide- and metal-mediated linkages. As illustrated in **Figure 10B**, the plane group symmetries suggest that ^{C98}RhuA tetramers adopt a checkerboard pattern (alternating up and down; $P42_12$ symmetry) whereas $^{H63/H98}$RhuA tetramers self-assemble in the same orientation with respect to the 2D plane ($P4$ symmetry). Together with the fact that $^{F88/C98}$RhuA possesses two-fold symmetry parallel to the 2D plane, the three distinct 2D molecular patterns were obtained with minimal alteration of a single protein building block. Different views of the three lattices are shown in **Figure 21**. It is

noteworthy that ^{C98}RhuA and $^{H63/H98}$RhuA molecules self-assemble in specific and distinct orientations in the 2D plane despite limited protein interaction surfaces. Although atomic resolution structures are necessary to determine how these orientational specificites arise, it was postulated that the energetic bias stemming from disulfide or metal coordination configurations and the surrounding protein-protein interactions must be sufficiently large to favor one orientation over others to yield long-range crystalline order.

[0179] The superior quality and the larger sizes of ^{C98}RhuA crystals compared to the $^{F88/C98}$RhuA and $^{H63/H98}$RhuA lattices can be readily explained by the bonding interactions that direct the self-assembly of the three variants. The $^{F88/C98}$RhuA building block presents a roughly circular distribution of eight cysteines (**Figure 10A**, bottom row). This arrangement renders the desired double-disulfide-mediated, side-to-side self-assembly mode non-unique and permits alternate attachment geometries between $^{F88/C98}$RhuA molecules (**Figure 18**). Moreover, the increased poly-Cys-valency of $^{F88/C98}$RhuA leads to considerably stronger, less reversible intermolecular interactions and therefore "stiffer" lattices: in fact, the dissolution of $^{F88/C98}$RhuA polycrystallites require significantly higher amounts of βME and longer incubation periods compared to the ^{C98}RhuA lattice (**Figure 19**). Consequently, $^{F88/C98}$RhuA crystals display frequently lattice vacancies as well as both high- (>30°) and low-angle (<10°) grain boundaries (**Figure 18B**). $^{H63/H98}$RhuA crystals possess significantly fewer such defects owing to the reversibility and the orientational specificity of Zn^{2+}-coordination interactions. Yet, each $^{H63/H98}$RhuA building block also contains numerous surface residues that can weakly coordinate Zn^{2+} ions, promoting crystal growth in the third dimension (**Figure 17A**).

[0180] In contrast to $^{F88/C98}$RhuA and $^{H63/H98}$RhuA, the self-assembly of ^{C98}RhuA is both chemically and orientationally specific. Moreover, the reversibility and inherent flexibility of single Cys-Cys linkages–containing five rotatable bonds–likely allows for the correction of any defects such as step or surface vacancies and grain boundaries, which would be difficult to accomplish in a rigid lattice composed of strongly interacting building blocks such as $^{F88/C98}$RhuA. Indeed, as TEM images of mono-layered ^{C98}RhuA crystals indicate, the outcomes are a) macroscopic crystal morphologies that reflect the molecular symmetry of the building blocks, b) molecularly sharp crystal boundaries, and c) lattices with very low defect frequencies. In hundreds of monocrystalline ^{C98}RhuA lattices with surface areas >1 μm^2 that

were examined closely, a single lattice defect was not detected (vacancies or grain boundaries), despite the fact that these crystals grow in 3D space in an unsupported fashion. In a rare instance where a single lattice vacancy was found, the defect frequency still was one missing ^{C98}RhuA molecule in a 2D grid of ~9000 molecules (~0.6 μm^2) (**Figure 22**).

[0181] A perhaps more striking consequence of the flexibility of Cys-Cys linkages is the coherent dynamicity of the ^{C98}RhuA crystals. While our initial preparations predominantly yielded open lattices with large pores (**Figure 11A**), the sample suspensions developed over several days a sediment of ^{C98}RhuA crystals, which featured a densely packed lattice arrangement. Upon resuspension of these sedimented crystals with gentle mechanical agitation and subsequent TEM analysis of the resulting samples, at least seven distinct types of 2D ^{C98}RhuA crystals in different conformational states (I through VII) were captured (**Figures 12A and 23**). These conformational snapshots implicate a continuous motion of the lattice between fully open and fully closed states, afforded by a remarkable extent of hinging about the flexible Cys-Cys linkages. The transition from the open to the closed state is accompanied by the compression of the inter-^{C98}RhuA hinge angle (α) from >80° to 17°, the decrease of the pore size from ~4.4 nm to ~1.0 nm (for the passage of a spherical object), and an increase in the relative protein/hole surface density (per unit cell) of 170% (**Figure 12B and Table 1**).

	Open (II)	Intermediate (V)	Closed (VII)
Unit cell (a=b, γ)	114.4 Å, 90°	110.0 Å, 90°	107.8 Å, 90°
Intertetramer hinge angle, α	79°	49°	17°
Protein surface area per unit cell, $A_{protein}$	84.9 nm^2	86.2 nm^2	88.0 nm^2
Pore surface area per unit cell, A_{pore}	46.0 nm^2	34.7 nm^2	28.2 nm^2
Relative protein/pore density, $A_{protein}/A_{pore}$	1.8	2.5	3.1

[0182] Table 1. Structural parameters for conformations II, V and VII of ^{C98}RhuA crystals derived from images shown in **Figure 12**.

[0183] Conformational dynamics of ^{C98}RhuA crystals are fully coherent: in each crystal examined, only one type of conformational state is observed throughout the lattice and the overall $P42_12$ plane group symmetry is preserved (**Figure 12B**). This observation implies that any mechanical deformation of a ^{C98}RhuA crystal is rapidly and cooperatively propagated in the 2D lattice, enabled by both the flexibility and short linker-length of the Cys-Cys linkages: a longer, more flexible type of linkage would preclude coherent dynamics, whereas an inflexible linkage would lead to non-adaptive lattices. Conformational dynamics of the ^{C98}RhuA crystals are reversible as indicated by the interconversion of the open and closed conformational states during repeated sedimentation/resuspension cycles (**Figure 12C**). It was posited that the energetic activation barriers between different ^{C98}RhuA lattice conformations (due to different Cys-Cys configurations and long-range protein-protein interactions) must be small enough to be overcome by mechanical agitation and internal protein dynamics.

[0184] Geometric considerations (**Figure 12D**) indicate that ^{C98}RhuA crystals are auxetic, with a Poisson's ratio of –1. Poisson's ratio (ν) is a scale-independent metric that describes the response of a material to strain; it is defined as the ratio between transverse (e_x) and longitudinal strains (e_y) under uniaxial loading (G. N. Greaves, A. Greer, R. Lakes, T. Rouxel, *Nat. Mater.* 10, 823 (2011)). e_x and e_y are, in turn, approximated by changes in material length in transverse (ΔX) and longitudinal (ΔY) directions (G. N. Greaves, A. Greer, R. Lakes, T. Rouxel, *Nat. Mater.* 10, 823 (2011)):

$$\nu = -\frac{e_y}{e_x} \approx -\frac{\Delta Y}{\Delta X}$$

where $-1 \leq \nu \leq 0.5$ for an isotropic material. Most materials possess positive Poisson's ratios, *i.e.*, they become thinner in the longitudinal direction when stretched transversely (G. N. Greaves, A. Greer, R. Lakes, T. Rouxel, *Nat. Mater.* 10, 823 (2011)). Materials with negative Poisson's ratios (*i.e.*, auxetic materials), on the other hand, display the counterintuitive behavior of longitudinal expansion upon transverse stretching. Thus, auxetic materials can be expected to possess enhanced toughness, resistance to indentation, and shear stiffness, and have been proposed for use in body armors, smart textiles, actuated filtration and piezoelectric devices, among many others (G. N. Greaves, A. Greer, R. Lakes, T. Rouxel,

Nat. Mater. 10, 823 (2011); K. E. Evans, A. Alderson, *Adv. Mater.* 12, 617 (2000); R. H. Baughman, *Nature* 425, 667 (2003)). Although natural and synthetic materials with negative Poisson's ratios exist, most fall in the range of $-0.4<\nu<0$, with the lowest value reported of –0.7, observed in reentrant polyurethane foams (R. Lakes, *Science* 235, 1038 (1987)). It was postulated that for a 2D lattice of rotating rigid squares with flexible hinges, the Poisson's ratio should be negative at all rotation angles and equal to the lowest thermodynamically permissible value of –1 (J. Grima, A. Alderson, K. Evans, *Phys. Stat. Sol. b* 242, 561 (2005)). ^{C98}RhuA lattices represent a true realization of this theoretical model at the molecular scale and represent–to our knowledge–the first synthetic or natural isotropic material with $\nu = -1$. In the embodiments described herein, the 2D crystalline material comprises a Poisson's ratio of -1.

It was envisioned that upon hierarchical assembly through physical methods, molecular architectures like 2D ^{C98}RhuA lattices can be used as feedstocks for adaptive and auxetic macroscopic materials. Of particular importance is the observation that compression and expansion of ^{C98}RhuA-type, "rotary" lattices occur without the deformation of individual building blocks, thereby opening the way for incorporating their inherent molecular functions and properties into higher-order assemblies. Due to their chemical tunability, reproducible production and high structural quality, ^{C98}RhuA lattices provide an ideal medium for studying molecular self-assembly, crystal nucleation and growth. The resulting understanding of structural/lattice dynamics at the nanoscale should greatly aid the fabrication of functional materials.

Example 1-Design of RhuA variants and site-directed mutagenesis

[0185] RhuA variants were designed as described above based on previously reported crystal structures (PDB ID: 1OJR for ^{C98}RhuA and $^{H63/H98}$RhuA (P. Ringler, G. E. Schulz, *Science* **302**, 106 (2003)) and PDB ID 2UYU for $^{F88/C98}$RhuA (D. Grueninger *et al.*, *Science* **319**, 206 (2008)). All RhuA variants also contain the mutations E192A and C126S as reported in (P. Ringler, G. E. Schulz, *Science* 302, 106 (2003)) and (D. Grueninger *et al.*, *Science* 319, 206 (2008)). The gene for ^{C98}RhuA, pre-inserted into the pJ414 expression vector optimized for expression in *E. coli* (Ampicillin resistant), was purchased from DNA2.0. $^{F88/C98}$RhuA and $^{H63/H98}$RhuA were prepared using QuikChange mutagenesis

(Stratagene) with primers obtained from Integrated DNA Technologies (Table 2). The mutant plasmids were transformed into XL-1 Blue *E. coli* cells followed by purification using the QIAprep Spin Miniprep kit (Qiagen). The presence of the mutations was verified by sequencing (Retrogen).

^{C98}RhuA Sequence (SEQ ID NO: 3):

MQNITQSWFVQGMIKATTDAWLKGWDERNGGNLTLRLDDADIAPYHDNFHQQPRY
IPLSQPMPLLANTPFIVTGSGKFFRNVQLDPAANLGIVKVDSCGAGYHILWGLTNEAV
PTSELPAHFLSHSERIKATNGKDRVIMHCHATNLIALTYVLENDTAVFTRQLWEGSTE
CLVVFPDGVGILPWMVPGTDAIGQATAQEMQKHSLVLWPFHGVFGSGPTLDETFGLI
DTAEKSAQVLVKVYSMGGMKQTISREELIALGKRFGVTPLASALAL

$^{H63/H98}$RhuA Sequence (SEQ ID NO: 4):

MQNITQSWFVQGMIKATTDAWLKGWDERNGGNLTLRLDDADIAPYHDNFHQQPRY
IPLSQPMHLLANTPFIVTGSGKFFRNVQLDPAANLGIVKVDSHGAGYHILWGLTNEAV
PTSELPAHFLSHSERIKATNGKDRVIMHCHATNLIALTYVLENDTAVFTRQLWEGSTE
CLVVFPDGVGILPWMVPGTDAIGQATAQEMQKHSLVLWPFHGVFGSGPTLDETFGLI
DTAEKSAQVLVKVYSMGGMKQTISREELIALGKRFGVTPLASALAL

$^{F88/C98}$RhuA Sequence (SEQ ID NO: 5):

MQNITQSWFVQGMIKATTDAWLKGWDERNGGNLTLRLDDADIAPYHDNFHQQPRY
IPLSQPMPLLANTPFIVTGSGKFFRNVQLDPAFNLGIVKVDSCGAGYHILWGLTNEAV
PTSELPAHFLSHSERIKATNGKDRVIMHCHATNLIALTYVLENDTAVFTRQLWEGSTE
CLVVFPDGVGILPWMVPGTDAIGQATAQEMQKHSLVLWPFHGVFGSGPTLDETFGLI
DTAEKSAQVLVKVYSMGGMKQTISREELIALGKRFGVTPLASALAL

Example 2-Protein expression and purification

[0186] Bacterial expression of RhuA variants was performed according to previously published procedures with slight modifications (M. Kroemer, G. E. Schulz, *Acta Cryst. D* **58**, 824 (2002)). Plasmids bearing the variants were transformed into BL21(DE3) *E. coli* cells, and the colonies were grown overnight at 37 °C on lysogeny broth (LB) agar plates (pH 7.4) containing 100 mg/L ampicillin. Starter cultures (5 mL with 100 mg/L ampicillin)

from single colonies were grown for ~4-6 h at 37 °C (with shaking at 250 rpm) before inoculation into 1-L LB cultures containing 100 mg/L ampicillin. After the cells were grown to an optical density of ~0.8 at 600 nm, protein expression was induced with 1 mM isopropyl β-D-1-thiogalactopyranoside (IPTG, Gold Biotechnology) for 12 – 13 h (at 37 °C with shaking at 250 rpm). Cells were pelleted by centrifugation (5,000 rpm at 4 °C for 10 min), and resuspended in a buffer solution containing 10 mM Tris(hydroxymethyl)aminomethane hydrochloride (TRIS) (pH 7.5), 1 mM $ZnCl_2$, and 10 mM β-mercaptoethanol (βME). For $^{H63/H98}$RhuA preparations, $ZnCl_2$ was excluded from buffer solutions to avoid possible protein precipitation during purification. Cell lysis was performed by sonication for 15 min on ice. The lysis solution was centrifuged for 30 min at 12,000 rpm at 4 °C. Polymin-P (Acros) was added to the supernatant at a final concentration of 0.15% (w/v) for nucleic acid precipitation and the resulting mixture was stirred for 30 min prior to centrifugation for 30 min at 12,000 rpm at 4 °C. The supernatant was loaded onto a DEAE-Sepharose CL-6B (GE Healthcare) column and eluted using a gradient of 0 – 500 mM NaCl in Tris buffer at 4 °C. Fractions containing RhuA which eluted at ~ 200 mM NaCl were added 1.7 M ammonium sulfate, and were centrifuged for 45 min at 12,000 rpm at 4 °C. The precipitate was dissolved in a buffer solution containing 5 mM sodium phosphate (NaPi) (pH 7.2), 1 mM $ZnCl_2$, and 10 mM βME, and then dialyzed three times against 5 L of the same buffer solution. Further purification was done using either a High Q cartridge column (BioRad) (at pH 8.0) using a 0-500 mM NaCl gradient or a Mini CHT™ Type I hydroxyapatite column (BioRad) (at pH 7.2) using a 5-500 mM NaPi gradient on a DuoFlow fast protein chromatography workstation (Bio-Rad). Pure protein fractions eluted at 350 mM NaCl and 200 mM NaPi, respectively. These fractions were combined, dialyzed three times against a buffer solution of 10 mM TRIS (pH 7.5), 1 mM $ZnCl_2$, and 10 mM β-mercaptoethanol (βME), and concentrated in an Amicon stirred cell at 4 °C. The protein was then flash frozen and kept at −80 °C until use. Protein purity was confirmed by SDS-PAGE (**Figure 13**) and ESI-MS (**Figure 14 and Table 3**), and stock concentrations (~100-175 μM for ^{C98}RhuA and $^{F88/C98}$RhuA; 100 μM for $^{H63/H98}$RhuA) was determined as previously reported (H. Edelhoch, *Biochemistry* **6**, 1948 (1967)).

[0187] Purification techniques can be performed using standard protein purification kits, columns, and methods and are known to those skilled in the art. In some embodiments described herein, the polypeptides or proteins purified for use in creating the 2D crystalline material is purified to a purity of 80%, 85%, 90%, 95% or 100% purity or any percent purity in between a range defined by any two aforementioned values.

Example 3-Preparation of 2D RhuA crystals

[0188] All 2D RhuA crystals reported herein were obtained in an unsupported fashion in solutions. Several solution conditions were screened for optimizing the formation of 2D protein crystals of ^{C98}RhuA, $^{F88/C98}$RhuA and $^{H63/H98}$RhuA variants. For all variants, these screening conditions included various pH's (6 to 8), starting protein concentrations (25 to 175 μM), buffer salt concentration and identity (5 – 20 mM bis-TRIS, CHES, MES, MOPS, NaPi, and TRIS), and temperature (4 – 37 °C).In some embodiments, the polypeptides are screened for formation of 2D crystals in buffers that comprise a pH of 5, 5.5, 6, 6.5, 7, 7.5, 8 or 8.5 or any pH in between a range defined by any two aforementioned values. For the disulfide-mediated self-assembly of ^{C98}RhuA and $^{F88/C98}$RhuA, various oxidizing conditions were additionally screened (1 – 2 mM total GSH/GSSG at ratios varying from 1:19 to 19:1, or 5 – 10 mM βME, which slowly decomposed in aqueous solution in the presence of metal ions). For the metal-mediated assembly of $^{H63/H98}$RhuA, 4 – 20 molar equivalents (over protein concentration) of $ZnCl_2$ and $CuCl_2$ were screened. As stated, in some of the embodiments herein, the best conditions were: ^{C98}RhuA and $^{F88/C98}$RhuA (≥125 μM protein, 10 mM βME, pH 7.5, 10 mM TRIS); $^{H63/H98}$RhuA (25 μM protein, 200 mM $ZnCl_2$, pH 7, 20 mM MOPS) at 4 °C. In general, the formation of crystals was either immediate (upon metal addition for $^{H63/H98}$RhuA) or lasted overnight to several days (for ^{C98}RhuA and $^{F88/C98}$RhuA). Crystal formation resulted in increasing cloudiness of the self-assembly solutions. The growth of ^{C98}RhuA crystals could be accelerated by gentle shaking (compare **Figures 15 and 16**). In some embodiments of the methods of forming the 2D crystalline material, the crystal formation is accelerated by gentle shaking.

Example 4-TEM measurements and image processing

[0189] For TEM sample preparation, 3 – 3.5 μL aliquots of crystal suspensions were applied onto a negatively glow-discharged carbon-coated Cu grids (Ted Pella, Inc),

washed with Milli-Q water, and stained with 1% uranyl acetate at 4 °C. Sample screening was preformed in an FEI Sphera transmission electron microscope equipped with a LaB_6 electron gun at 200 keV and imaged on Gatan $2K^2$ CCD.

[0190] Selected micrographs were each processed separately using the 2dx software package (B. Gipson, X. Zeng, Z. Y. Zhang, H. Stahlberg, *J. Struct. Biol.* 157, 64 (2007)) to determine 2D plane group lattice symmetry of each crystal, to calculate their unit cell dimensions and to generate a projection density map of each crystal. The estimated resolution limit of each image (between 15 and 30 Å) was assessed by visual inspection of its computed Fourier transform.

Example 5-Structural modeling and simulations

[0191] Projected electron density maps were used as a reference in the visualization software UCSF Chimera (E. F. Pettersen *et al.*, *J. Comput. Chem.* 25, 1605 (2004)) to determine the orientation of the RhuA molecules in each crystal. The atomic coordinates were extracted from the PDB entries 1OJR (C_4-symmetric tetramer for ^{C98}RhuA and $^{H63/H98}$RhuA) and 2UYU (D_4-symmetric octamer for $^{F88/C98}$RhuA) and placed manually to fit the position of one subunit in the observed projected density map. The orientation of the molecule was refined in an iterative manner by comparing the experimental density with the density simulated from a model of the unit cell, obtained as explained below.

[0192] Simulated projected electron density maps were computed using Bsoft (lsbr.niams.nih.gov/bsoft) (J. B. Heymann, *J. Struct. Biol.* 133, 156 (2001)) and EMAN2 (blake.bcm.edu/emanwiki/EMAN2) (G. Tang *et al.*, *J. Struct. Biol.* 157, 38 (2007)). Starting from the estimated position and orientation of a single subunit, multiple copies of the model were generated to cover one unit cell (*bmoledit* in Bsoft) and converted to electron density (*e2pdb2mrc.py* in EMAN2) with a resolution limit of 30 Å. Finally, the density volume was projected along the vertical direction (*bproject* in Bsoft) to generate a 2D density map comparable to the experimental map.

Example 6-Classification of the conformational states of 2D ^{C98}RhuA crystals

[0193] TEM micrographs of ^{C98}RhuA crystals were analyzed computationally to categorize different conformational states of the 2D lattice. Essentially, for each raw image it was determined a roundness index number derived from the shape of the pores in the lattice,

and used this value to classify the images. The analysis was performed using an *ad hoc* algorithm coded as a macro in Fiji (fiji.sc/Fiji) (J. Schindelin *et al.*, *Nat. Meth.* 9, 676 (2012)) and ImageJ (imagej.nih.gov/ij/) (C. A. Schneider, W. S. Rasband, K. W. Eliceiri, *Nat. Methods* 9, 671 (2012)). Each image was initially processed by applying a 3×3 mean filter applied three times, and then it was converted to a binary image after automatic thresholding to segment out the pores. The mask was then filtered using the opening morphological operator to smooth the shape of the pores and to remove small outliers. Pores that were distorted from potential bending of the crystal in some regions of the field of view were discarded using their size for screening. For images acquired at a nominal magnification of × 50,000 and × 68,000 (calibrated pixel size = 2.033 Å and 1.646 Å, respectively), only pores with areas that covered 500–1200 pixels were kept. The remaining pores were modeled as ellipses and their roundness index was determined as the ratio between the lengths of the major and the minor elliptical axes. A single index value was assigned to each micrograph as the average from all the segmented pores. The images were assigned to one of the seven identified states using the following criterion: State I: >0.85; State II: >0.75 – 0.85; State III: >0.65 – 0.75; State IV: >0.55 – 0.65; State V: >0.35 – 0.45; State VI: >0.35 – 0.45; State VII <0.35.

Variant	Mutation	Primer Sequence
$^{F88/C98}$RhuA	A88F	5'-CGCAATGTCCAGTTGGACCCAGCGTTTAACCTGGGCATTG TTAAGGTGG-3' (SEQ ID NO: 6) 5'-CCACCTTAACAATGCCCAGGTTAAACGCTGGGTCCAACTG GACATTGCG-3' (SEQ ID NO: 7)
$^{H63/H98}$RhuA	P63H C98H	5'- CGCTGAGCCAGCCGATGCATCTGTTGGCGAATACCC -3' (SEQ ID NO: 8) 5'- GGGTATTCGCCAACAGATGCATCGGCTGGCTCAGCG -3' (SEQ ID NO: 9) 5'- GGGCATTGTTAAGGTGGATAGCCATGGTGCAGGTTACCAC ATCC-3' (SEQ ID NO: 10)

		5'- GGATGTGGTAACCTGCACCATGGCTATCCACCTTAACAAT GCCC -3' (SEQ ID NO: 11)

Table 2. List of primers used in constructing site-directed mutants of RhuA using C98RhuA as a base.

Variant	Calculated Mass (Da)	Observed Mass (Da)
^{C98}RhuA	30059.5	30060.0
$^{F88/C98}$RhuA	30135.6	30136.0
$^{H63/H98}$RhuA	30133.5	30134.0

[0194] Table 3. Positive ESI-MS characterization of RhuA mutants. For the actual mass spectra, refer to **Figure 14**.

[0195] Two-dimensional (2D) crystalline materials possess unique structural, mechanical, and electronic properties (Mas-Balleste, R., Gomez-Navarro, C., Gomez-Herrero, J. & Zamora, F. 2D materials: to graphene and beyond. *Nanoscale* 3, 20-30, (2011); Butler, S. Z. *et al.* Progress, challenges, and opportunities in two-dimensional materials beyond graphene. *ACS Nano* 7, 2898-2926, (2013)), which have rendered them highly attractive in many applications (Schedin, F. *et al.* Detection of individual gas molecules adsorbed on graphene. *Nat. Mater.* 6, 652-655, (2007); Lu, C.-H., Yang, H.-H., Zhu, C.-L., Chen, X. & Chen, G.-N. A Graphene Platform for Sensing Biomolecules. *Angew. Chem. Int. Ed. Engl.* 121, 4879-4881, (2009); Joshi, R. K. *et al.* Precise and Ultrafast Molecular Sieving Through Graphene Oxide Membranes. *Science* 343, 752-754, (2014)). Although there have been advances in preparing 2D materials that consist of one or few atomic/molecular layers (Nicolosi, V., Chhowalla, M., Kanatzidis, M. G., Strano, M. S. & Coleman, J. N. Liquid exfoliation of layered materials. *Science* 340, 1226419, (2013); Li, D., Muller, M. B., Gilje, S., Kaner, R. B. & Wallace, G. G. Processable aqueous dispersions of graphene nanosheets. *Nat. Nano.* 3, 101-105, (2008)), bottom-up assembly of 2D crystalline materials remains a considerable challenge and an active area of development (Colson, J. W. *et al.* Oriented 2D

covalent organic framework thin films on single-layer graphene. *Science* 332, 228-231, (2011; Kissel, P., Murray, D. J., Wulftange, W. J., Catalano, V. J. & King, B. T. A nanoporous two-dimensional polymer by single-crystal-to-single-crystal photopolymerization. *Nat. Chem.* 6, 774-778, (2014); Kory, M. J. *et al.* Gram-scale synthesis of two-dimensional polymer crystals and their structure analysis by X-ray diffraction. *Nat. Chem.* 6, 779-784, (2014)). Even more challenging is the design of dynamic 2D lattices that can undergo large-scale motions without loss of crystallinity. Dynamicity in porous 3D crystalline solids has been exploited for stimuli-responsive functions and adaptive behavior (Shimomura, S. *et al.* Selective sorption of oxygen and nitric oxide by an electron-donating flexible porous coordination polymer. *Nat. Chem.* 2, 633-637, (2010); Rabone, J. *et al.* An adaptable peptide-based porous material. *Science* 329, 1053-1057, (2010); Serre, C. *et al.* Role of solvent-host interactions that lead to very large swelling of hybrid frameworks. *Science* 315, 1828-1831, (2007)). As in the case of such 3D materials, integrating flexibility/adaptiveness into crystalline 2D lattices would greatly broaden the functional scope of 2D materials. As described herein is the self-assembly of unsupported, 2D protein lattices with precise spatial arrangements and patterns through a readily accessible design strategy. Three single- or double-point mutants of the C_4 symmetric protein RhuA were designed to assemble via different modes of intermolecular interactions (single disulfide, double disulfide and metal coordination) into crystalline 2D arrays. Owing to the flexibility of the single disulfide interactions, the lattices of one of the variants (^{C98}RhuA) are essentially defect-free and undergo substantial but fully correlated changes in molecular arrangement, giving coherently dynamic 2D molecular lattices. Notably, ^{C98}RhuA lattices possess a Poisson's ratio of –1, the lowest thermodynamically possible value for an isotropic material. In some of the embodiments described herein, the 2D crystalline material comprises a Poisson's ratio of -1.

[0196] Proteins are attractive building blocks for 2D materials because of their structural/chemical diversity and inherent functions. Examples for natural, protein-based 2D materials can include, but are not limited to bacterial S-layer proteins and purple-membrane assemblies, which form crystalline arrays in association with cell walls and membranes, respectively, and have been employed in diverse technological applications (Sleytr, U. B.,

Schuster, B., Egelseer, E. M. & Pum, D. S-layers: principles and applications. *FEMS Microbiol. Rev.* 38, 823 – 864, (2014), Hampp, N. Bacteriorhodopsin as a photochromic retinal protein for optical memories. *Chem. Rev.* 100, 1755-1776, (2000)). On the synthetic front, methods for 2D protein crystallization have been developed for the structural characterization of membrane proteins (Engel, A. *et al.* Assembly of 2-D membrane protein crystals: dynamics, crystal order, and fidelity of structure analysis by electron microscopy. *J. Struct. Biol.* 109, 219-234, (1992); Stahlberg, H. *et al.* Two-dimensional crystals: a powerful approach to assess structure, function and dynamics of membrane proteins. *FEBS Lett.* 504, 166-172, (2001)) or functional applications (Saboe, P. O. *et al.* Two-Dimensional Protein Crystals for Solar Energy Conversion. *Adv. Mater.* 26, 7064-7069, (2014)), generally relying on lipid layers as supports. Recently, 2D or 3D supramolecular protein arrays have been designed through the symmetric polymerization of protein building blocks via computationally designed protein-protein interactions or fusion of protein components (Sinclair, J. C., Davies, K. M., Venien-Bryan, C. & Noble, M. E. M. Generation of protein lattices by fusing proteins with matching rotational symmetry. *Nat. Nanotechnol.* 6, 558-562, (2011); Brodin, J. D. *et al.* Metal-directed, chemically tunable assembly of one-, two- and three-dimensional crystalline protein arrays. *Nat. Chem.* 4, 375-382, (2012); Gonen, S., DiMaio, F., Gonen, T. & Baker, D. Design of ordered two-dimensional arrays mediated by noncovalent protein-protein interfaces. *Science* 348, 1365-1368, (2015); Lanci, C. J. *et al.* Computational design of a protein crystal. *Proc. Natl. Acad. Sci. USA* 109, 7304-7309, (2012)). While elegant, these approaches are engineering-intensive and highly dependent on the accuracy of the design, and the integration of dynamic/adaptive behavior has not been explored.

[0197] In order to address these issues, described herein is a developed simple chemical bonding strategy to control protein self-assembly. It was reasoned that both cysteine (Cys)-mediated disulfide bonds and metal coordination interactions between protein building blocks can produce crystalline and dynamic arrays with minimal design, because these bonds are: 1) strong but reversible (to minimize the surface area to be designed and ensure self-healing), 2) short yet sufficiently flexible (to simultaneously afford crystallinity and adaptiveness), and 3) chemically tunable (to exert external control over self-assembly and

enable stimuli-responsiveness), and 4) easily designed and engineered. In some embodiments described herein, cysteine (Cys)-mediated disulfide bonds and metal coordination interactions between protein building blocks can produce crystalline and dynamic arrays with minimal design. In some embodiments, the cysteine bonds are strong but flexible. In some embodiments, the cysteine bonds and metal coordination interactions are strong but flexible. In some embodiments, the bonds are short yet sufficiently flexible. In some embodiments, the bonds are chemically tunable. In some embodiments, the bonds are easily designed and engineered.

[0198] The most straightforward route to obtaining 2D lattices is the tesselation of C_3, C_4 or C_6 symmetric building blocks through appropriately positioned C_2 symmetric linkages such as disulfide bonds or many metal coordination interactions. As such, as described in several embodiments herein, 2D lattices were produced by the methods herein to have C_3, C_4 or C_6 symmetric building blocks through appropriately positioned C_2 symmetric linkages such as disulfide bonds or many metal coordination interactions . As a model building block, L-rhamnulose-1-phosphate aldolase (RhuA), and a C_4 symmetric homotetramer (dimensions: 7×7×5 nm) that was previously used as a synthon for supramolecular assemblies, were chosen (Ringler, P. & Schulz, G. E. Self-assembly of proteins into designed networks. *Science* 302, 106-109, (2003)) (**Figure 10A**). An inspection of RhuA indicated protrusions in the four corner positions as ideal locations to incorporate single Cys or two histidine (His) residues for disulfide- or metal-directed self-assembly, respectively. As described in some embodiments described herein, two variants were generated, ^{C98}RhuA and $^{H63/H98}$RhuA, with four conditionally self-associating corners for forming square lattices (**Figure. 10A, 10B**, top and middle rows). The relative positions of residues 63 and 98 were deemed to be conducive to forming a bis-His metal coordination motif to afford a tetrahedral or square planar coordination geometry for metal-mediated RhuA pairing interactions. Additionally, it was noted that RhuA could be converted into a stable D_4 symmetric octamer through a single point mutation (A88F) (Grueninger, D. *et al.* Designed protein-protein association. *Science* 319, 206-209, (2008)). Thus, a third variant, $^{F88/C98}$RhuA, was prepared, which presents eight symmetry-related cysteines at roughly 45° angles in a 2D projection (**Figure. 10A**, bottom row). It was envisioned that the C_4

symmetric ^{C98}RhuA and $^{H63/H98}$RhuA variants could yield square lattices with two distinct patterns in terms of the orientation of the building blocks with respect to the 2D plane (**Figure 10B**). On the other hand, the D_4 symmetry of $^{F88/C98}$RhuA would dictate a 2D lattice with equivalent faces (**Figure 10B**). These RhuA building blocks would also provide three distinct modes of inter-building-block interactions, whose effects on self-assembly were to be investigated, such as single disulfide, double disulfide and bis-His-anchored metal coordination.

[0199] For the oxidative self-assembly of ^{C98}RhuA and $^{F88/C98}$RhuA, various strategies were tested including air oxidation, redox buffer systems containing reduced and oxidized glutathione (GSH and GSSG) or low concentrations (≤10 mM) of the reductant β-mercaptoethanol (βME), which slowly decomposes in aqueous solution and results in gradually more oxidizing conditions. In these experiments, solutions of purified ^{C98}RhuA and $^{F88/C98}$RhuA were first rapidly exchanged via repeated centrifugal filtration into solutions that varied in terms of their pH (6 to 8.5), buffering species (sodium phosphate, CHES, MES, MOPS, TRIS; at 5 to 20 mM), different compositions of the redox buffering system (1:19 or 19:1 GSH:GSSG; at 1 mM total concentration) or different concentrations of βME (0-10 mM). After adjustment to the desired final protein concentration (25 – 175 μM), these solutions were monitored for the formation of self-assembled structures by visual inspection for emergence of cloudiness and by transmission electron microscopy (TEM). Likewise, for metal-directed assembly, purified $^{H63/H98}$RhuA was exchanged into solutions with varying pH's and buffer ions (to modulate metal binding kinetics and thermodynamics), with the exception that these solutions did not contain any reductants. Self-assembly was initiated by addition of 4 – 40 molar equivalents of Zn^{2+} and Cu^{2+} (1-10 equiv. per bis-His motif), both of which can accommodate the desired four-coordinate geometries to link $^{H63/H98}$RhuA building blocks at their corners.

[0200] It was found that the assembly of all variants into 2D arrays was robust and occurred under a wide range of conditions. As expected, crystalline self-assembly was favored by conditions that promoted slow, controlled oxidation or slow metal-binding kinetics. For example, uncontrolled air oxidation of ^{C98}RhuA solutions or addition of large molar excess of Zn^{2+} and Cu^{2+} to $^{H63/H98}$RhuA samples resulted largely in amorphous

aggregates in addition to some crystalline domains (**Figure 10C and 10D**). The following solution conditions yielded 2D assemblies that were optimized in terms of size, crystallinity, and yield: ^{C98}RhuA and $^{F88/C98}$RhuA (≥125 μM protein, 10mM βME, pH 7.5, 10 mM TRIS); $^{H63/H98}$RhuA (25 μM protein, 200 μM $ZnCl_2$, pH 7, 20 mM MOPS). Under these conditions, ^{C98}RhuA reproducibly assembled into straight-edged, single- or few-layered 2D crystals that grew to several μm's over several days (**Figure 11A**). Negative-stain and cryo-TEM, scanning electron microscopy (SEM) and atomic force microscopy (AFM) measurements revealed that the ^{C98}RhuA crystals were highly ordered and possessed uniform square/rectangular shapes with molecularly sharp boundaries (**Figure 11A, 11D, 11E 12G, 12H and 12I**); these features have not been previously observed in designed 2D protein crystals (Sinclair, J. C., Davies, K. M., Venien-Bryan, C. & Noble, M. E. M. Generation of protein lattices by fusing proteins with matching rotational symmetry. *Nat. Nanotechnol.* 6, 558-562, (2011); Gonen, S., DiMaio, F., Gonen, T. & Baker, D. Design of ordered two-dimensional arrays mediated by noncovalent protein-protein interfaces. *Science* 348, 1365-1368, (2015)). 2D crystals of $^{H63/H98}$RhuA (**Figure 11B and 17**) and $^{F88/C98}$RhuA (**Figure 11C and 18**) were several hundred nm's to 1 μm in size, but typically displayed irregular morphologies. $^{H63/H98}$RhuA lattices were monocrystalline, but tended to grow in 3D over time, whereas $^{F88/C98}$RhuA crystals consisted of poly-crystalline domains.

[0201] As monitored by TEM and dynamic light scattering (DLS), self-assembly of all variants was reversible, either upon addition of high concentrations of βME (>10 mM) in the case of ^{C98}RhuA and $^{F88/C98}$RhuA crystals or ethylene-diaminetetraacetic acid (EDTA, >10 mM) in the case of $^{H63/H98}$RhuA (**Figure 19**). The variant ^{D98}RhuA, which bears the native D98 residue and is devoid of corner Cys's or the bis-His motifs, was not competent to self-assemble upon oxidation or metal addition (**Figure 60A**). These observations confirm the proposed modes of disulfide- or metal-mediated self-assembly. Two additional variants (^{C133}RhuA and ^{C266}RhuA) were prepared with surface cysteines located on the sides of the tetramers (**Figures 60B and 60C**). Theoretically, these variants could be envisioned to self-associate into close-packed 2D square lattices through disulfide linkages. Instead, they both formed non-crystalline aggregates upon oxidation, which was ascribed to the steric crowding around the C133 and C266 positions that precludes the orientation of RhuA molecules for

planar self-assembly. These experiments suggest that the placement of Cys residues at sterically isolated, corner locations is preferable for the formation of 2D crystalline arrays.

[0202] Exhaustive TEM analyses involving many crystals of each variant indicated $p42_12$ plane group symmetry for ^{C98}RhuA and $^{F88/C98}$RhuA, and p4 symmetry for $^{H63/H98}$RhuA crystals (**Figure 11**, **Figures. 61A, 61B, and Table** 8). These assignments were corroborated by electron diffraction (ED) data for ^{C98}RhuA and $^{H63/H98}$RhuA crystals (**Figure 61C**). Experimental 2D EM projection maps agree very well with those calculated from structural models (**Figure20**A) and confirm the expected protein-protein interaction geometries: corner-attached ^{C98}RhuA and $^{H63/H98}$RhuA, and side-attached $^{F88/C98}$RhuA (**Figure 11**, columns iv and v). Plane group symmetries suggest that ^{C98}RhuA tetramers adopt a checkerboard pattern ($p42_12$ symmetry) whereas $^{H63/H98}$RhuA tetramers self-assemble in the same orientation with respect to the 2D plane (p4 symmetry). Together with the fact that $^{F88/C98}$RhuA possesses two-fold symmetry parallel to the 2D plane, thus three distinct 2D molecular patterns with minimal alteration of a single protein building block were obtained (**Figure 20B**). It is noteworthy that ^{C98}RhuA and $^{H63/H98}$RhuA molecules self-assemble in distinct orientations in the 2D plane, suggesting that the energetic bias stemming from disulfide or metal bonding configurations and surrounding protein-protein interactions must be sufficiently large to favor one orientation over others to yield long-range order.

[0203] Superior quality and larger sizes of ^{C98}RhuA crystals compared to $^{F88/C98}$RhuA and $^{H63/H98}$RhuA lattices are readily explained by interactions that direct the self-assembly of the variants. $^{F88/C98}$RhuA presents a roughly circular distribution of eight cysteines (**Figure 10A**, bottom row). This arrangement renders the desired double-disulfide-mediated, side-to-side self-assembly mode non-unique and permits alternate attachment geometries between $^{F88/C98}$RhuA molecules (**Figure 18**). Moreover, the increased Cys-valency of $^{F88/C98}$RhuA leads to considerably stronger interactions and therefore "stiffer" lattices: in fact, the dissolution of $^{F88/C98}$RhuA polycrystallites requires significantly higher amounts of βME and longer incubation periods compared to ^{C98}RhuA lattices (**Figure 19**). Consequently, $^{F88/C98}$RhuA lattices display vacancies as well as both high- (>30°) and low-angle (<10°) grain boundaries (**Figure 18**). $^{H63/H98}$RhuA crystals possess fewer such defects owing to the reversibility of Zn^{2+}-coordination interactions. Yet, each $^{H63/H98}$RhuA building

block also contains numerous surface residues that can weakly coordinate Zn^{2+} ions, promoting crystal growth in the third dimension (**Figure 17A**).

[0204] In contrast to $^{F88/C98}$RhuA and $^{H63/H98}$RhuA, self-assembly of ^{C98}RhuA is both chemically and orientationally specific. Moreover, the reversibility and inherent flexibility of single Cys-Cys linkages–containing five rotatable bonds–likely allows for the correction of any defects such as vacancies and grain boundaries, which would be difficult to accomplish in a rigid lattice composed of strongly interacting building blocks such as $^{F88/C98}$RhuA. Indeed, as TEM images of mono-layered ^{C98}RhuA crystals illustrate, the outcomes are a) macroscopic crystal morphologies that reflect the molecular symmetry of the building blocks, b) molecularly sharp crystal boundaries, and c) lattices with extremely low defect frequencies. In hundreds of monocrystalline ^{C98}RhuA lattices with surface areas >1 μm^2 that were examined closely, a lattice defect was rarely found, despite the fact that these crystals grow in 3D space in an unsupported fashion. Even in a rare instance such as that shown in **Figure. 20C**, the defect frequency still was one missing ^{C98}RhuA molecule within a lattice grid of ~9000 molecules (~0.6 μm^2).

[0205] A more striking consequence of the disulfide bond flexibility is the coherent dynamicity of ^{C98}RhuA crystals. While the initial sample preparations of ^{C98}RhuA crystals predominantly yielded open lattices with large pores (**Figure 11A**), it was noticed that these crystal suspensions developed a dense sediment over a period of 1-3 days at 4 °C (**Figure 21A**). TEM analysis of these sedimented crystals indicated a close-packed lattice arrangement (**Figure 12A and 12B**, right panels). Upon resuspension of the sedimented crystals by repeated gentle mixing with a pipette and subsequent TEM imaging of the resulting samples, a total of at least seven types of 2D ^{C98}RhuA crystals in distinct conformational states were captured (I through VII) (**Figure 12A and 21B**). These conformational states were categorized by computational image analysis according to the roundness indices of the lattice pores, ranging from ≥0.85 for State I to ≤0.35 for State VII (see Methods). As evidenced by the retention of $p42_12$ symmetry and nearly equal unit cell dimensions, these seven conformational states are clearly interconnected and implicate a continuous lattice motion between fully open and fully closed states. These large amplitude motions of the ^{C98}RhuA lattices are afforded by a remarkable extent of hinging about the

flexible disulfide linkages and their placement at corner locations of RhuA molecules. The transition from the open to the closed state is accompanied by the compression of the inter-^{C98}RhuA hinge angle (α) from >80° to 17°, decrease of the pore size from ~4.4 nm to ~1.0 nm (for the passage of a spherical object), and increase in the relative protein/hole surface density of 170% (**Figure 12B, Table 4**).

	State II	State V	State VII
Unit cell (a=b, γ)	114.4 Å, 90°	110 Å, 90°	107.8 Å, 90°
Plane-group symmetry	$p42_12$	$p42_12$	$p42_12$
Intertetramer hinge angle, α	79°	49°	17°
Protein surface area per unit cell, $A_{protein}$	82.7 nm^2	86.2 nm^2	88.0 nm^2
Pore surface area per unit cell, A_{pore}	44.7 nm^2	34.7 nm^2	28.2 nm^2
Relative protein/pore density, $A_{protein}/A_{pore}$	1.9	2.5	3.1

[0206] Table 4. Structural parameters for conformations II, V and VII of C98RhuA crystals derived from images shown in **Figure12(A-F)**.

[0207] Conformational dynamics of ^{C98}RhuA crystals are fully coherent: in each crystal examined, only one type of conformational state (I-VII) was observed throughout the lattice (**Figure 12B**). This observation implies that any mechanical deformation of a ^{C98}RhuA crystal is cooperatively propagated along the 2D plane, enabled by both the flexibility and short linker-length of single disulfide linkages: longer, more flexible linkages would preclude coherent dynamics, whereas inflexible linkages would lead to non-adaptive lattices. Indeed, $^{F88/C98}$RhuA and $^{H63/H98}$RhuA lattices do not display any apparent dynamic behavior because their double-disulfide- or metal-mediated modes of assembly do not allow rotation of the neighboring protein molecules with respect to one another.

[0208] To establish that the conformational dynamics of ^{C98}RhuA crystals are reversible, the ^{C98}RhuA crystals were subjected to repeated sedimentation/resuspension

cycles within the solutions in which they self-assembled at 4 °C. In each cycle, TEM images of >100 individual crystals from the same container were obtained, collected either a) from the sediments that formed overnight, or b) from the suspensions immediately after mixing the sediments by repeated pipetting. As shown in **Figure 12C**, the conversion between the closed states (VI and VII) and open/intermediate states (I-V) is completely reversible and absolute. Sedimented samples do not contain any open/intermediate states and resuspended samples do not contain any closed states, providing unambiguous evidence that ^{C98}RhuA lattices are reversibly dynamic. Based on the observed distribution profiles, the opening of the lattices by mechanical agitation and their distribution among conformational states I-V appear to be immediate (at least within the ~ 5-min time scale of TEM sample preparation), whereas their full closure takes several hours. It was posited that the energetic barriers between different ^{C98}RhuA lattice conformations (due to different disulfide bond configurations and long-range protein-protein interactions) must be small enough to be overcome by mechanical agitation and internal protein dynamics. The fully closed conformation (state VII) appears to be a kinetically stable conformation that accumulates over time in unagitated solutions at 4 °C. This kinetic stability may be ascribed to the dense protein packing interactions in state VII and the resulting restriction of the dynamics of both the lattice and the individual building blocks.

[0209] Geometric considerations based on the retention of $p42_12$ symmetry (**Figures. 12B**, **12D**) as well as a strain analysis of the seven conformational states by digital image correlation (**Figure 12E and23C**) indicate that ^{C98}RhuA crystals are auxetic and possess a Poisson's ratio of –1.00±0.01 (**Figure 12F**). Poisson's ratio (ν) is a scale-independent metric that describes the response of a material to strain; it is defined as the ratio between transverse (e_x) and longitudinal strains (e_y) under uniaxial loading (Greaves, G. N., Greer, A., Lakes, R. & Rouxel, T. Poisson's ratio and modern materials. *Nat. Mater.* 10, 823-837, (2011)). e_x and e_y are, in turn, approximated by changes in material length in transverse (ΔX) and longitudinal (ΔY) directions (**Figure 12D**) (Greaves, G. N., Greer, A., Lakes, R. & Rouxel, T. Poisson's ratio and modern materials. *Nat. Mater.* 10, 823-837, (2011)):

$$\nu = -\frac{e_y}{e_x} \approx -\frac{\Delta Y}{\Delta X}$$

where $-1 \leq \nu \leq 0.5$ for an isotropic 3D material and $-1 \leq \nu \leq 1$ for an isotropic 2D material (Grima, J., Alderson, A. & Evans, K. Auxetic behaviour from rotating rigid units. *Phys. Stat. Sol. b* 242, 561-575, (2005)). Most materials possess positive ν's, *i.e.*, they become thinner in the longitudinal direction when stretched transversely (Greaves, G. N., Greer, A., Lakes, R. & Rouxel, T. Poisson's ratio and modern materials. *Nat. Mater.* 10, 823-837, (2011)). Materials with negative ν's (*i.e.*, auxetic materials), in contrast, display the counterintuitive behavior of longitudinal expansion upon transverse stretching. Thus, auxetic materials can be expected to possess enhanced toughness, resistance to indentation and shear stiffness as well as favorable damping and acoustic response, and have been proposed for use in protective armors, smart textiles, actuated filtration, piezoelectric and biomedical devices (Greaves, G. N., Greer, A., Lakes, R. & Rouxel, T. Poisson's ratio and modern materials. *Nat. Mater.* 10, 823-837, (2011); Evans, K. E. & Alderson, A. Auxetic materials: functional materials and structures from lateral thinking! *Adv. Mater.* 12, 617-628, (2000); Baughman, R. H. Auxetic materials: Avoiding the shrink. *Nature* 425, 667-667, (2003); Scarpa, F., Ciffo, L. & Yates, J. Dynamic properties of high structural integrity auxetic open cell foam. *Smart Mat. Struct.* 13, 49, (2004)). Although materials with negative ν's exist, most fall in the range of $-0.4 < \nu < 0$, with lowest reported values of –0.7 to –0.8 observed in reentrant foams (Lakes, R. Foam structures with a negative Poisson's ratio. *Science* 235, 1038-1040, (1987); Choi, J. B. & Lakes, R. S. Non-linear properties of metallic cellular materials with a negative Poisson's ratio. *J. Mater. Sci.* 27, 5375-5381, (1992)). Grima *et al.* postulated that for a 2D lattice of rotating rigid squares with flexible hinges, ν should be equal to the lowest thermodynamically permissible value of –1 at all rotation angles (Grima, J., Alderson, A. & Evans, K. Auxetic behaviour from rotating rigid units. *Phys. Stat. Sol. b* 242, 561-575, (2005)). ^{C98}RhuA lattices represent a true realization of this theoretical model and represent the first isotropic material with $\nu = -1$ designed and constructed at the molecular scale. Assuming Grima's model, it was calculated that ^{C98}RhuA crystals should shrink or expand simultaneously in x and y dimensions by at least 24% during the conversion between fully open (state I) and fully closed states (state VII) (**Figure 23D**).

[0210] It was envisioned that upon hierarchical assembly through physical methods or incorporation into polymeric materials through chemical strategies, molecular architectures like 2D ^{C98}RhuA lattices may be used as feedstocks for adaptive and auxetic macroscopic materials. In general, in some embodiments described herein, this study underscores the utility of dynamic covalent bonds in the construction of highly ordered yet adaptive protein materials. Specifically, due to their high structural quality and chemically tunable assembly under ambient conditions, ^{C98}RhuA crystals provide a unique medium for studying molecular self-assembly and crystallization as well as for investigating the energy landscape of lattice dynamics. The resulting understanding of structural dynamics at the nanoscale should greatly aid the fabrication of functional materials.

[0211] MORE ALTERNATIVES

METHODS

[0212] **Example 7: Design of RhuA variants and site-directed mutagenesis**. RhuA variants were designed as described in some of the embodiments herein, and were based on previously reported crystal structures (PDB ID: 1GT7[23] for ^{C98}RhuA, $^{H63/H98}$RhuA, ^{D98}RhuA, ^{C133}RhuA, and ^{C266}RhuA and PDB ID: 2UYU (Grueninger, D. *et al.* Designed protein-protein association. *Science* 319, 206-209, (2008)) for $^{F88/C98}$RhuA. All RhuA variants also contain the mutations E192A and C126S as previously reported (Ringler, P. & Schulz, G. E. Self-assembly of proteins into designed networks. *Science* 302, 106-109, (2003); Grueninger, D. *et al.* Designed protein-protein association. *Science* 319, 206-209, (2008)). The gene for ^{C98}RhuA, pre-inserted into the pJ414 expression vector optimized for expression in *E. coli*, was purchased from DNA2.0. $^{F88/C98}$RhuA, $^{H63/H98}$RhuA, ^{D98}RhuA, ^{C133}RhuA, and ^{C266}RhuA were prepared using QuikChange mutagenesis (Stratagene) with primers obtained from Integrated DNA Technologies (**Table 5**). The mutant plasmids were transformed into XL-1 Blue *E. coli* cells followed by purification using the QIAprep Spin Miniprep kit (Qiagen). The presence of the mutations was verified by sequencing (Retrogen). Amino acid sequences of RhuA variants are shown in **Table 6**.

Variant	Mutation	Primer Sequence
$^{F88/C98}$RhuA	A88F	5'-CGCAATGTCCAGTTGGACCCAGCGTTTAACCTGGGCATTGTTAAGGTGG-3' (SEQ ID NO: 6) 5'-CCACCTTAACAATGCCCAGGTTAAACGCTGGGTCCAACTGGACATTGCG-3' (SEQ ID NO: 7)
$^{H63/H98}$RhuA	P63H C98H	5'- CGCTGAGCCAGCCGATGCATCTGTTGGCGAATACCC -3' (SEQ ID NO: 8) 5'- GGGTATTCGCCAACAGATGCATCGGCTGGCTCAGCG -3' (SEQ ID NO: 9) 5'- GGGCATTGTTAAGGTGGATAGCCATGGTGCAGGTTACCACATCC-3' (SEQ ID NO: 10) 5'- GGATGTGGTAACCTGCACCATGGCTATCCACCTTAACAATGCCC -3' (SEQ ID NO: 11)
^{D98}RhuA	C98D	5'- GCATTGTTAAGGTGGATAGCGACGGTGCAGGTTACCACATCC -3' (SEQ ID NO: 13) 5'- GGATGTGGTAACCTGCACCGTCGCTATCCACCTTAACAATGC -3' (SEQ ID NO: 14)
^{C133}RhuA	N133C	5'- GCGAGCGTATCAAGGCGACCTGCGGCAAAGACCGCG-3' (SEQ ID NO: 15) 5'- CGCGGTCTTTGCCGCAGGTCGCCTTGATACGCTCGC-3' (SEQ ID NO: 16)
^{C266}RhuA	T266C	5'- GGTAAGCGTTTTGGTGTCTGTCCGCTGGCGTCCGCGCTGG-3' (SEQ ID NO: 17) 5'- CCAGCGCGGACGCCAGCGGACAGACACCAAAACGCTTACC-3' (SEQ ID NO: 18)

[0213] Table 5 | List of primers used in constructing site-directed mutants of RhuA using ^{C98}RhuA as a base.

Variant	Amino Acid Sequence
^{C98}RhuA	MQNITQSWFVQGMIKATTDAWLKGWDERNGGNLTLRLDDADIAPYHDNFHQQPRYIPLSQ PMPLLANTPFIVTGSGKFFRNVQLDPAANLGIVKVDS**C**GAGYHILWGLTNEAVPTSELPAH FLSHSERIKATNGKDRVIMHCHATNLIALTYVLENDTAVFTRQLWEGSTECLVVFPDGVGIL PWMVPGTDAIGQATAQEMQKHSLVLWPFHGVFGSGPTLDETFGLIDTAEKSAQVLVKVYS MGGMKQTISREELIALGKRFGVTPLASALAL (SEQ ID NO: 3)
$^{H63/H98}$RhuA	MQNITQSWFVQGMIKATTDAWLKGWDERNGGNLTLRLDDADIAPYHDNFHQQPRYIPLSQ PM**H**LLANTPFIVTGSGKFFRNVQLDPAANLGIVKVDS**H**GAGYHILWGLTNEAVPTSELPAH FLSHSERIKATNGKDRVIMHCHATNLIALTYVLENDTAVFTRQLWEGSTECLVVFPDGVGIL PWMVPGTDAIGQATAQEMQKHSLVLWPFHGVFGSGPTLDETFGLIDTAEKSAQVLVKVYS MGGMKQTISREELIALGKRFGVTPLASALAL (SEQ ID NO: 4)
$^{F88/C98}$RhuA	MQNITQSWFVQGMIKATTDAWLKGWDERNGGNLTLRLDDADIAPYHDNFHQQPRYIPLSQ PMPLLANTPFIVTGSGKFFRNVQLDPA**F**NLGIVKVDS**C**GAGYHILWGLTNEAVPTSELPAHF LSHSERIKATNGKDRVIMHCHATNLIALTYVLENDTAVFTRQLWEGSTECLVVFPDGVGILP WMVPGTDAIGQATAQEMQKHSLVLWPFHGVFGSGPTLDETFGLIDTAEKSAQVLVKVYS MGGMKQTISREELIALGKRFGVTPLASALAL (SEQ ID NO: 5)
^{D98}RhuA	MQNITQSWFVQGMIKATTDAWLKGWDERNGGNLTLRLDDADIAPYHDNFHQQPRYIPLSQ PMPLLANTPFIVTGSGKFFRNVQLDPAANLGIVKVDS**D**GAGYHILWGLTNEAVPTSELPAH FLSHSERIKATNGKDRVIMHCHATNLIALTYVLENDTAVFTRQLWEGSTECLVVFPDGVGIL PWMVPGTDAIGQATAQEMQKHSLVLWPFHGVFGSGPTLDETFGLIDTAEKSAQVLVKVYS MGGMKQTISREELIALGKRFGVTPLASALAL (SEQ ID NO: 19)
^{C133}RhuA	MQNITQSWFVQGMIKATTDAWLKGWDERNGGNLTLRLDDADIAPYHDNFHQQPRYIPLSQ PMPLLANTPFIVTGSGKFFRNVQLDPAANLGIVKVDSDGAGYHILWGLTNEAVPTSELPAH FLSHSERIKAT**C**GKDRVIMHCHATNLIALTYVLENDTAVFTRQLWEGSTECLVVFPDGVGIL PWMVPGTDAIGQATAQEMQKHSLVLWPFHGVFGSGPTLDETFGLIDTAEKSAQVLVKVYS MGGMKQTISREELIALGKRFGVTPLASALAL (SEQ ID NO: 20)
^{C266}RhuA	MQNITQSWFVQGMIKATTDAWLKGWDERNGGNLTLRLDDADIAPYHDNFHQQPRYIPLSQ PMPLLANTPFIVTGSGKFFRNVQLDPAANLGIVKVDSDGAGYHILWGLTNEAVPTSELPAH FLSHSERIKATNGKDRVIMHCHATNLIALTYVLENDTAVFTRQLWEGSTECLVVFPDGVGIL PWMVPGTDAIGQATAQEMQKHSLVLWPFHGVFGSGPTLDETFGLIDTAEKSAQVLVKVYS MGGMKQTISREELIALGKRFGV**C**PLASALAL (SEQ ID NO: 21)

Table 6 | Amino acid sequences of RhuA variants. Point mutation positions are underlined.

[0214] Example 8 Protein expression and purification. Bacterial expression of RhuA variants was performed according to previously published procedures with slight

modifications (Kroemer, M. & Schulz, G. E. The structure of L-rhamnulose-1-phosphate aldolase (class II) solved by low-resolution SIR phasing and 20-fold NCS averaging. *Acta Cryst. D.* 58, 824-832, (2002)). Plasmids bearing the variants were transformed into BL21(DE3) *E. coli* cells, and the colonies were grown overnight at 37 °C on lysogeny broth (LB) agar plates (pH 7.4) containing 100 mg/L ampicillin. Starter cultures (5 mL with 100 mg/L ampicillin) from single colonies were grown for ~4-6 h at 37 °C (with shaking at 250 rpm) before inoculation into 1-L LB cultures containing 100 mg/L ampicillin. After the cells were grown to an optical density of ~0.8 at 600 nm, protein expression was induced with 1 mM isopropyl β-D-1-thiogalactopyranoside (IPTG, Gold Biotechnology) for 12 – 13 h (at 37 °C with shaking at 250 rpm). Cells were pelleted by centrifugation (5,000 rpm at 4 °C for 10 min), and resuspended in a buffer solution containing 10 mM Tris(hydroxymethyl)aminomethane hydrochloride (TRIS) (pH 7.5), 1 mM $ZnCl_2$, and 10 mM β-mercaptoethanol (βME). For $^{H63/H98}$RhuA preparations, $ZnCl_2$ was excluded from buffer solutions to avoid possible protein precipitation during purification. Cell lysis was performed by sonication for 15 min on ice. The lysis solution was centrifuged for 30 min at 12,000 rpm at 4 °C. Polymin-P (Acros) was added to the supernatant at a final concentration of 0.15% (w/v) for nucleic acid precipitation and the resulting mixture was stirred for 30 min prior to centrifugation for 30 min at 12,000 rpm at 4 °C. The supernatant was loaded onto a DEAE-Sepharose CL-6B (GE Healthcare) column and eluted using a gradient of 0 – 500 mM NaCl in Tris buffer at 4 °C. Fractions containing RhuA which eluted at ~200 mM NaCl were added 1.7 M ammonium sulfate, and were centrifuged for 45 min at 12,000 rpm at 4 °C. The precipitate was dissolved in a buffer solution containing 5 mM sodium phosphate (NaPi) (pH 7.2), 1 mM $ZnCl_2$, and 10 mM βME, and then dialyzed three times against 5 L of the same buffer solution. Further purification was done using either a High Q cartridge column (BioRad) (at pH 8.0) using a 0-500 mM NaCl gradient or a Mini CHT Type I hydroxyapatite column (BioRad) (at pH 7.2) using a 5-500 mM NaPi gradient on a DuoFlow fast protein chromatography workstation (Bio-Rad). Pure protein fractions eluted at 350 mM NaCl and 200 mM NaPi, respectively. These fractions were combined, dialyzed three times against a buffer solution of 10 mM TRIS (pH 7.5), 1 mM $ZnCl_2$, and 10 mM β-mercaptoethanol (βME), and concentrated in an Amicon stirred cell at 4 °C. The protein was then flash frozen

and kept at −80 °C until use. Protein purity was confirmed by SDS PAGE (**Figure 13**) and ESI-MS (**Figure 14 and Table 7**), and stock concentrations were determined as previously reported (Edelhoch, H. Spectroscopic determination of tryptophan and tyrosine in proteins. *Biochemistry* 6, 1948-1954, (1967)).

Variant	Calculated Mass (Da)	Observed Mass (Da)
^{C98}RhuA	30059.5	30060.0
$^{F88/C98}$RhuA	30135.6	30136.0
$^{H63/H98}$RhuA	30133.5	30134.0
^{D98}RhuA	30071.4	30075.0
^{C133}RhuA	30060.4	30061.0
^{C266}RhuA	30073.4	30073.0

[0215] Table 7 | Molecular masses of RhuA mutants. For the actual mass spectra, refer to **Figure 14**.

a, ^{C98}RhuA

2D plane group	Phase Residual[a] (°)	Number of comparisons	Target Residual[b] (°)
p1	22.4[c]	126	
p2	29.6*	63	32.5
p12_b	74.6	45	23.1
p12_a	73.8	45	23.1
$p12_1$_b	18.1*	45	23.1
$p12_1$_a	12.8*	45	23.1
c12_b	74.6	45	23.1
c12_a	73.8	45	23.1
p222	56.1	153	26.6
$p222_1$_b	54.2	153	26.6
$p222_1$_a	56.6	153	26.6
$p22_12_1$	21.6*	153	26.6

c222	56.1	153	26.6
p4	26.7*	155	26.5
p422	52.6	333	24.3
$p42_12$	24.4*	333	24.3

[a] Phase residual versus other spots (90° = random).
[b] Expected residual based on the quality of the reflections involved in the calculation.
[c] Theoretical, based on the quality of the reflections observed

* acceptable (better than target or within 1°)
† to be considered (within 5° from target)
§ possibility (within 10° from target)

Table 8 | Symmetry analysis for the 2D lattices of RhuA variants. Internal phase residuals for all possible non-hexagonal plane groups. Residuals were determined from the power spectra shown in **Figure 23A** using the program ALLSPACE, as described in Methods. Reflections up to 11 Å and with IQ less than 6 were included in the calculations.

b, $^{H63/H98}$RhuA

2D plane group	Phase Residual[a] (°)	Number of comparisons	Target Residual[b] (°)
p1	21.8[c]	96	
p2	29.4[*]	48	31.6
p12_b	44.7	28	23.2
p12_a	46.0	31	24.0
$p12_1$_b	73.0	28	23.2
$p12_1$_a	79.5	31	24.0
c12_b	44.7	28	23.2
c12_a	46.0	31	24.0
p222	38.5	107	26.2
$p222_1$_b	64.7	107	26.2
$p222_1$_a	70.9	107	26.2
$p22_12_1$	62.6	107	26.2
c222	38.5	107	26.2
p4	23.1[*]	112	26.0
p422	31.9[§]	231	23.8
$p42_12$	62.1	231	23.8

Table 8, continued

[a] Phase residual versus other spots (90° = random).
[b] Expected residual based on the quality of the reflections involved in the calculation.
[c] Theoretical, based on the quality of the reflections observed

[*] acceptable (better than target or within 1°)
[†] to be considered (within 5° from target)
[§] possibility (within 10° from target)

c, $^{F88/C98}$RhuA

2D plane group	Phase Residual[a] (°)	Number of comparisons	Target Residual[b] (°)
p1	26.8[c]	160	
p2	26.4*	80	39.3
p12_b	71.2	54	27.7
p12_a	70.4	56	28.1
$p12_1$_b	14.1*	54	27.7
$p12_1$_a	13.1*	56	28.1
c12_b	71.2	54	27.7
c12_a	70.4	56	28.1
p222	52.1	190	32.1
$p222_1$_b	56.9	190	32.1
$p222_1$_a	58.3	190	32.1
$p22_12_1$	19.3*	190	32.1
c222	52.1	190	32.1
p4	17.3*	204	31.7
p422	45.7	431	29.1
$p42_12$	16.0*	431	29.1

Table 8, continued.

[a] Phase residual versus other spots (90° = random).
[b] Expected residual based on the quality of the reflections involved in the calculation.
[c] Theoretical, based on the quality of the reflections observed

* acceptable (better than target or within 1°)
† to be considered (within 5° from target)
§ possibility (within 10° from target)

[0216] Example 9: Preparation of 2D RhuA crystals. All 2D RhuA crystals reported herein were obtained in an unsupported fashion in solutions. As described in the in several embodiments herein, several solution conditions were screened for optimizing the formation of 2D protein crystals of ^{C98}RhuA, $^{F88/C98}$RhuA and $^{H63/H98}$RhuA variants. For all

variants, these screening conditions included various pH's (6 to 8), starting protein concentrations (25 to 175 μM), buffer salt concentration and identity (5 – 20 mM bis-TRIS, CHES, MES, MOPS, NaPi, and TRIS), and temperature (4 – 37 °C). For the disulfide-mediated self-assembly of ^{C98}RhuA and $^{F88/C98}$RhuA, various oxidizing conditions (1 – 2 mM total GSH/GSSG at ratios varying from 1:19 to 19:1, or 5–10 mM βME, which slowly decomposed in aqueous solution in the presence of metal ions) were additionally screened. For the metal-mediated assembly of $^{H63/H98}$RhuA, 4 – 20 molar equivalents (over tetrameric protein concentration) of $ZnCl_2$ and $CuCl_2$ were screened. As stated previously, the best conditions were: ^{C98}RhuA and $^{F88/C98}$RhuA (≥125 μM protein, 10 mM βME, pH 7.5, 10 mM TRIS); $^{H63/H98}$RhuA (25 μM protein, 200 μM $ZnCl_2$, pH 7, 20 mM MOPS) at 4 °C. In general, the formation of crystals was either immediate (upon metal addition for $^{H63/H98}$RhuA) or lasted overnight to several days (for ^{C98}RhuA and $^{F88/C98}$RhuA). Crystal formation resulted in increasing cloudiness of the self-assembly solutions. The growth of ^{C98}RhuA crystals could be accelerated by gentle shaking (**Figures.=11A, 11B**). In additional experiments, the thermo- and chemo-stability of ^{C98}RhuA crystals as shown in **Figure 62** were tested.

[0217] **Example 10:** Electron microscopy. For negative-stain TEM sample preparation, 3 – 3.5 μL aliquots of crystal suspensions were applied onto negatively glow-discharged carbon-coated Cu grids (Ted Pella, Inc.), washed with Milli-Q water, and stained with 1% uranyl acetate at 4 °C. For cryo-EM sample preparation, 3 – 3.5 μl aliquots of 25 μM ^{C98}RhuA sample (diluted sample) were deposited onto negatively glow-discharged Quantifoil grids, and then plunged into liquid ethane after blotting. The sample was then stored under liquid nitrogen until analysis. Sample screening was performed in an FEI Sphera transmission electron microscope equipped with a LaB6 electron gun at 200 keV and imaged on Gatan $2K^2$ CCD. A complete electron crystallographic analysis was done on 43, 50 and 33 micrographs for ^{C98}RhuA, $^{H63/H98}$RhuA and $^{F88/C98}$RhuA, respectively, which were selected by visual assessment. Micrographs were each processed separately using the 2dx software[33], which implements a semi-automatic processing pipeline mostly based on programs from the MRC suite (Crowther, R., Henderson, R. & Smith, J. MRC image processing programs. *J. Struct. Biol.* 116, 9-16, (1996)). The program allows one to determine the 2D plane group lattice symmetry of each crystal, to calculate its unit cell dimensions and to generate a

projection density map. The processing involves estimation of the Contrast Transfer Function (CTF) by CTFFIND3 (Mindell, J. A. & Grigorieff, N. Accurate determination of local defocus and specimen tilt in electron microscopy. *J. Struct. Biol.* 142, 334-347, (2003)), spot-list determination, automatic lattice determination, crystal masking, unbending and generation of projection map after CTF correction. Within this program, the symmetry plane group is determined using ALLSPACE (Valpuesta, J. M. a., Carrascosa, J. L. & Henderson, R. Analysis of electron microscope images and electron diffraction patterns of thin crystals of Ø29 connectors in ice. *J. Mol. Biol.* 240, 281-287, (1994)) by comparing the internal phase residual for each symmetry to its expected value. Lattice unit cell dimensions were determined on a subset of images, screened by the quality of the reflections, of 12, 44 and 13 for ^{C98}RhuA, $^{H63/H98}$RhuA and $^{F88/C98}$RhuA, respectively. The estimated resolution limit of each image (between 15 and 30 Å) was assessed both by visual inspection of its computed Fourier transform and by comparison with simulated images filtered at different levels of resolution.

[0218] Example 11: AFM measurements. For AFM sample preparation, 2 µL of crystal suspensions were applied on freshly cleaved mica, washed with deionized water and dried. AFM images were collected using a Dimension Icon microscope (Bruker, USA) using Scan Asyst peak force tapping (in air) mode at a resolution of 512 lines per image and a scan rate of 0.3 – 0.5 Hz. AFM images obtained were processed using Nanoscope Analysis (Bruker, USA).

[0219] Example 12: SEM measurements. For SEM sample preparation, 2 µL of crystal suspensions were applied onto SiO_2 substrates. Sample was sputter-coated with iridium oxide before analysis to reduce charging effects. SEM micrographs were collected on an FEIXL 30UHR scanning electron microscope operated at 5 keV.

[0220] Example 13: DLS measurements. DLS experiments were performed using Wyatt DynaPro NanoStar instrument. The experiment runs were performed to collect 10 acquisitions with 657 nm excitation at a power setting of 100%. Measurements were plotted using a Rayleigh sphere model. Peak radius cutoffs were fixed according to default settings (0.5 – 10000 nm).

[0221] **Example 14:** Structural modelling and simulations. Projected electron density maps were used as a reference in the visualization software UCSF Chimera (Pettersen, E. F. *et al.* UCSF Chimera—a visualization system for exploratory research and analysis. *J. Comput. Chem.* 25, 1605-1612, (2004)) to determine the orientation of the RhuA molecules in each crystal. The atomic coordinates were extracted from the PDB entries 1GT7 (C_4-symmetric tetramer for ^{C98}RhuA and $^{H63/H98}$RhuA) and 2UYU (D_4-symmetric octamer for $^{F88/C98}$RhuA) and placed manually to fit the position of one subunit in the observed projected density map. The orientation of the molecule was refined in an iterative manner by comparing the experimental density with the density simulated from a model of the unit cell, obtained as explained below. Simulated projected electron density maps were computed using Bsoft (lsbr.niams.nih.gov/bsoft) (Heymann, J. B. Bsoft: image and molecular processing in electron microscopy. *J. Struct. Biol.* 133, 156-169, (2001)) and EMAN2 (blake.bcm.edu/emanwiki/EMAN2) (Tang, G. *et al.* EMAN2: an extensible image processing suite for electron microscopy. *J. Struct. Biol.* 157, 38-46, (2007)). Software for calculating projected electron density maps are readily available and are known to those skilled in the art. Starting from the estimated position and orientation of a single subunit, multiple copies of the model were generated to cover one unit cell (*bmoledit* in Bsoft) and converted to electron density (*e2pdb2mrc.py* in EMAN2) with a resolution limit of 30 Å. Finally, the density volume was projected along the vertical direction (*bproject* in Bsoft) to generate a 2D density map comparable to the experimental map.

[0222] **Example 15:** Classification of the conformational states of 2D ^{C98}RhuA crystals. TEM micrographs of ^{C98}RhuA crystals were analyzed computationally to categorize different conformational states of the 2D lattice. Essentially, for each raw image a roundness index number derived from the shape of the pores in the lattice was determined, and used this value to classify the images. The analysis was performed on 982 images using an *ad hoc* algorithm coded as a macro in Fiji (fiji.sc/Fiji) (Schindelin, J. *et al.* Fiji: an open-source platform for biological-image analysis. *Nat. Meth.* 9, 676-682, (2012)) and ImageJ (imagej.nih.gov/ij) (Schneider, C. A., Rasband, W. S. & Eliceiri, K. W. NIH Image to ImageJ: 25 years of image analysis. *Nat. Methods* 9, 671-675, (2012)). Each image was initially processed by applying a 3×3 mean filter applied three times and then converted to a

binary image after automatic thresholding to segment out the pores. The mask was then filtered using the opening morphological operator to smooth the shape of the pores and to remove small outliers. Pores that were distorted from potential bending of the crystal in some regions of the field of view were discarded using their size for screening. For images acquired at nominal magnifications of ×50,000 and ×68,000 (calibrated pixel size = 2.033 Å and 1.646 Å, respectively), only pores with areas that covered 500–1200 pixels were kept. The remaining pores were modeled as ellipses and their roundness index was determined as the ratio between the lengths of the major and the minor elliptical axes. A single index value was assigned to each micrograph as the average from all the segmented pores. The images were assigned to one of the seven identified states using the following criterion: State I: >0.85; State II: >0.75 – 0.85; State III: >0.65 – 0.75; State IV: >0.55 – 0.65; State V: >0.35 – 0.45; State VI: >0.35 – 0.45; State VII <0.35.

[0223] Example 16: Generation of video simulating the lattice motions. A video (Supplementary Video 1) to illustrate the dynamics of 2D ^{C98}RhuA crystals was generated starting from the TEM snapshots of the seven conformational states (I-VII) (**Figure 12A**). All projected density images were rescaled to include the same field of view (*bint* and *bimg* from Bsoft). Twenty four intermediate image frames were created between each pair in the sequence by pseudo-morphing, using the program *convert* from the software suite ImageMagick®. Finally, the video was generated with *ffmpeg* (www.ffmpeg.org) by combining the images as frames.

[0224] Example 17: Digital Image Correlation for Poisson's value determination. Using Matlab, digital image processing of the reconstructed 2D TEM images of dynamic ^{C98}RhuA crystals for evaluating Poisson's ratios was performed. As a first step, histogram normalization was performed taking as a reference the image of conformational state I in order to normalize the intensity of the images (**Figure 23C**). This normalization guarantees that the thresholds used for pixel selection have the same meaning through all the images. After normalizing, the representative volume element (RVE) in each one of the images was selected. The RVE considered has a rectangular section whose vertices correspond to the centroid of the lattice pores (shown as the squares with the vertices labeled 1, 2, 3 and 4 in **Figure 23C** and rectangles with the vertices 1, 2, 3 and 4 and in **Figure 12E**). To find the

position of the centroids, the edges of the pores using the Sobel edge detection method was determined. The edges of the pores are shown as circles in **Figure 23C** and **Figure 12E**. Then, centroid calculation was performed by taking the mean of the coordinates in *x* and *y* for each pixel in the border. After the selection of the RVE, the size of the RhuA building blocks was measured on each image by defining the circle that is circumscribed to each square (shown as blue circles in **Figure 23C**). Since the square shape of the RhuA building blocks can be assumed to remain rigid in each conformational state, it was determined that the images were at slightly different scales; thus, appropriate magnification factors were calculated taking as a reference the image corresponding to conformational state I. The applied scaling factors are shown in **Figure 23C**. The position of the vertices of the RVE on each conformational state was then calculated and was then proceeded with the calculation of the Poisson's ratio. For each RVE, local values of engineering strains e_x and e_y can be calculated from the vectors ***M***, ***N*** and ***m***, ***n*** that span the RVE on its reference (state I) and deformed configurations (states II-VII), respectively (see **Figure 12E**):

$$M = \begin{bmatrix} M_x \\ M_y \end{bmatrix}, N = \begin{bmatrix} N_x \\ N_y \end{bmatrix} \text{ and } m = \begin{bmatrix} m_x \\ m_y \end{bmatrix}, n = \begin{bmatrix} n_x \\ n_y \end{bmatrix}$$

and considering that the deformed and undeformed configurations can be related through the deformation gradient F:

$$\begin{bmatrix} m_x \\ m_y \end{bmatrix} = \begin{bmatrix} 1 + e_x & e_{xy} \\ e_{yx} & 1 + e_y \end{bmatrix} \begin{bmatrix} M_x \\ M_y \end{bmatrix} \text{ and } \begin{bmatrix} n_x \\ n_y \end{bmatrix} = \begin{bmatrix} 1 + e_x & e_{xy} \\ e_{yx} & 1 + e_y \end{bmatrix} \begin{bmatrix} N_x \\ N_y \end{bmatrix}$$

where

$$F = \begin{bmatrix} 1 + e_x & e_{xy} \\ e_{yx} & 1 + e_y \end{bmatrix}$$

Then, homogenized values of the engineering strains for the RVE can be calculated as:

$$\begin{bmatrix} 1 + e_x & e_{xy} \\ e_{yx} & 1 + e_y \end{bmatrix} = \begin{bmatrix} n_x & m_x \\ n_y & m_y \end{bmatrix} \begin{bmatrix} N_x & M_x \\ N_y & M_y \end{bmatrix}^{-1}$$

Finally, the Poisson's ratio is calculated as:

$$\nu = -\frac{e_y}{e_x}$$

[0225] **Example 18:** Development of templating and growth of functionalities on ^{C98}RhuA crystals:C98 with meleimido Au. Monomaleimino Nanogold® at 6nmol was used for staining instead of UA. (**See Figure 24-33).** The covalent modification of the RhuA lattices is carried out via the reaction of peripheral cysteines with monomaleimido nanogold or iodoacetamidofluorescein. The nucleation/growth of gold nanoparticle was also tested on ^{C98}RhuA crystals using Gold(III) chloride trihydrate ($HAuCl_4$) under various reducing reagents.

[0226] As shown in **Figure 26** is a ^{C98}RhuA crystal with monomaleimido nanogold. For making the crystal,_3 – 3.5 μL aliquots of crystal suspensions were applied onto negatively glow-discharged carbon-coated Cu grids, washed with Milli-Q water, and treated with 5 μL of 6 nmol Monomaleimido Nanogold (Nanoprobes, Inc) for 3 hours or overnight at 4 °C. As shown in **Figure 27,** ^{C98}RhuA crystals were treated with iodoacetamidofluorescein._4 μL aliquots of crystal suspensions were mixed into 200 μM iodoacetamidofluorescein for 1 day, and sample was deposited onto negatively glow-discharged carbon-coated Cu grids, washed with Milli-Q water, and stained with 1% uranyl acetate at 4 °C. Sample was also tested by confocal microscopy to determine the addition of *iodoacetamidofluorescein.*

[0227] As shown in **Figure 28,** are ^{C98}RhuA crystals with $HAuCl_4$.4 μL aliquots of crystal suspensions were mixed into 0.5 mM $HAuCl_4$ with various reducing reagents in 5 mM NaPi pH 7.2 for indicated time, and sample was deposited onto negatively glow-discharged carbon-coated Cu grids, washed with Milli-Q water at 4 °C.

[0228] **Example 19:** The results for making the C98-CD with HAuCl4 is shown in Figures 28-34. For making the crystalline structures, 4 μL aliquots of crystal suspensions were mixed into 0.5 mM $HAuCl_4$ with various reducing reagents in 5 mM NaPi pH 7.2 for indicated time, and sample was deposited onto negatively glow-discharged carbon-coated Cu grids, washed with Milli-Q water at 4 °C.

[0229] As shown in Figure 28, 4uL sheet was added into 0.5 mM $HAuCl_4$ for 1 day. As shown in Figure 29, RhuA-C98 (4uL) added into 0.5 mM $HAuCl_4$ in 5 mM NaPi pH 7.2 6 days then added 5 mM bME for 1 day. As shown in Figure 30, RhuA-C98 (4uL) added

into 100 μL of Au(I) ($HAuCl_4$ + 2 eq thiodiethanol) in 5 mM NaPi pH 7.2 for 4 days and then the crystals were examined. As shown in Figure 31, RhuA-C98 sheet/$HAuCl_4$ on grids followed by $HAuCl_4/K_2CO_3/NaBH_4$ for 1 hr then in 10 % formaldehyde for 2 hours. As shown in Figure 32, RhuA-C98 sheet/HAuCl4 on grids followed by HAuCl4/K2CO3/NaBH4 in NaPi pH 7.2 for 2 hours. As shown in Figure 33, RhuA-C98 sheet/HAuCl4 on grids followed by HAuCl4/K2CO3/Formaldehyde in NaPi pH 7.2 for 2 hours.

[0230] Example 20: Investigation of new connectivity's via covalent modification of C98RhuA. In order to broaden the connectivity of lattices, the covalent modifications of cysteine on ^{C98}RhuA were carried out, and their self-assemblies were tested via addition of metals, small molecule, or counter partner.

[0231] Example 21: Addition of functional groups onto ^{C98}RhuA. 500 uM ^{C98}RhuA was reduced with 18 eq TCEP for a hour followed by reaction with 20 eq of N-(1,10-Phenanthrolin-5-yl)*iodoacetamide*, dmco(cycloakyne)maleimide, or 4-phenylazomaleinanil in 10 mM Tris pH 7.5 with 5 % DMF. Sample was dialyzed against 10 mM Tris (with 5 % DMF if necessary) pH 7.5. $^{dmco(cycloakyne)maleimidoC98}$RhuA was then reacted with 20 eq of mono-6-Azido-6-deoxy-beta-cyclodextrin followed by dialysis.

[0232] Example 22: Metal directed self-assembly of $^{iPhen\text{-}C98}$RhuA (and $^{iPhen\text{-}C133}$RhuA). 2 eq of $ZnCl_2$, $CuCl_2$, or $NiSO_4$ was mixed with 100 μM ^{iPhenC98}RhuA at pH 5.5 in 20 mM MES for 1 day (or as indicated) to assemble 2D crystals. Sample was deposited onto negatively glow-discharged carbon-coated Cu grids, washed with Milli-Q water at 4 °C, and stained with 1% uranyl acetate at 4 °C.

[0233] ^{C133}RhuA (control) was also tested in this experiment. Even though ^{C133}RhuA could not form ordered array via disulfide bonds, $^{iPhen\text{-}C133}$RhuA (modification of cysteines) was able to form crystals via metal directed assembly due to additional space between protein-protein interactions. (See **Figures 63, 38 and 41)**

[0234] Example 23: Small molecule (curcumin) directed self-assembly of $^{CD\text{-}C98}$RhuA. 100 uM $^{CD\text{-}C98}$RhuA was incubated with 1 mM or 5 mM curcumin (stock in DMF) in 10 mM TRIS pH 7.5 with 5 % DMF at 4 °C for indicated time. Sample was deposited onto negatively glow-discharged carbon-coated Cu grids, washed with Milli-Q water at 4 °C, and stained with 1% uranyl acetate at 4 °C. (See **Figures 43, 44, 49, 51 and 52)**

[0235] **Example 24:** Self-assembly of $^{CD\text{-}C98}$RhuA and $^{Azo\text{-}C98}$RhuA

[0236] 100 μM of $^{CD\text{-}C98}$RhuA and $^{Azo\text{-}C98}$RhuA was mixed for 1 day at 4°C. Sample was deposited onto negatively glow-discharged carbon-coated Cu grids, washed with Milli-Q water at 4 °C, and stained with 1% uranyl acetate at 4 °C. (**Figures 42, 55, 58 and 59)**

[0237] **Example 25:** The 2D protein lattices can be modified with inorganic compounds as shown in **Figures 24-26.** As shown, 2D crystalline material comprising a polypeptide building block of any one of the alternatives described herein is provided. The polypeptide building block can comprise the non-naturally occurring symmetrical polypeptide building block described herein. The non-naturally occurring symmetrical polypeptide building block can comprise a plurality of cysteine residues positioned such that formation of disulfide bonds between some or all of said plurality of cysteine residues facilitates formation of 2D crystals. polypeptide building block comprises a symmetrical polypeptide comprising a single set of surface cysteine residues in the corner positions. In some embodiments, said polypeptide has inherent C3, C4, C6, D3, D4 or D6 symmetry. In some embodiments, at least one of said cysteine residues has been introduced into said polypeptide building block through genetic engineering. In some embodiments, said polypeptide is generated via solid phase synthesis. In some embodiments, said polypeptide is genetically engineered. In some embodiments, said polypeptide further comprises an additional modification, wherein said additional modification is selected from the group consisting of a chemical modification, a modification made via an enzymatic reaction, and a modification made via genetic engineering. In some embodiments, said additional modification is selected from the group consisting of functional groups, tags, other polypeptides, peptide tags, detectable labels, fluorophores, and nanoparticles. In some embodiments, said polypeptide comprises the RhuA protein. In some embodiments, the polypeptide building block can be chemically modified with inorganic nanoparticles. In some embodiments, the polypeptide building block can be modified with organic functional groups (fluorophores, metal chelating groups or host complexes) for different modes of controllable self-assembly. In some embodiments, the polypeptide building block can be genetically modified/fused with functional proteins and peptides. In some embodiments, said 2D

crystalline material is auxetic. In some embodiments, the 2D crystalline material comprises a Poisson's ratio of at least -1. In some embodiments, the 2D crystalline material comprises a Poisson's ratio of -1. In some embodiments, the 2D crystalline material can be chemically modified with inorganic nanoparticles. In some embodiments, the 2D crystalline material can be modified with organic functional groups (fluorophores, metal chelating groups or host complexes) for different modes of controllable self-assembly. In some embodiments, the 2D crystalline material can be genetically modified/fused with functional proteins and peptides. The 2D crystalline material can be modified with maleimido AU and with the addition of $HAuCl_4$. The 2D crystalline material can also be fused to a protein.

[0238] **Example 26: 2D protein lattices can be used as templates for inorganic nanoparticle growth**. C98-CD with $HAuCl_4$. As shown in **Figures 28-33**, the 2D crystalline structures as described herein, can be used as templates for inorganic nanoparticle growth such as nanotubes for example. These can be shown in which the crystals have grown in 0.5mM Au(I) to 0.125mM Au(I).

[0239] **Example 27: 2D Crystalline structures can be modified with functional groups. (Figures 34-53).** As shown, 2D crystalline material comprising a polypeptide building block of any one of the alternatives described herein is provided. The polypeptide building block can comprise the non-naturally occurring symmetrical polypeptide building block described herein. The non-naturally occurring symmetrical polypeptide building block can comprise a plurality of cysteine residues positioned such that formation of disulfide bonds between some or all of said plurality of cysteine residues facilitates formation of 2D crystals. polypeptide building block comprises a symmetrical polypeptide comprising a single set of surface cysteine residues in the corner positions. In some embodiments, said polypeptide has inherent C3, C4, C6, D3, D4 or D6 symmetry. In some embodiments, at least one of said cysteine residues has been introduced into said polypeptide building block through genetic engineering. In some embodiments, said polypeptide is generated via solid phase synthesis. In some embodiments, said polypeptide is genetically engineered. In some embodiments, said polypeptide further comprises an additional modification, wherein said additional modification is selected from the group consisting of a chemical modification, a modification made via an enzymatic reaction, and a

modification made via genetic engineering. In some embodiments, said additional modification is selected from the group consisting of functional groups, tags, other polypeptides, peptide tags, detectable labels, fluorophores, and nanoparticles. In some embodiments, said polypeptide comprises the RhuA protein. In some embodiments, the polypeptide building block can be chemically modified with inorganic nanoparticles. In some embodiments, the polypeptide building block can be modified with organic functional groups (fluorophores, metal chelating groups or host complexes) for different modes of controllable self-assembly. In some embodiments, the polypeptide building block can be genetically modified/fused with functional proteins and peptides. In some embodiments, said 2D crystalline material is auxetic. In some embodiments, wherein the 2D crystalline material can be assembled by visible light and dissembled by UV light. In some embodiments, the 2D crystalline material comprises a Poisson's ratio of at least -1. In some embodiments, the 2D crystalline material comprises a Poisson's ratio of -1. In some embodiments, the 2D crystalline material can be chemically modified with inorganic nanoparticles. In some embodiments, the 2D crystalline material can be modified with organic functional groups (fluorophores, metal chelating groups or host complexes) for different modes of controllable self-assembly. In some embodiments, the 2D crystalline material can be genetically modified/fused with functional proteins and peptides. The 2D crystalline material can be modified with maleimido AU and with the addition of $HAuCl_4$. The 2D crystalline material can also be fused to a protein. In the alternatives shown in Figures 34-53, the 2D crystalline materials can be modified by the addition of Iodo-Fl. Additionally there was covalent modification of the 2D crystalline materials with metal chelators anc cyclodextrin.

[0240] As shown in Figure 36, RhuA-Cys-iphen was synthesized. The Cys of RhuA-C133 and RhuA-C266 are conjugated with iPhen as of RhuA-C98. In the presence of CuCl2, there is the formation of a crystalline structure (**Figure 38**). This is also seen in the presence of nickel and zinc as shown in **Figure 39 and 41.** Crystals were also formed in the presence of imidazole (**Figure 40**).

[0241] Protein assembly was also shown to be photoswitchable as seen in Figure **42.**

[0242] Furthermore, the 2D crystalline materials can be further modified in some embodiments by Bis-azobenzene and curcumin (See **Figure 43-53**).

[0243] **Example 28: Genetic Fusions.** As described herein, the 2D crystalline structures or materials of any one of the embodiments described herein can be further modified by a point mutation of an extra cysteine, covalent modification of the lattices (metal chealtors, cyclodextran), as well as any genetic fusions. This can include a His tag, a Pd4Tag or manufacuturing of a ACP fusion protein for use (**Figures 54-59**).

[0244] As shown in **Figure 54,** concentrated samples of C98C18 RhuA mutants (100uM) were treated with iodo Fl for modification.

[0245] As shown in **Figures 55-56,** the RhuA-C98-HisTag (100 μM) was treated in 20 mM MOPS at pH 7 in Redox Condition after 1 Day and observed for crystalline materials.

[0246] Assembly of ^{C98}RhuA-Pd4 (125 μM) under various conditions (after 1 day w/ shake) was also examined **(Figure 57)**.

[0247] Assembly of ^{C98}RhuA-Pd4 (125 μM) under various conditions (after 1 day w/ shake) was also examined in the presence of beta mercaptoethanol and zinc chloride. (**Figure 58**)

[0248] As shown in **Figure 59,** Fusion Protein 2D Assemblies of RhuA-ACP was studied under various conditions. In some embodiments described herein, polypeptide can be genetically engineered to present a fusion peptide for lattice assembly.

[0249] **Example 29: Addition of functionalities onto ^{C98}RhuA via genetic fusions.** To investigate the functionalities on C98RhuA crystals, genetically added HisTag, Pd4, or acyl carrier protein (ACP) at C-terminus of C98RhuA, and their self-assemblies via disulfide formation were tested accordingly. In addition, additional cysteine (C18 or C22) inside of cavity at ^{C98}RhuA for chemical handle was also tested, not for self-assembly.

[0250] The gene for ^{C98}RhuA-HisTag, ^{C98}RhuA-Pd4, and ^{C98}RhuA-ACP based on ^{C98}RhuA were pre-inserted into the pJ414 expression vector optimized for expression in *E. coli*, was purchased from DNA2.0. Protein expression and purification was followed as of ^{C98}RhuA.

[0251] Right after C98RhuA sequence, below sequence was added:

[0252] ^{C98}RhuA-HisTag: GSGSGHHHHHH (Linker-HisTag) (SEQ ID NO: 22) **(Figure 55)**

[0253] ^{C98}RhuA-Pd4: GSGSGTSNAVHPTLRHL (Linker-Pd4 peptide) (SEQ ID NO: 23) **(Figure 58)**

[0254] ^{C98}RhuA-ACP: GSGSGSTIEERVKKIIGEQLGVKQEEVTNNASFVEDLGADSLDTVELVMALEEEFDTE IPDEEAEKITTVQAAIDYINGHQA (Linker-ACP protein) (SEQ ID NO: 24) **(Figure 59)**

[0255] Additional Cys onto ^{C98}RhuA: ^{C18C98}RhuA and ^{C22C98}RhuA **(Figure 64)**

[0256] Several solution conditions were screened for optimizing the formation of 2D protein crystals of fusion proteins and best condition so far was indicated in figures.

[0257] The disclosures of all references listed herein and each of the following references are incorporated herein by reference in their entireties:

References:

[0258] U.S. Pat. No. 9,030,079

[0259] U.S. Publication No. 2011/0059291

[0260] U.S. Publication No. 2011/0156314

[0261] U.S. Publication No. 2015/0075033

[0262] WO 2010/070505 A2

[0263] Baker/King et al., Nature 2014, 510:103–108.

[0264] Baneyx, F. & Matthaei, J. F. Curr. Opin. Biotech. 2014, 28:39.

[0265] Baughman, R. H. Auxetic materials: Avoiding the shrink. Nature 2003, 425:667-667.

[0266] Brodin, J. D. et al. Metal-directed, chemically tunable assembly of one-, two- and three-dimensional crystalline protein arrays. Nat. Chem. 2012, 4:375-382.

[0267] Buehler, Nat. Nanotech., 2011

[0268] Butler, S. Z.; Hollen, S. M.; Cao, L.; Cui, Y.; Gupta, J. A.; Gutiérrez, H. R.; Heinz, T. F.; Hong, S. S.; Huang, J.; Ismach, A. F.; Johnston-Halperin, E.; Kuno, M.; Plashnitsa, V. V.; Robinson, R. D.; Ruoff, R. S.; Salahuddin, S.; Shan, J.; Shi, L.; Spencer, M. G.; Terrones, M.; Windl, W.; & Goldberger, J. E. Progress, Challenges, and Opportunities in Two-Dimensional Materials Beyond Graphene. ACS Nano 2013, 7:2898-2926.

[0269] Choi, J. B. & Lakes, R. S. Non-linear properties of metallic cellular materials with a negative Poisson's ratio. J. Mater. Sci. 1992, 27:5375-5381.

[0270] Colson, J. W. et al. Oriented 2D covalent organic framework thin films on single-layer graphene. Science 2011, 332:228-231.

[0271] Colson, J. W.; Dichtel, W. R. Rationally synthesized two-dimensional polymers. Nat. Chem. 2013, 5:453-465.

[0272] Crowther, R., Henderson, R. & Smith, J. MRC image processing programs. J. Struct. Biol. 1996, 116:9-16.

[0273] Edelhoch, H. Spectroscopic determination of tryptophan and tyrosine in proteins. Biochemistry 1967, 6:1948-1954.

[0274] Engel, A. et al. Assembly of 2-D membrane protein crystals: dynamics, crystal order, and fidelity of structure analysis by electron microscopy. J. Struct. Biol. 1992, 109:219-234.

[0275] Evans, K. E. & Alderson, A. Auxetic materials: functional materials and structures from lateral thinking! Adv. Mater. 2000, 12:617-628.

[0276] Geim, A. K., & Novoselov, K. S., Nat. Mater. 2007, 6:183.

[0277] Gipson, B., Zeng, X., Zhang, Z. Y., & Stahlberg, H., J. Struct. Biol. 2007, 157:64.

[0278] Gonen, S., DiMaio, F., Gonen, T. & Baker, D. Design of ordered two-dimensional arrays mediated by noncovalent protein-protein interfaces. Science 2015, 348:1365-1368.

[0279] Greaves, G. N., Greer, A., Lakes, R. & Rouxel, T. Poisson's ratio and modern materials. Nat. Mater. 2011, 10:823-837.

[0280] Grima, J., Alderson, A. & Evans, K. Auxetic behaviour from rotating rigid units. Phys. Stat. Sol. b 2005, 242:561-575.

[0281] Grueninger, D. et al. Designed protein-protein association. Science 2008, 319:206-209.

[0282] Hampp, N. Bacteriorhodopsin as a photochromic retinal protein for optical memories. Chem. Rev. 2000, 100:1755-1776.

[0283] Heymann, J. B. Bsoft: image and molecular processing in electron microscopy. J. Struct. Biol. 2001, 133:156-169.

[0284] Joshi, R. K. et al. Precise and Ultrafast Molecular Sieving Through Graphene Oxide Membranes. Science 2014, 343:752-754.

[0285] King, N. P.; Sheffler, W.; Sawaya, M. R.; Vollmar, B. S.; Sumida, J. P.; Andro, I.; Gonen, T.; Yeates, T. O.; Baker, D. Computational Design of Self-Assembling Protein Nanomaterials with Atomic Level Accuracy. Science 2012, 336:1171-1174.

[0286] Kissel, P., Murray, D. J., Wulftange, W. J., Catalano, V. J. & King, B. T. A nanoporous two-dimensional polymer by single-crystal-to-single-crystal photopolymerization. Nat. Chem. 2014, 6:774-778.

[0287] Kory, M. J. et al. Gram-scale synthesis of two-dimensional polymer crystals and their structure analysis by X-ray diffraction. Nat. Chem. 2014, 6:779-784.

[0288] Kroemer, M. & Schulz, G. E. The structure of L-rhamnulose-1-phosphate aldolase (class II) solved by low-resolution SIR phasing and 20-fold NCS averaging. Acta Cryst. D. 2002, 58:824-832.

[0289] Kroemer, Biochemistry, Vol. 42 (2003), pp. 10560-10568, Structure and Catalytic Mechanism of L-Rhamnulose-1-phosphate Aldolase.

[0290] Lai, Y.-T.; Cascio, D.; Yeates, T. O. Structure of a 16-nm Cage Designed by Using Protein Oligomers. Science 2012, 336:1129.

[0291] Lakes, R. Foam structures with a negative Poisson's ratio. Science 1987, 235:1038-1040.

[0292] Lanci, C. J.; MacDermaid, C. M.; Kang, S.-g.; Acharya, R.; North, B.; Yang, X.; Qiu, X. J.; DeGrado, W. F.; Saven, J. G. Computational design of a protein crystal. Proc. Natl. Acad. Sci. USA 2012, 109:7304-7309.

[0293] Lebeau, L. et al., Two-dimensional crystallization of a membrane protein on a detergent- resistant lipid monolayer. J. Mol. Biol, 2001, 306:639-647.

[0294] Li, D., Muller, M. B., Gilje, S., Kaner, R. B. & Wallace, G. G. Processable aqueous dispersions of graphene nanosheets. Nat. Nano. 2008, 3:101-105.

[0295] Lu, C.-H., Yang, H.-H., Zhu, C.-L., Chen, X. & Chen, G.-N. A Graphene Platform for Sensing Biomolecules. Angew. Chem. Int. Ed. Engl. 2009, 121:4879-4881.

[0296] Lukowski. M. A.. et al., J. Am. Chem. Soc. 2013, 135:10274.

[0297] Mas-Balleste, R., Gomez-Navarro, C., Gomez-Herrero, J. & Zamora, F. 2D materials: to graphene and beyond. Nanoscale 2011, 3:20-30.

[0298] Mindell, J. A. & Grigorieff, N. Accurate determination of local defocus and specimen tilt in electron microscopy. J. Struct. Biol. 2003, 142:334-347.

[0299] Nicolosi, V., Chhowalla, M., Kanatzidis, M. G., Strano, M. S. & Coleman, J. N. Liquid exfoliation of layered materials. Science 2013, 340:1226419.

[0300] Pettersen, E. F. et al. UCSF Chimera—a visualization system for exploratory research and analysis. J. Comput. Chem. 2004, 25:1605-1612.

[0301] Rabone, J. et al. An adaptable peptide-based porous material. Science 2010, 329:1053-1057.

[0302] Ringler, P. & Schulz, G. E. Self-assembly of proteins into designed networks. Science 2003, 302:106-109.

[0303] Saboe, P. O. et al. Two-Dimensional Protein Crystals for Solar Energy Conversion. Adv. Mater. 2014, 26:7064-7069.

[0304] Scarpa, F., Ciffo, L. & Yates, J. Dynamic properties of high structural integrity auxetic open cell foam. Smart Mat. Struct. 2004, 13:49.

[0305] Schedin, F. et al. Detection of individual gas molecules adsorbed on graphene. Nat. Mater. 2007, 6:652-655.

[0306] Schindelin, J. et al. Fiji: an open-source platform for biological-image analysis. Nat. Meth. 2012, 9:676-682.

[0307] Schneider, C. A., Rasband, W. S. & Eliceiri, K. W. NIH Image to ImageJ: 25 years of image analysis. Nat. Methods 2012, 9:671-675.

[0308] Serre, C. et al. Role of solvent-host interactions that lead to very large swelling of hybrid frameworks. Science 2007, 315:1828-1831.

[0309] Shimomura, S. et al. Selective sorption of oxygen and nitric oxide by an electron-donating flexible porous coordination polymer. Nat. Chem. 2010, 2:633-637.

[0310] Sinclair, J. C.; Davies, K. M.; Venien-Bryan, C.; Noble, M. E. M. Generation of protein lattices by fusing proteins with matching rotational symmetry. Nat. Nanotechnol. 2011, 6:558-562.

[0311] Sleytr, U. B., Schuster, B., Egelseer, E. M. & Pum, D. S-layers: principles and applications. FEMS Microbiol. Rev. 2014, 38:823–864.

[0312] Stahlberg, H. et al. Two-dimensional crystals: a powerful approach to assess structure, function and dynamics of membrane proteins. FEBS Lett. 2001, 504:166-172.

[0313] Suzuki, et al. Self-assembly of coherently dynamic, auxetic, two-dimensional protein crystals. Nature, 2016, 533:369-385.

[0314] Tang, G. et al. EMAN2: an extensible image processing suite for electron microscopy. J. Struct. Biol. 2007, 157:38-46.

[0315] Valpuesta, J. M. a., Carrascosa, J. L. & Henderson, R. Analysis of electron microscope images and electron diffraction patterns of thin crystals of Ø29 connectors in ice. J. Mol. Biol. 1994, 240:281-287.

[0316] Uzgiris, E. & Kornberg, R. Two-dimensional crystallization technique for imaging macromolecules with application to antigen-antibody-complement complexes. Nature 1983, 301:125-129.

[0317] Yeates, T. O. Nanobiotechnology: Protein arrays made to order. Nat. Nanotechnol. 2011, 6:541-542.

WHAT IS CLAIMED IS:

1. A non-naturally occurring symmetrical polypeptide building block comprising a plurality of cysteine residues positioned such that formation of disulfide bonds between some or all of said plurality of cysteine residues facilitates formation of 2D crystals.

2. The polypeptide building block of Claim 1, wherein said polypeptide building block comprises a symmetrical polypeptide comprising a single set of surface cysteine residues in the corner positions.

3. The polypeptide building block of any one of Claims 1 and 2, wherein said polypeptide has inherent C3, C4, C6, D3, D4 or D6 symmetry.

4. The polypeptide building block of any one of Claims 1-3, wherein at least one of said cysteine residues has been introduced into said polypeptide building block through genetic engineering.

5. The polypeptide building block of any one of Claims 1-3, wherein said polypeptide is generated via solid phase synthesis.

6. The polypeptide building block of any one of Claims 1-4, wherein said polypeptide is genetically engineered.

7. The polypeptide building block of any one of Claims 1-7, wherein said polypeptide comprises the RhuA protein.

8. The polypeptide building block of any one of Claims 1-6 further comprising an additional polypeptide modification.

9. The polypeptide building block of Claim 8, wherein said additional modification is selected from the group consisting of a chemical modification, a modification made via an enzymatic reaction, and a modification made via genetic engineering.

10. The polypeptide building block of Claim 9, wherein said additional modification is selected from the group consisting of functional groups, tags, other polypeptides, peptide tags, detectable labels, fluorophores, and nanoparticles.

11. The polypeptide building block of Claim 10, wherein the peptide tag comprises a His tag.

12. The polypeptide building block of Claim 11, wherein the His tag comprises a sequence set forth in SEQ ID NO: 22.

13. The polypeptide of any one of Claims 10-12, wherein the peptide tag comprises a Pd4 peptide.

14. The polypeptide building block of Claim 13, wherein the Pd4 peptide comprises a sequence set forth in SEQ ID NO: 23.

15. The polypeptide of any one of Claims 10-14, wherein the peptide tag comprises a ACP protein.

16. The polypeptide building block of Claim 13, wherein the ACP protein comprises a sequence set forth in SEQ ID NO: 24.

17. The polypeptide building block of any one of Claims 1-16, wherein the polypeptide building block can be chemically modified.

18. The polypeptide of claim 17, wherein the polypeptide is chemically modified with inorganic nanoparticles.

19. The polypeptide building block of any one of Claims 1-18, wherein the polypeptide building block is modified with one or more organic functional groups.

20. The polypeptide of any one of Claims 1-19, wherein the polypeptide building block is modified for different modes of controllable self-assembly.

21. The polypeptide building block of Claim 19 or 20, wherein the organic functional group is a fluorophore, metal chelating group or a host complex.

22. The polypeptide building block of any one of Claims 1-21, wherein the polypeptide building block can be genetically modified/fused with functional proteins and peptides.

23. A 2D crystalline material comprising a polypeptide building block of any one of Claims 1-22.

24. The 2D crystalline material of Claim 23, wherein said 2D crystalline material is auxetic.

25. The 2D crystalline material of Claim 23 or 24 wherein the 2D crystalline material comprises a Poisson's ratio of at least -1.

26. The 2D crystalline material of any one of Claims 23-25 wherein the 2D crystalline material comprises a Poisson's ratio of -1.

27. The 2D crystalline material of any one of Claims 23-26, wherein the 2D crystalline material can be chemically modified.

28. The 2D crystalline material of claim 27, wherein the 2D crystalline material is chemically modified with inorganic nanoparticles.

29. The 2D crystalline material of any one of Claims 23-28, wherein the 2D crystalline material is modified with one or more organic functional groups.

30. The 2D crystalline material of any one of Claims 23-29, wherein the 2D crystalline material is modified for different modes of controllable self-assembly.

31. The 2D crystalline material of Claim 29 or 30, wherein organic functional group is a fluorophore, metal chelating group or a host complex.

32. The 2D crystalline material of any one of Claims 23-31, wherein the 2D crystalline material can be genetically modified/fused with functional proteins and peptides.

33. A lab-on-a-chip comprising the 2D crystalline material of any one of Claims 23-32.

34. A molecular membrane comprising the 2D crystalline material of any one of Claims 23-32.

35. A molecular template comprising the 2D crystalline material of any one of Claims 23-32.

36. A stabilized polypeptide formulation comprising the 2D crystalline material of any one of Claims 23-32.

37. The stabilized polypeptide formulation of Claim 36, wherein the stabilized polypeptide comprises an enzyme or protein.

38. A molecular scaffold comprising the 2D crystalline material of any one of Claims 23-32.

39. A protective armor comprising the 2D crystalline material of any one of Claims 23-32.

40. A smart textile comprising the 2D crystalline material of any one of Claims 23-32.

41. A piezo electronic component comprising the 2D crystalline material of any one of Claims 23-32.

42. An adaptive membrane or sieve comprising the 2D crystalline material of any one of Claims 23-32.

43. A controlled drug release formulation comprising the 2D crystalline material of any one of Claims 23-32.

44. A run-flat tire comprising the 2D crystalline material of any one of Claims 23-32.

45. A method of making a crystalline material comprising:

placing a plurality of polypeptide building blocks of any one of Claims 1-22 under oxidizing conditions; and

allowing said plurality of polypeptide building blocks to self-assemble into said crystalline material.

46. The method of Claim 45, wherein said oxidizing conditions are controllable.

47. The method of any one of Claims 45-46, wherein said plurality of polypeptide building blocks are incubated in solution under said oxidizing conditions.

48. A non-naturally occurring symmetrical polypeptide building block comprising a plurality of histidine residues positioned such that coordination of some or all of said plurality of histidine residues with one or more metal ions facilitates formation of 2D crystals.

49. The polypeptide building block of Claim 48, wherein said polypeptide building block comprises a symmetrical polypeptide comprising surface histidine residues in the corner positions.

50. The polypeptide building block of any one of Claims 48 and 49, wherein said polypeptide has inherent C3, C4, C6, D3, D4 or D6 symmetry.

51. The polypeptide building block of any one of Claims 48-50, wherein at least one of said histidine residues has been introduced into said polypeptide building block through genetic engineering.

52. The polypeptide building block of any one of Claims 48-51, wherein said polypeptide is generated via solid phase synthesis.

53. The polypeptide building block of any one of Claims 48-51, wherein said polypeptide is genetically engineered.

54. The polypeptide building block of any one of Claims 48-53, further comprising an additional modification.

55. The polypeptide building block of Claim 54, wherein said additional modification is selected from the group consisting of a chemical modification, a modification made via an enzymatic reaction, and a modification made via genetic engineering.

56. The polypeptide building block of Claim 55, wherein said additional modification is selected from the group consisting of functional groups, tags, other polypeptides, peptide tags, detectable labels, fluorophores, and nanoparticles.

57. The polypeptide building block of any one of Claims 48-56, wherein said symmetrical polypeptide comprises the RhuA protein.

58. The polypeptide building block of Claim 56 or 57, wherein the peptide tag comprises a His tag.

59. The polypeptide building block of Claim 58, wherein the His tag comprises a sequence set forth in SEQ ID NO: 22.

60. The polypeptide of any one of Claims 56-59, wherein the peptide tag comprises a Pd4 peptide.

61. The polypeptide building block of Claim 60, wherein the Pd4 peptide comprises a sequence set forth in SEQ ID NO: 23.

62. The polypeptide of any one of Claims 56-61, wherein the peptide tag comprises a ACP protein.

63. The polypeptide building block of Claim 62, wherein the ACP protein comprises a sequence set forth in SEQ ID NO: 24.

64. The polypeptide building block of any one of Claims 48-63, wherein the polypeptide building block can be chemically modified.

65. The polypeptide of claim 64, wherein the polypeptide is chemically modified with inorganic nanoparticles.

66. The polypeptide building block of any one of Claims 48-65, wherein the polypeptide building block is modified with one or more organic functional groups.

67. The polypeptide of any one of Claims 48-66, wherein the polypeptide building block is modified for different modes of controllable self-assembly.

68. The polypeptide building block of Claim 66 or 67, wherein the organic functional group is a fluorophore, metal chelating group or a host complex.

69. The polypeptide building block of any one of Claims 48-68, wherein the polypeptide building block can be genetically modified/fused with functional proteins and peptides.

70. A 2D crystalline material comprising a polypeptide building block of any one of Claims 48-69.

71. The 2D crystalline material of Claim 70, wherein said 2D crystalline material is auxetic.

72. The 2D crystalline material of Claim 71 or 72, wherein the 2D crystalline material comprises a Poisson's ratio of at least -1.

73. The 2D crystalline material of any one of Claims 70-72, wherein the 2D crystalline material comprises a Poisson's ratio of -1.

74. The 2D crystalline material of any one of Claims 70-73, wherein the 2D crystalline material can be chemically modified.

75. The 2D crystalline material of claim 74, wherein the 2D crystalline material is chemically modified with inorganic nanoparticles.

76. The 2D crystalline material of any one of Claims 70-75, wherein the 2D crystalline material is modified with one or more organic functional groups.

77. The 2D crystalline material of any one of Claims 70-76, wherein the 2D crystalline material is modified for different modes of controllable self-assembly.

78. The 2D crystalline material of Claim 76 or 77, wherein organic functional group is a fluorophore, metal chelating group or a host complex.

79. The 2D crystalline material of any one of Claims 70-78, wherein the 2D crystalline material can be genetically modified/fused with functional proteins and peptides.

80. A lab-on-a-chip comprising the 2D crystalline material of any one of Claims 70-79.

81. A molecular membrane comprising the 2D crystalline material of any one of Claims 70-79.

82. A molecular template comprising the 2D crystalline material of any one of Claims 70-79.

83. A stabilized polypeptide formulation comprising the 2D crystalline material of any one of Claims 70-79.

84. The stabilized polypeptide formulation of Claim 83, wherein the stabilized polypeptide comprises an enzyme or protein.

85. A molecular scaffold comprising the 2D crystalline material of any one of Claims 70-79.

86. A protective armor comprising the 2D crystalline material of any one of Claims 70-79.

87. A smart textile comprising the 2D crystalline material of any one of Claims 70-79.

88. A piezo electronic component comprising the 2D crystalline material of any one of Claims 70-79.

89. An adaptive membrane or sieve comprising the 2D crystalline material of any one of Claims 70-79.

90. A controlled drug release formulation comprising the 2D crystalline material of any one of Claims 70-79.

91. A run-flat tire comprising the 2D crystalline material of any one of Claims 70-79.

92. A method of making a crystalline material comprising:

placing a plurality of polypeptide building blocks of any one of Claims 48-69 under conditions in which said histidine residues form metal coordinates; and

allowing said plurality of polypeptide building blocks to self-assemble into said crystalline material.

93. The method of Claim 92, wherein said conditions in which said histidine residues form metal coordinates are controllable.

94. The method of any one of Claims 92 and 93, wherein said metal coordinates comprise a metal selected from the group consisting of Zn^{2+} and Cu^{2+}.

95. A polypeptide comprising an amino acid sequence selected from the group consisting of SEQ ID NO: 3, SEQ ID NO: 4 and SEQ ID NO: 5.

96. The polypeptide of Claim 95, further comprising an additional modification.

97. The polypeptide of Claim 96, wherein said additional modification is selected from the group consisting of a chemical modification, a modification made via an enzymatic reaction, and a modification made via genetic engineering.

98. The polypeptide of Claim 97, wherein said additional modification is selected from the group consisting of functional groups, tags, other polypeptides, peptide tags, detectable labels, fluorophores, and nanoparticles.

99. The polypeptide building block of Claim 98, wherein the peptide tag comprises a His tag.

100. The polypeptide building block of Claim 99, wherein the His tag comprises a sequence set forth in SEQ ID NO: 22.

101. The polypeptide of Claims 98, wherein the peptide tag comprises a Pd4 peptide.

102. The polypeptide building block of Claim 101, wherein the Pd4 peptide comprises a sequence set forth in SEQ ID NO: 23.

103. The polypeptide of Claim 98, wherein the peptide tag comprises a ACP protein.

104. The polypeptide of Claim 103, wherein the ACP protein comprises a sequence set forth in SEQ ID NO: 24.

105. The polypeptide of any one of Claims 95-104, wherein the polypeptide building block can be chemically modified.

106. The polypeptide of claim 105, wherein the polypeptide is chemically modified with inorganic nanoparticles.

107. The polypeptide building block of any one of Claims 95-106, wherein the polypeptide building block is modified with one or more organic functional groups.

108. The polypeptide of any one of Claims 95-107, wherein the polypeptide building block is modified for different modes of controllable self-assembly.

109. The polypeptide building block of Claim 107 or 108, wherein the organic functional group is a fluorophore, metal chelating group or a host complex.

110. The polypeptide building block of any one of Claims 95-110, wherein the polypeptide building block can be genetically modified/fused with functional proteins and peptides.

111. A 2D crystalline material comprising the polypeptide of any one of Claims 95-110.

112. The 2D crystalline material of Claim 111, wherein said 2D crystalline material is auxetic.

113. The 2D crystalline material of Claim 111 or 112, wherein the 2D crystalline material comprises a Poisson's ratio of at least -1.

114. The 2D crystalline material of any one of Claims 111-113, wherein the 2D crystalline material comprises a Poisson's ratio of -1.

115. The 2D crystalline material of any one of Claims 111-114, wherein the 2D crystalline material can be chemically modified.

116. The 2D crystalline material of claim 115, wherein the 2D crystalline material is chemically modified with inorganic nanoparticles.

117. The 2D crystalline material of any one of Claims 111-116, wherein the 2D crystalline material is modified with one or more organic functional groups.

118. The 2D crystalline material of any one of Claims 111-117, wherein the 2D crystalline material is modified for different modes of controllable self-assembly.

119. The 2D crystalline material of Claim 117 or 118, wherein organic functional group is a fluorophore, metal chelating group or a host complex.

120. The 2D crystalline material of any one of Claims 111-119, wherein the 2D crystalline material can be genetically modified/fused with functional proteins and peptides.

121. A polypeptide comprising the amino acid sequence of SEQ ID NO: 2, 19, 20 21 or 24.

122. The polypeptide of Claim 121, further comprising an additional modification.

123. The polypeptide of Claim 122, wherein said additional modification is selected from the group consisting of a chemical modification, a modification made via an enzymatic reaction, and a modification made via genetic engineering.

124. The polypeptide of Claim 123, wherein said additional modification is selected from the group consisting of functional groups, tags, other polypeptides, peptide tags, detectable labels, fluorophores, and nanoparticles.

125. The polypeptide building block of Claim 124, wherein the peptide tag comprises a His tag.

126. The polypeptide building block of Claim 125, wherein the His tag comprises a sequence set forth in SEQ ID NO: 22.

127. The polypeptide of Claims 124, wherein the peptide tag comprises a Pd4 peptide.

128. The polypeptide building block of Claim 127, wherein the Pd4 peptide comprises a sequence set forth in SEQ ID NO: 23.

129. The polypeptide of any one of Claims 124, wherein the peptide tag comprises a ACP protein.

130. The polypeptide building block of Claim 129, wherein the ACP protein comprises a sequence set forth in SEQ ID NO: 24.

131. The polypeptide building block of any one of Claims 121-130, wherein the polypeptide building block can be chemically modified.

132. The polypeptide of claim 131, wherein the polypeptide is chemically modified with inorganic nanoparticles.

133. The polypeptide building block of any one of Claims 121-132, wherein the polypeptide building block is modified with one or more organic functional groups.

134. The polypeptide of any one of Claims 121-133, wherein the polypeptide building block is modified for different modes of controllable self-assembly.

135. The polypeptide building block of Claim 133 or 134, wherein the organic functional group is a fluorophore, metal chelating group or a host complex.

136. The polypeptide building block of any one of Claims 121-135, wherein the polypeptide building block can be genetically modified/fused with functional proteins and peptides.

137. A 2D crystalline material comprising the polypeptide of any one of Claims 121-136.

138. The 2D crystalline material of Claim 137, wherein said 2D crystalline material is auxetic.

139. The 2D crystalline material of Claim 137 or 138, wherein the 2D crystalline material comprises a Poisson's ratio of at least -1.

140. The 2D crystalline material of any one of Claims 137-139, wherein the 2D crystalline material comprises a Poisson's ratio of -1.

141. The 2D crystalline material of any one of Claims 137-140, wherein the 2D crystalline material can be chemically modified.

142. The 2D crystalline material of claim 141, wherein the 2D crystalline material is chemically modified with inorganic nanoparticles.

143. The 2D crystalline material of any one of Claims 137-142, wherein the 2D crystalline material is modified with one or more organic functional groups.

144. The 2D crystalline material of any one of Claims 137-143, wherein the 2D crystalline material is modified for different modes of controllable self-assembly.

145. The 2D crystalline material of Claim 143 or 144, wherein organic functional group is a fluorophore, metal chelating group or a host complex.

146. The 2D crystalline material of any one of Claims 137-145, wherein the 2D crystalline material can be genetically modified/fused with functional proteins and peptides.

147. The 2D crystalline material of any one of Claims 23-32, 70-79, 111-120, or 137-146, wherein the 2D crystalline material can be assembled by visible light and dissembled by UV light.

FIG. 1 **A majority of biological machines and materials are self-assembled, dynamic/responsive multiprotein architectures**

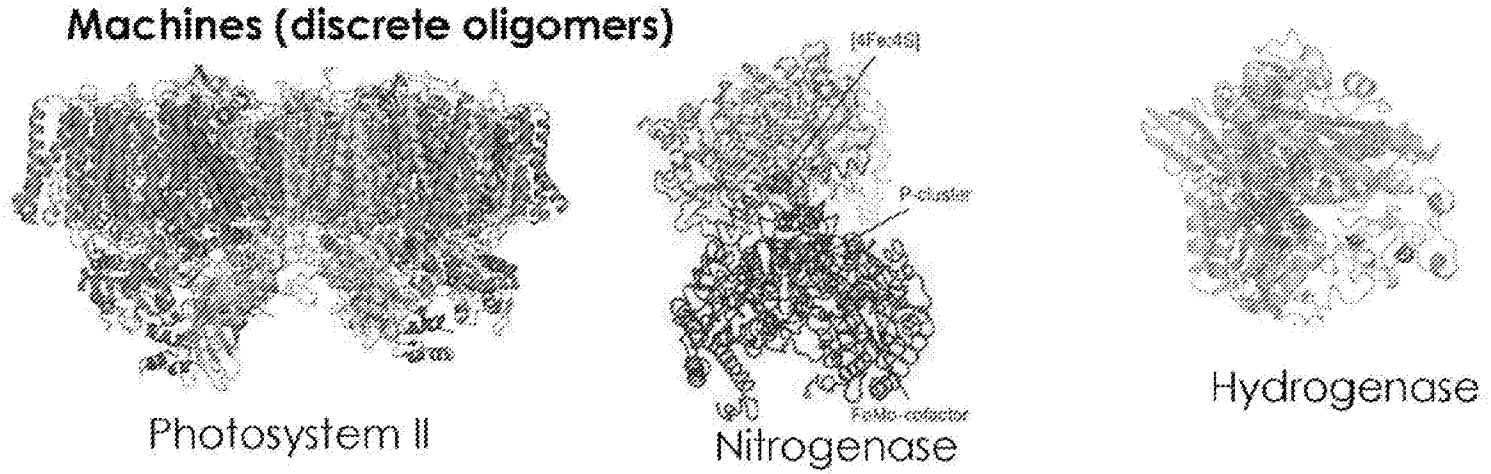


FIG. 2

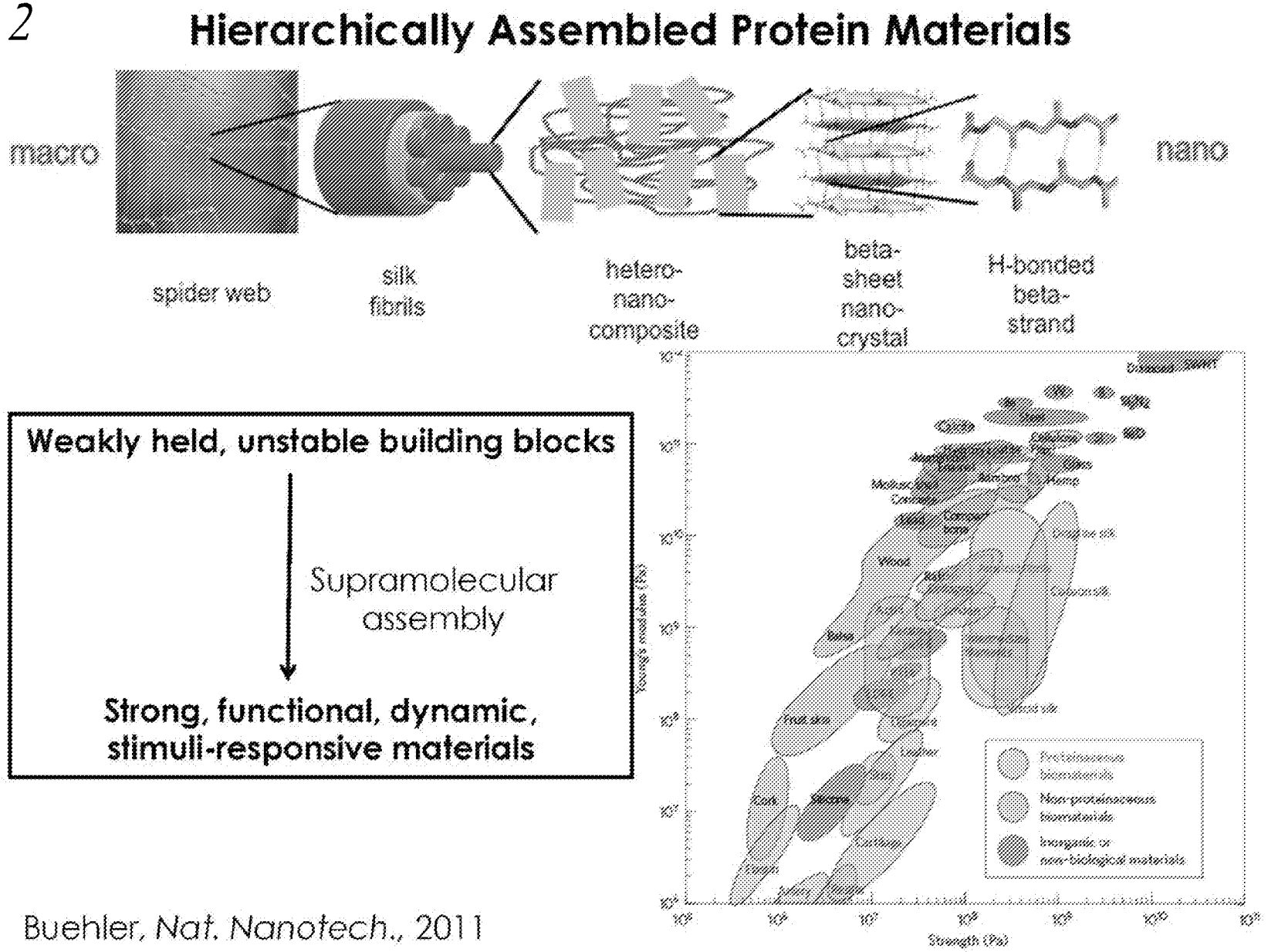

Hierarchically Assembled Protein Materials
macro
nano
spider web
silk fibrils
hetero-nano-composite
beta-sheet nano-crystal
H-bonded beta-strand
Weakly held, unstable building blocks
Supramolecular assembly
Strong, functional, dynamic, stimuli-responsive materials
Strength (Pa)
Buehler, Nat. Nanotech., 2011

FIG. 3

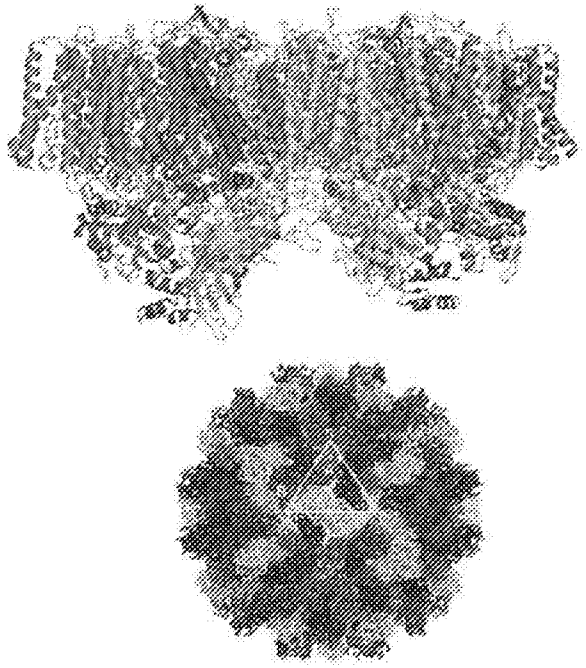
Proteins as building blocks for functional nanomaterials

Advantages

– 20 distinct components (i.e., amino acids) → nearly infinite structural and functional diversity

– inherently nanoscale

– genetically encoded → producible and evolvable in living systems



Disadvantages

– 20 distinct components → structure, self assembly and function difficult to program

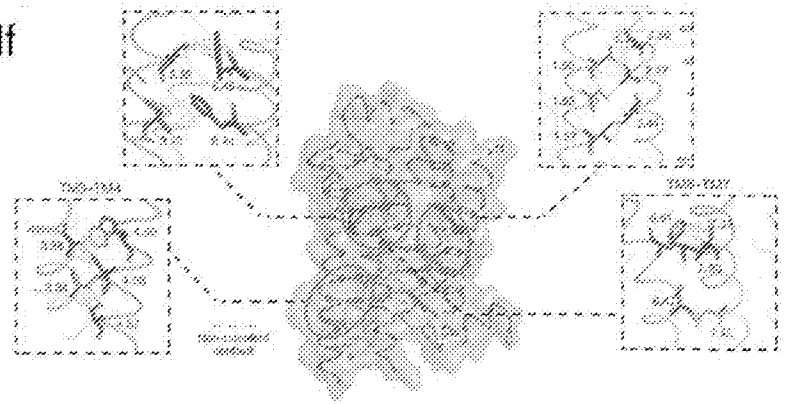
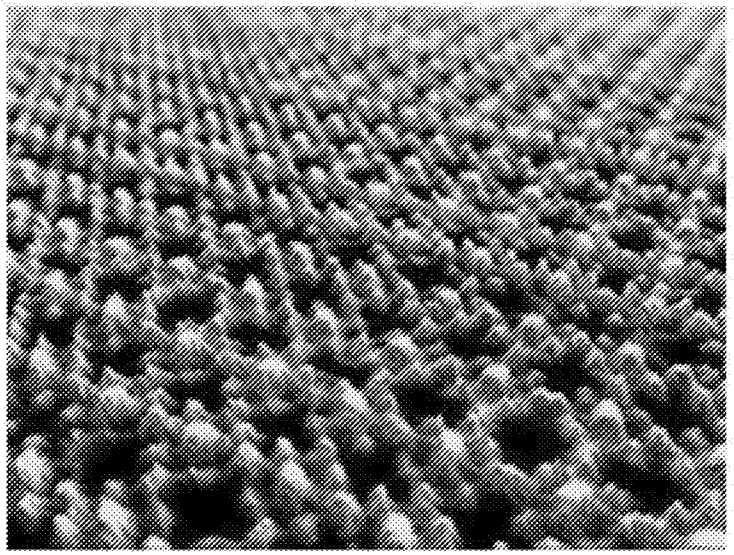
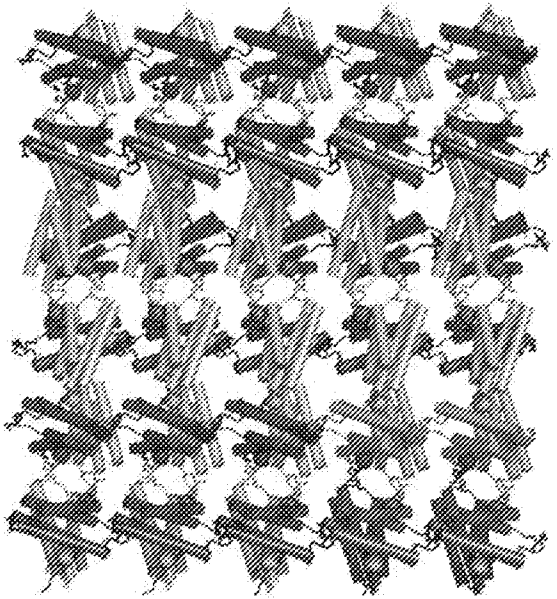


FIG. 4 **What would we gain by fabricating 2D supramolecular protein assemblies?**

-high surface area/volume ratio
-dense display of a diverse set of chemical functionalities in a highly ordered, yet dynamic fashion
-innately functional building blocks (e.g., functional enzymes)
-potential for smart materials, lab-on-a-chip technologies, heterogeneous catalyst platforms



Bacterial S-layers



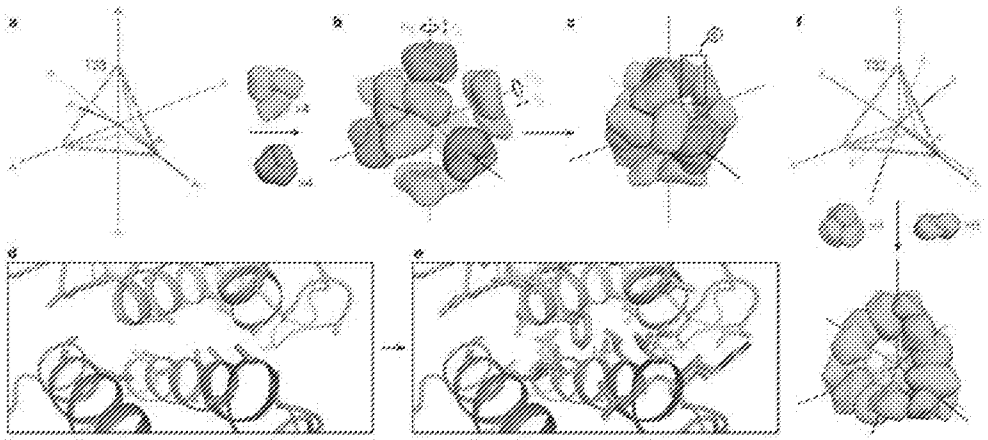
Zn-RIDC3 arrays

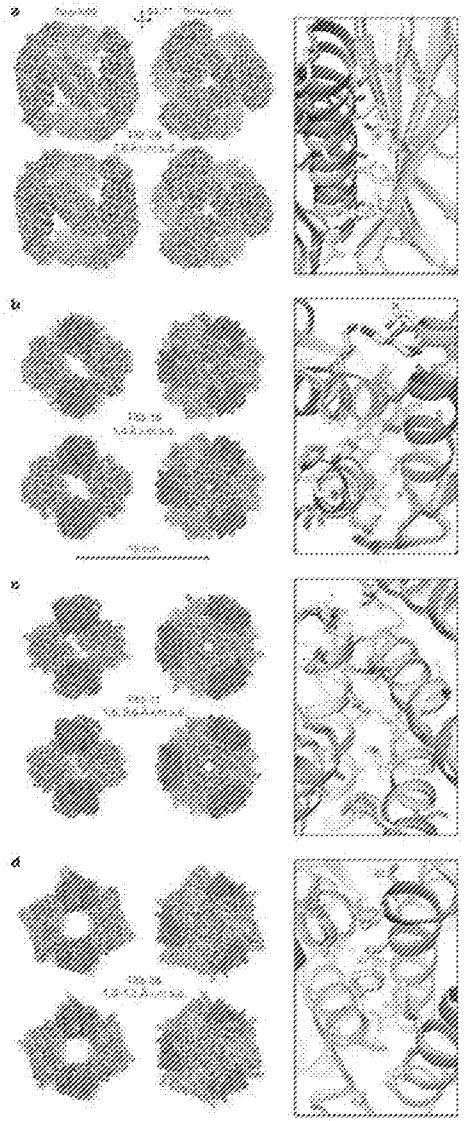
FIG. 5

Existing approaches for designed protein assembly

Computational design of new protein interfaces between symmetrical, homooligomeric proteins

Baker/King et al., Nature 510, 103–108 (2014)





Drawbacks:

-Too design-intensive

- Involves sophisticated, but not sure-fire computational methods or protein fusion strategies that do not always give the desired product

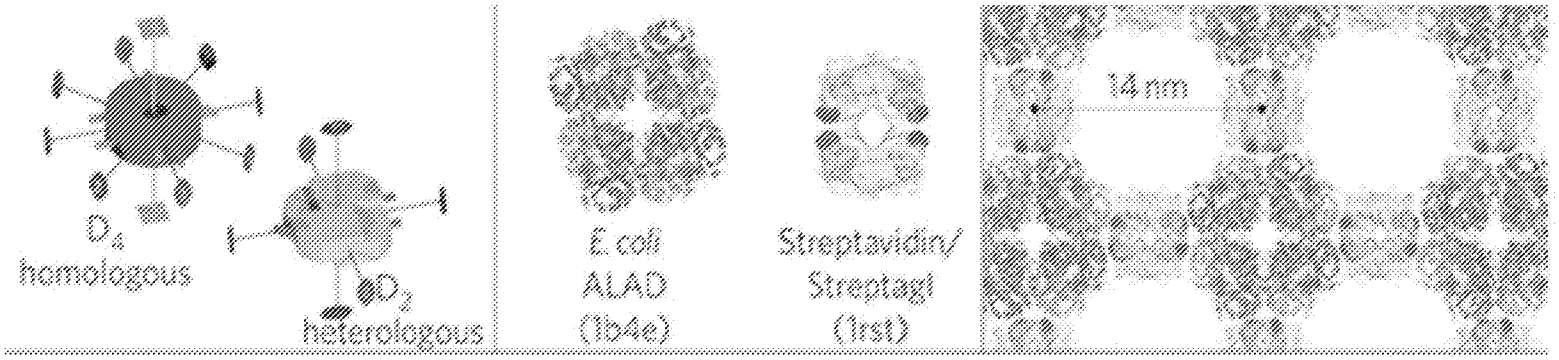
-The desired products are not scalable, do not always possess superior materials properties (e.g. perfect structural order, stimuli-responsiveness, etc.)

FIG. 6

Existing approaches for designed protein assembly

Covalent fusion of homooligomeric proteins or self-assembling protein monomers

Sinclair, Yeates etc. Nat. Nanotech. 6, 558–562 (2011)



Drawbacks:

-Too design-intensive

- Involves sophisticated, but not sure-fire computational methods or protein fusion strategies that do not always give the desired product

-The desired products are not scalable, do not always possess superior materials properties (e.g. perfect structural order, stimuli-responsiveness, etc.)

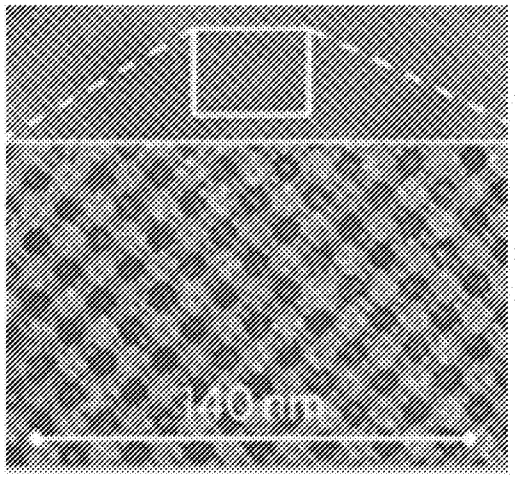


FIG. 7

Our approach: Disulfide-mediated assembly of 2D protein materials

- Bypasses the need for time-/cost-intensive computational design or protein-fusion: the only step is the engineering of cysteine residues at proper positions on a protein building block of choice.
- The requirement is a C3, C4 or C6-symmetric protein that is expressible in bacteria.
- Experimental flow/feasibility testing is highly streamlined: 1) protein expression/purification, 2) testing of different oxidative conditions for self-assembly (air oxidation or redox buffer systems). 3) characterization by electron microscopy)

FIG. 8

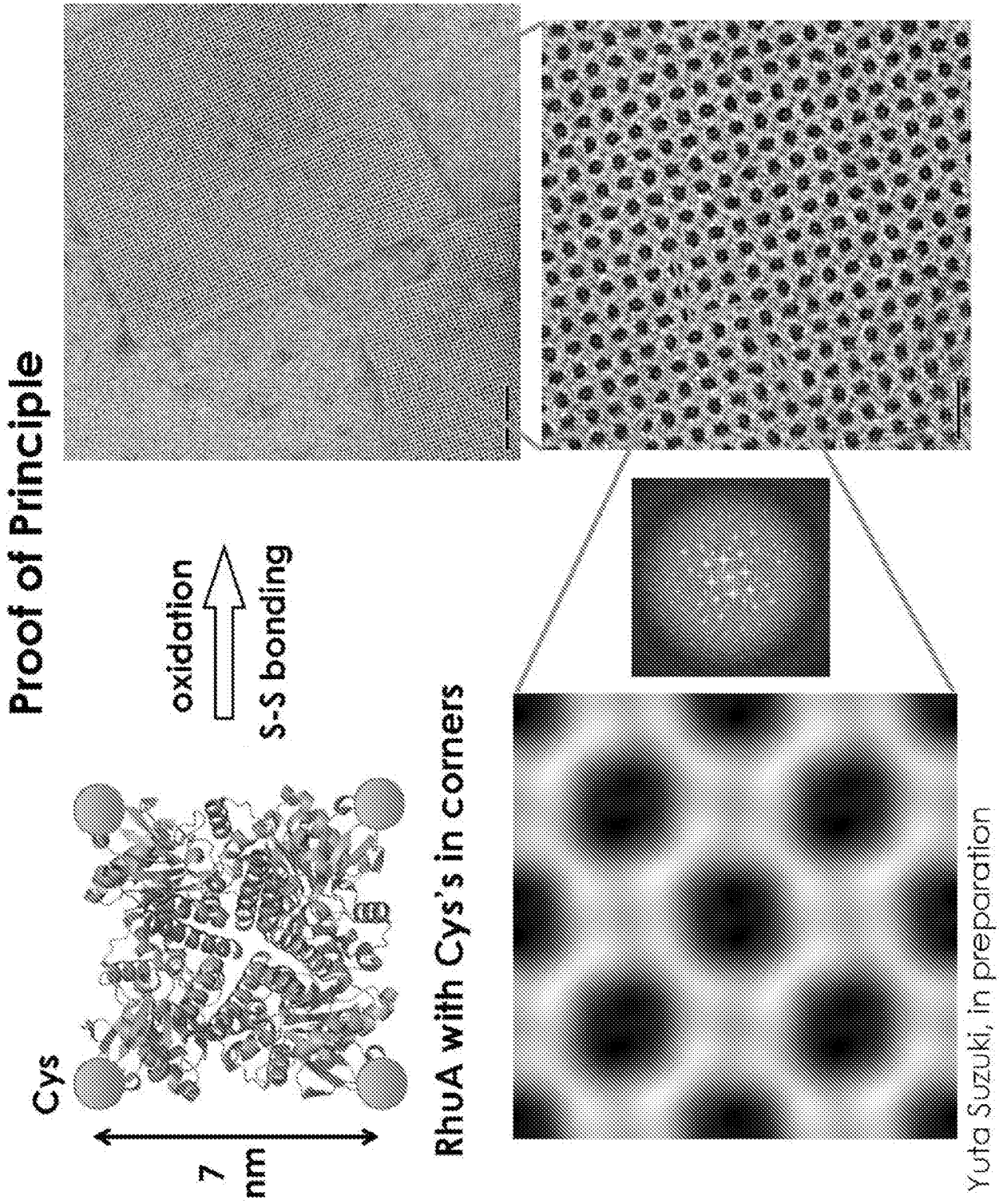
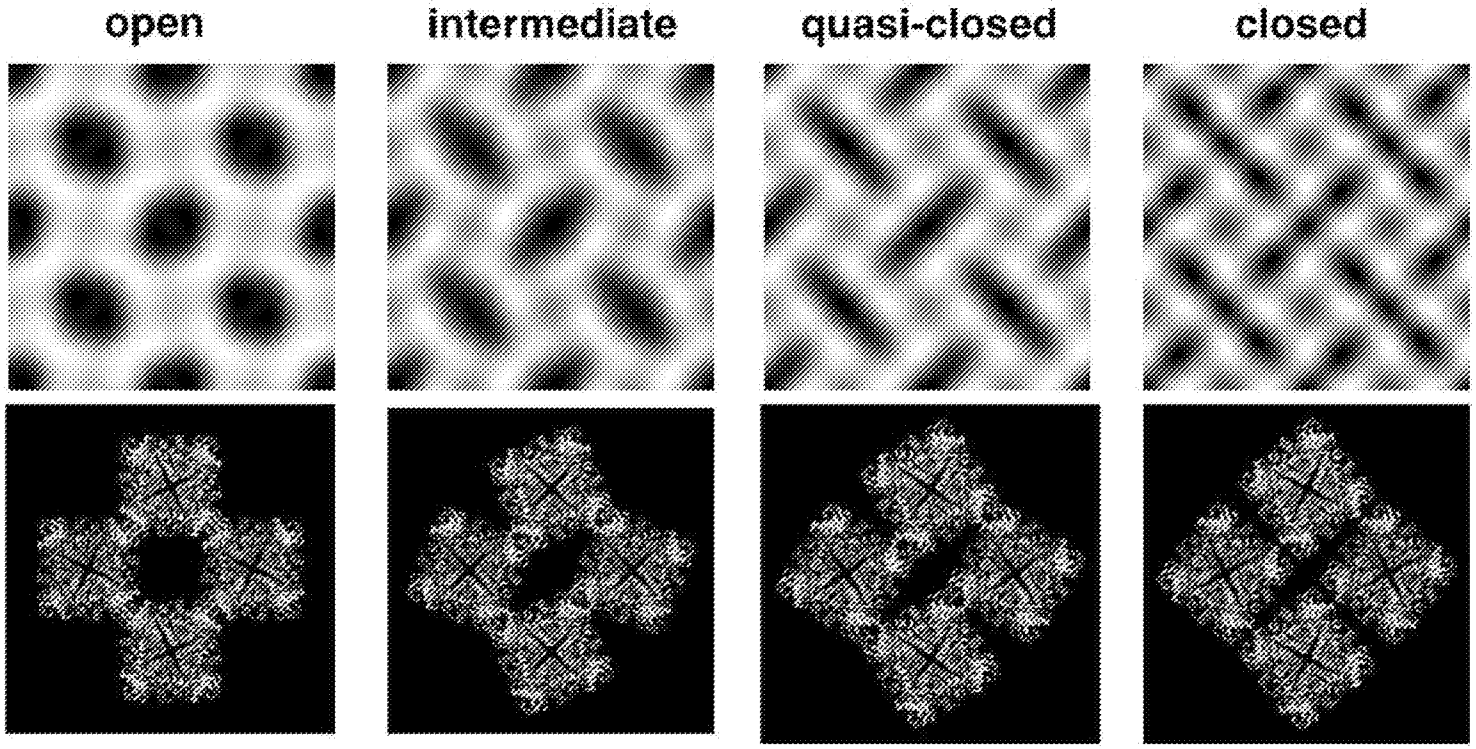

Proof of Principle
Cys
7 nm
oxidation
S-S bonding
RhuA with Cys's in corners
Yuta Suzuki, in preparation

FIG. 9

Disulfide-linker 2D C98-RhuA crystals

- Extremely easily designed (took us 10 min to find proper locations for Cys incorporation) and tested
- Robust, reproducible self-assembly
- Crystalline order over large length-scales (up to several microns)
- Single-layered
- Essentially defect-free
- **And DYNAMIC!!!** (no precedent for dynamic 2D crystalline protein materials)



→ New potential for smart/stimuli-responsive nano- and bio-materials, mechanical nanodevices

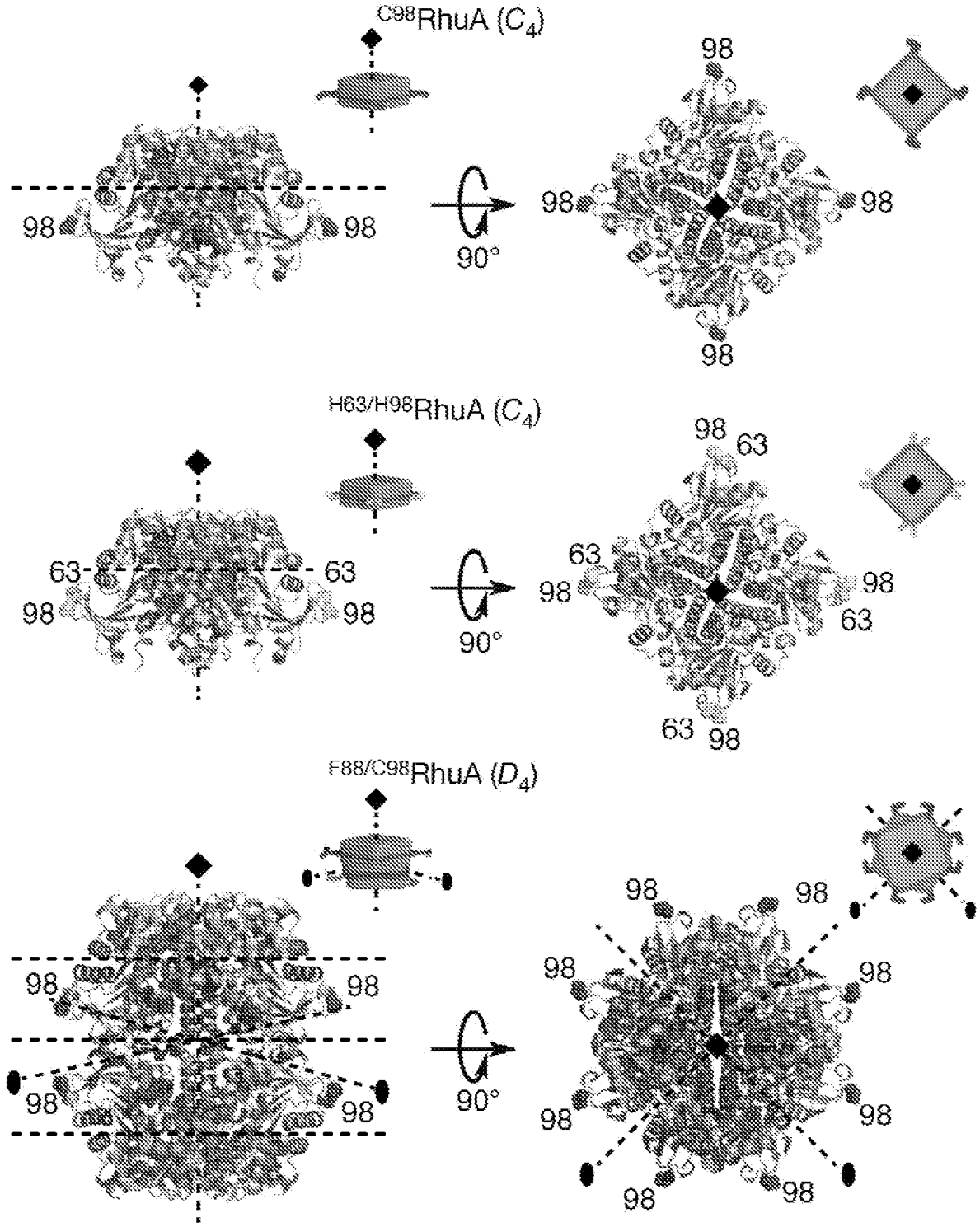

C98RhuA (C4)
98
98
90°
98
98
98
H63/H98RhuA (C4)
63
63
98
90°
98
63
63
98
98
63
63
98
F88/C98RhuA (D4)
98
98
98
98
90°
98
98
98
98
98
98
98
98

FIG. 10A

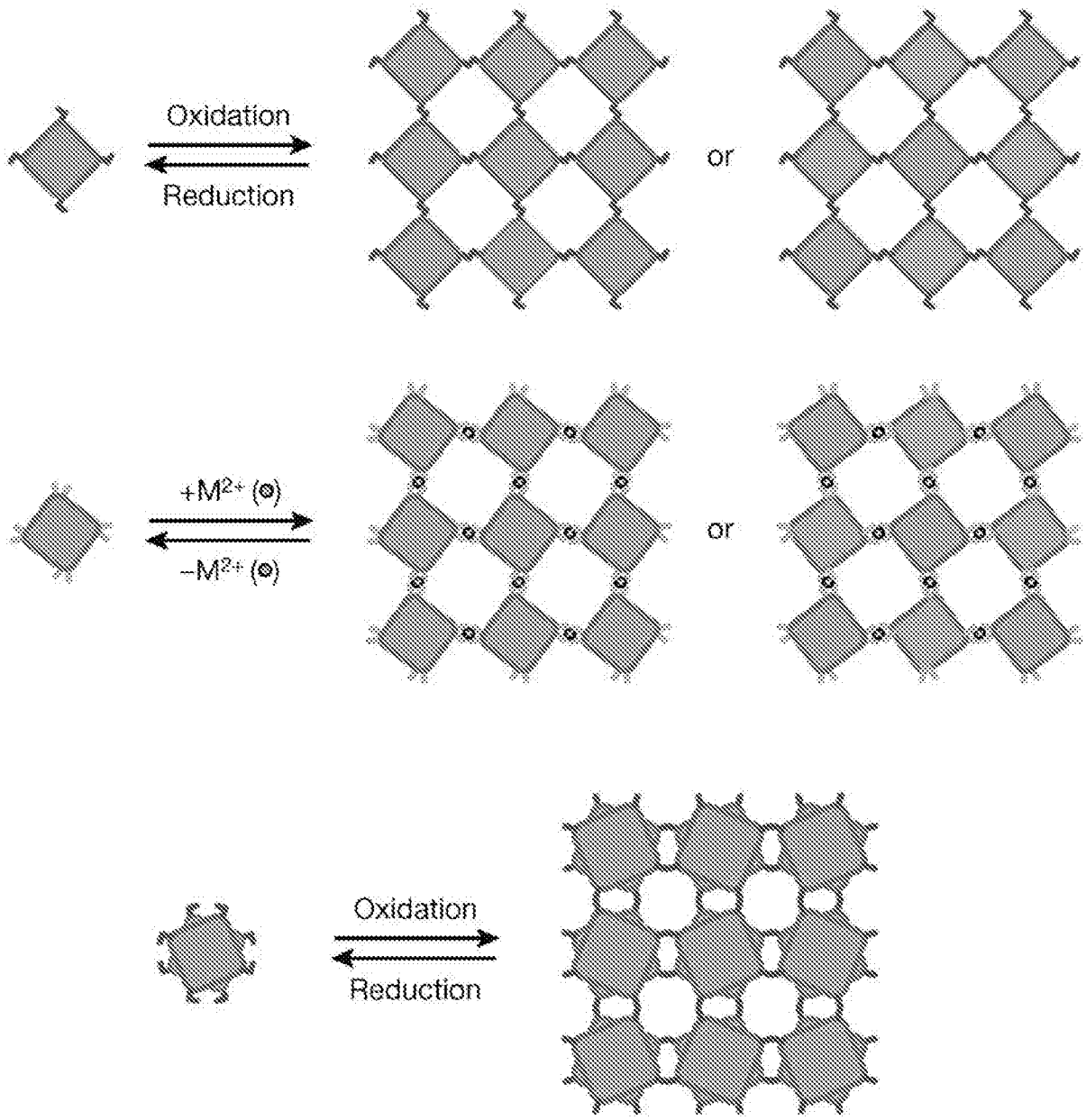


FIG. 10B

FIG. 10C

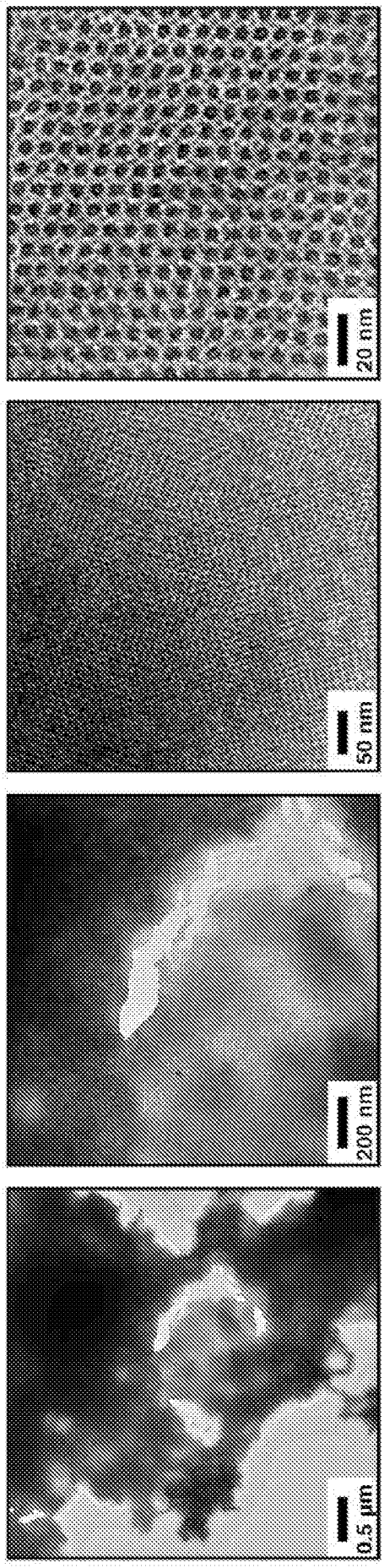
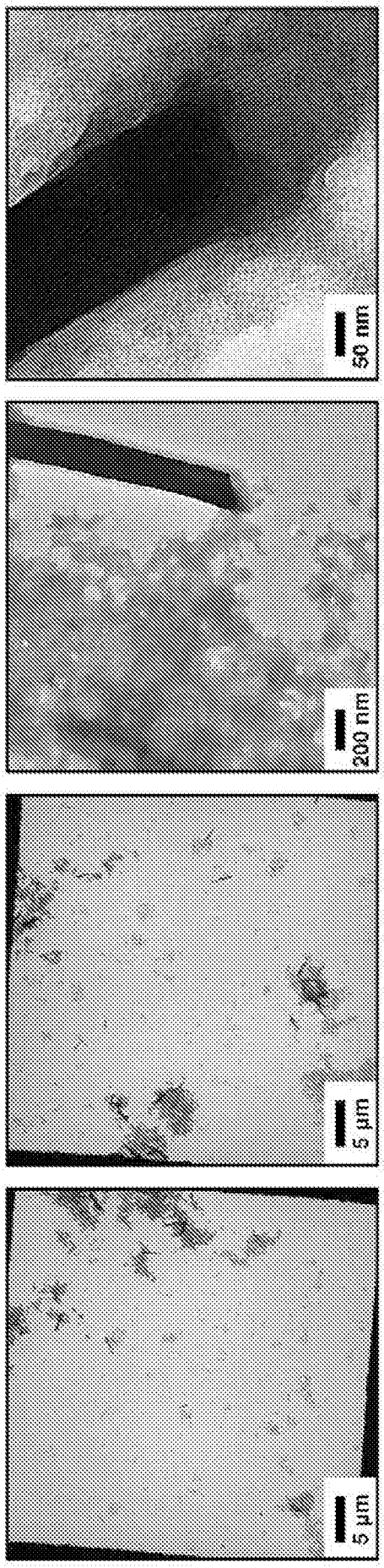


FIG. 10D



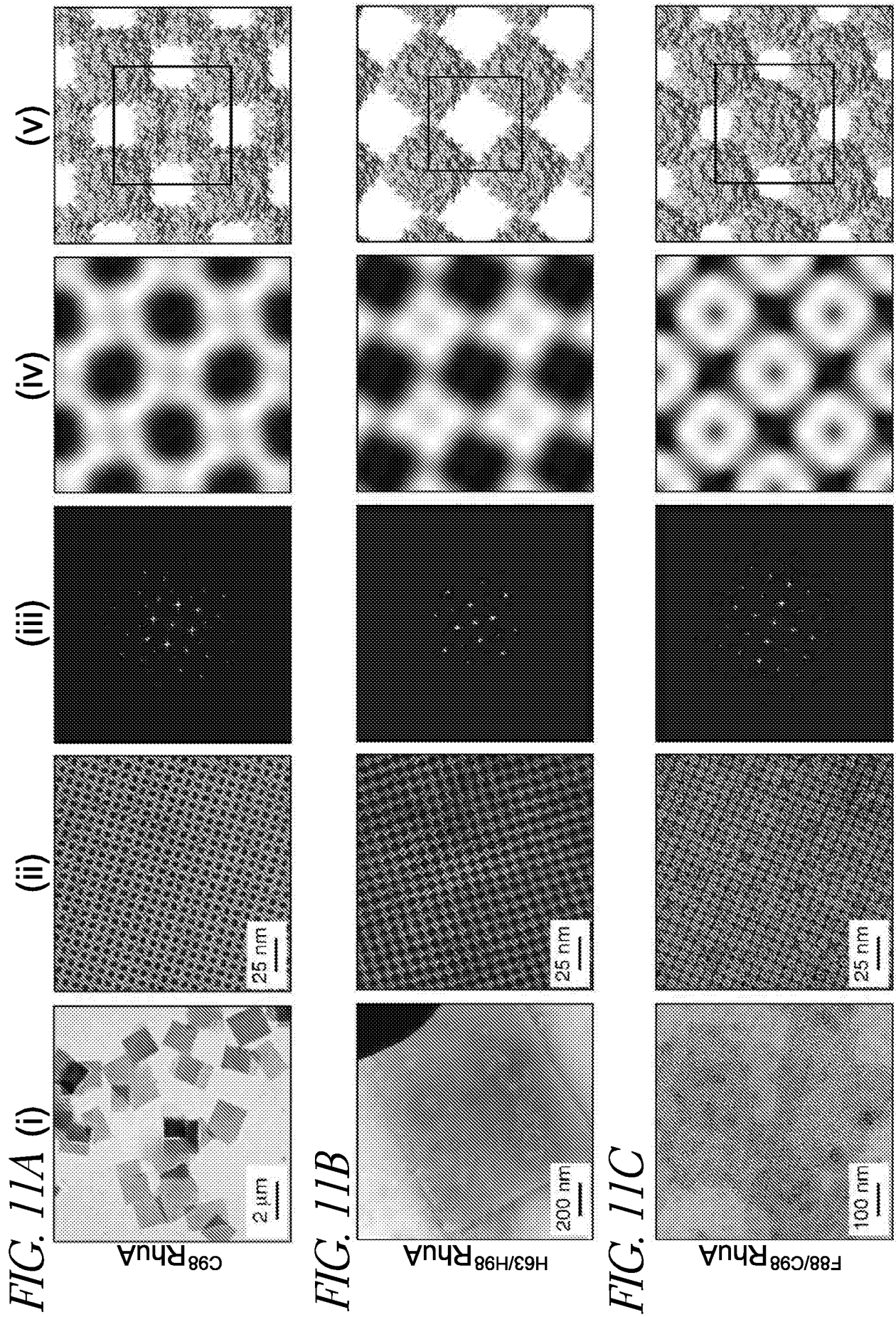


FIG. 11A

FIG. 11B

FIG. 11C

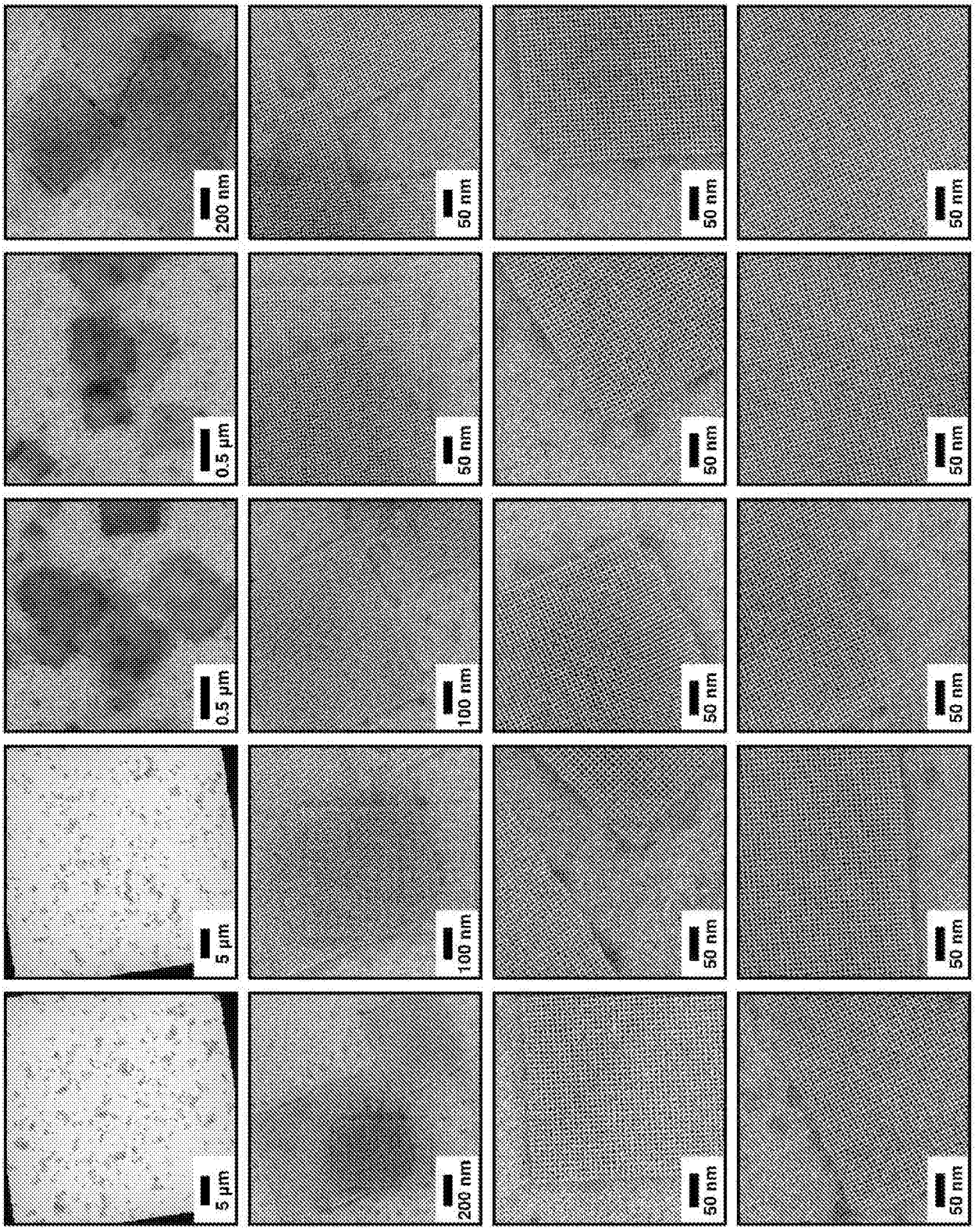

5 µm
0.5 µm
0.5 µm
200 nm
200 nm
100 nm
100 nm
50 nm
50 nm
50 nm
50 nm
50 nm
50 nm
50 nm
50 nm
50 nm
50 nm
50 nm

FIG. 11D

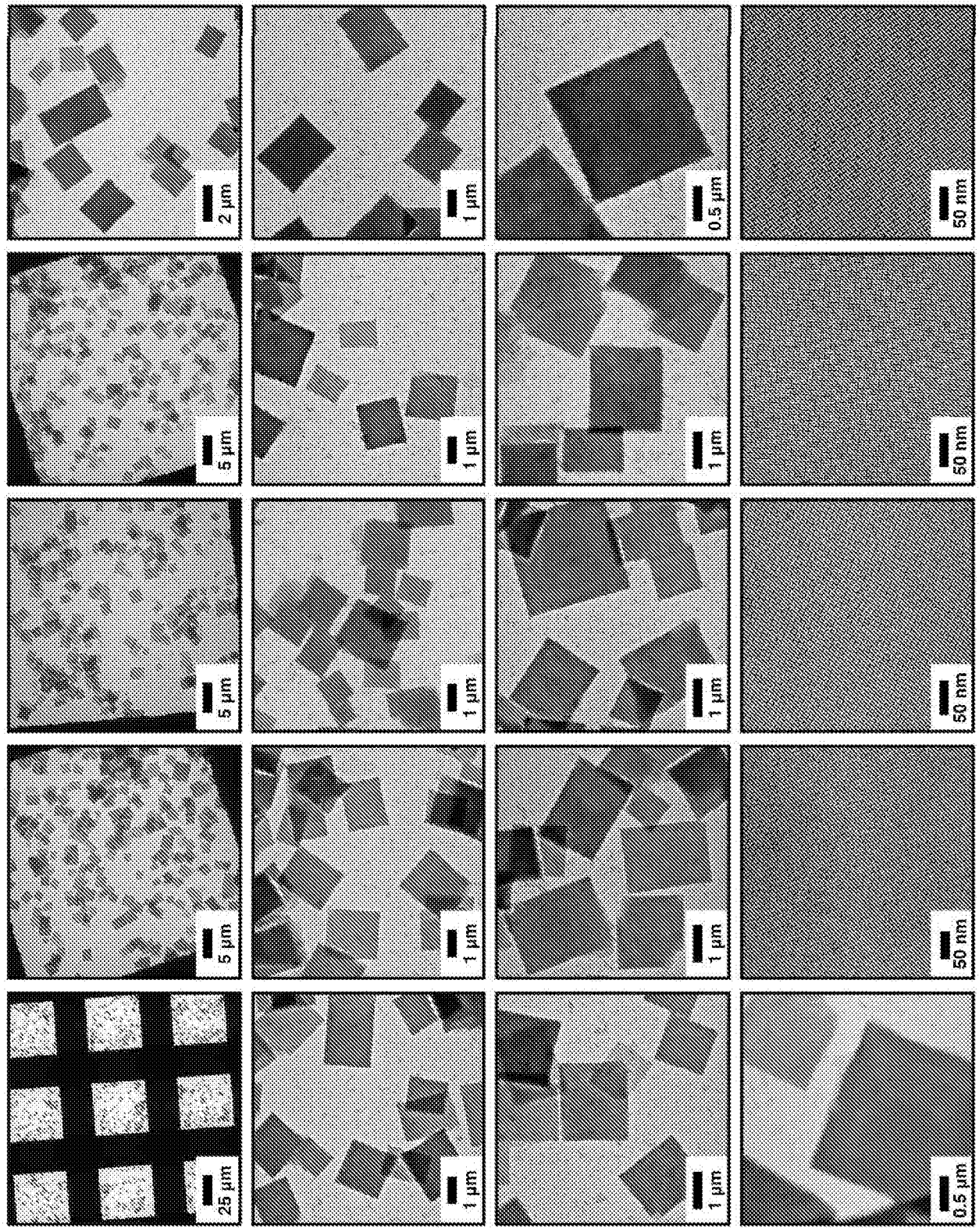

25 µm
5 µm
5 µm
5 µm
2 µm
1 µm
1 µm
1 µm
1 µm
1 µm
1 µm
1 µm
0.5 µm
50 nm
50 nm
50 nm
50 nm
0.5 µm

FIG. 11E

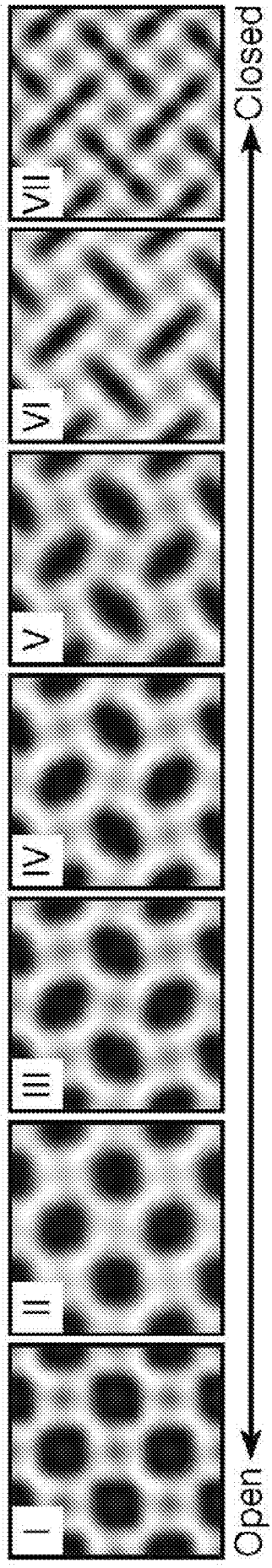


FIG. 12A

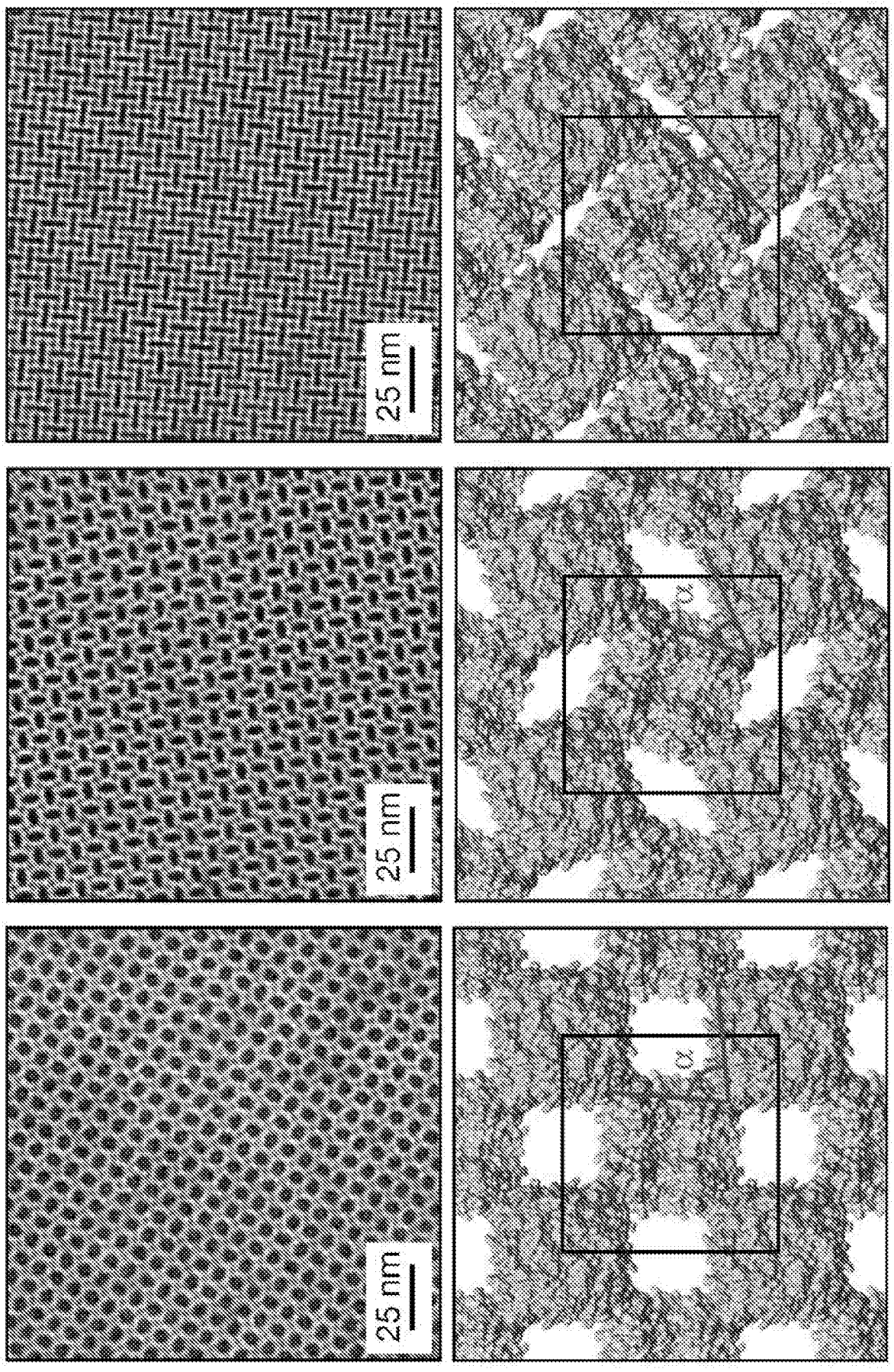


FIG. 12B

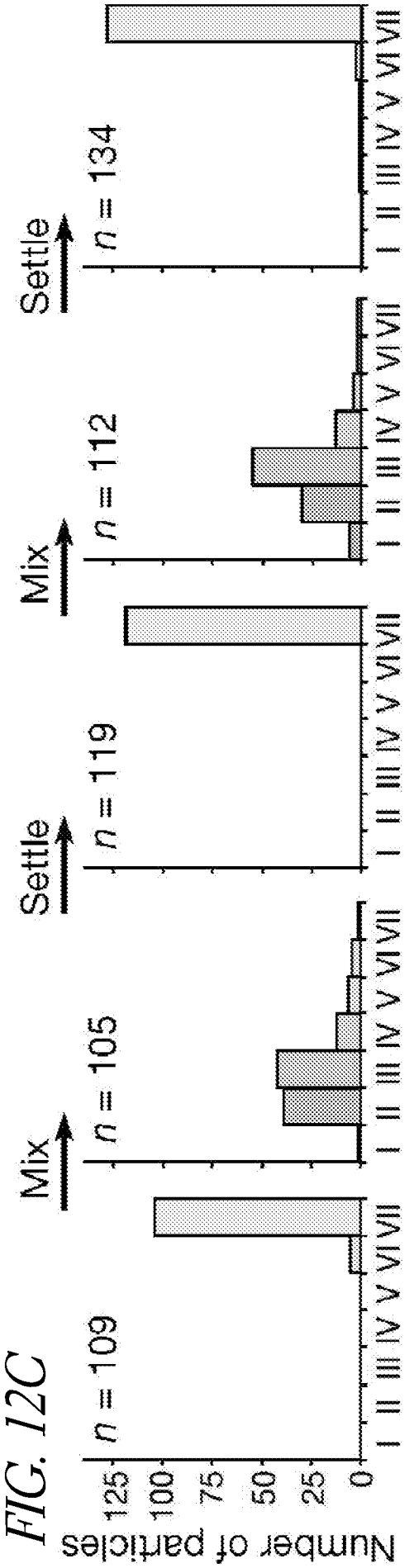


FIG. 12C

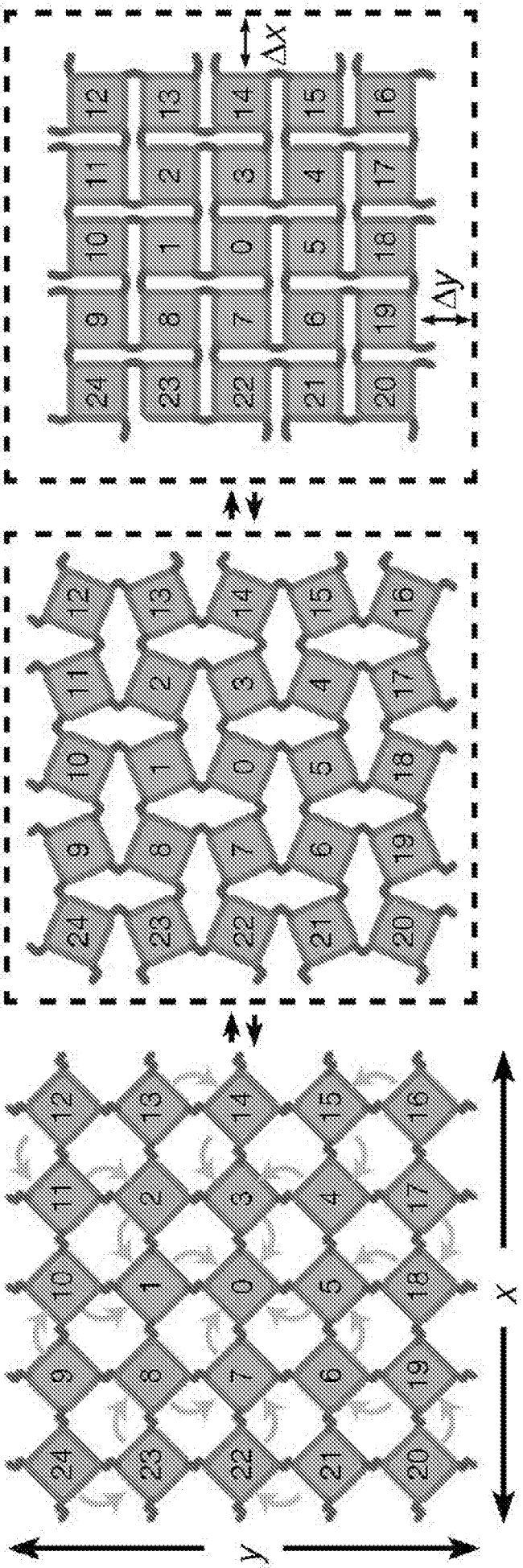


FIG. 12D

FIG. 12E

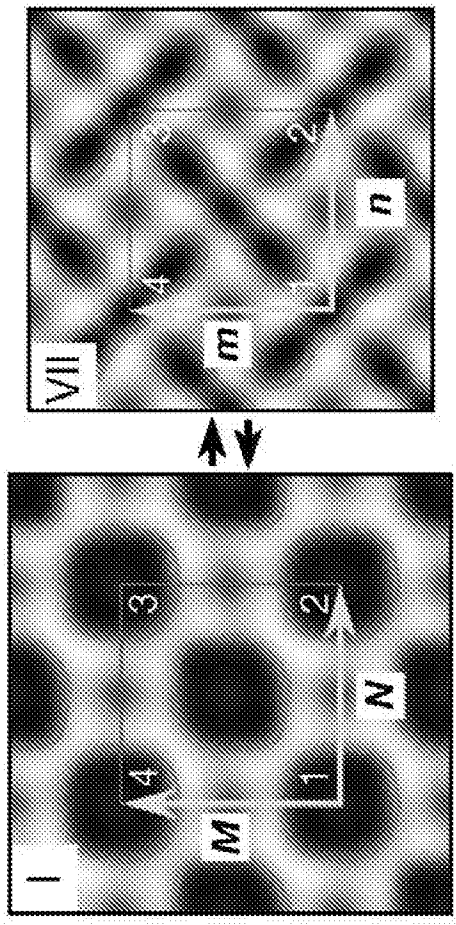
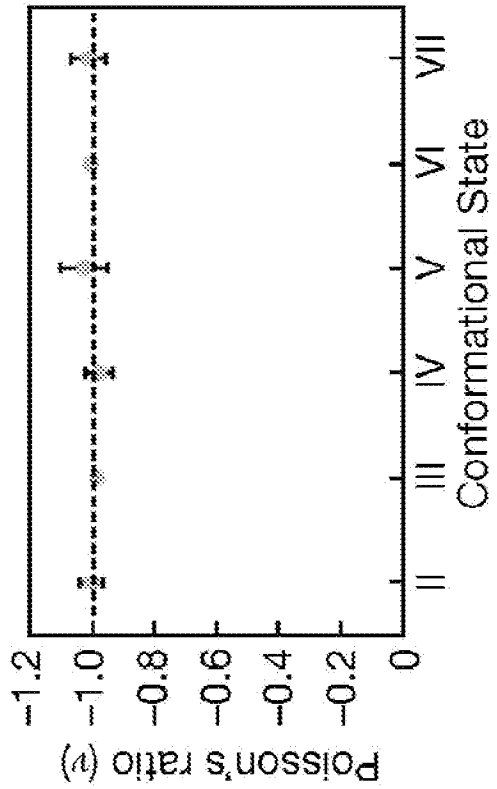


FIG. 12F



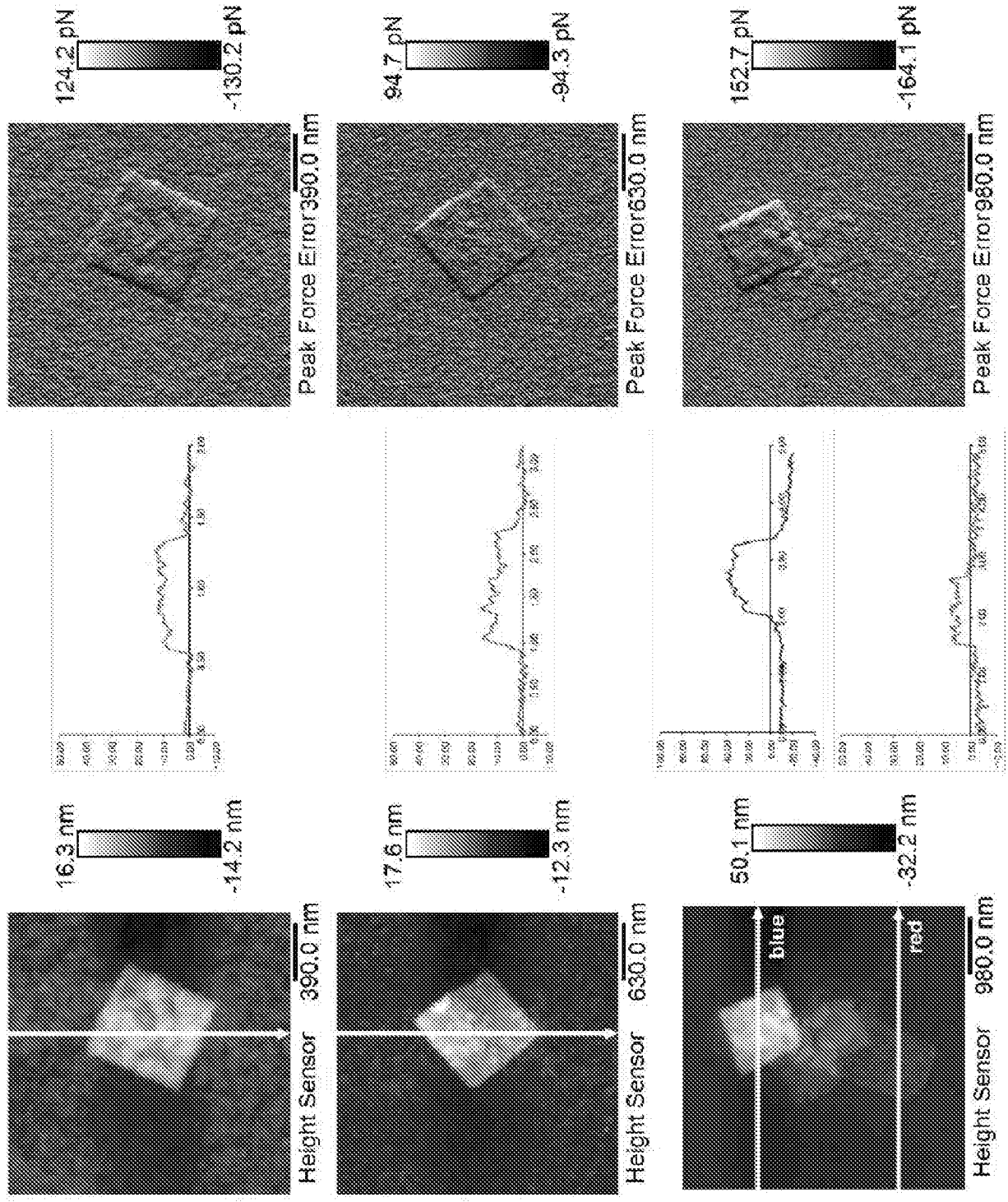

124.2 pN
-130.2 pN
Peak Force Error 390.0 nm
16.3 nm
-14.2 nm
Height Sensor 390.0 nm
94.7 pN
-94.3 pN
Peak Force Error 630.0 nm
17.6 nm
-12.3 nm
Height Sensor 630.0 nm
152.7 pN
-164.1 pN
Peak Force Error 980.0 nm
50.1 nm
-32.2 nm
blue
red
Height Sensor 980.0 nm

FIG. 12G

FIG. 12H

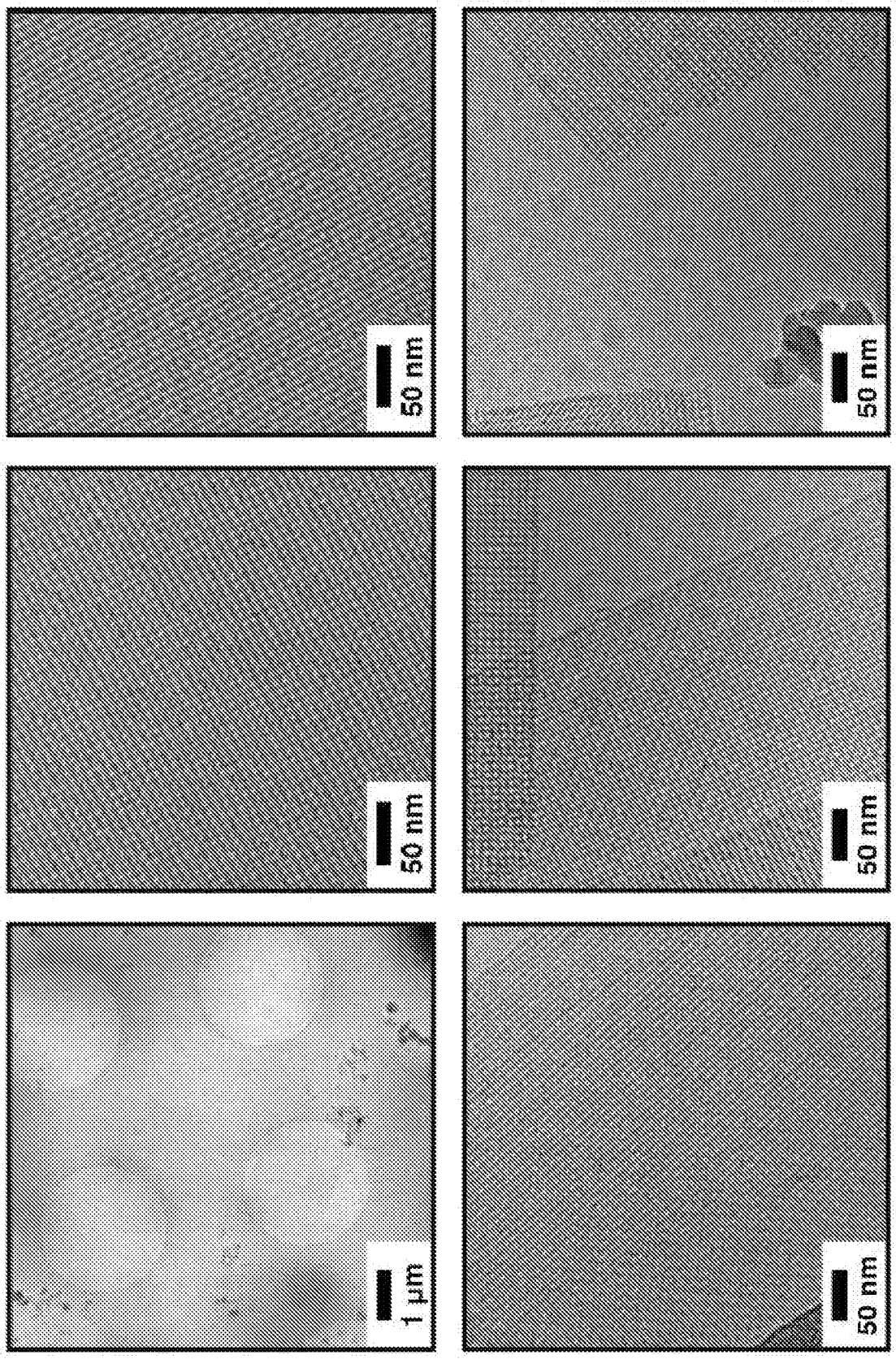


FIG. 12I

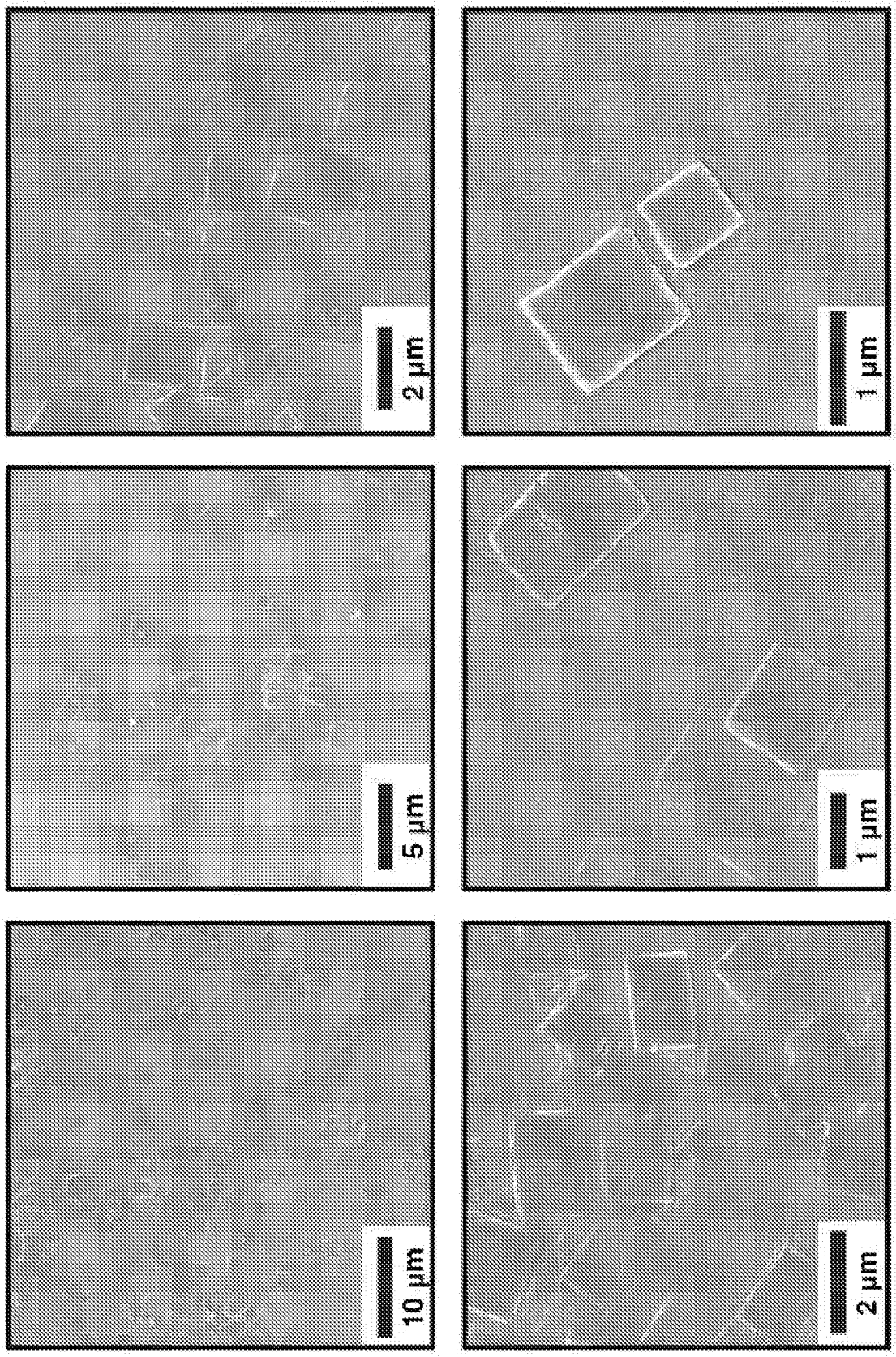


FIG. 13

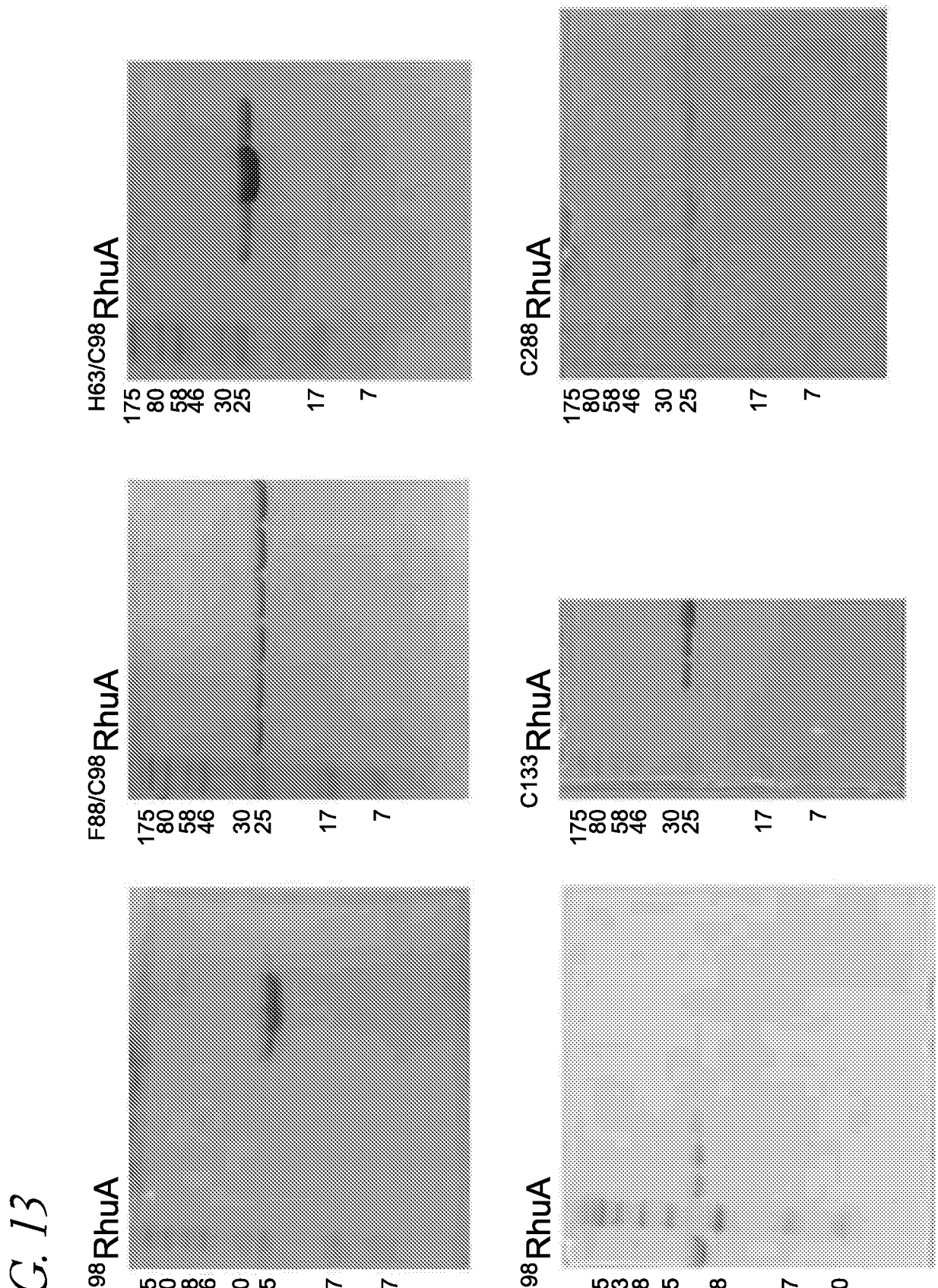

C98 RhuA
F88/C98 RhuA
H63/C98 RhuA
C133 RhuA
C288 RhuA
D98 RhuA
175
80
58
46
30
25
17
7
75
63
48
35
28
10

FIG. 14

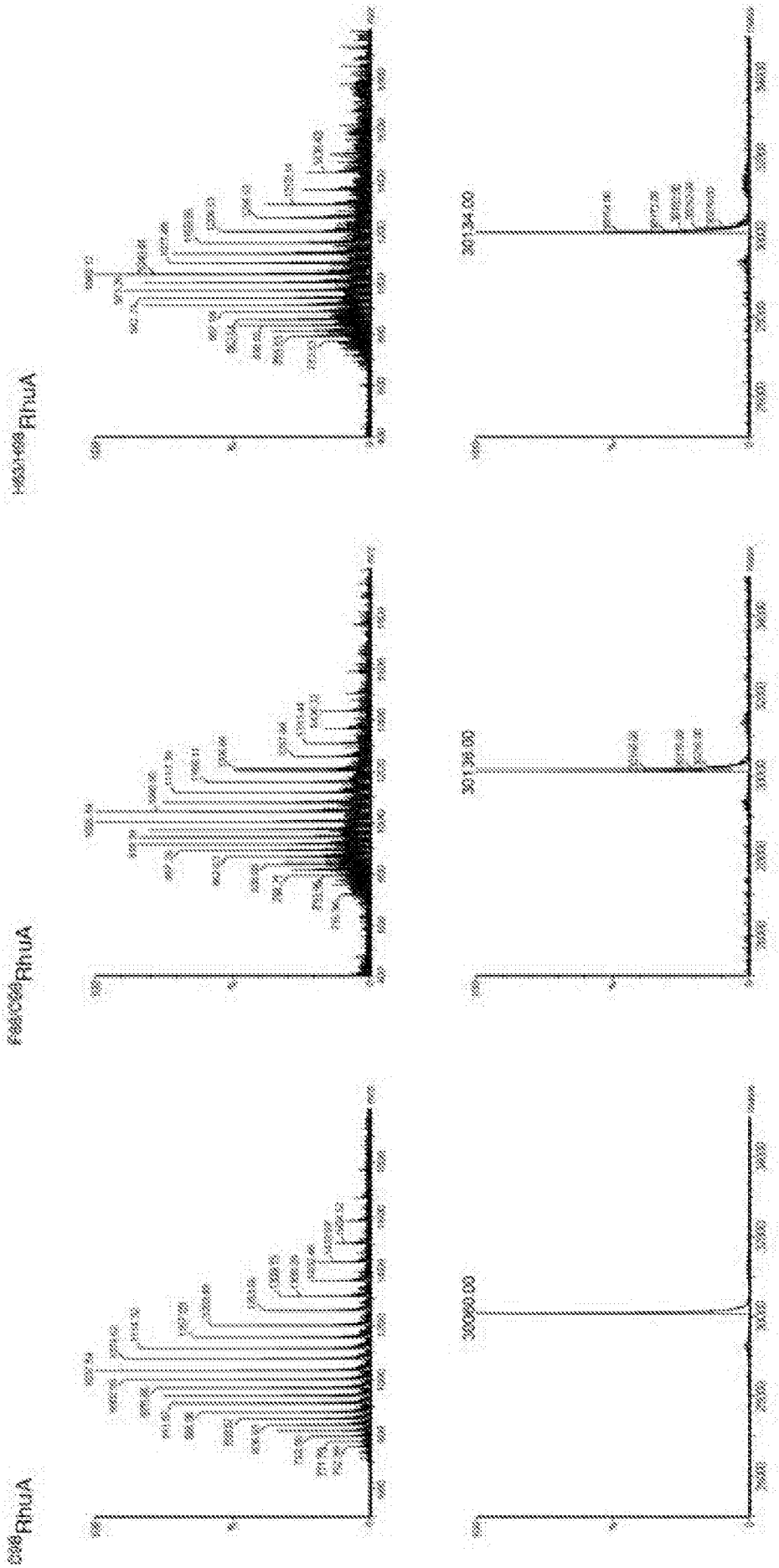
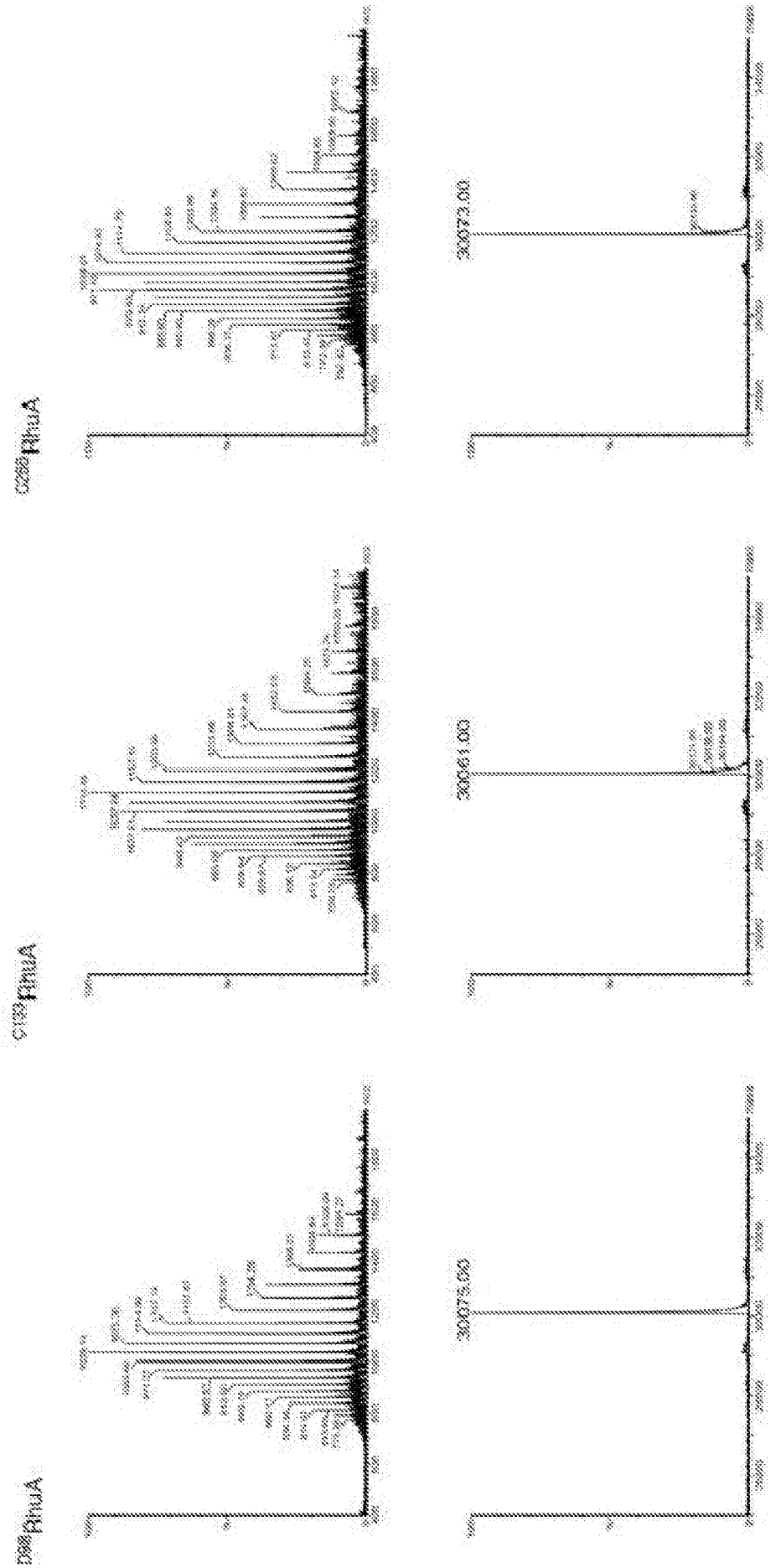


FIG. 14 (Con'd)



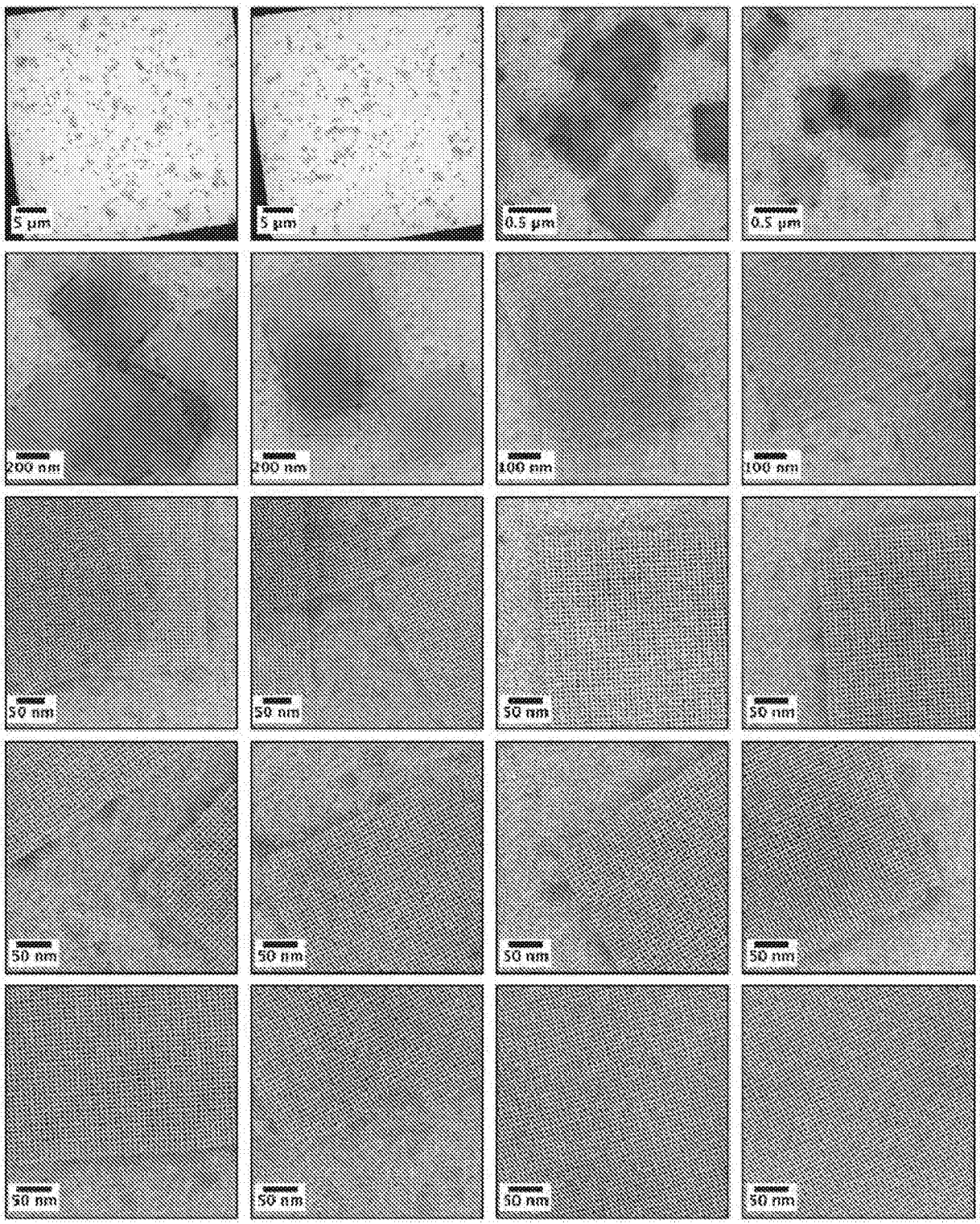

5 µm
5 µm
0.5 µm
0.5 µm
200 nm
200 nm
100 nm
100 nm
50 nm
50 nm
50 nm
50 nm
50 nm
50 nm
50 nm
50 nm
50 nm
50 nm
50 nm
50 nm

FIG. 15

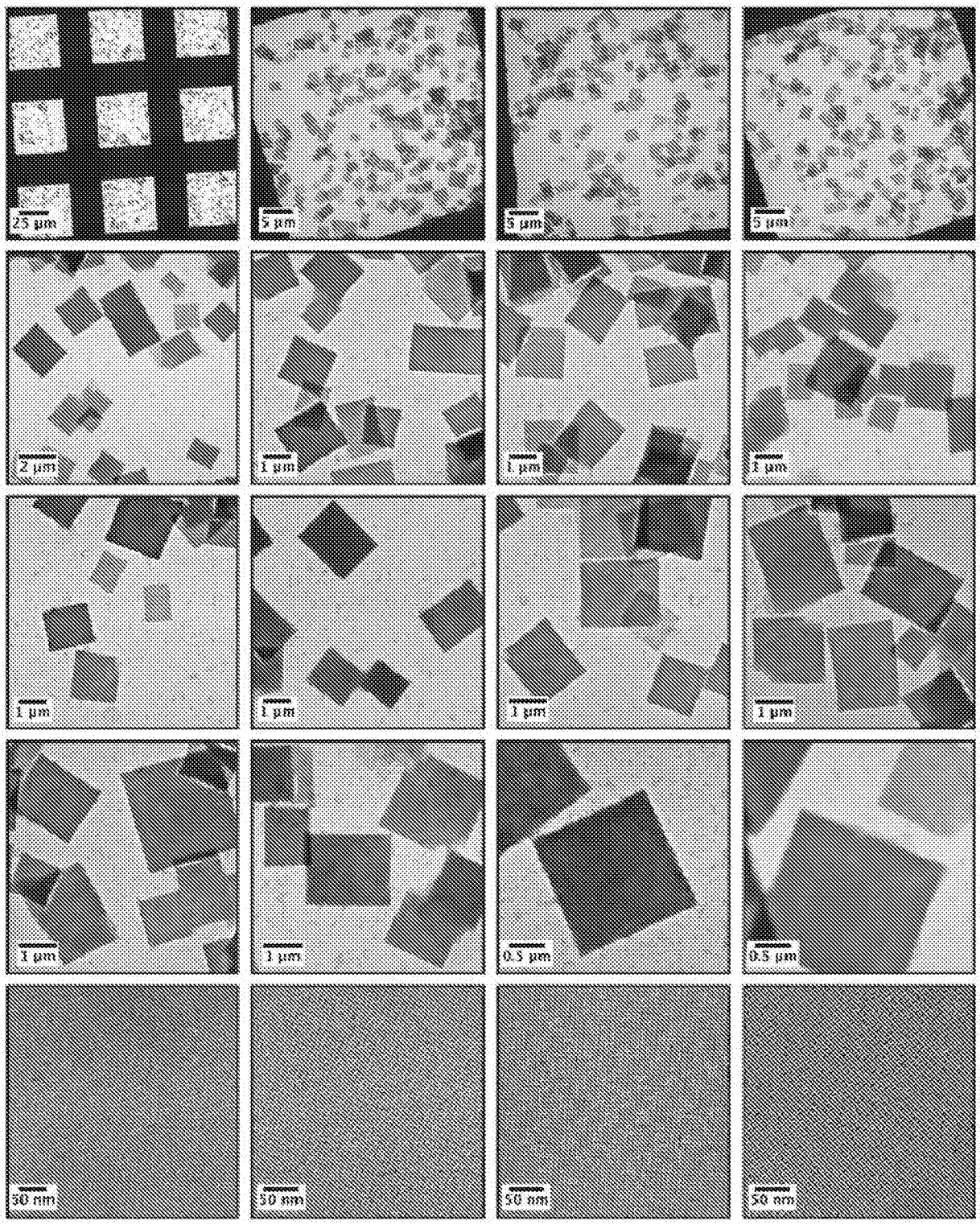

25 µm
5 µm
5 µm
5 µm
2 µm
1 µm
1 µm
1 µm
1 µm
1 µm
1 µm
1 µm
1 µm
1 µm
0.5 µm
0.5 µm
50 nm
50 nm
50 nm
50 nm

FIG. 16

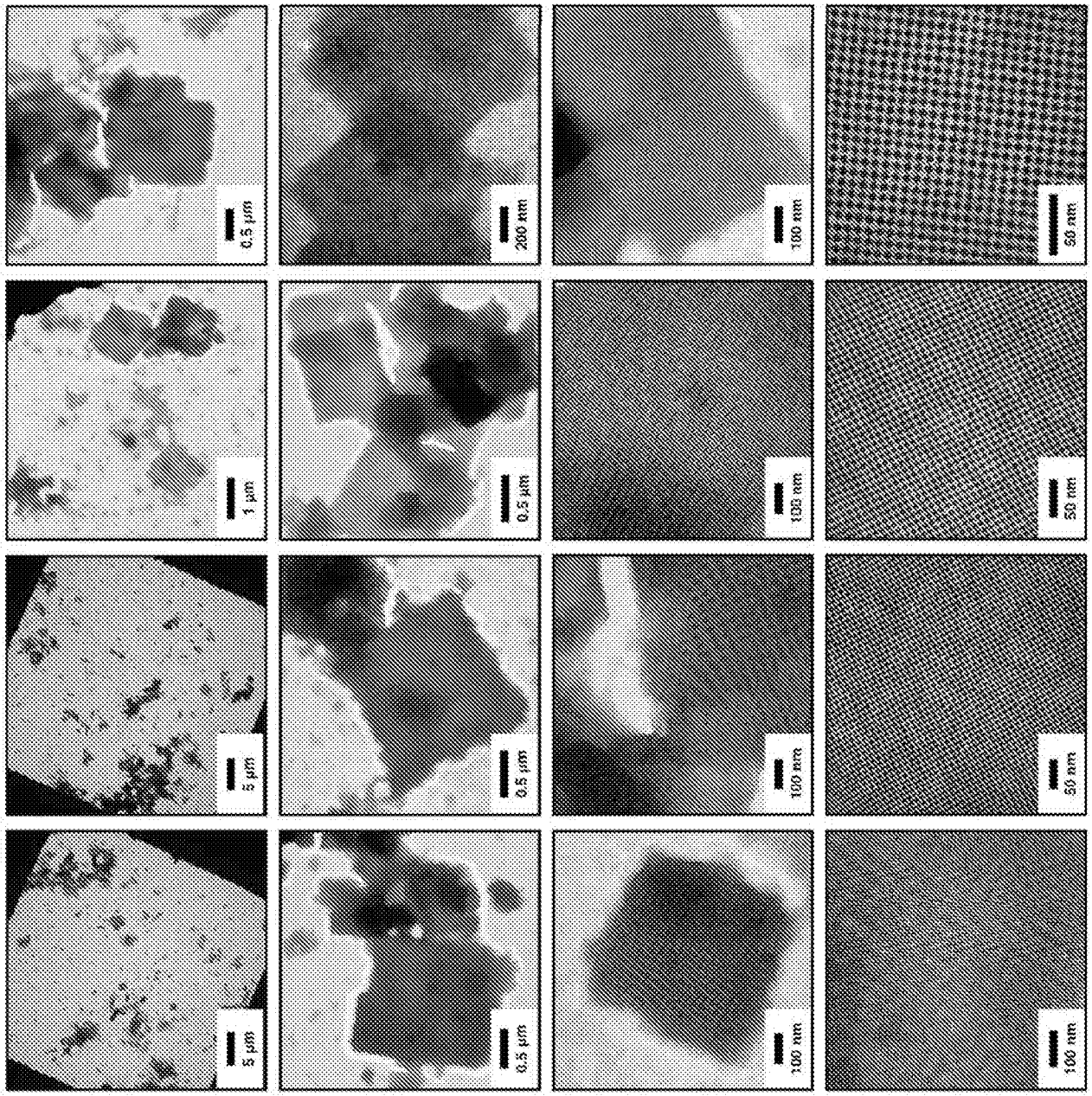

5 μm
1 μm
0.5 μm
0.5 μm
0.5 μm
1 μm
0.5 μm
200 nm
100 nm
100 nm
100 nm
100 nm
100 nm
50 nm
50 nm
50 nm

FIG. 17A

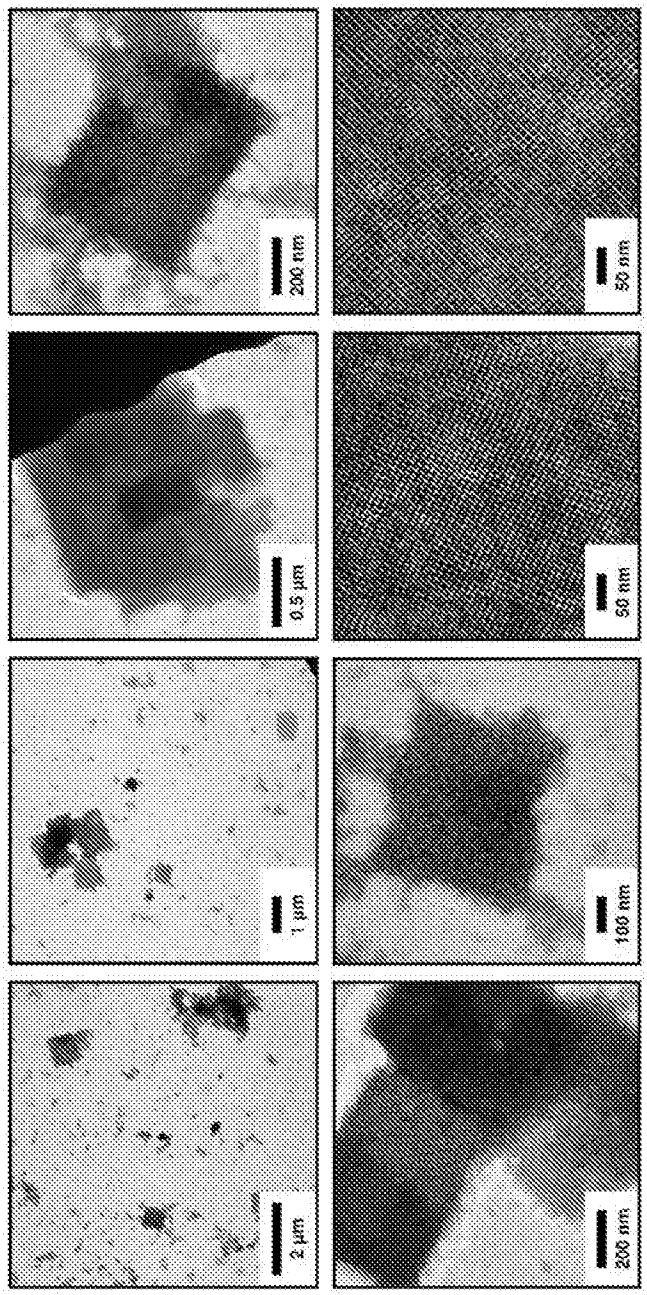


FIG. 17B

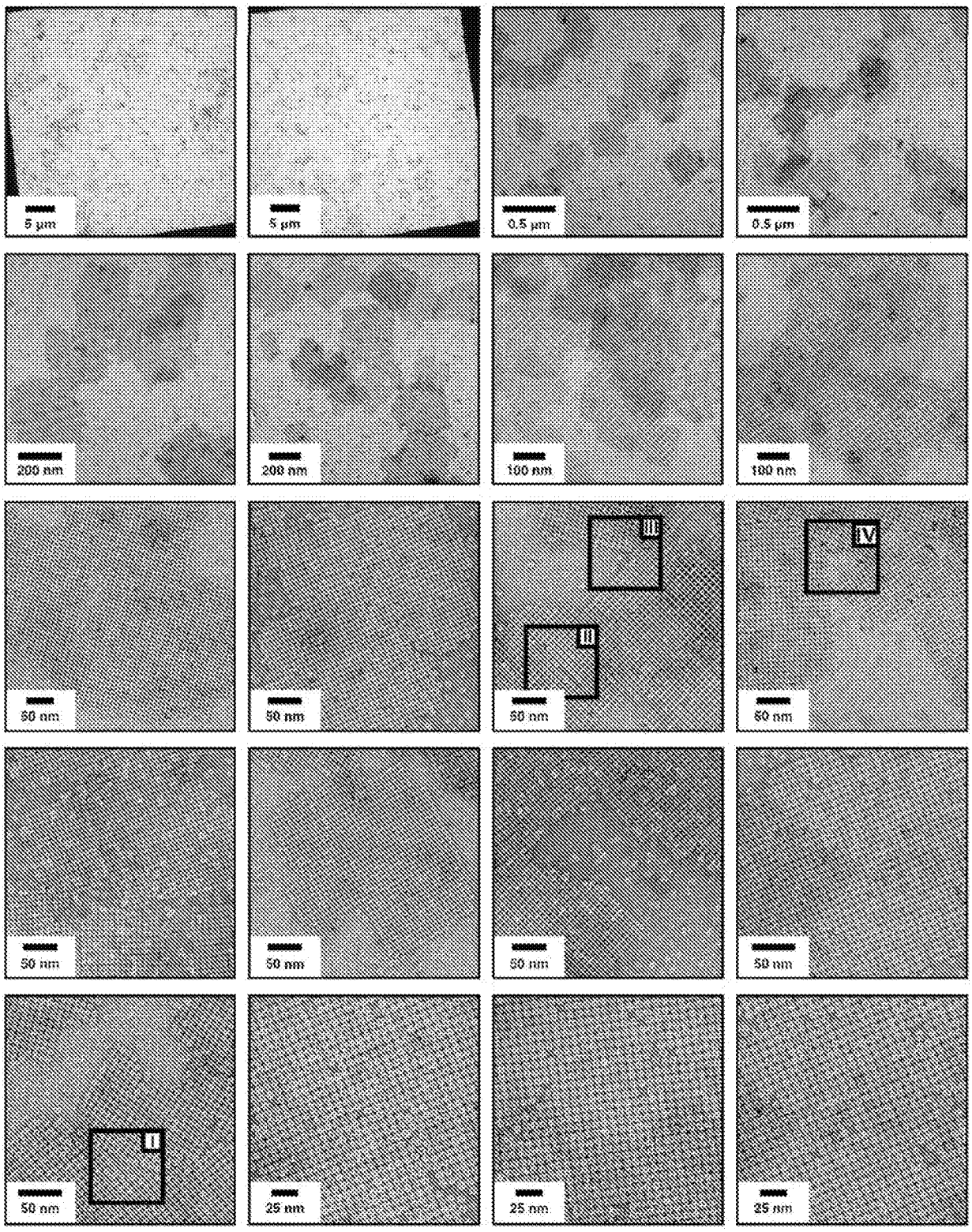

5 µm
5 µm
0.5 µm
0.5 µm
200 nm
200 nm
100 nm
100 nm
50 nm
50 nm
III
II
50 nm
IV
50 nm
50 nm
50 nm
50 nm
50 nm
I
50 nm
25 nm
25 nm
25 nm

FIG. 18A

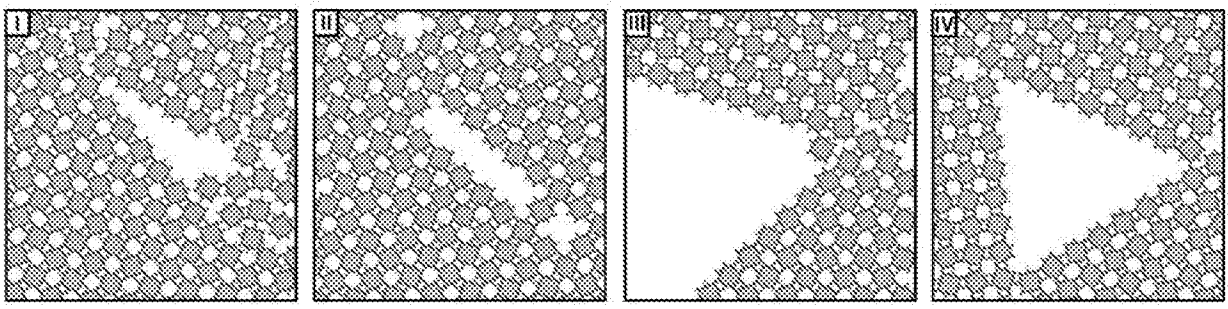
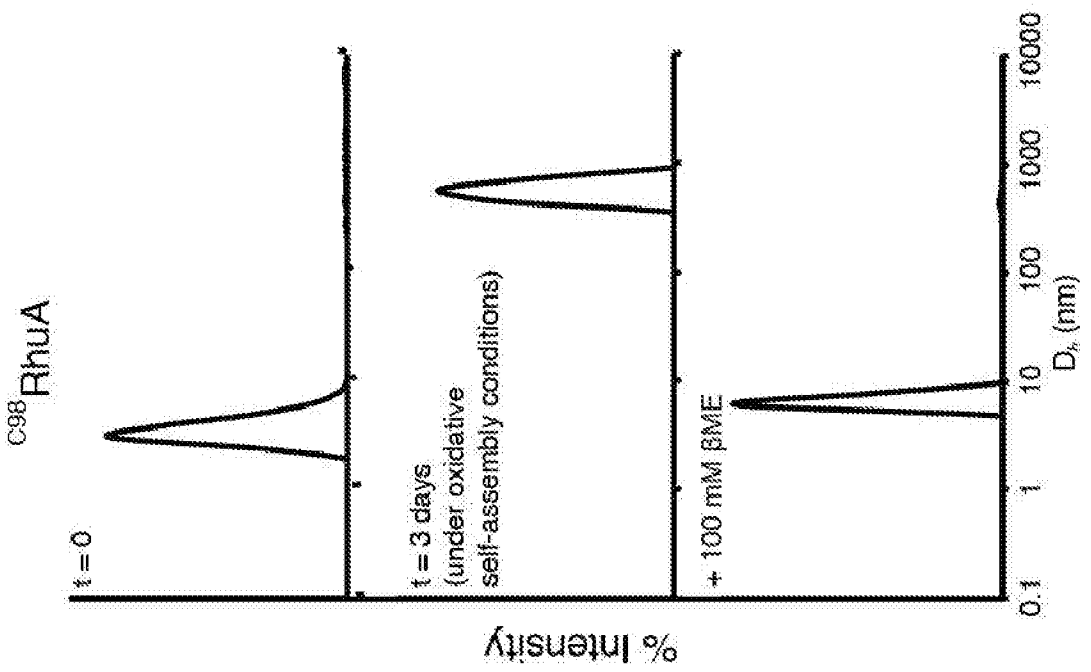
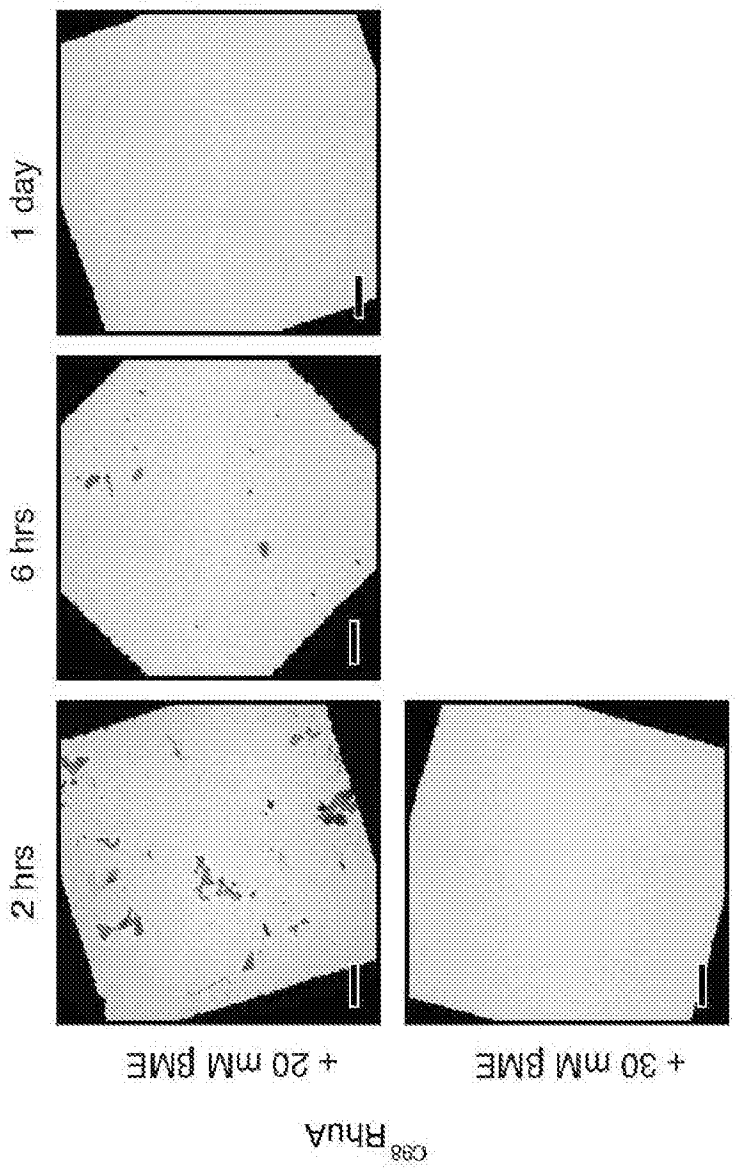
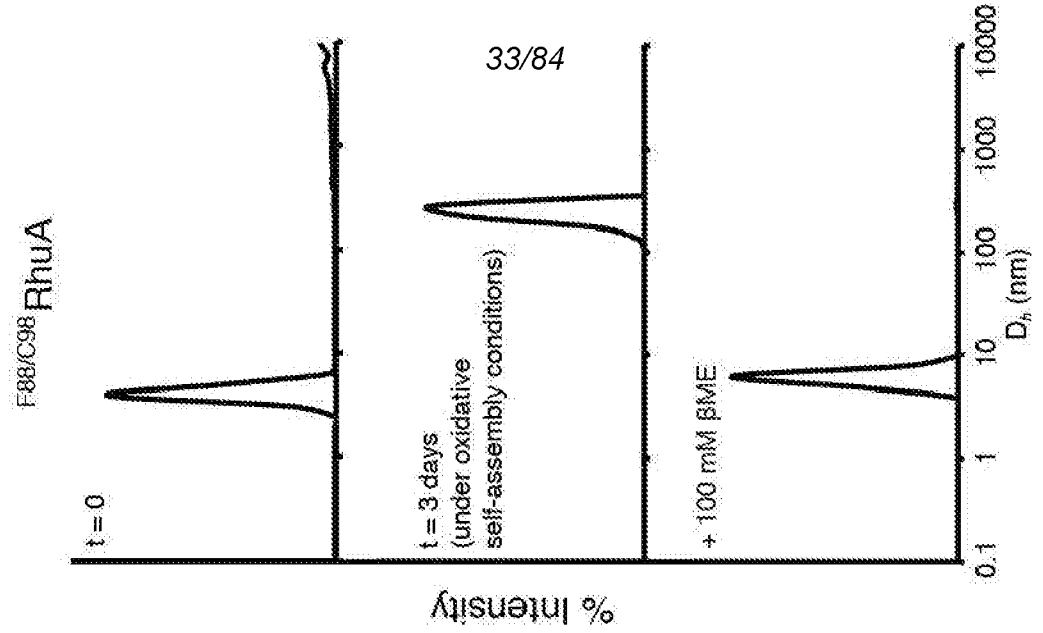


FIG. 18B

FIG. 19A


C98RhuA
t = 0
t = 3 days
(under oxidative
self-assembly conditions)
+ 100 mM βME
% Intensity
0.1
1
10
100
1000
10000
D_h (nm)


C98RhuA
+ 20 mM βME
+ 30 mM βME
2 hrs
6 hrs
1 day


F88/C98 RhuA
t = 0
t = 3 days
(under oxidative
self-assembly conditions)
+ 100 mM βME
% Intensity
0.1
1
10
100
1000
10000
D_h (nm)

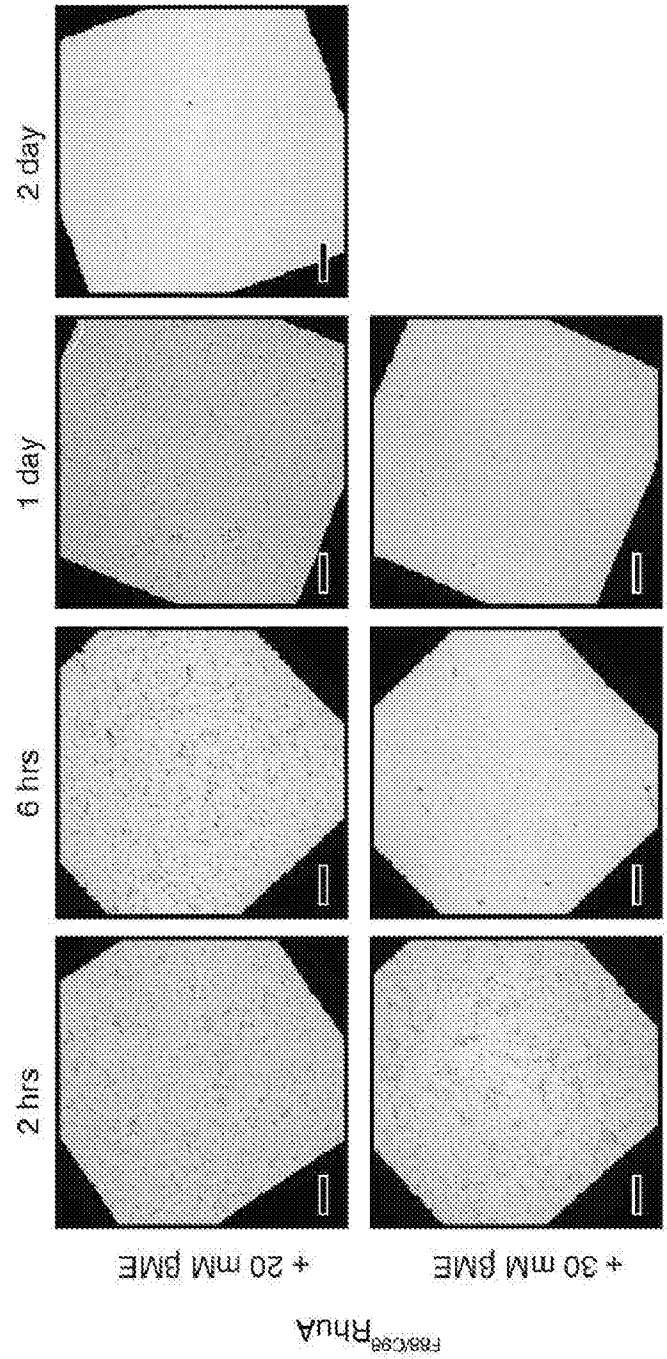

F88/C98 RhuA
+ 30 mM βME
+ 20 mM βME
2 hrs
6 hrs
1 day
2 day

FIG. 19B

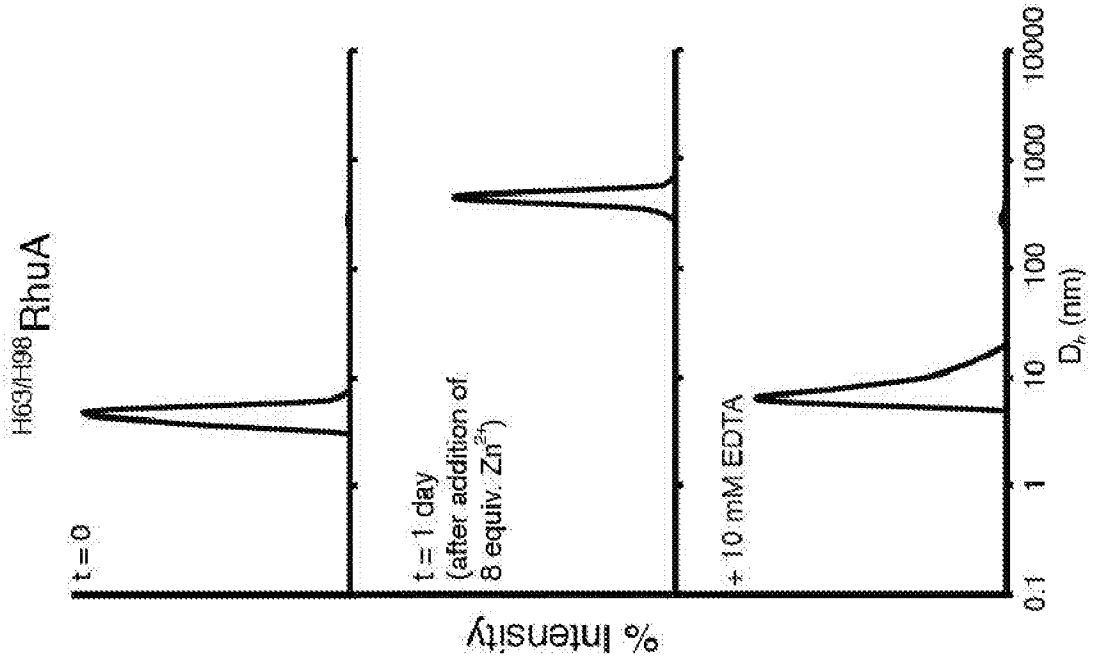
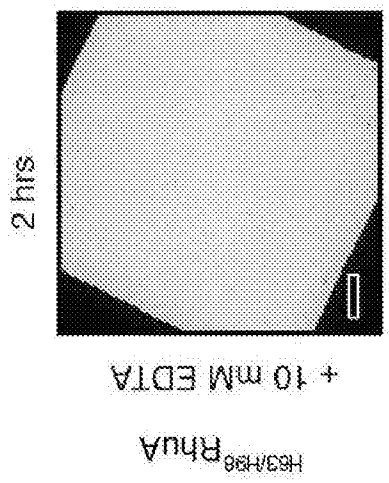

H63A/H98 RhuA
t = 0
t = 1 day
(after addition of
8 equiv. Zn2+)
+ 10 mM EDTA
% Intensity
0.1
1
10
100
1000
10000
Dh (nm)

FIG. 19C


H63A/H98 RhuA
+ 10 mM EDTA
2 hrs

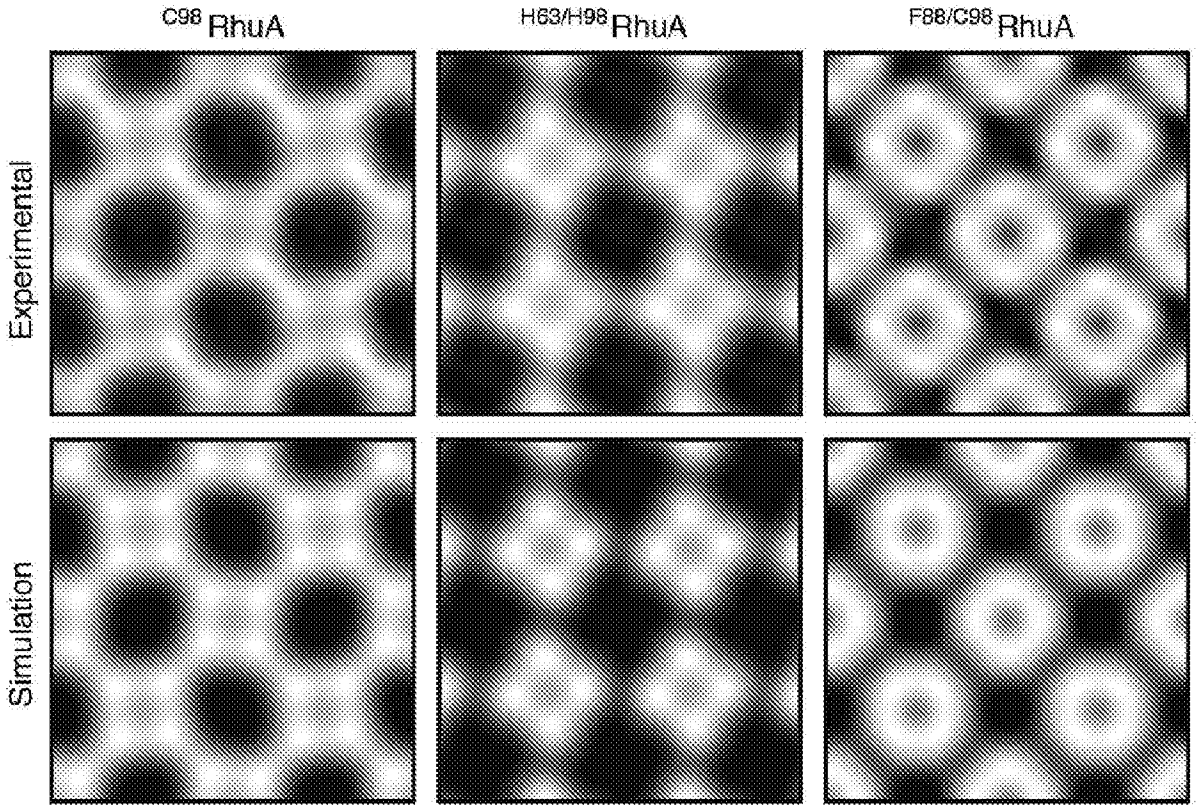


FIG. 20

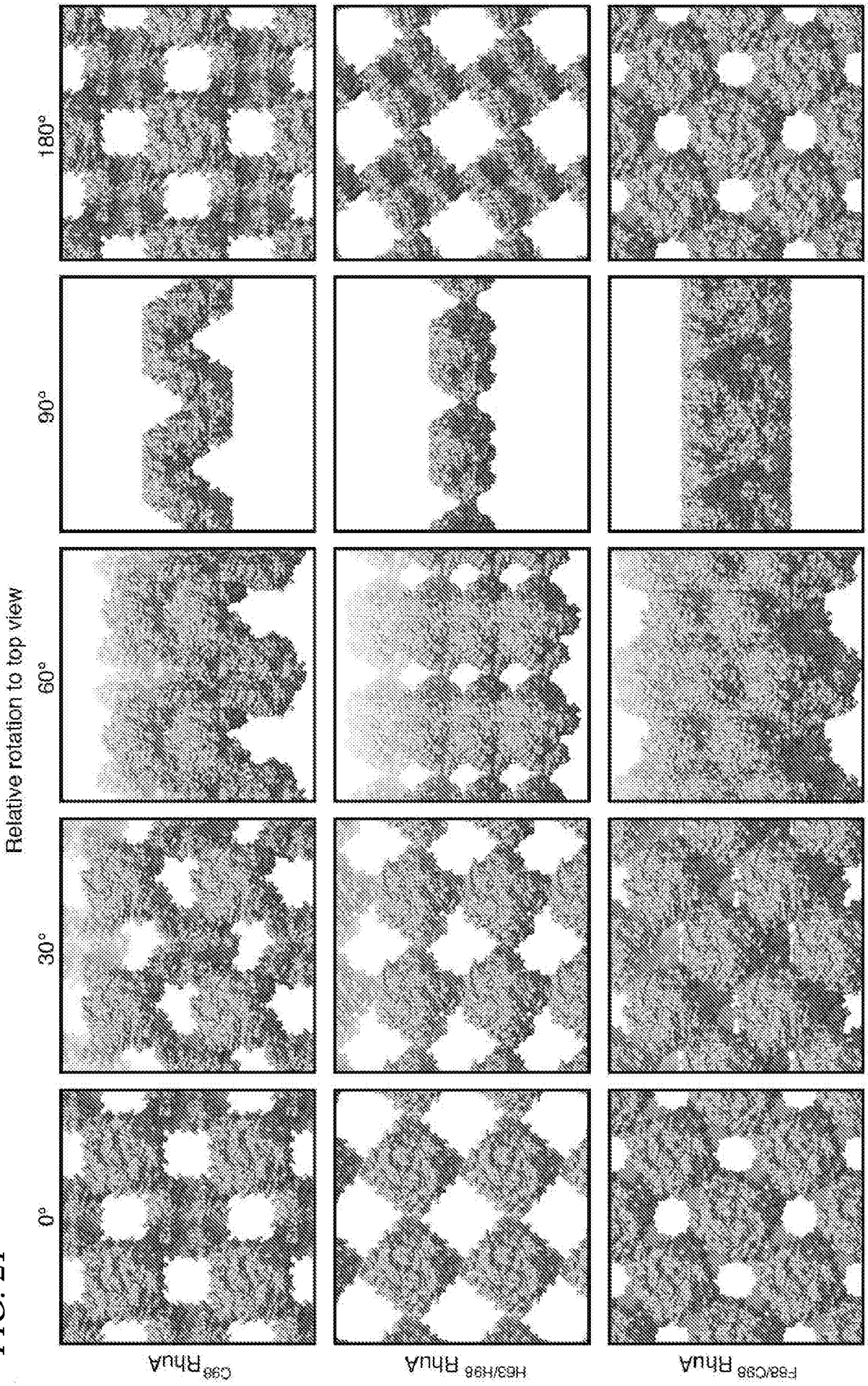

Relative rotation to top view
0°
30°
60°
90°
180°
C98 RhuA
H63/H98 RhuA
F58/C98 RhuA

FIG. 21

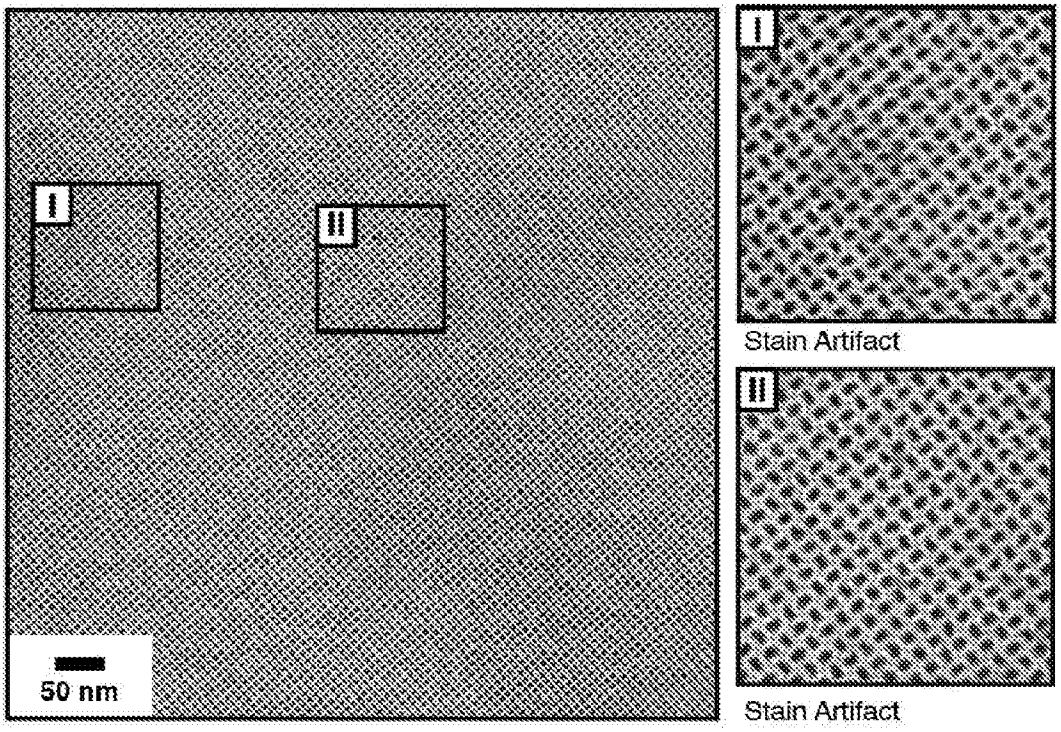


FIG. 22A

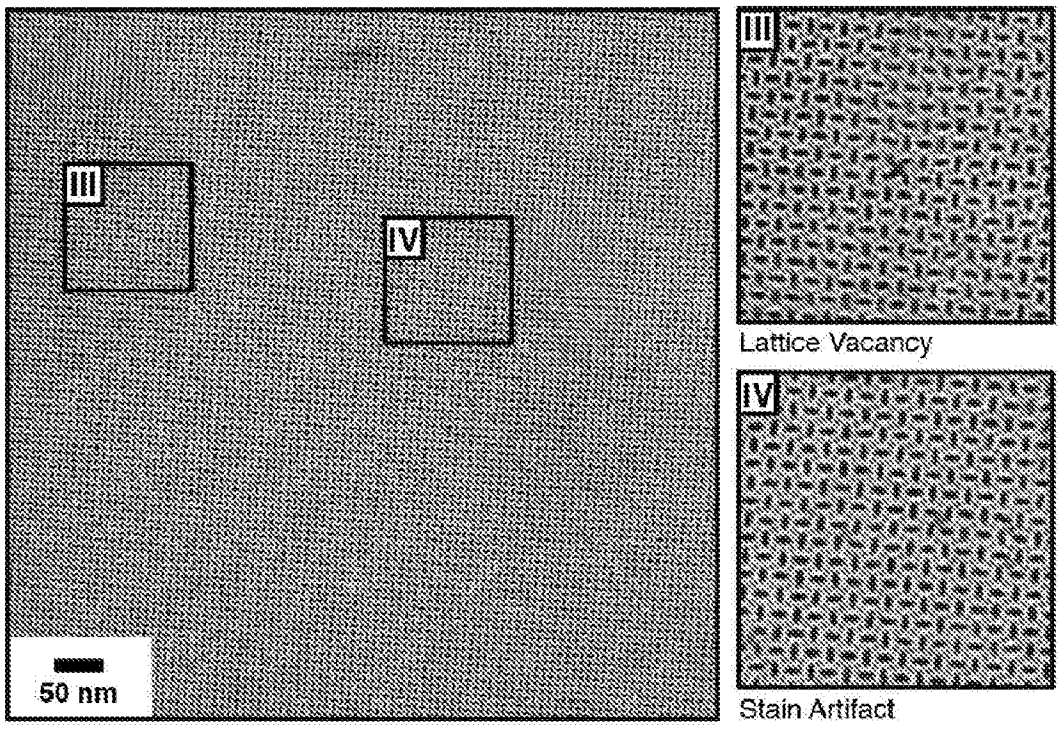


FIG. 22B

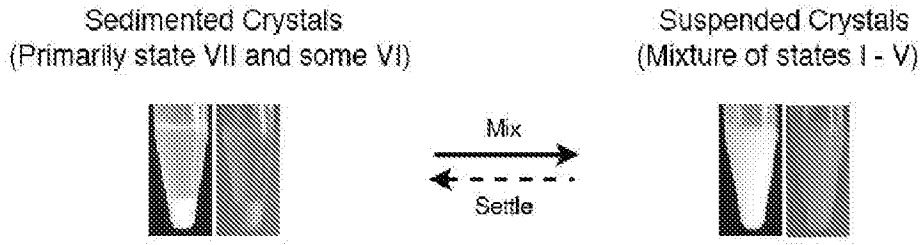


FIG. 23A

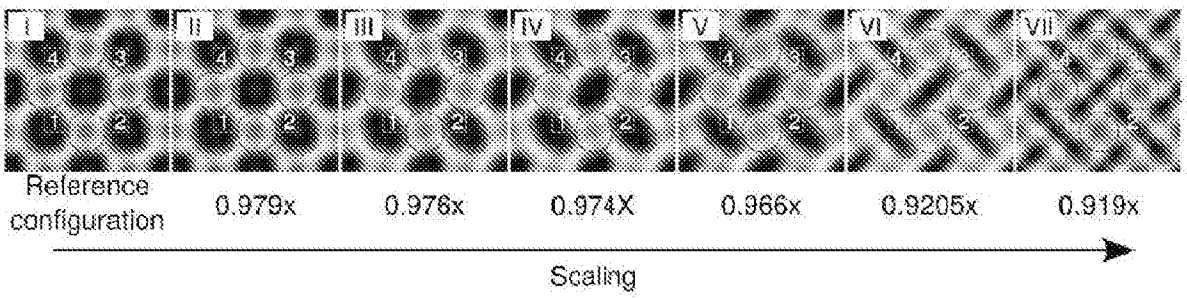


FIG. 23C

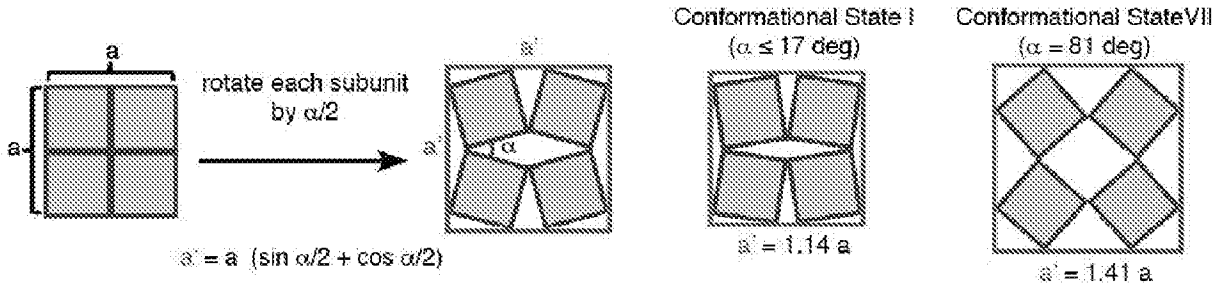


FIG. 23D

FIG. 23B

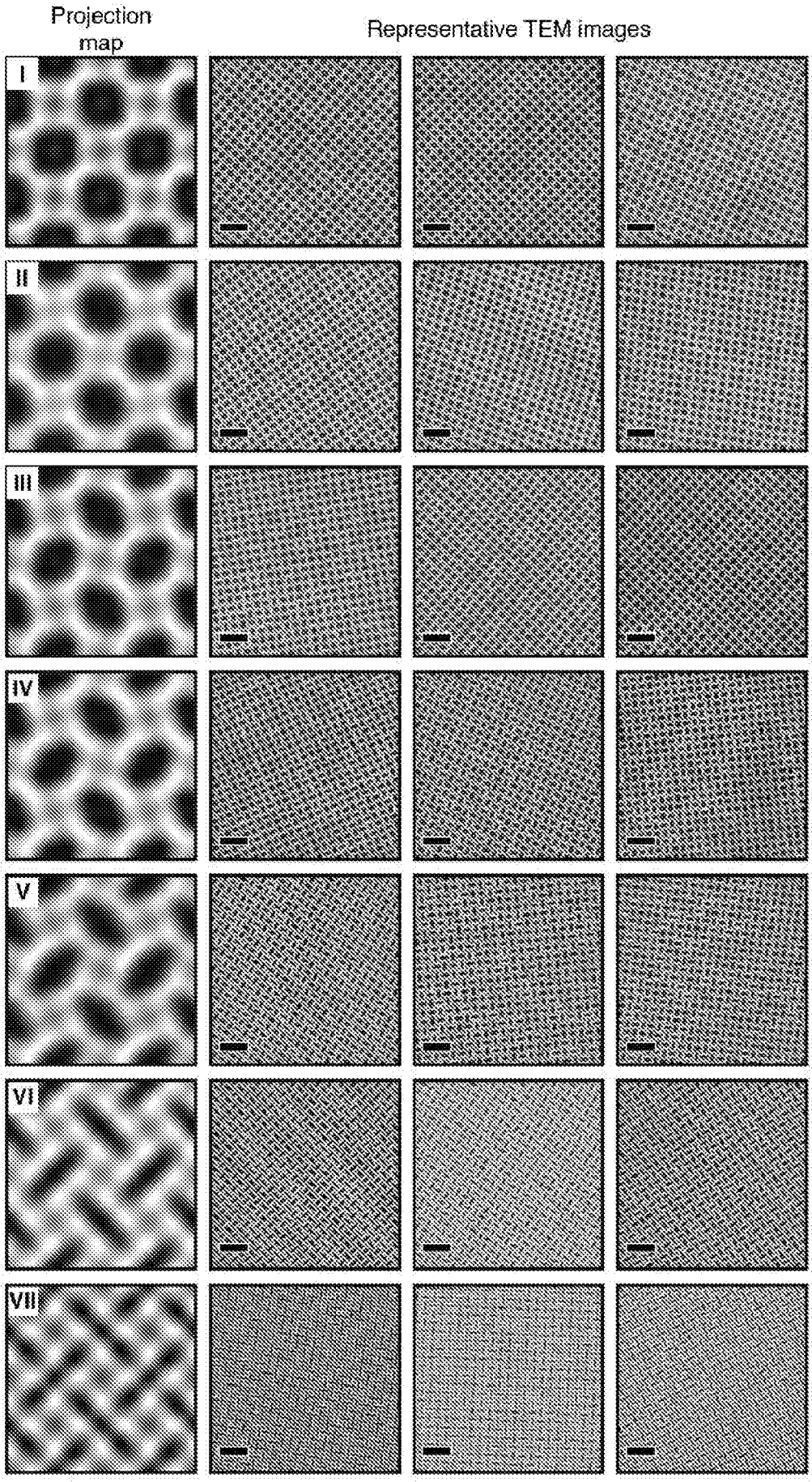

Projection map
Representative TEM images
I
II
III
IV
V
VI
VII

FIG. 24 RhuA-C98 Sheet on Grid Followed by Addition of Maleimido-Au for 2 Hours

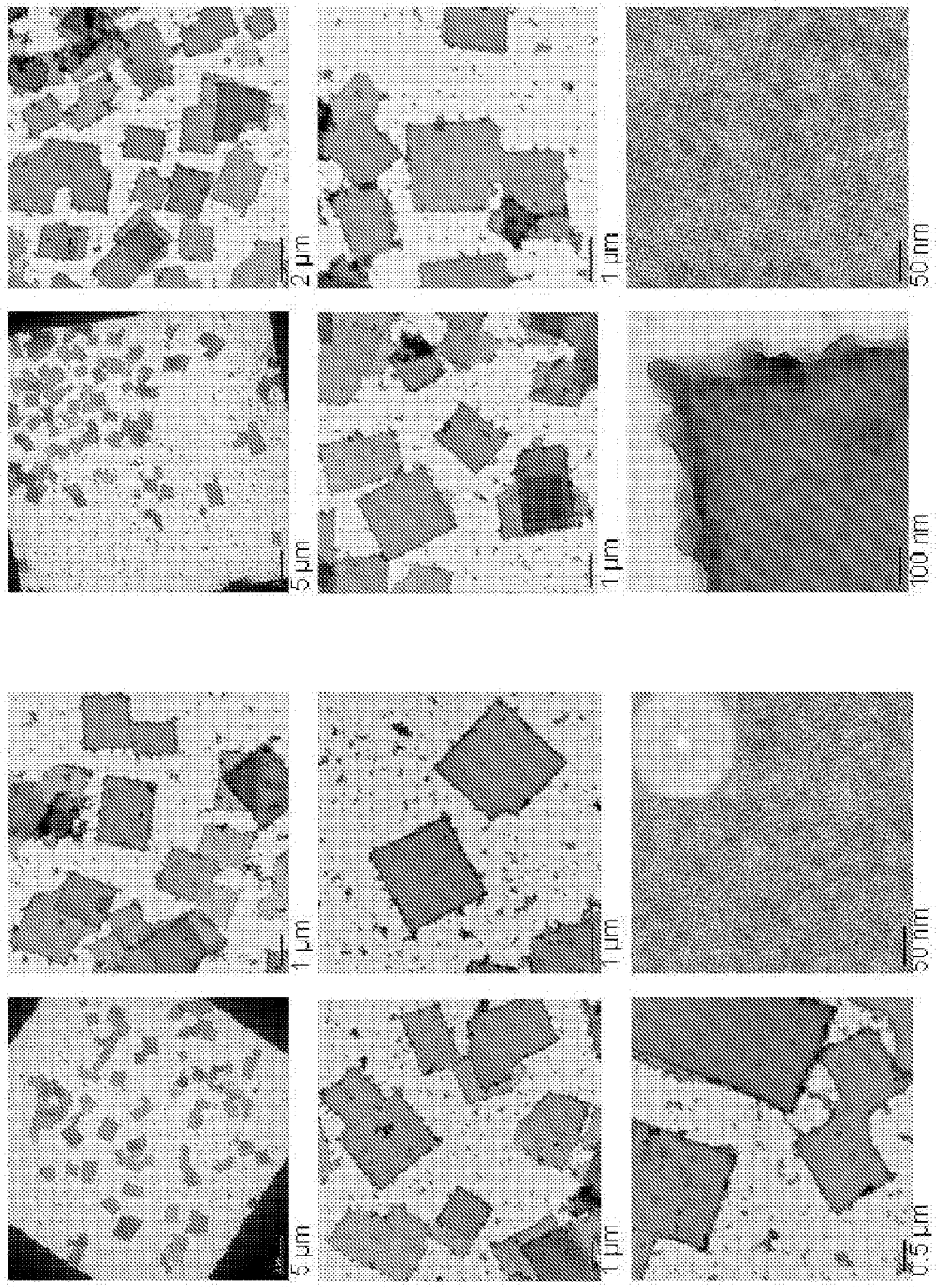
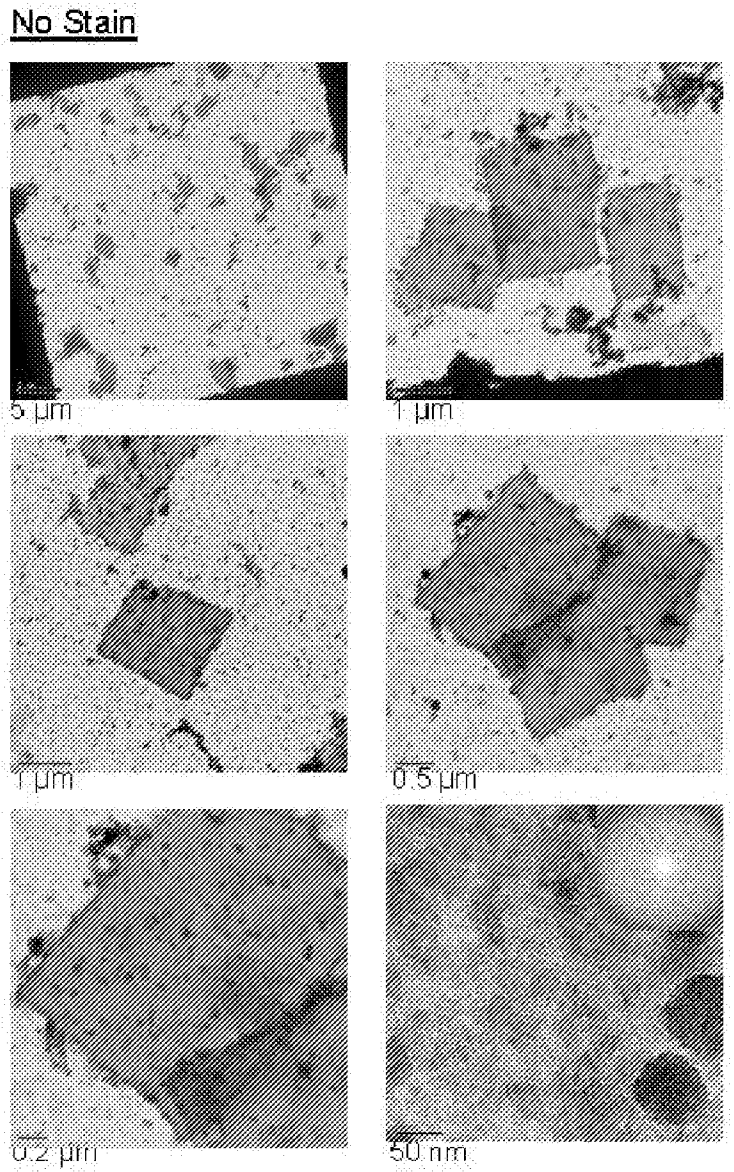


FIG. 25 *RhuA-C98 Sheet on Grid Followed by Addition of Maleimido-Au for 2 Hours*



*Different preparation from previous slide
- This sample was prepared on grid
- Sample showed in previous slide was prepared in crystal tray

FIG. 26 RhuA-C98 Sheet on Grid Followed by Addition of Maleimido-Au for Overnight

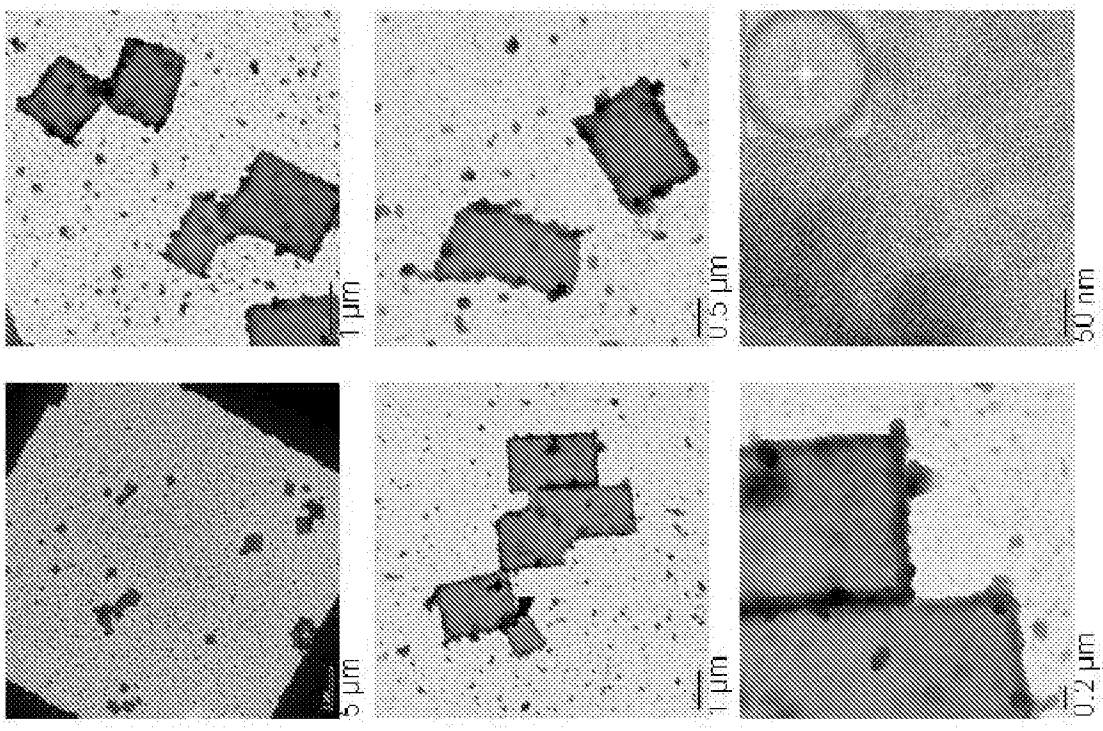


FIG. 27

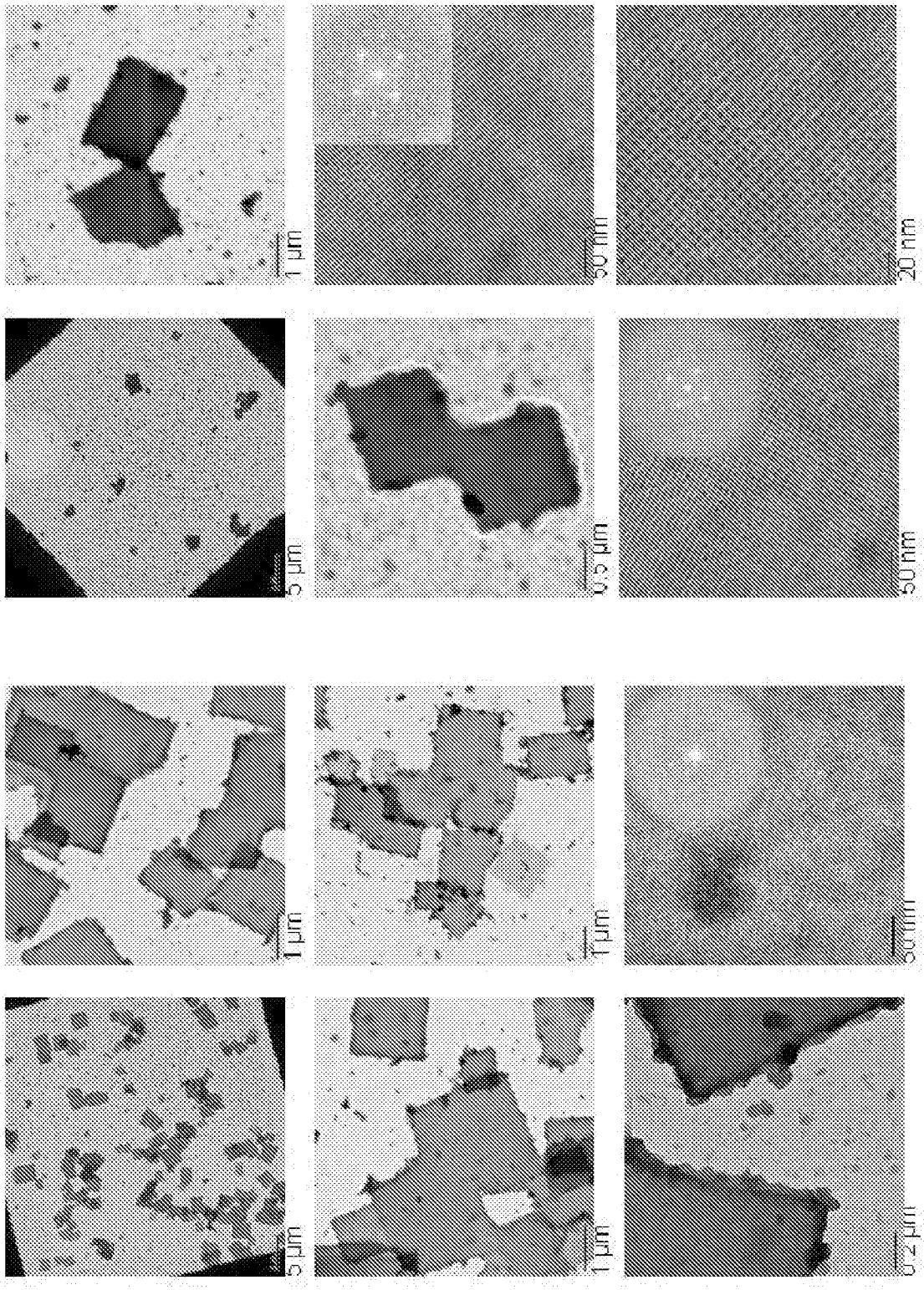
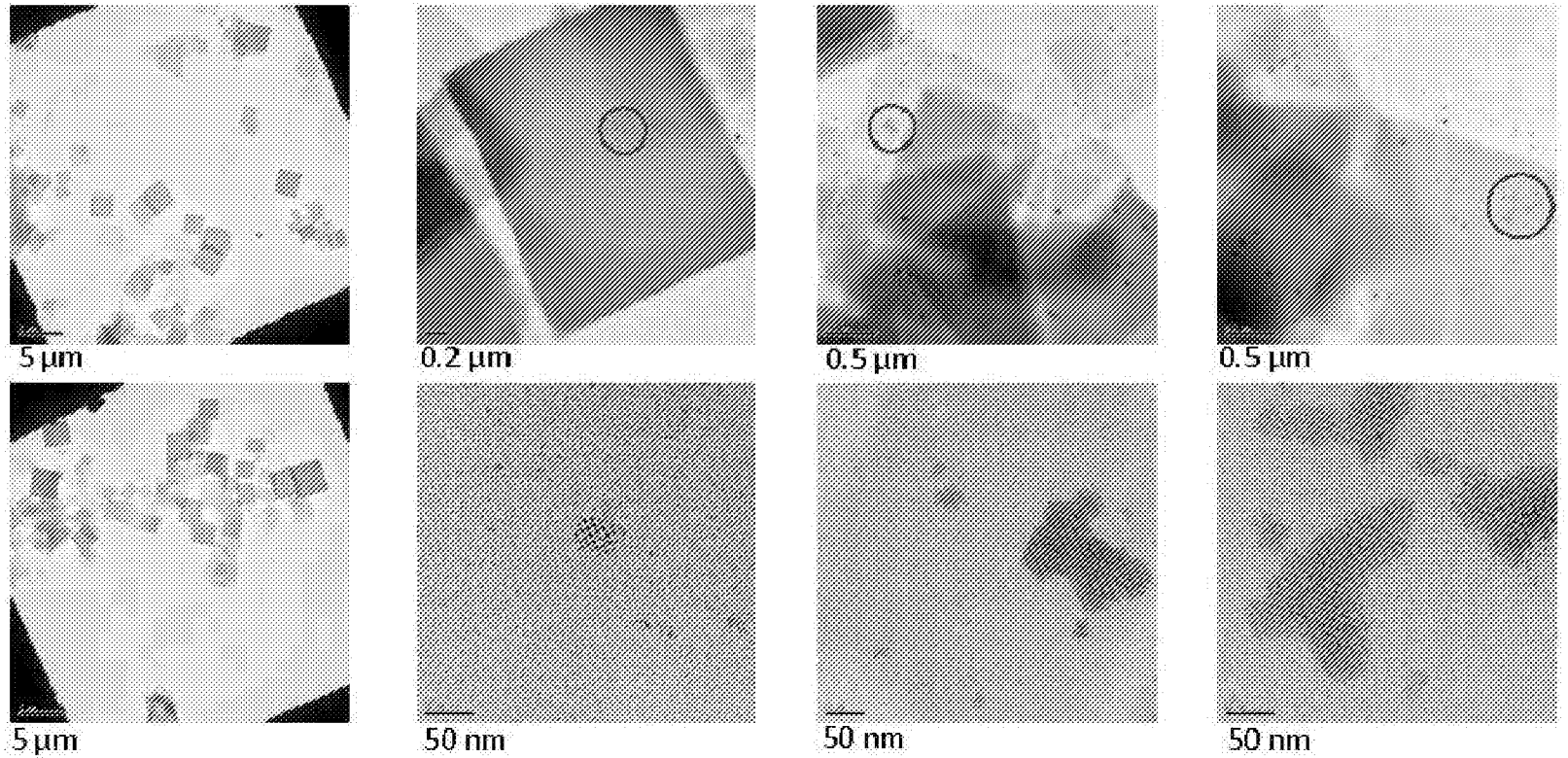

RhuA-C98 Sheet on Grid Followed by Addition of Maleimido-Au for 3 Hours (Repeat)
No Stain
UA Stain
5 µm
1 µm
1 µm
5 µm
0.5 µm
50 nm
50 nm
20 nm
1 µm
1 µm
50 nm
0.2 µm

FIG. 28 *RhuA-C98 Sheet: Stock Sample with $HAuCl_4$*

4uL sheet was added into 0.5 mM $HAuCl_4$ for 1 day



I chekced after 2 days and could not see these...

I also tried different concentrations of $HAuCl_4$ (1 mM and 2 mM) for 1 day, but did not see these.

FIG. 29 RhuA-C98 (4uL) added into 0.5 mM $HAuCl_4$ in 5 mM NaPi pH 7.2 6 days then added 5 mM bME for 1 day

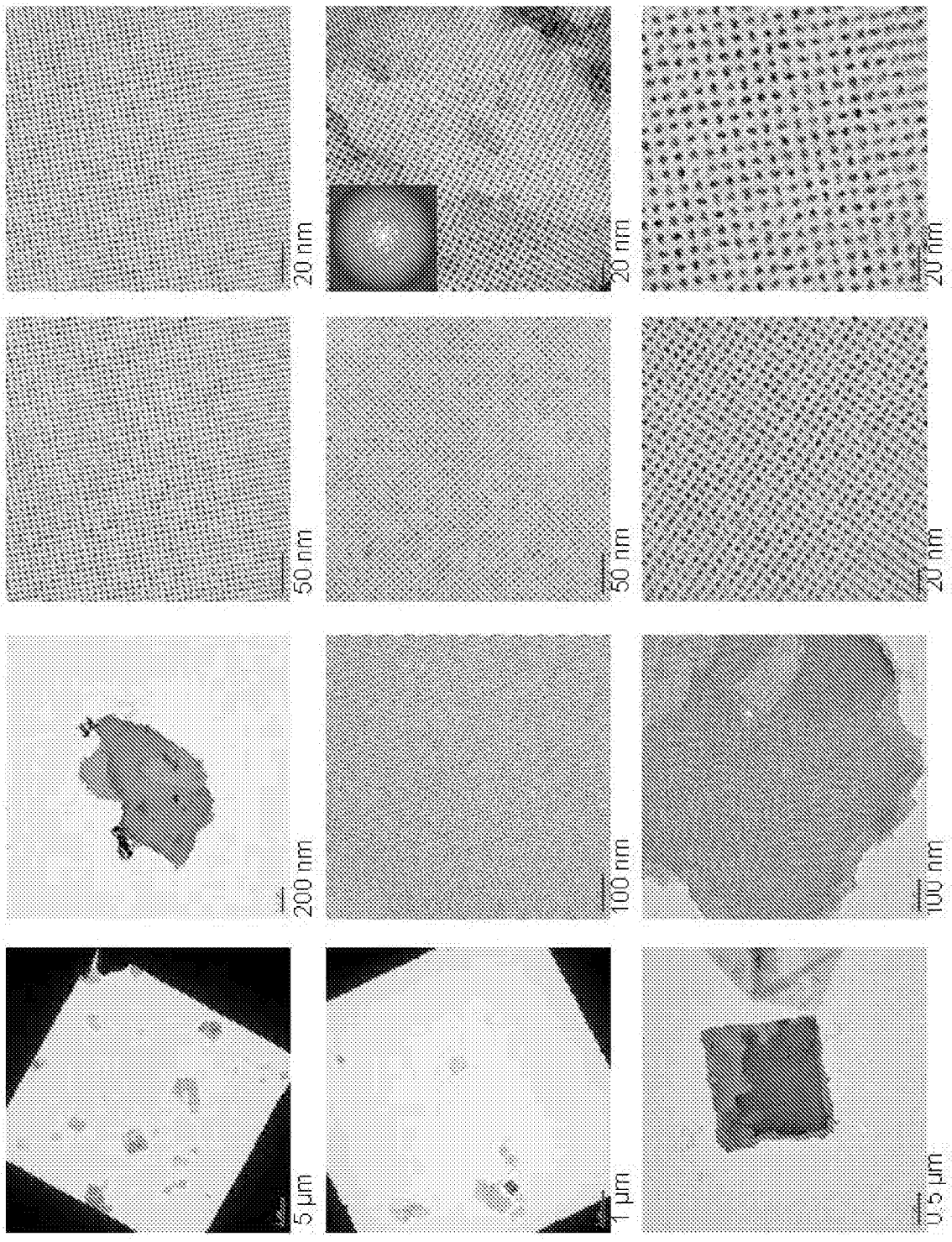


FIG. 30 RhuA-C98 (4uL) added into 100 µL of Au(I) ($HAuCl_4$ + 2 eq thiodiethanol) in 5 mM NaPi pH 7.2 for 4 days

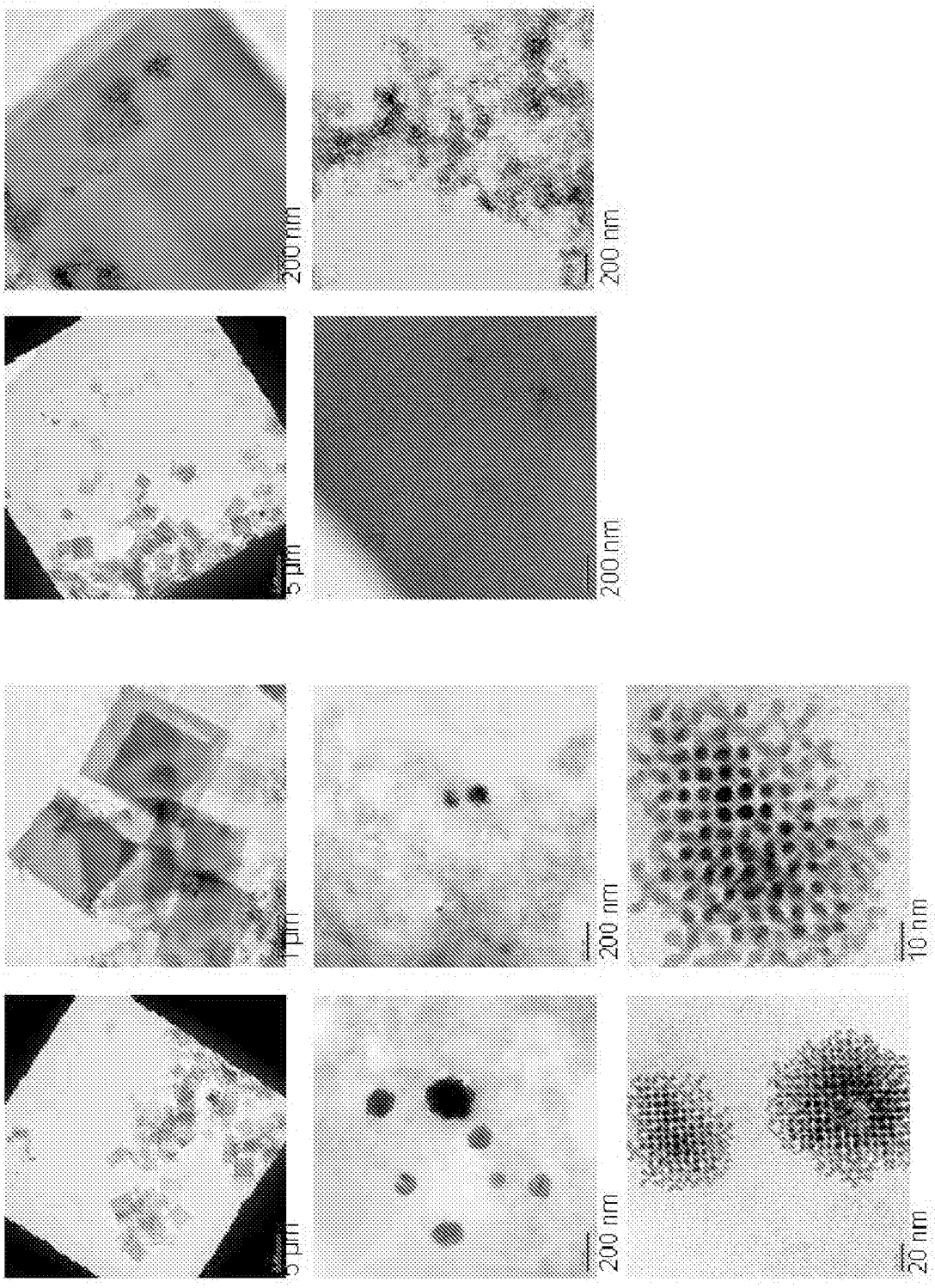


FIG. 31

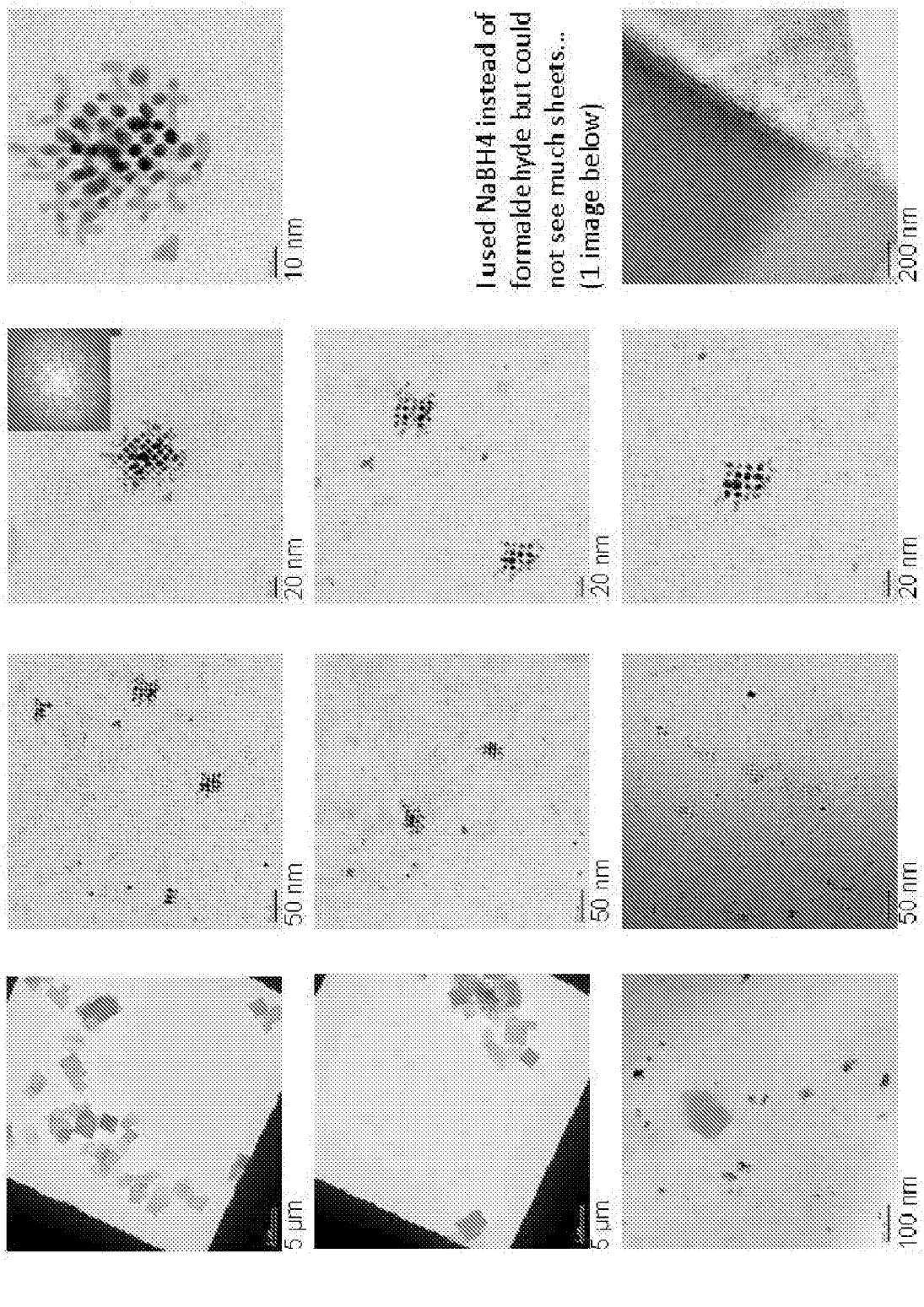

RhuA-C98 sheet/HAuCl4 on grids followed by HAuCl4/K2CO3/NaBH4 for 1 hr then in 10 % formaldehyde for 2 hours
5 µm
50 nm
20 nm
10 nm
I used NaBH4 instead of formaldehyde but could not see much sheets... (1 image below)
5 µm
50 nm
20 nm
200 nm
100 nm
50 nm
20 nm

FIG. 32

RhuA-C98 sheet/$HAuCl_4$ on grids followed by $HAuCl_4/K_2CO_3/NaBH_4$ in NaPi pH 7.2 for 2 hours

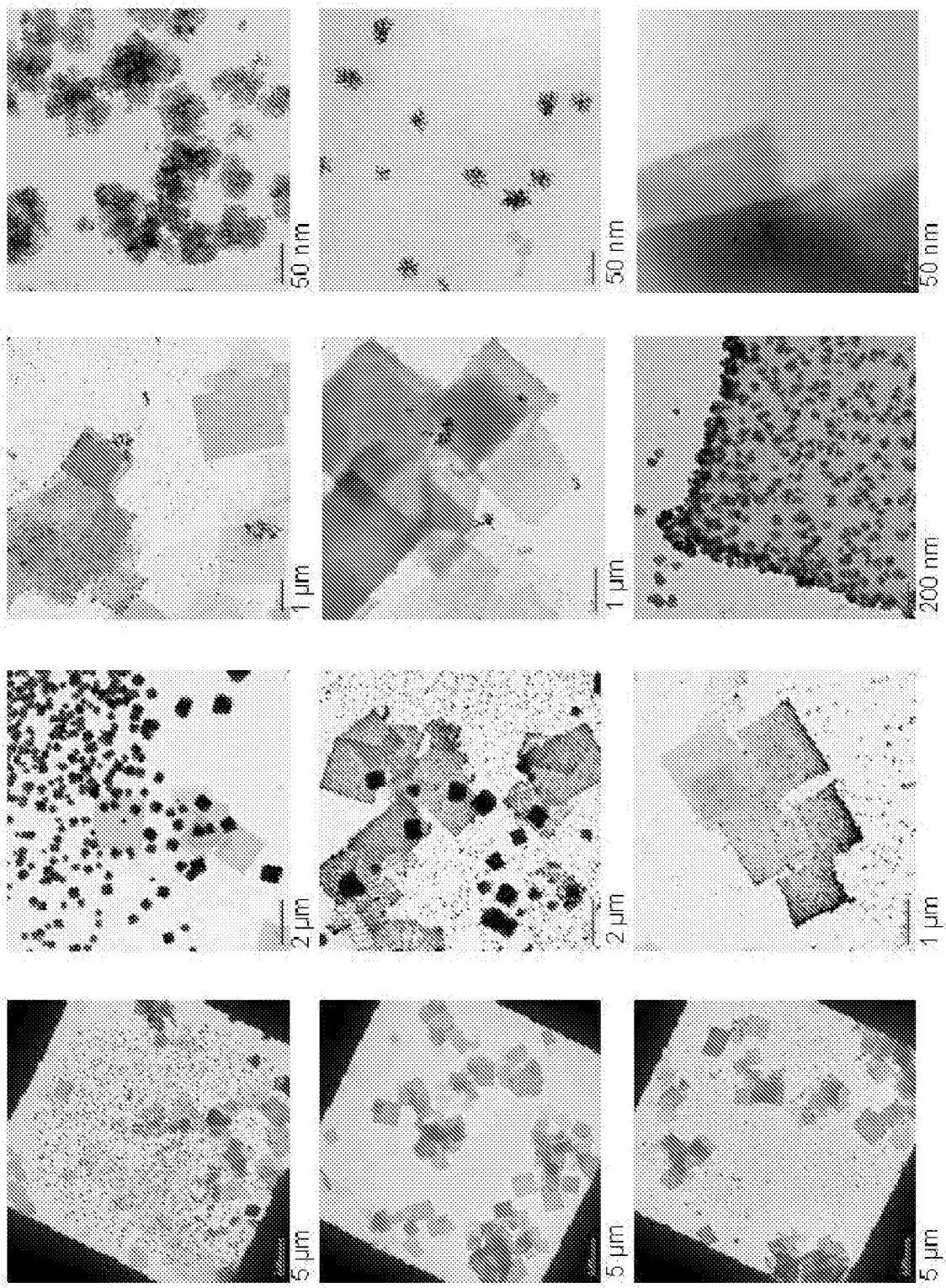
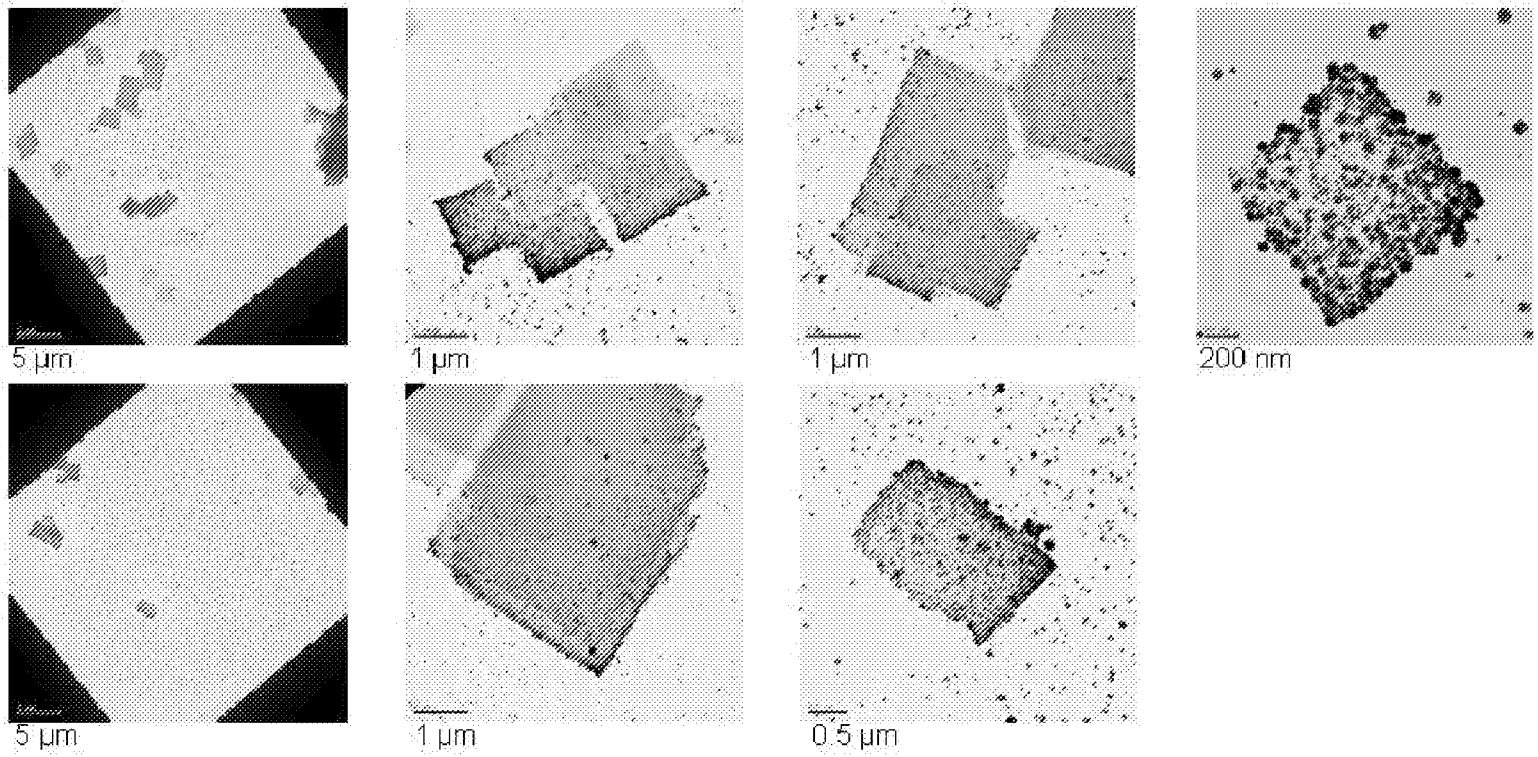


FIG. 33 *RhuA-C98 sheet/$HAuCl_4$ on grids followed by $HAuCl_4$/K_2CO_3/Formaldehyde in NaPi pH 7.2 for 2 hours*



Other conditions:

Sheet/HAuCl4/K2CO3 for 1day on grid; then grids into HAuCl4/K2CO3/NaBH4 for 2hours

Sheet/HAuCl4/K2CO3 for 1day on grid; then grid into HAuCl4/K2CO3/formaldehyde for 2hours

Sheet/HAuCl4/K2CO3 for 1day then mixed formaldehyde for 2hours

Sheet/HAuCl4/K2CO3 for 1day then mixed NaBH4 for 2hours

Sheet/HAuCl4 mixed 10percent formaldehyde for 2hours

Mix HAuCl4/K2CO3 for 2hr then added sheet for 1day; then mixed NaBH4 for 2hours

Sheet/HAuCl4 mixed NaBH4 for 2hours

FIG. 34 RhuA-C98 Sheet: Addition of 200 μM Iodo-Fl

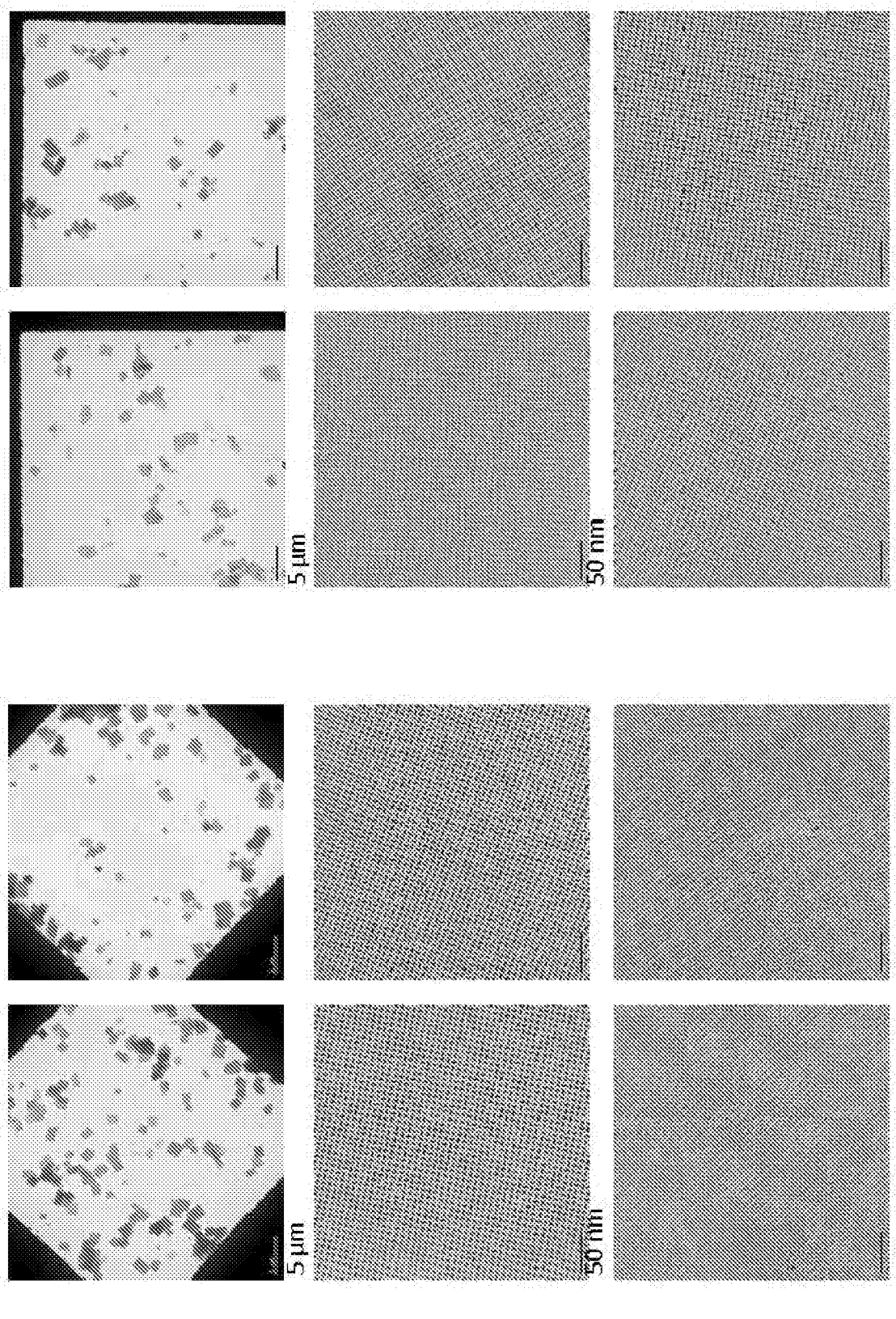
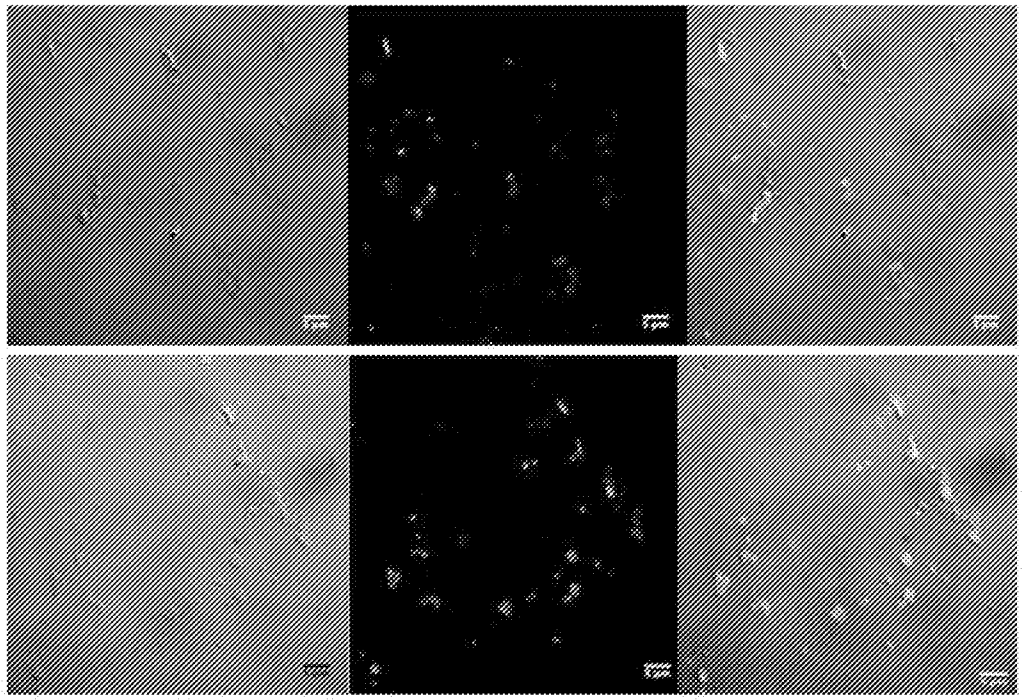
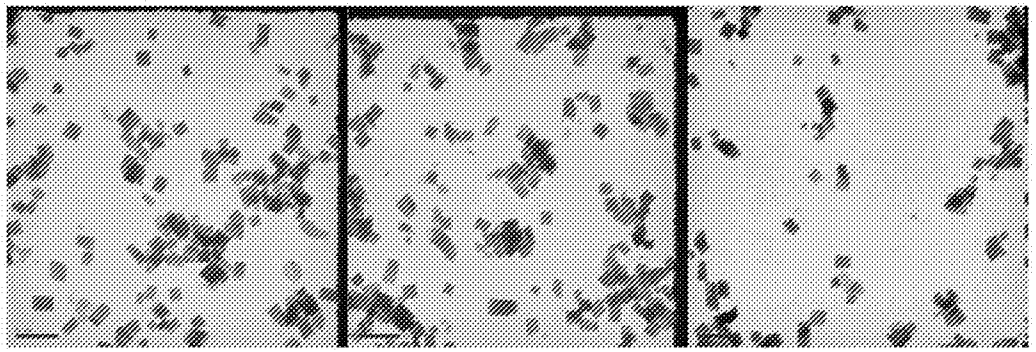


FIG. 35 *RhuA-C98 Sheet: Addition of 200 μM Iodo-Fl*

Confocal Microscopy Images

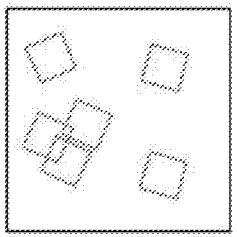


Relevant TEM Images



To see if outside of protein sheet thiols are able to protect by iodoFl in solution as of maleimido-Au (on grid).

Expectation:

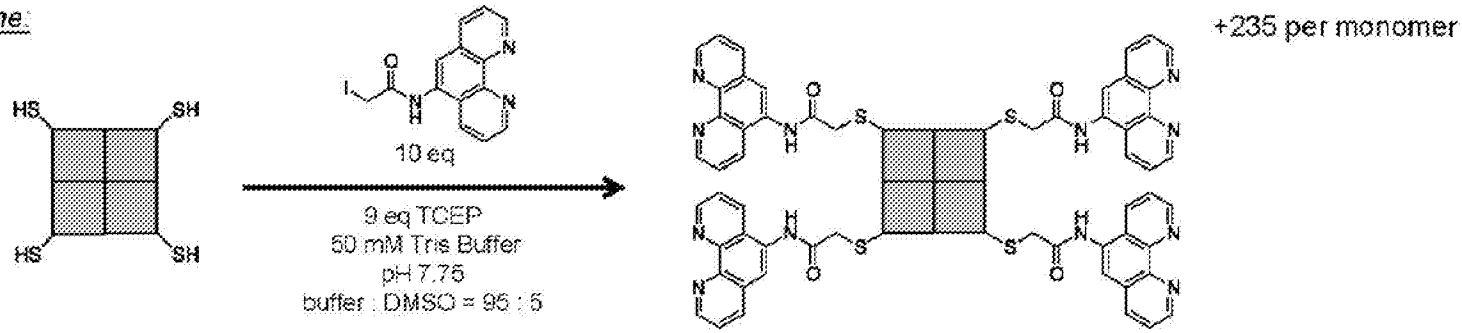


Result:
Inside of sheet was also fluorescent...

Next: Analysis of this sheet

FIG. 36 Synthesis of RhuA-Cys-iPhen

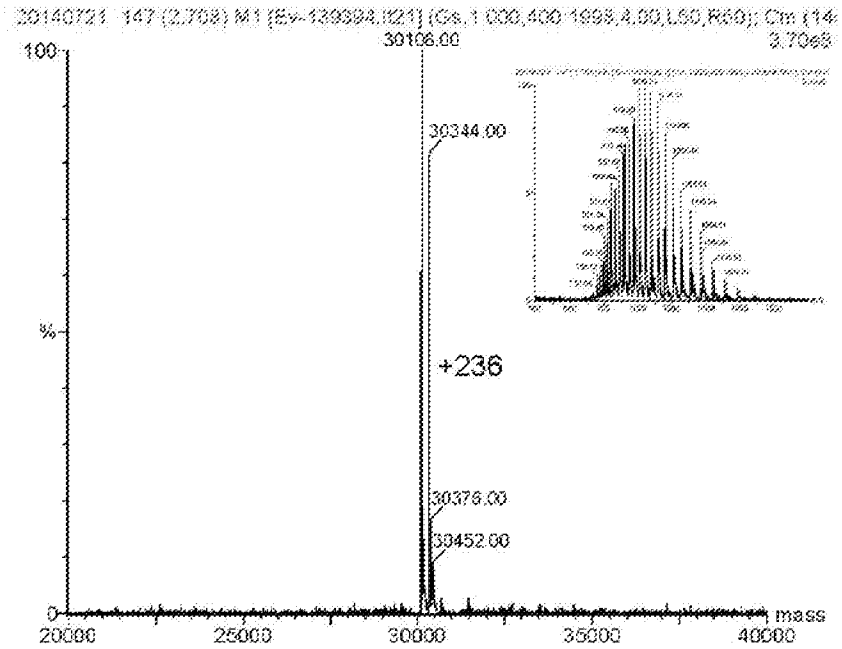
Reaction Scheme:



**Scheme (position of Cys) is C98*

ESI-MS

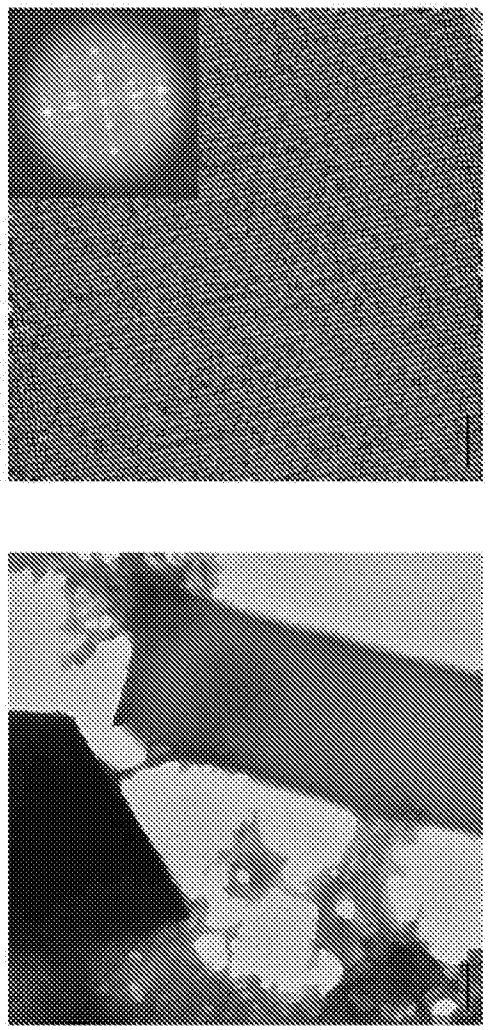
RhuA-C257-iPhen



- ✓ Cys of RhuA-C133 and RhuA-C266 are conjugated with iPhen as of RhuA-C98.
- ✓ After 10 DG column, it was still clouded (even after the addition of EDTA)
- ✓ Reaction was not completed as result of ESI-MS.
- ✓ RhuA-C273-iPhen was also synthesized; however, it was lost while concentrating amicon – seems filter was broken....

FIG. 37

RhuA-C98-iphen (100 μM) with 2eqNiCl$_2$ in 20 mM Mes at pH5.5 after 1day



2014C E1 C98iphen 2eqNi pH5.5 1day 28

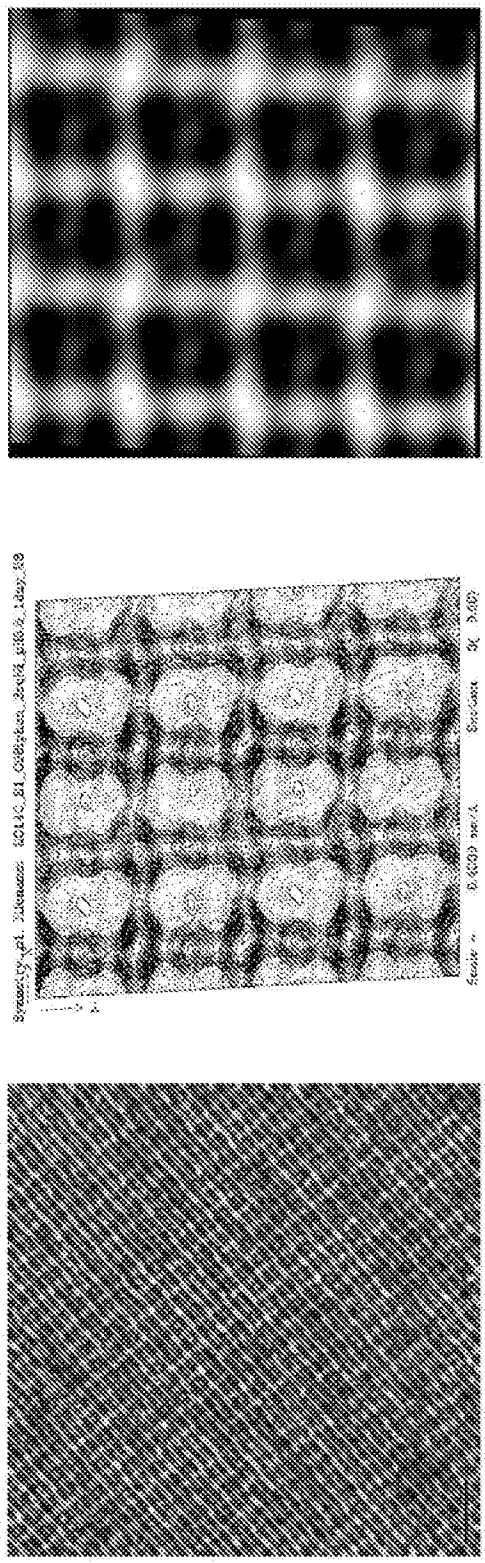


FIG. 38

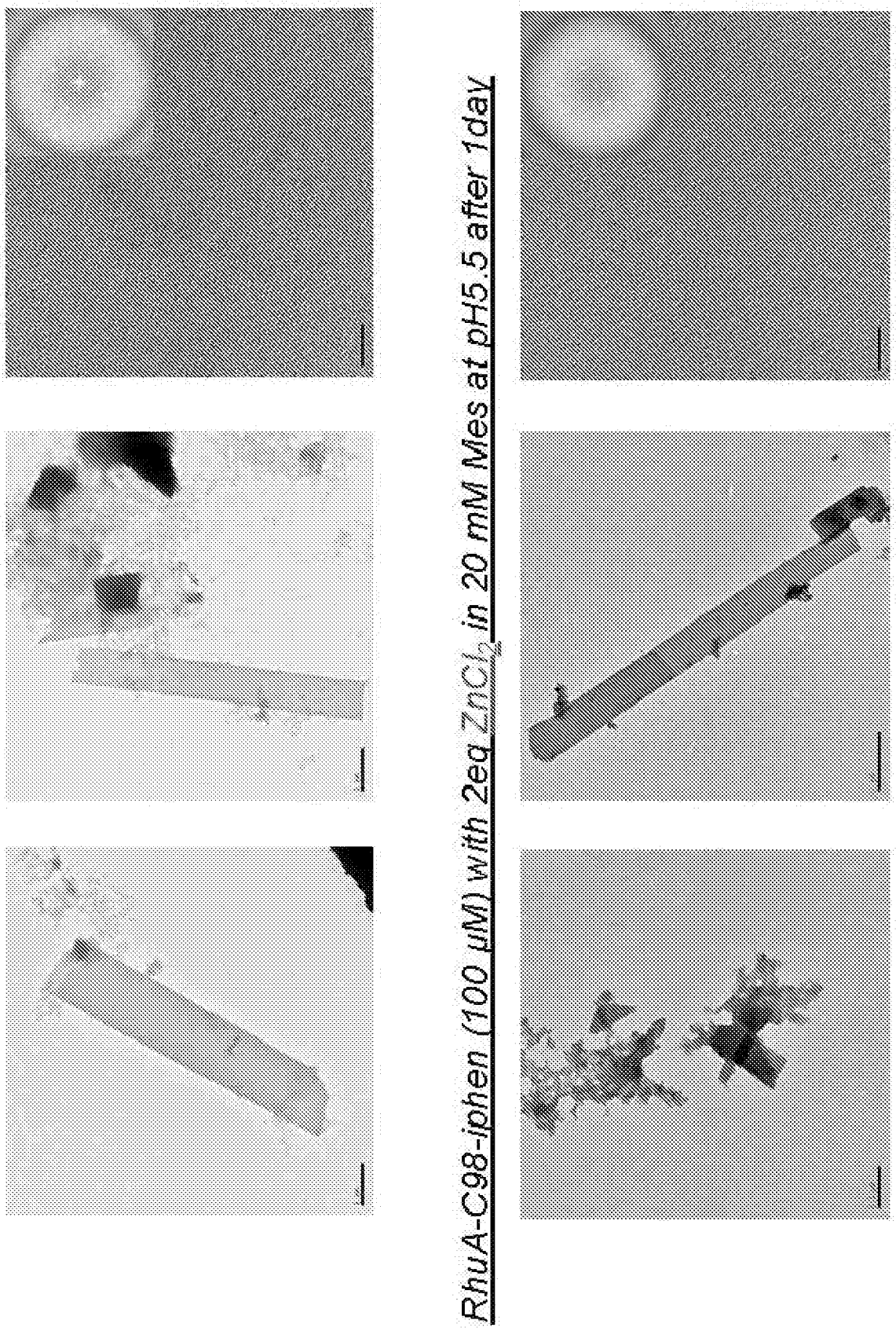
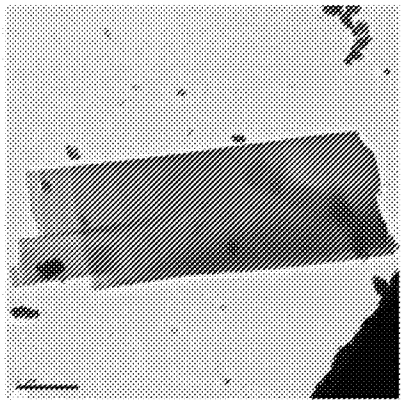
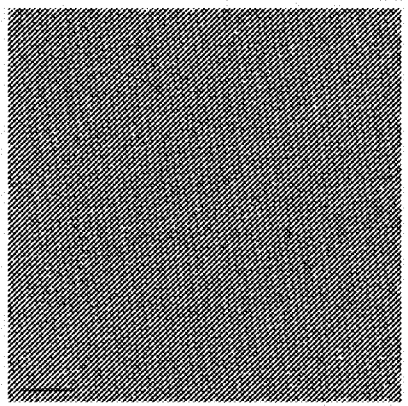

RhuA-C98-iphen (100 μM) with 2eq $CuCl_2$ in 20 mM Mes at pH5.5 after 1day
RhuA-C98-iphen (100 μM) with 2eq $ZnCl_2$ in 20 mM Mes at pH5.5 after 1day

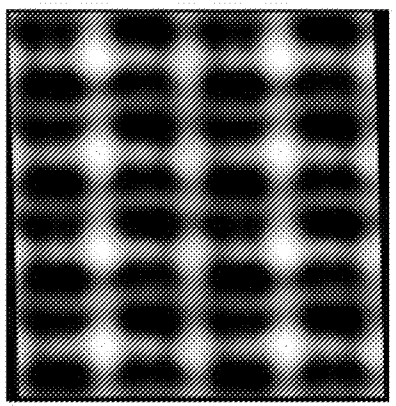
FIG. 39 2014D_C1_C98iPhen_2eqNi_pH5.5_2days

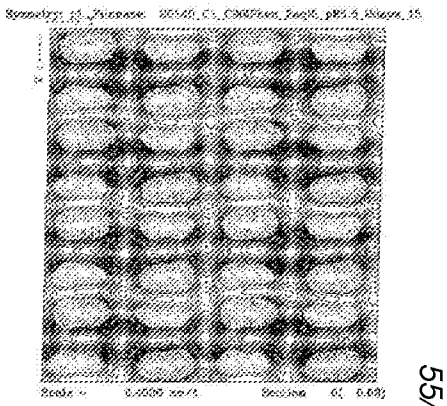
Sheet observed



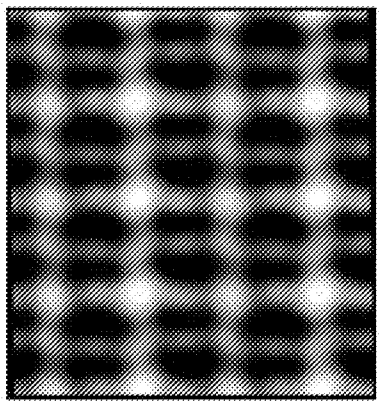
2014D_C1_C98iPhen_2eqNi_pH5.5_2days_15

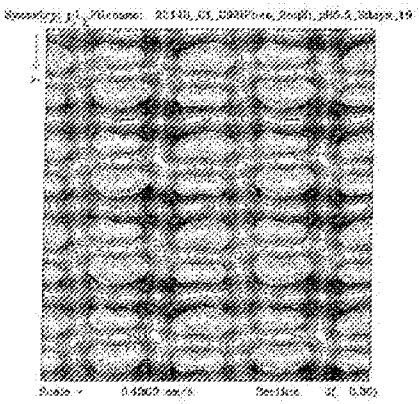




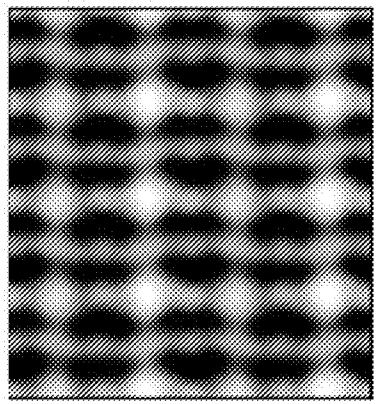


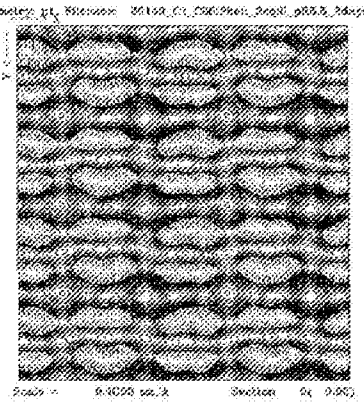
2014D_C1_C98iPhen_2eqNi_pH5.5_2days_19





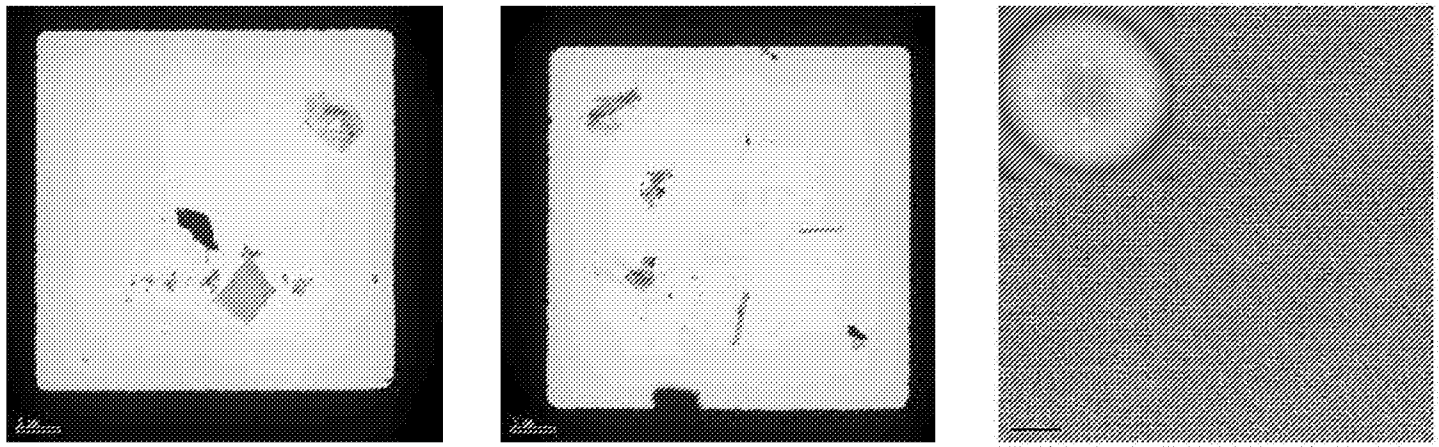
2014D_C1_C98iPhen_2eqNi_pH5.5_2days_29



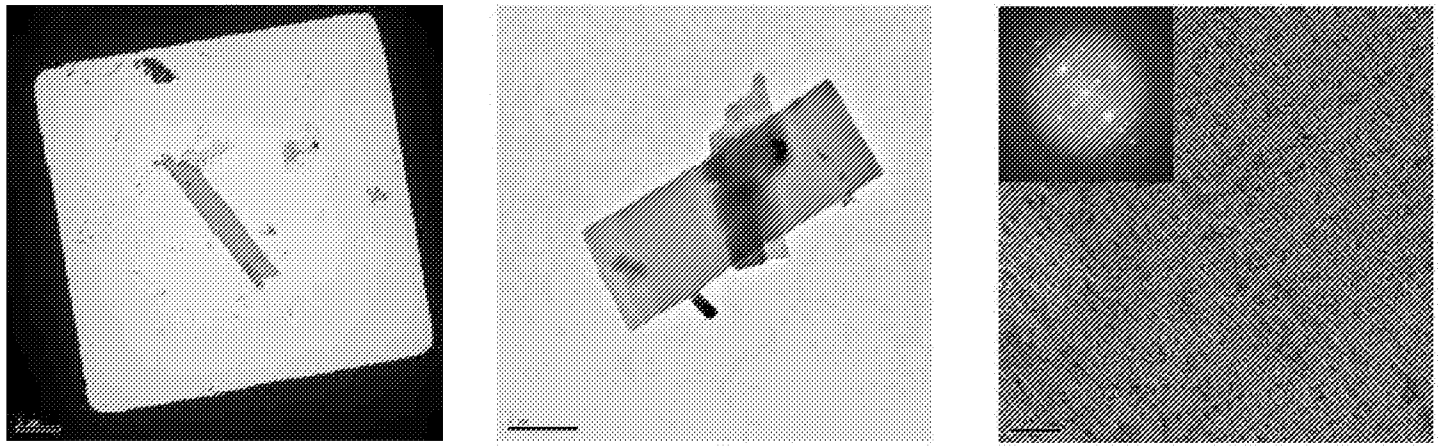


More data for Cu and Zn as well in 20140723

FIG. 40 RhuA-C98-iphen (100 μM) with 2 eq $NiCl_2$ in 20 mM Mes at pH5.5 after 12 days



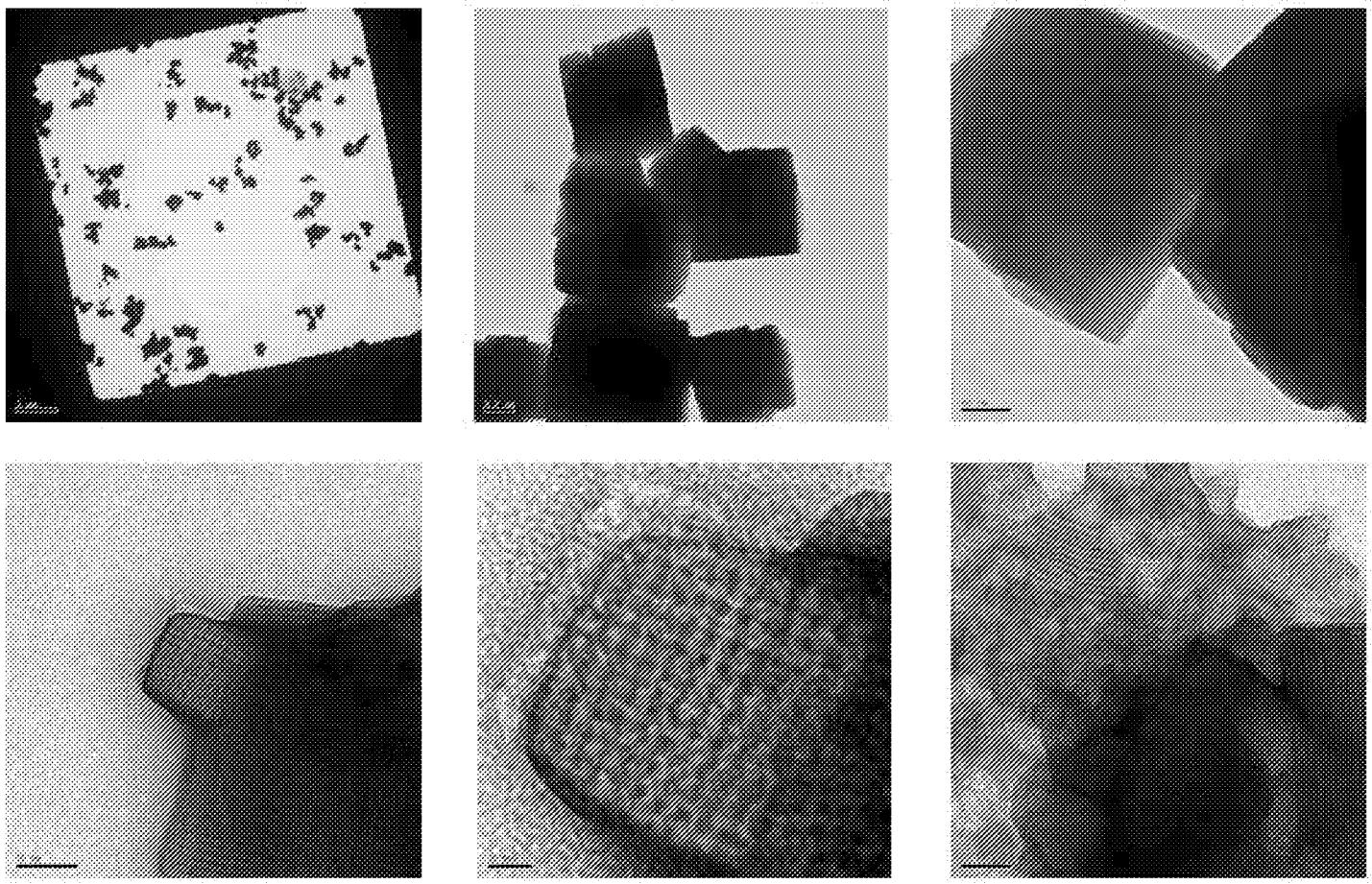
with additiona of 4 eq Imidazole



Samples were prepared on July 21.
TEM samples were prepared on Aug 2nd

FIG. 41 *RhuA-C133-iphen (100 μM) with 2 eq $NiCl_2$ in 20 mM Mes at pH5.5 after 12 days*

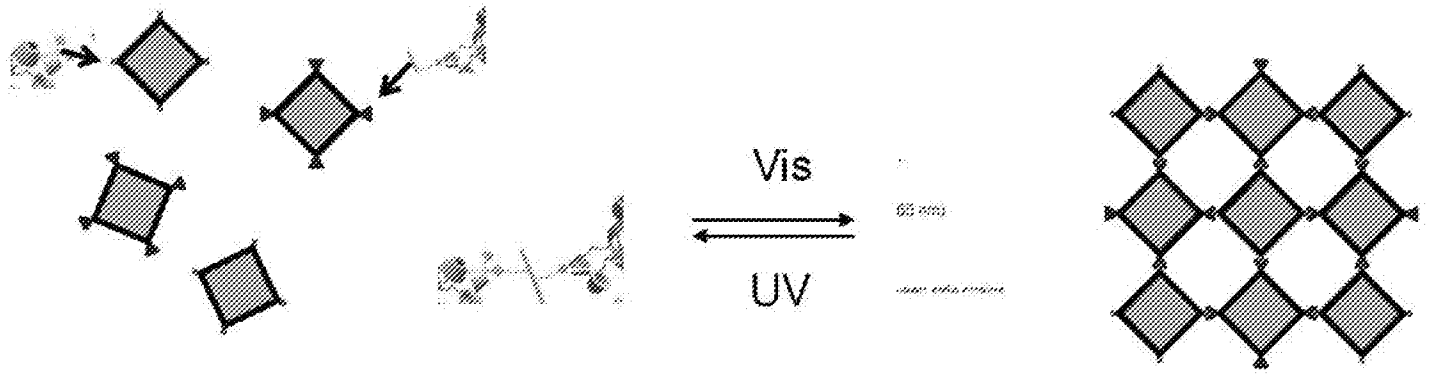
w/ 2eq Zinc



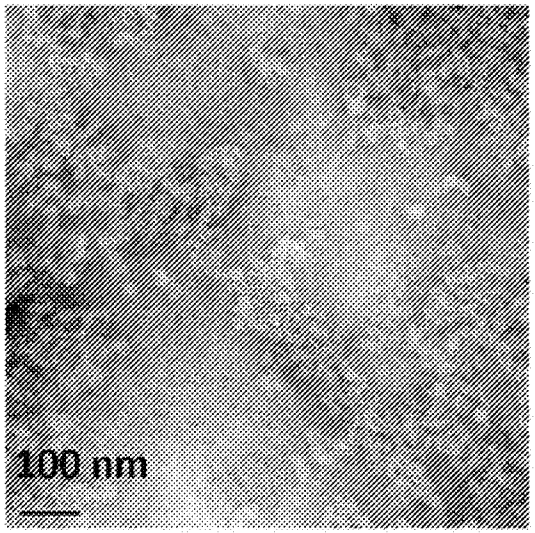
Samples were prepared on July 21.
TEM samples were prepared on Aug 2nd

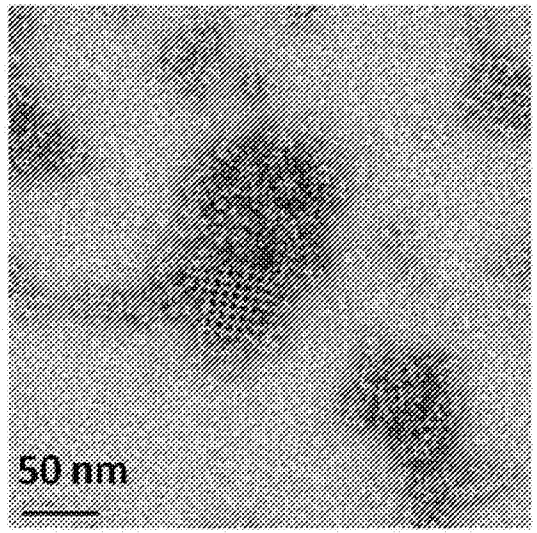
FIG. 42 *Photoswitchable Protein Assembly Via Azo-CD*

Scheme



- Still reaction was incomplete, I took partial solution and removed small molecules, then mixed C98-CD and C98-Azo





Found two partial sheet formation.

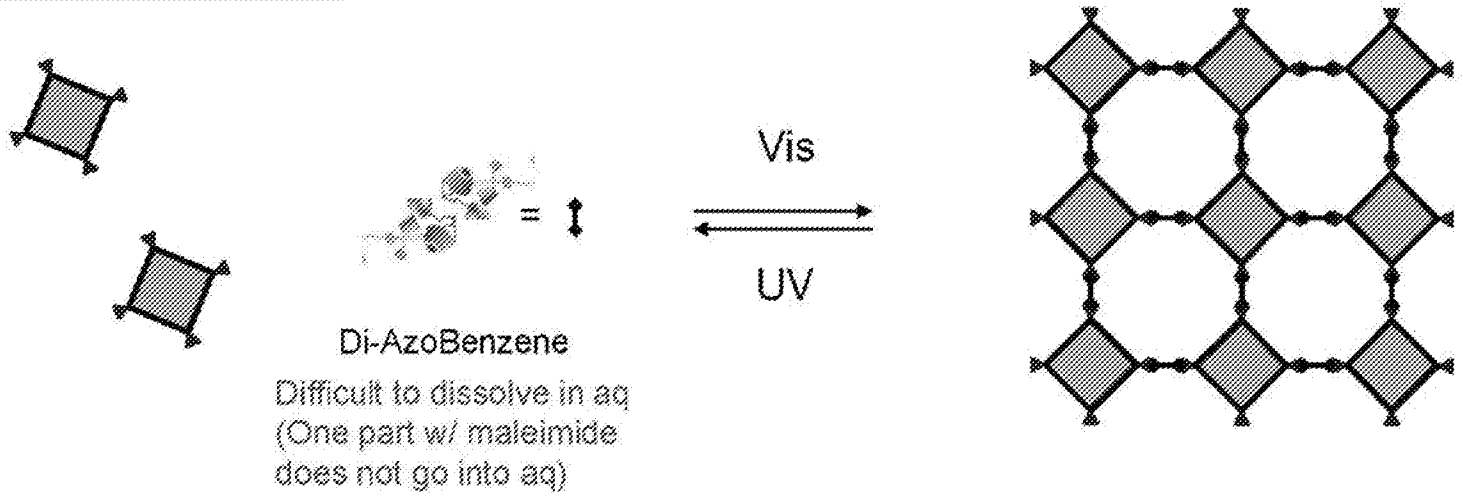
It is possible to be C98 sheet since reaction of RhuA-Azo was not complete.

~100 uM each

FIG. 43

Protein Assembly Via Small Molecule

First Idea: Bis-Azobenzene



Using Curcumin as binding partner

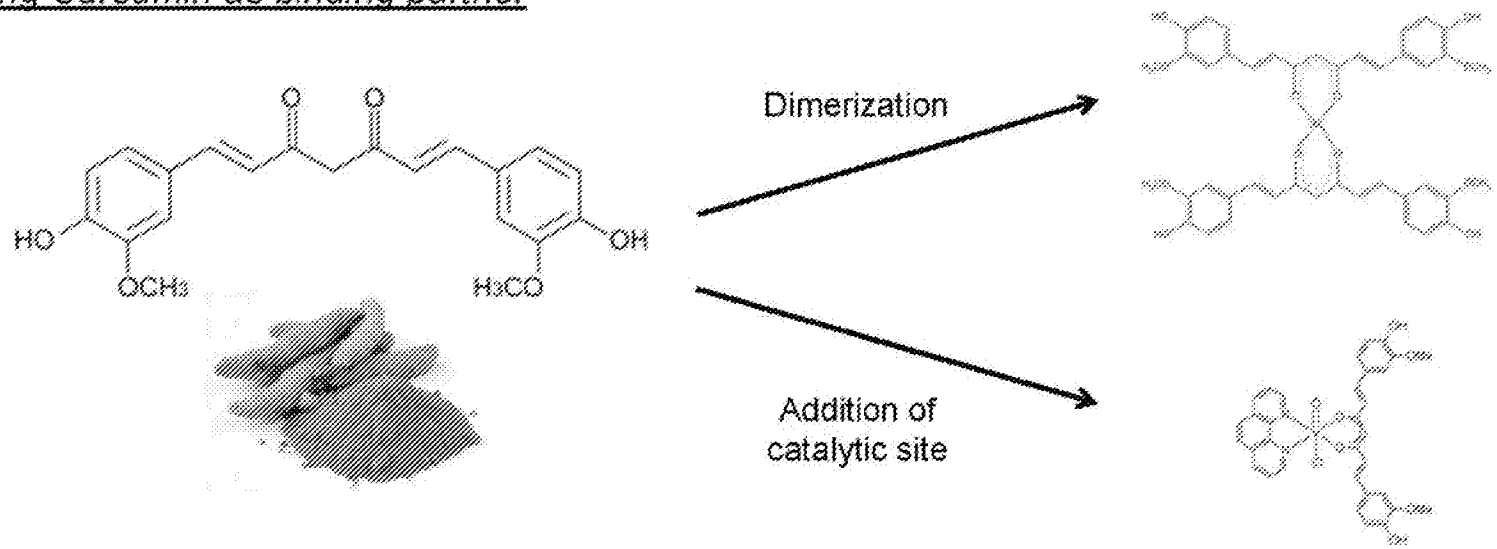


FIG. 44 Protein Assembly Via Small Molecule - 1 mM Curcumin After 1 hr

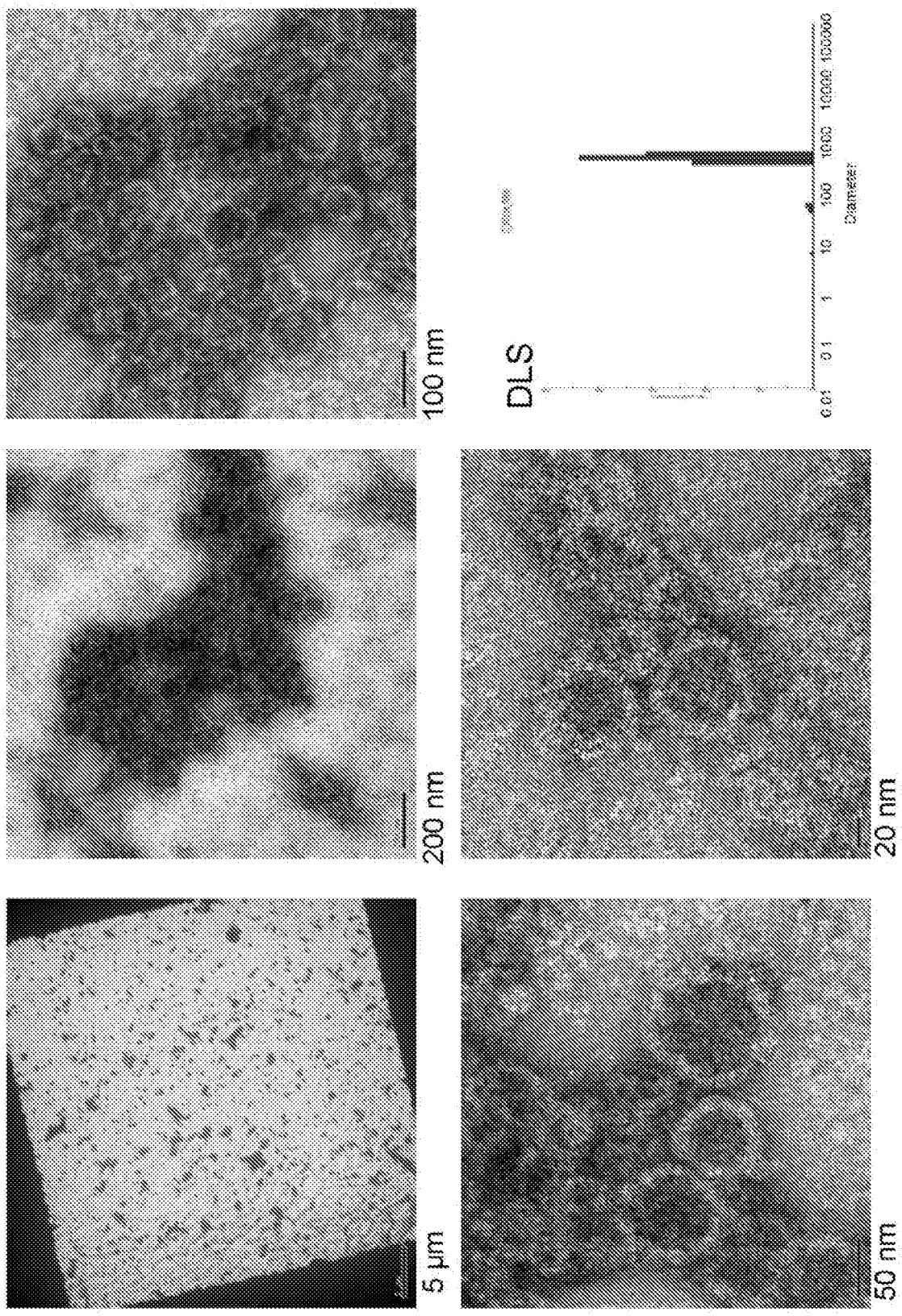


FIG. 45

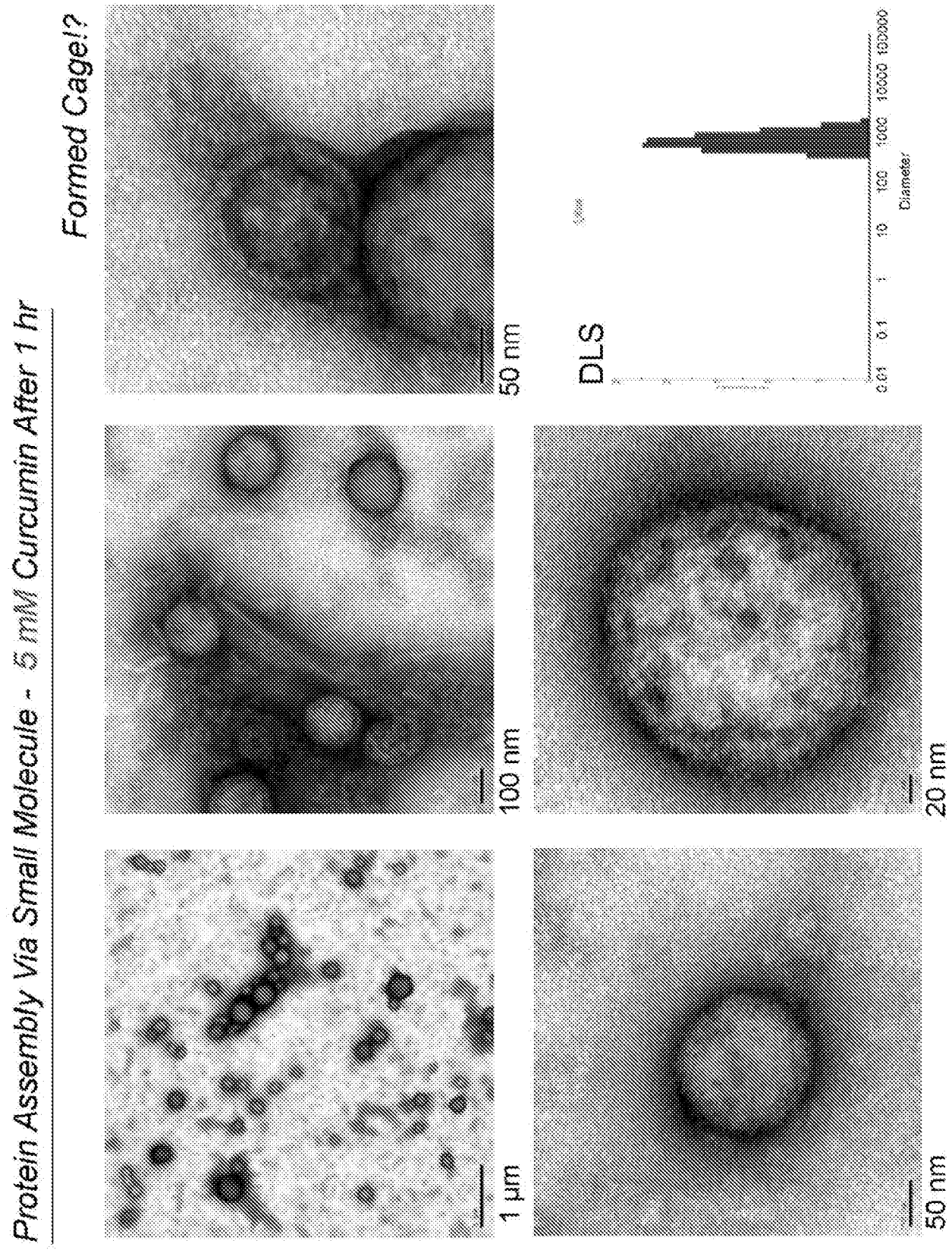
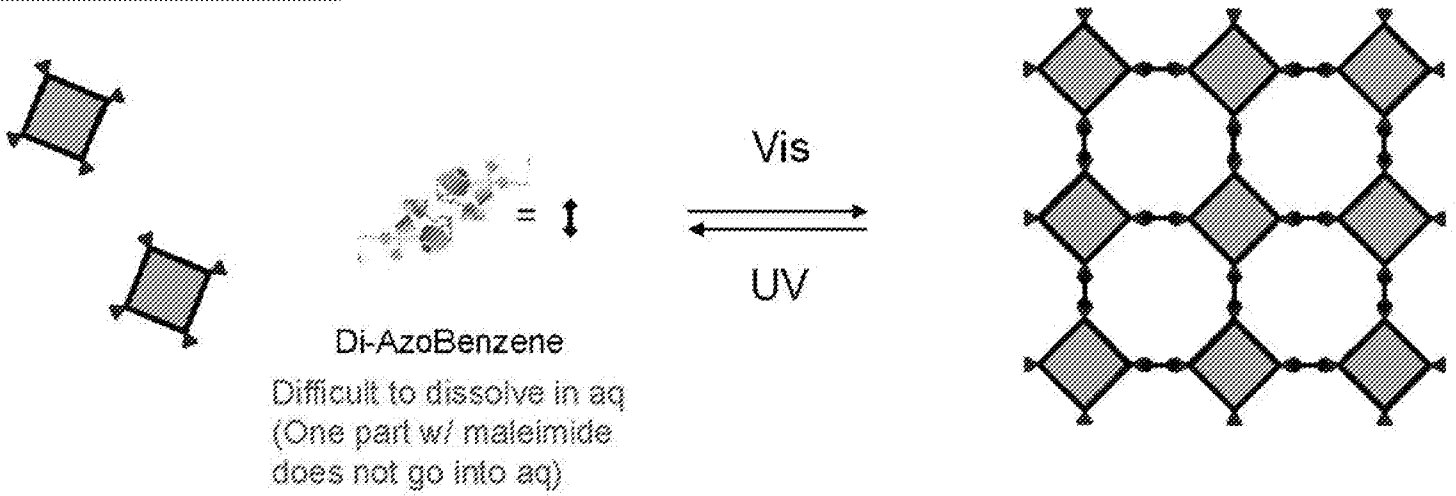

Protein Assembly Via Small Molecule - 5 mM Curcumin After 1 hr
Formed Cage!?
50 nm
100 nm
1 µm
20 nm
50 nm
DLS
Diameter

FIG. 46 *Protein Assembly Via Small Molecule*

First Idea: Bis-Azobenzene



Using Curcumin as binding partner

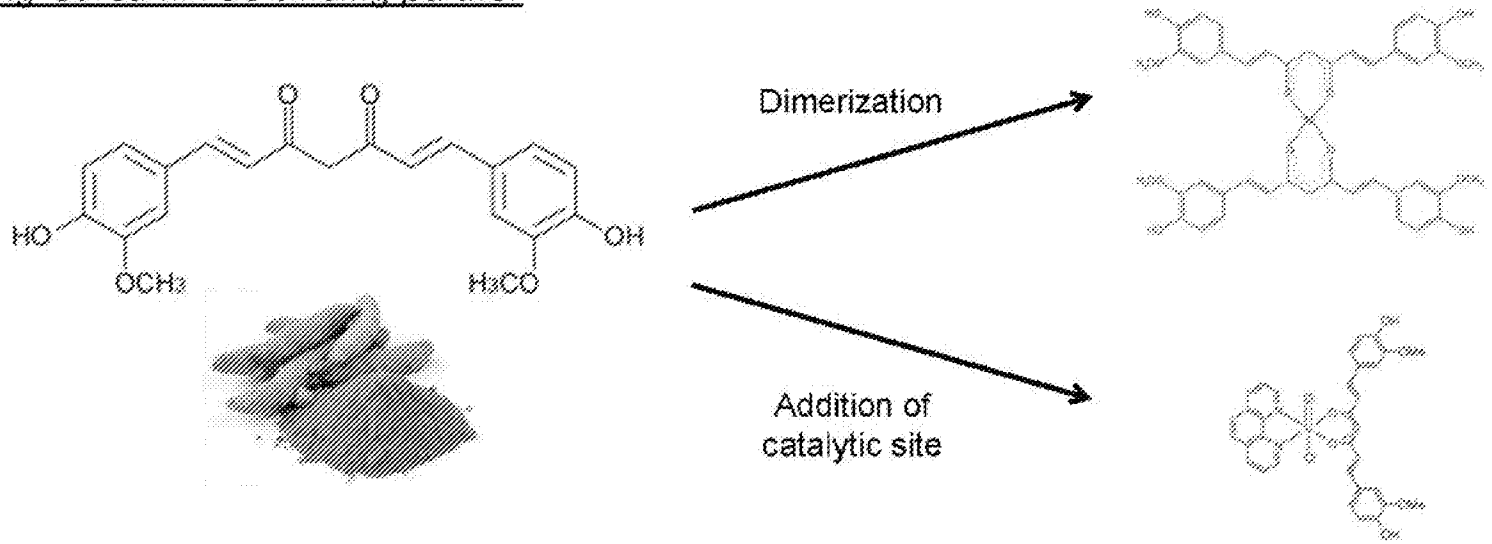


FIG. 47 *Protein Assembly Via Small Molecule - 100 μM Curcumin After 1 hr*

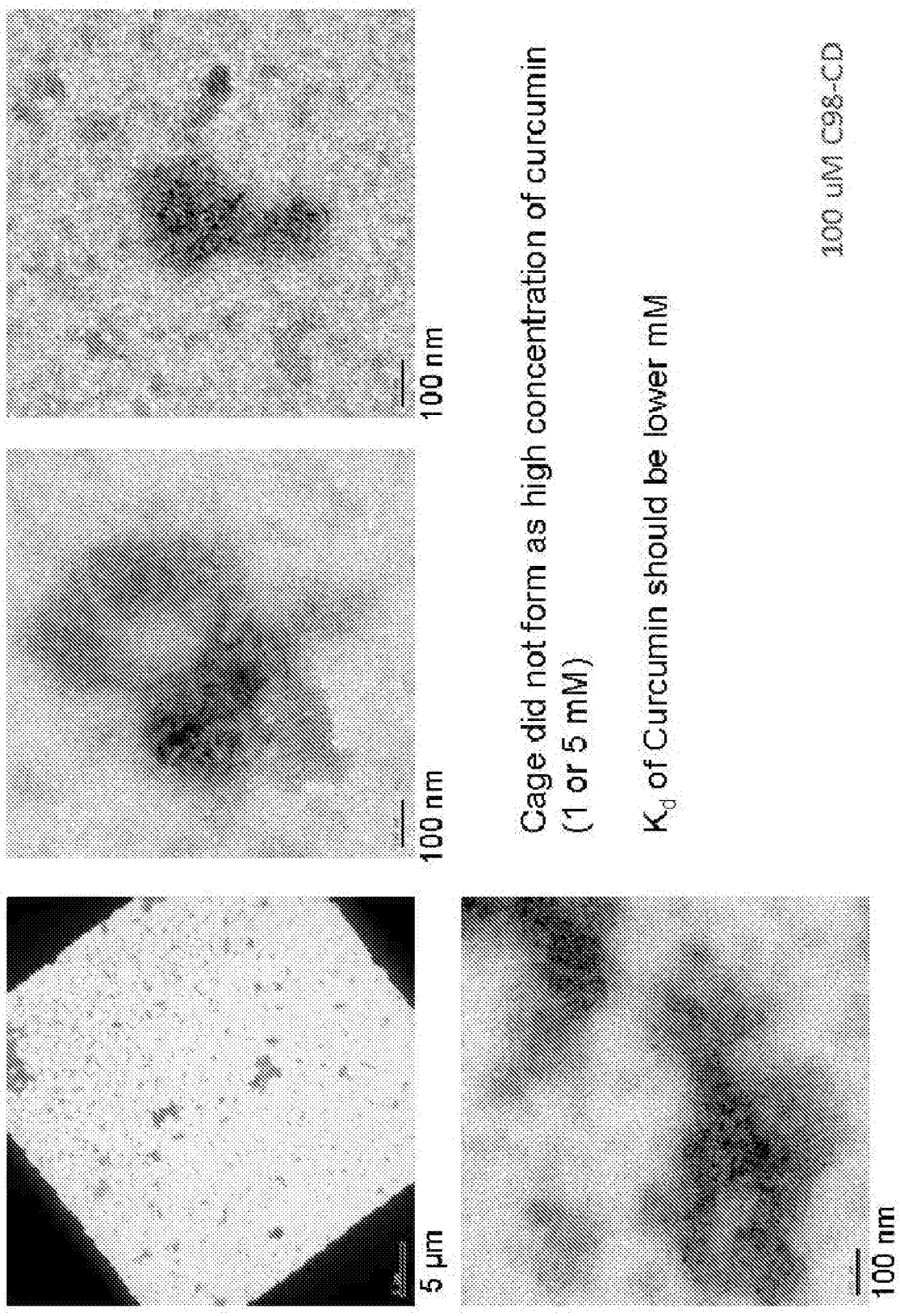


FIG. 48

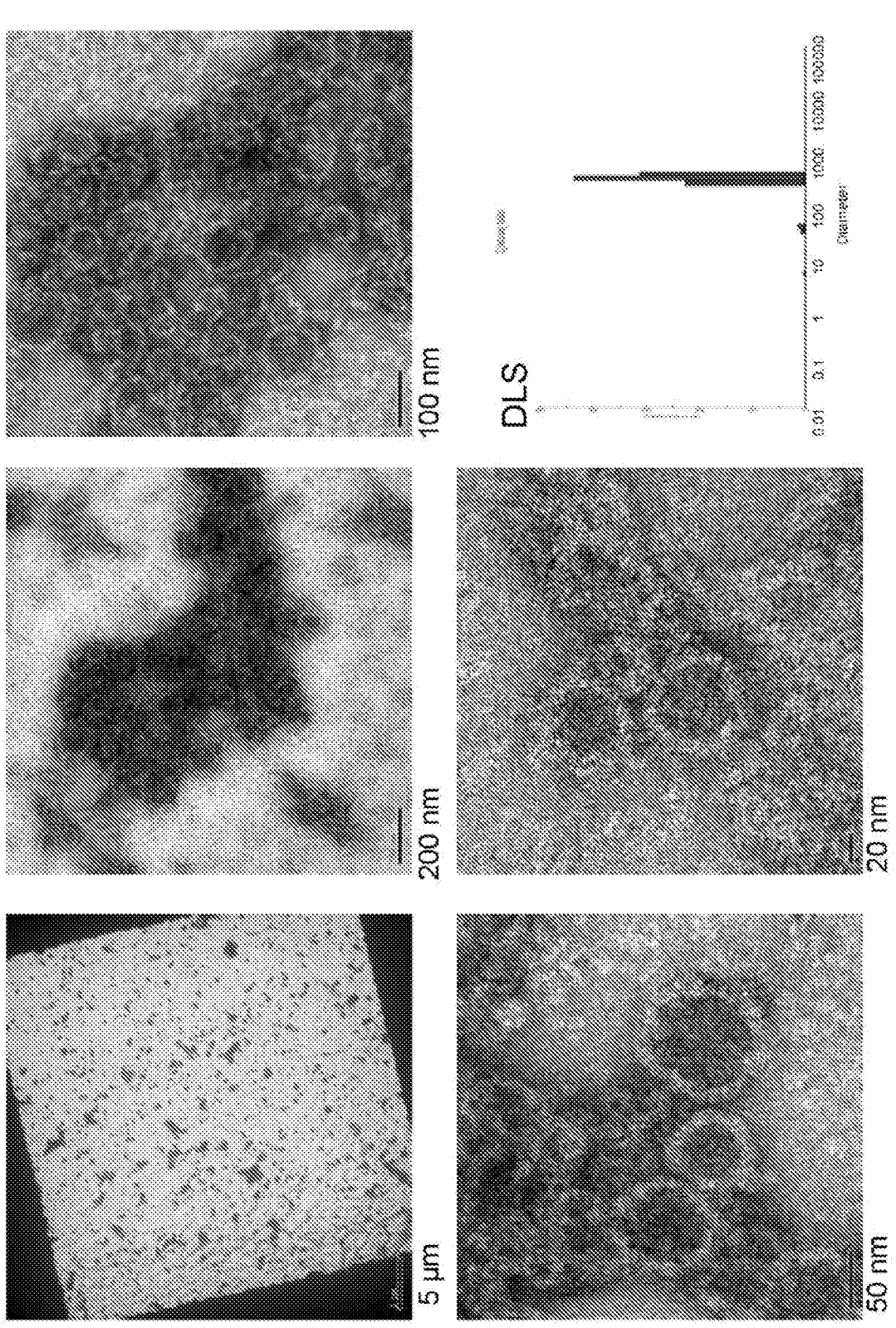

Protein Assembly Via Small Molecule - 1 mM Curcumin After 1 hr
Previous week
Formed Cage!?
100 nm
200 nm
5 µm
DLS
20 nm
50 nm

FIG. 49 Protein Assembly Via Small Molecule - 1 mM Curcumin After 3 Days

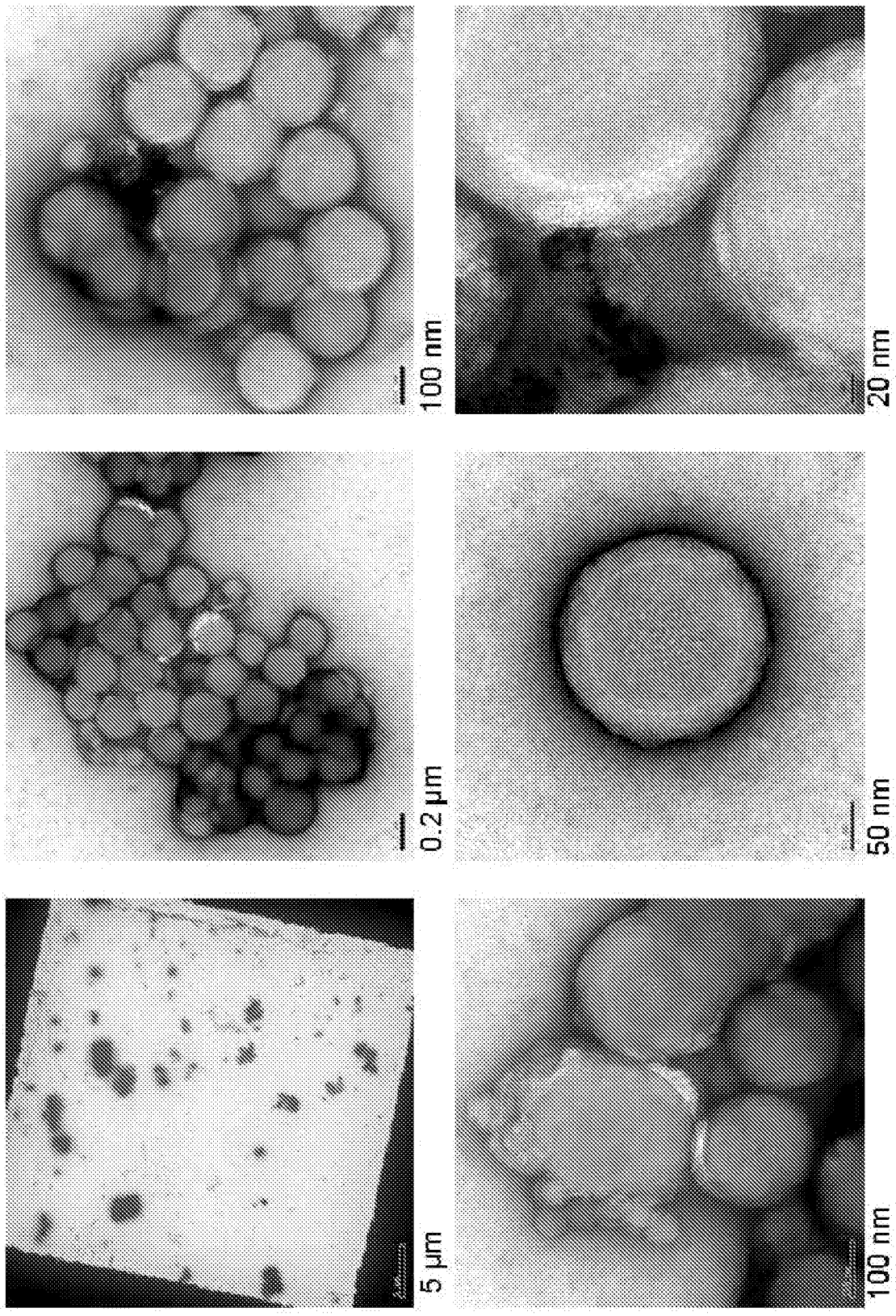
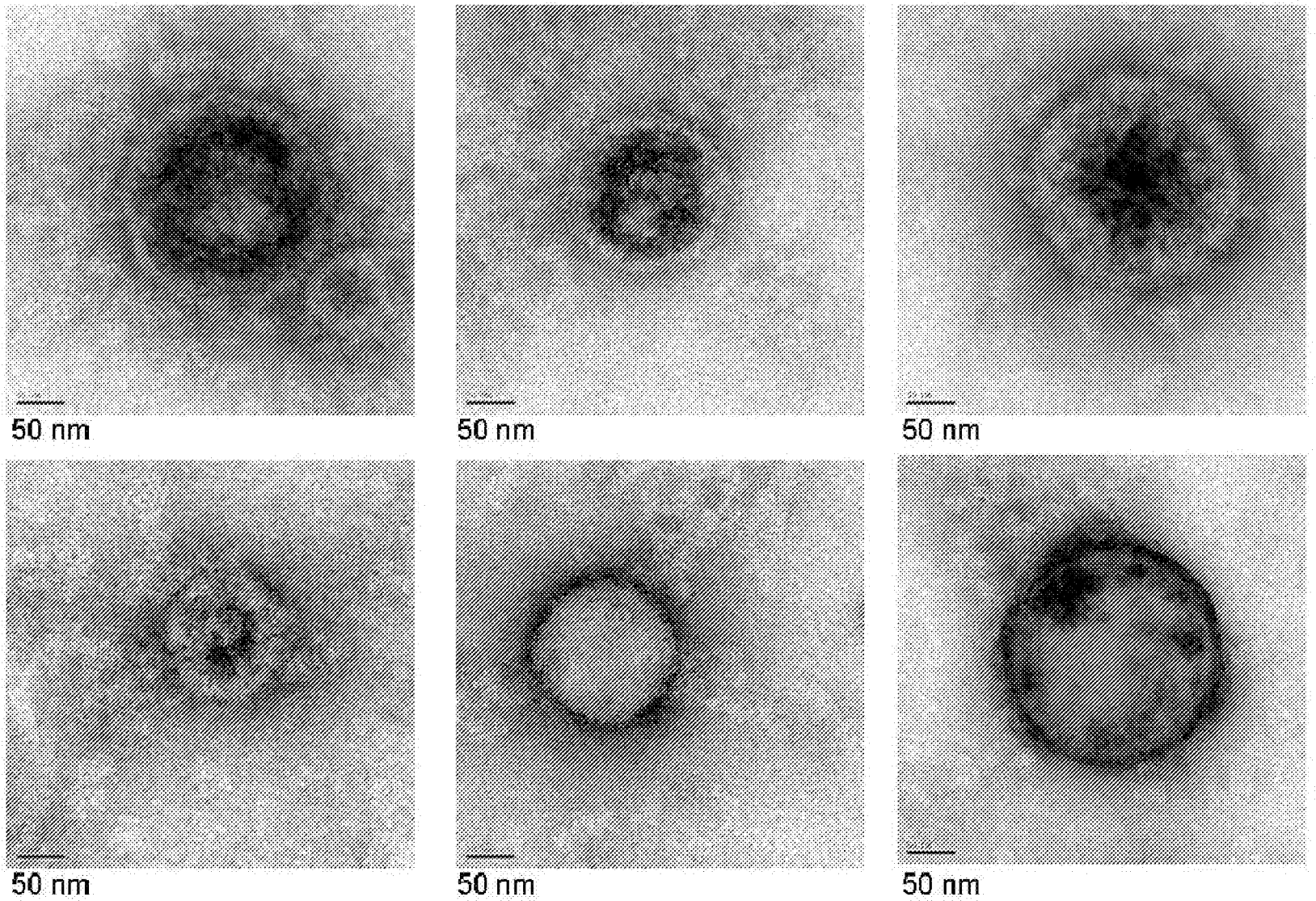


FIG. 50 2nd Trial: Protein Assembly Via Small Molecule - 1 mM Curcumin After 1 hr



Repeatable!!

Pathway of cage formation??

FIG. 51

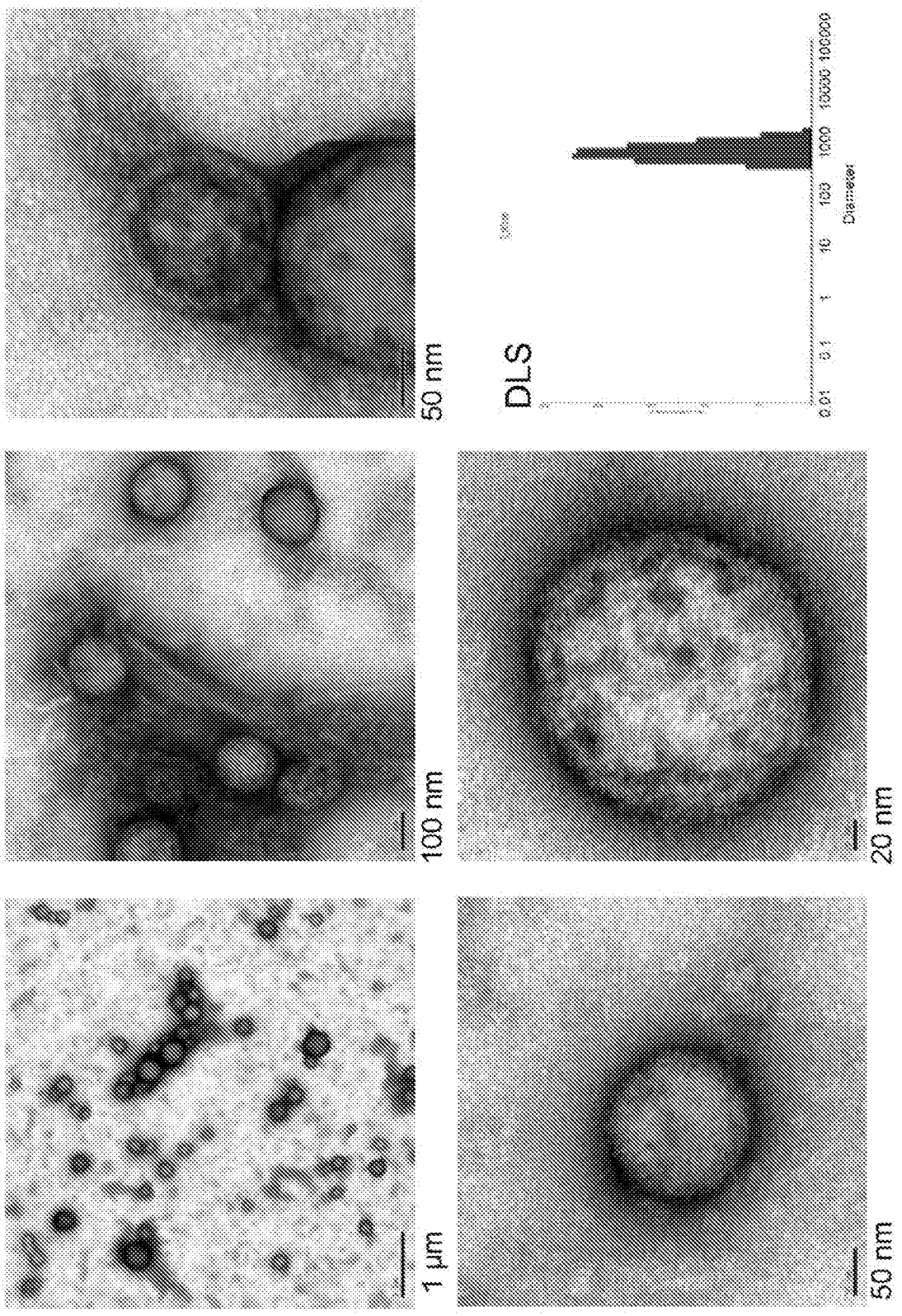

Protein Assembly Via Small Molecule - 5 mM Curcumin After 1 hr
Previous week
Formed Cage!?
50 nm
100 nm
1 µm
DLS
20 nm
50 nm
Diameter

FIG. 52 Protein Assembly Via Small Molecule - 5 mM Curcumin After 3Days

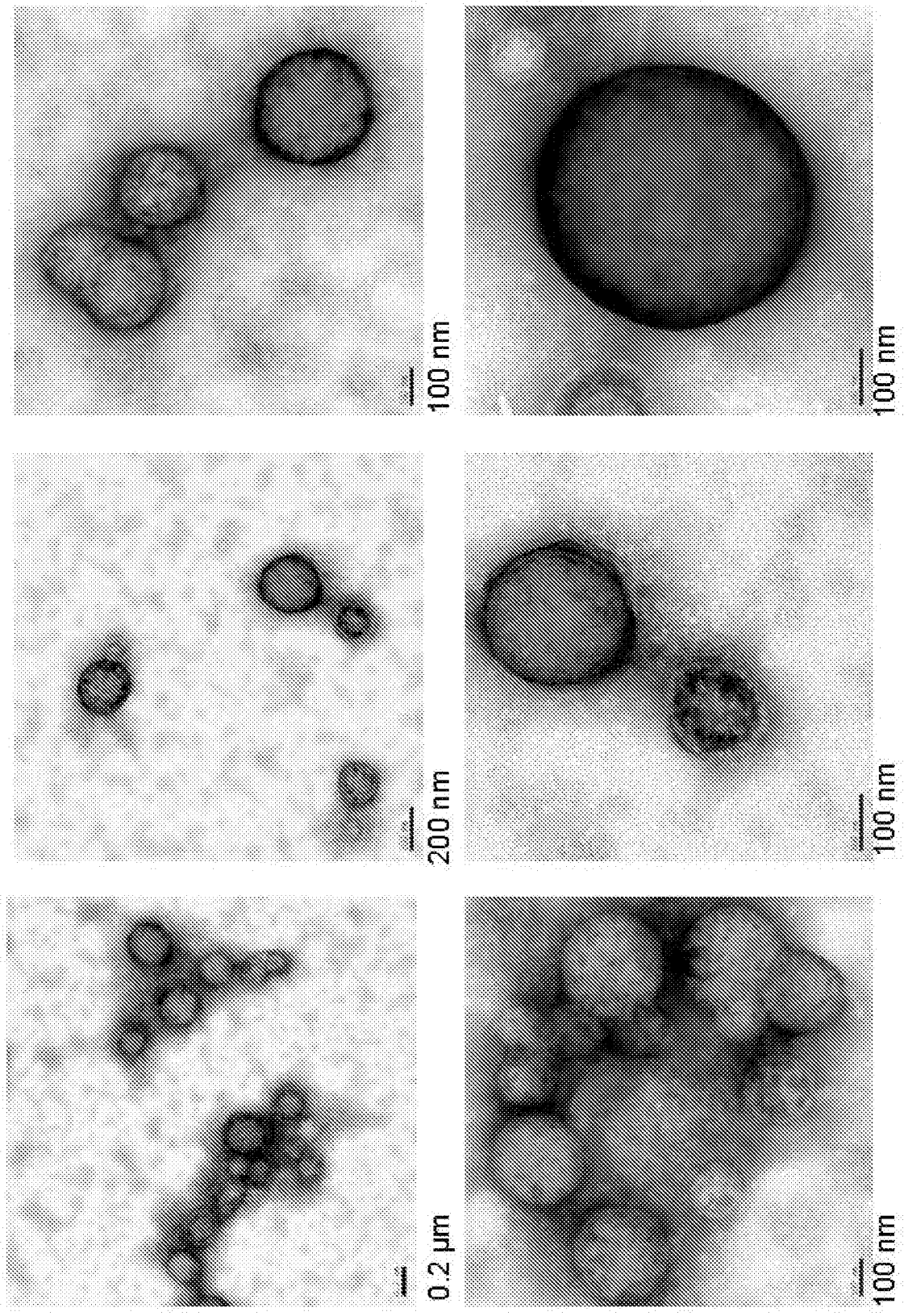


FIG. 53

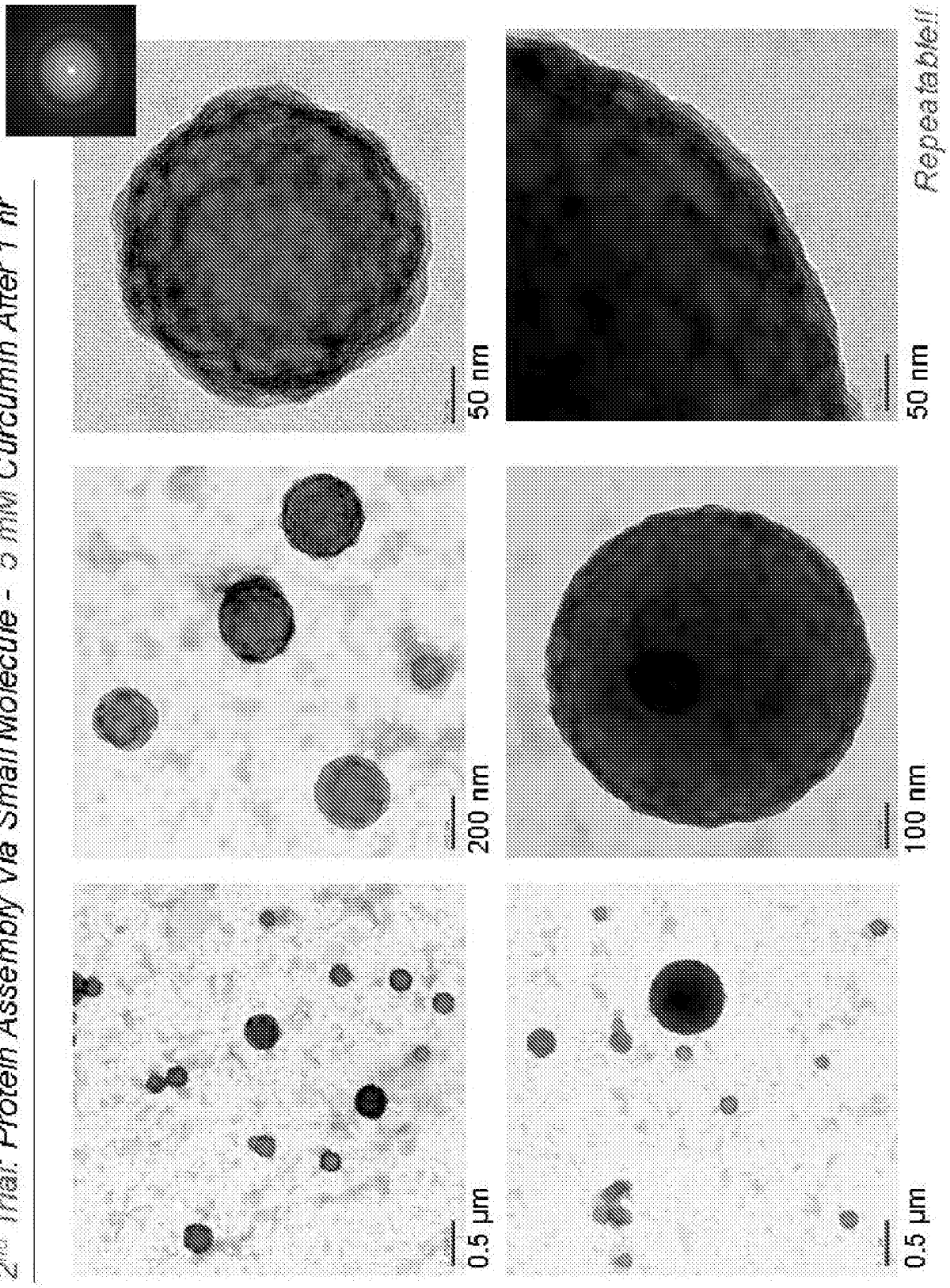
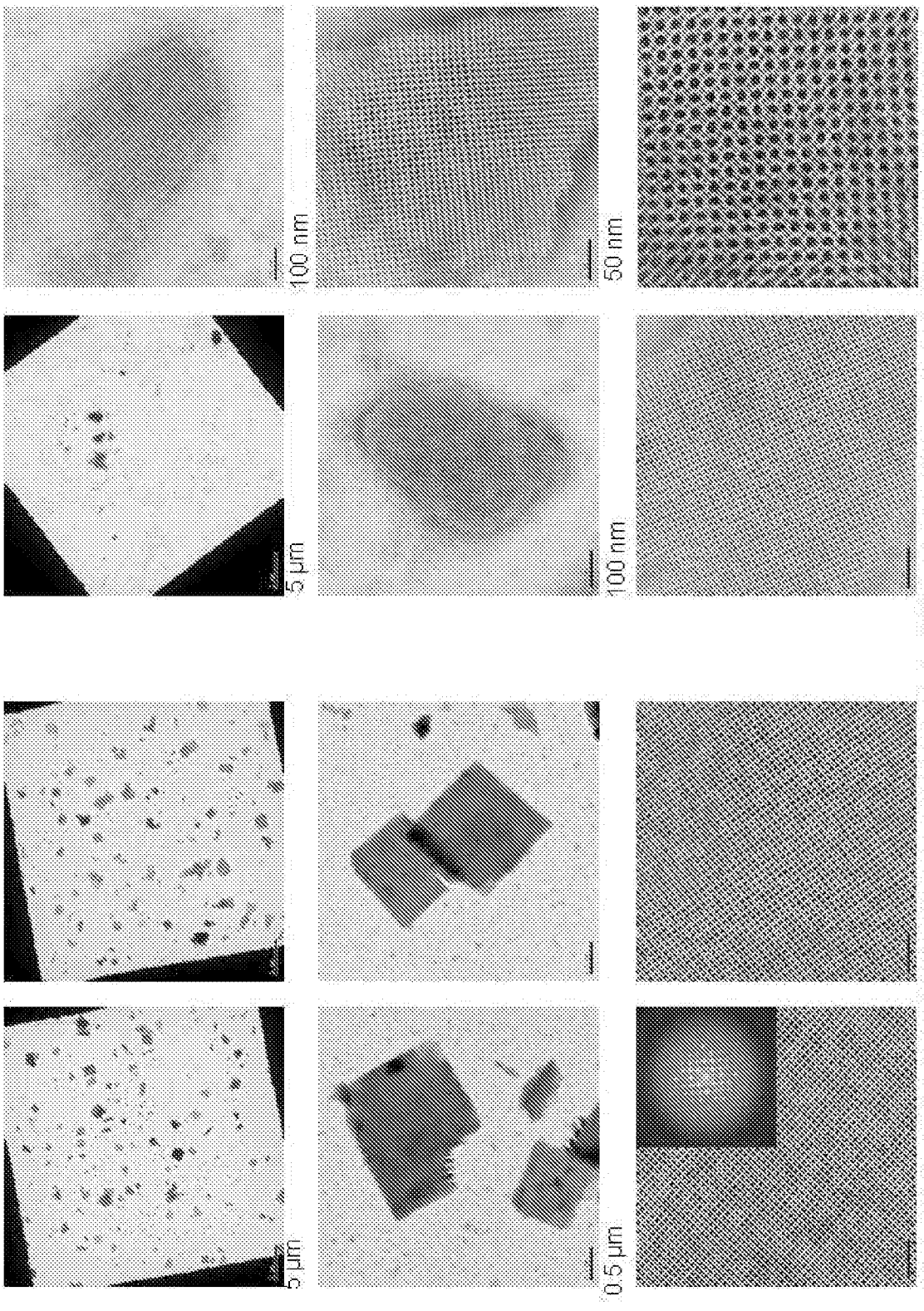

2nd Trial: Protein Assembly Via Small Molecule - 5 mM Curcumin After 1 hr
0.5 µm
200 nm
50 nm
0.5 µm
100 nm
50 nm
Repeatable!!

FIG. 54



Concentrated samples (~100 µM) were shaked for 1 day (I also tested after 4 days and did not see as well...)
These were mixed with iodo-FL, but I could not observe sheets – even without iodo-FL as mentioned above.

FIG. 55 RhuA-C98-HisTag (100 μM) in 20 mM MOPS at pH 7 in Reduced Condition After 5 Days

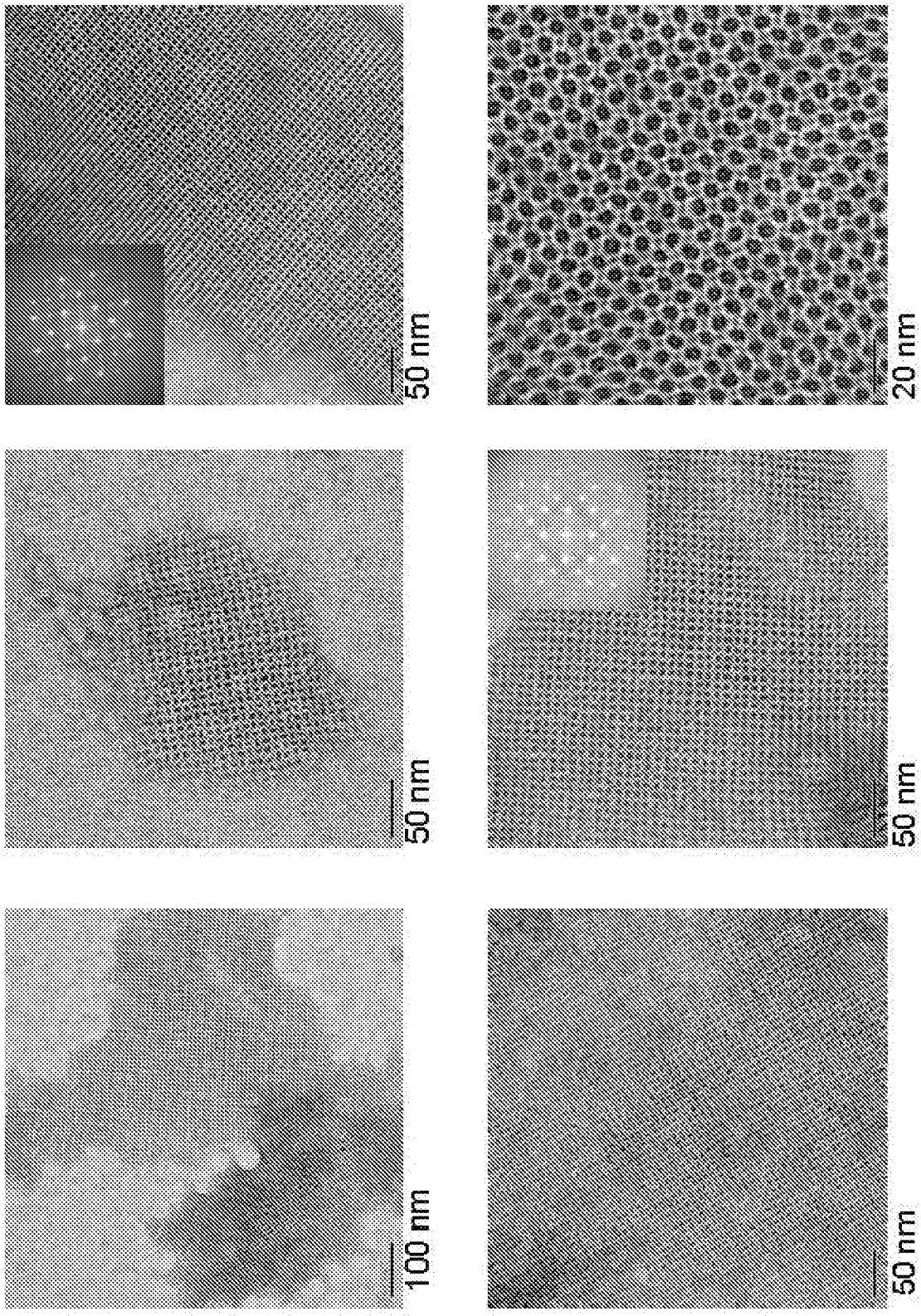


FIG. 56

RhuA-C98-HisTag (100 μM) in 20 mM MOPS at pH 7 in Redox Condition after 1 Day

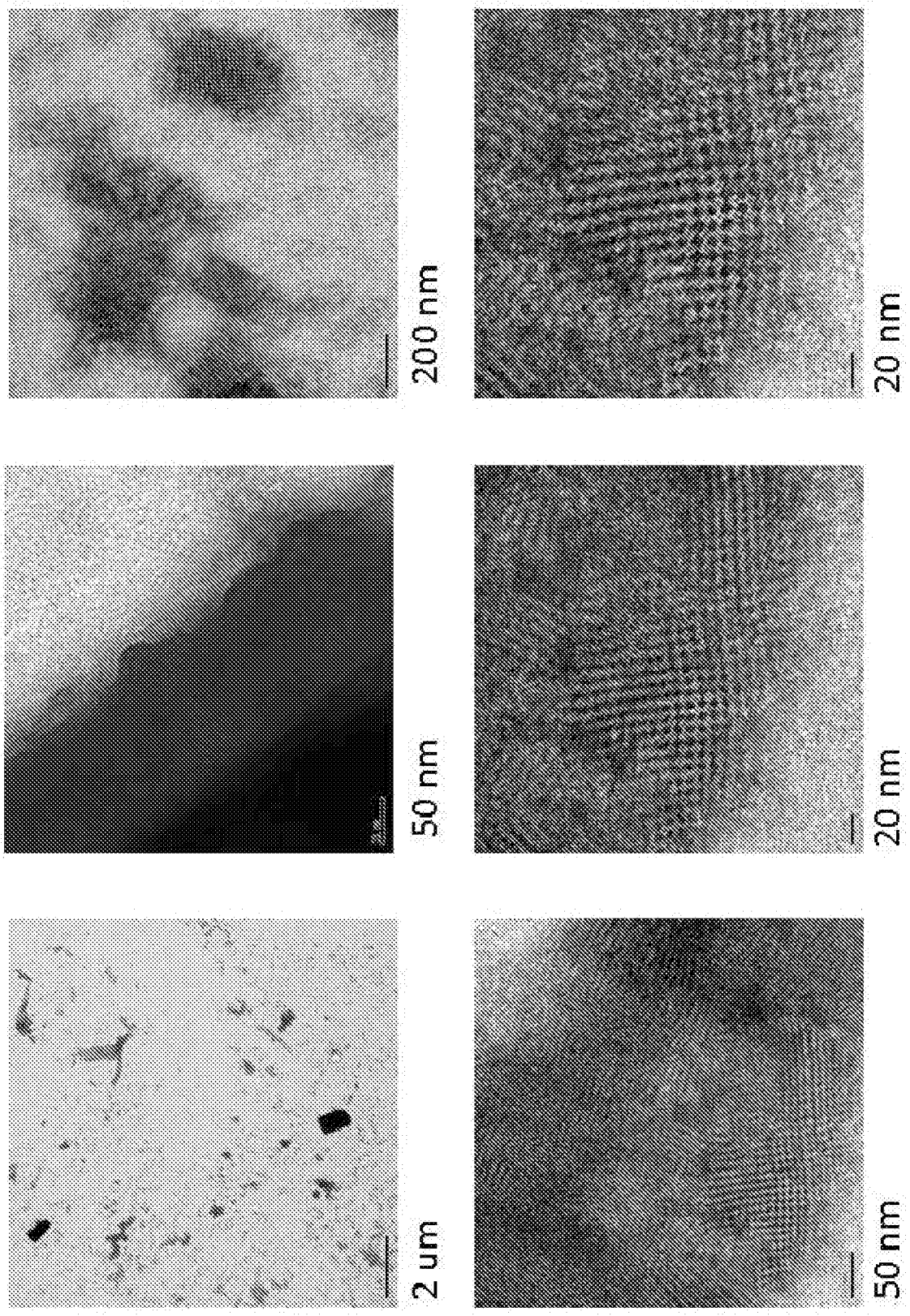


FIG. 57 *Assembly of ^{C98}RhuA-Pd4 (125 μM) under various conditions (after 1 day w/ shake)*

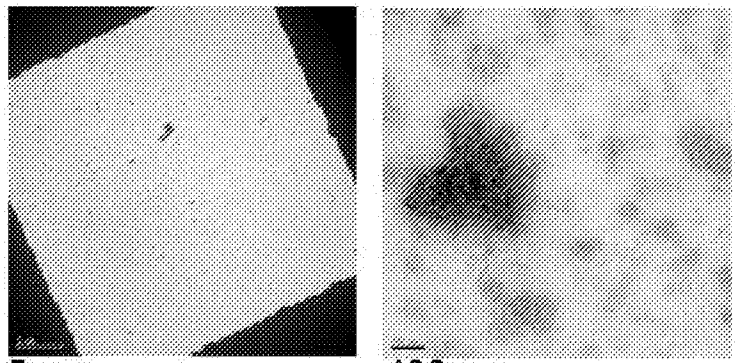
RhuA-Pd4

^{C98}RhuA

MQNITQSWFVQGMIKATTDAWLKGWDERNGGNLTLRLDDADIAPYHDNFHQQPRYIPLSQPMPL
LANTPFIVTGSGKFFRNVQLDPAANLGIVKVDSCGAGYHILWGLTNEAVPTSELPAHFLSHSERIKATN
GKDRVIMHCHATNLIALTYVLENDTAVFTRQLWEGSTECLVVFPDGVGILPWMVPGTDAIGQATAQ
EMQKHSLVLVVPFHGVFGSGPTLDETFGLIDTAEKSAQVLVKVYSMGGMKQTISREELIALGKRFGVT
PLASALALGSGSGTSNAVHPTLRHL

Pd4 peptide

20 mM Mes pH 5.5, 10 mM βME, no $ZnCl_2$



Immediately became cloudy

10 mM Tirs pH 7.5, 10 mM βME, no $ZnCl_2$

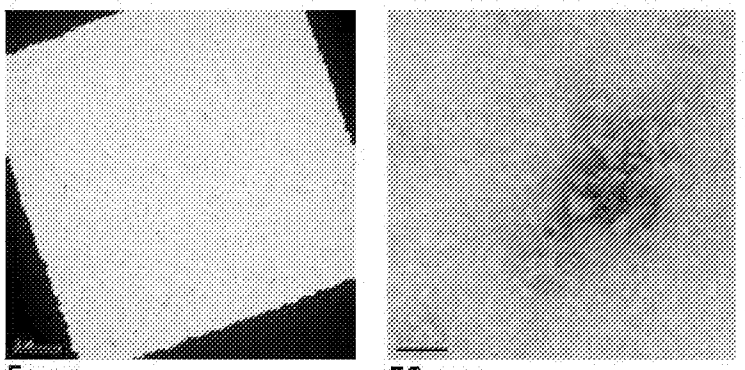


FIG. 58

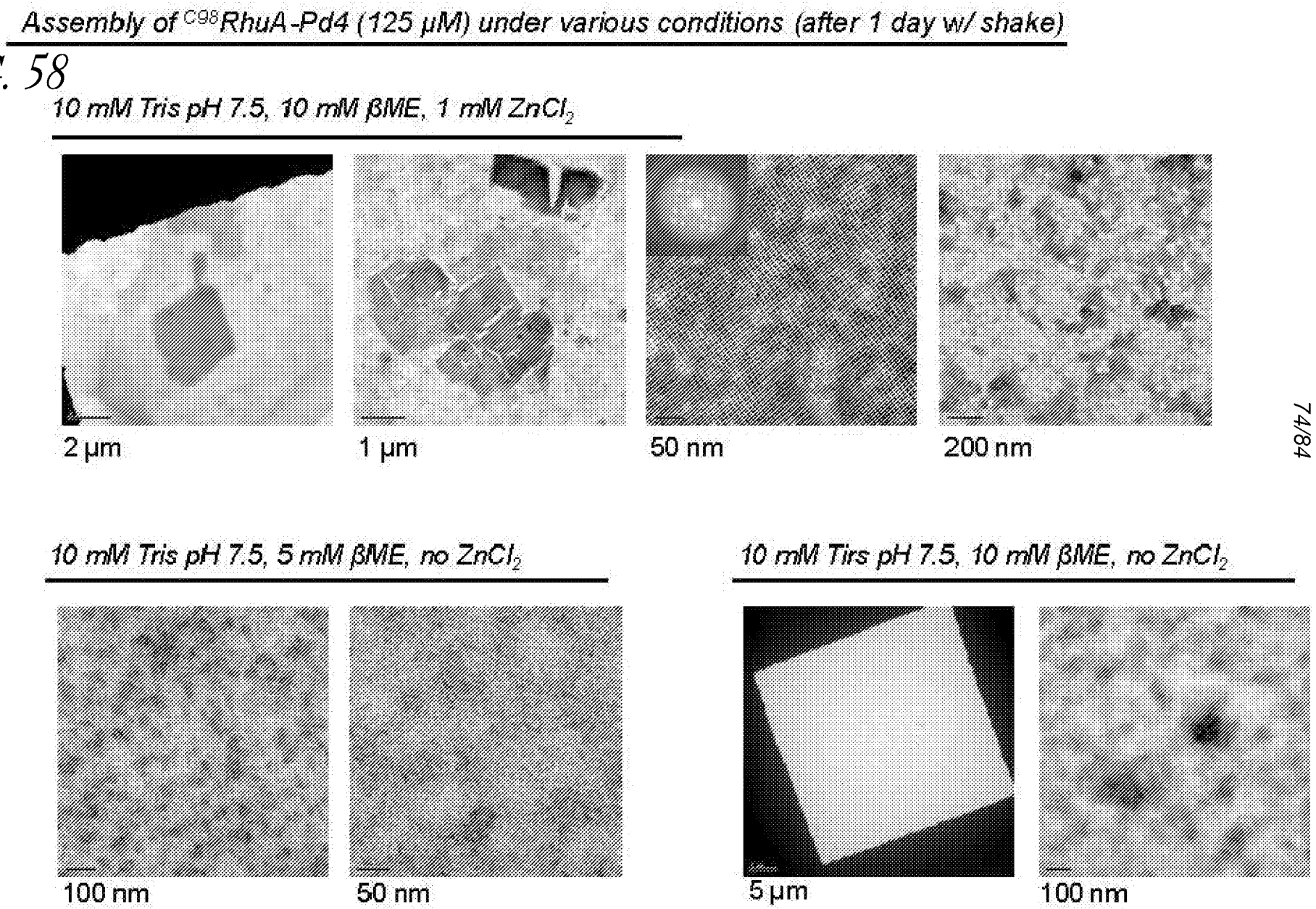
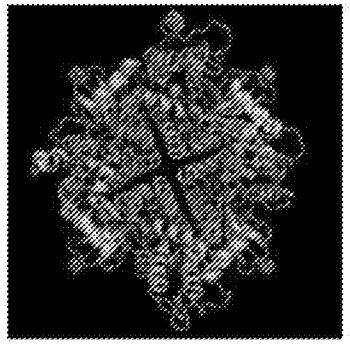
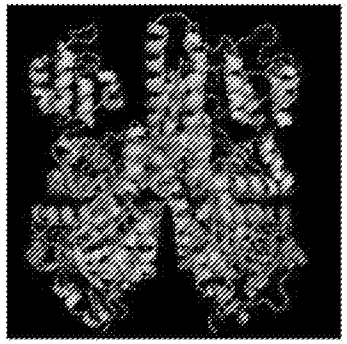

Assembly of C98RhuA-Pd4 (125 μM) under various conditions (after 1 day w/ shake)
10 mM Tris pH 7.5, 10 mM βME, 1 mM ZnCl2
2 μm
1 μm
50 nm
200 nm
10 mM Tris pH 7.5, 5 mM βME, no ZnCl2
100 nm
50 nm
10 mM Tirs pH 7.5, 10 mM βME, no ZnCl2
5 μm
100 nm

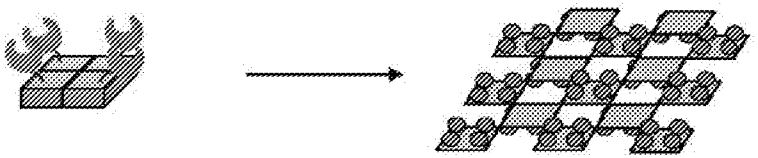
FIG. 59 Fusion Protein 2D Assemblies: RhuA-ACP – Most up-to-date Data

Crude sample: [C] not known.
Should be lower than 50 uM.
It was just a quick test.





Design



Construct of fusion protein: RhuA-C98 – GSGSG – e.coli. ACP

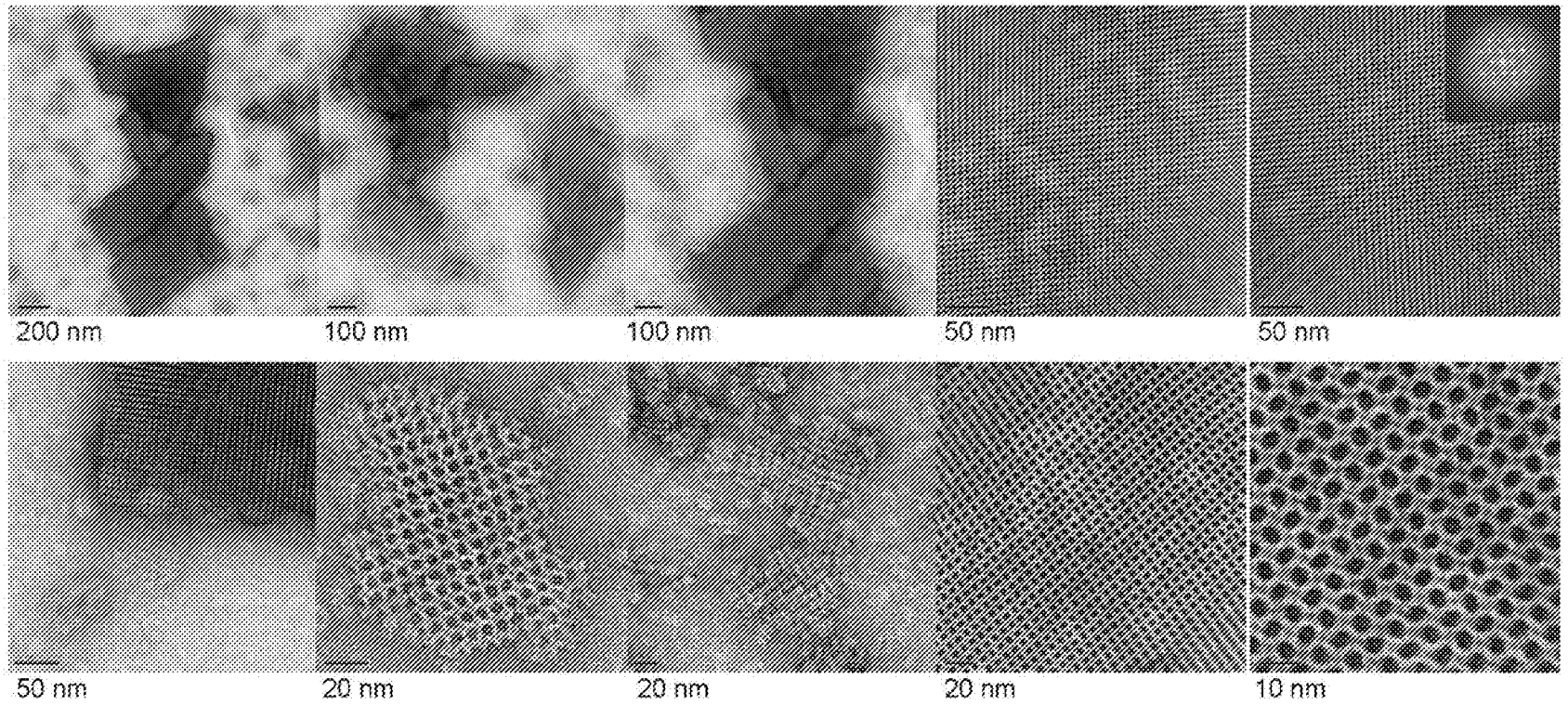
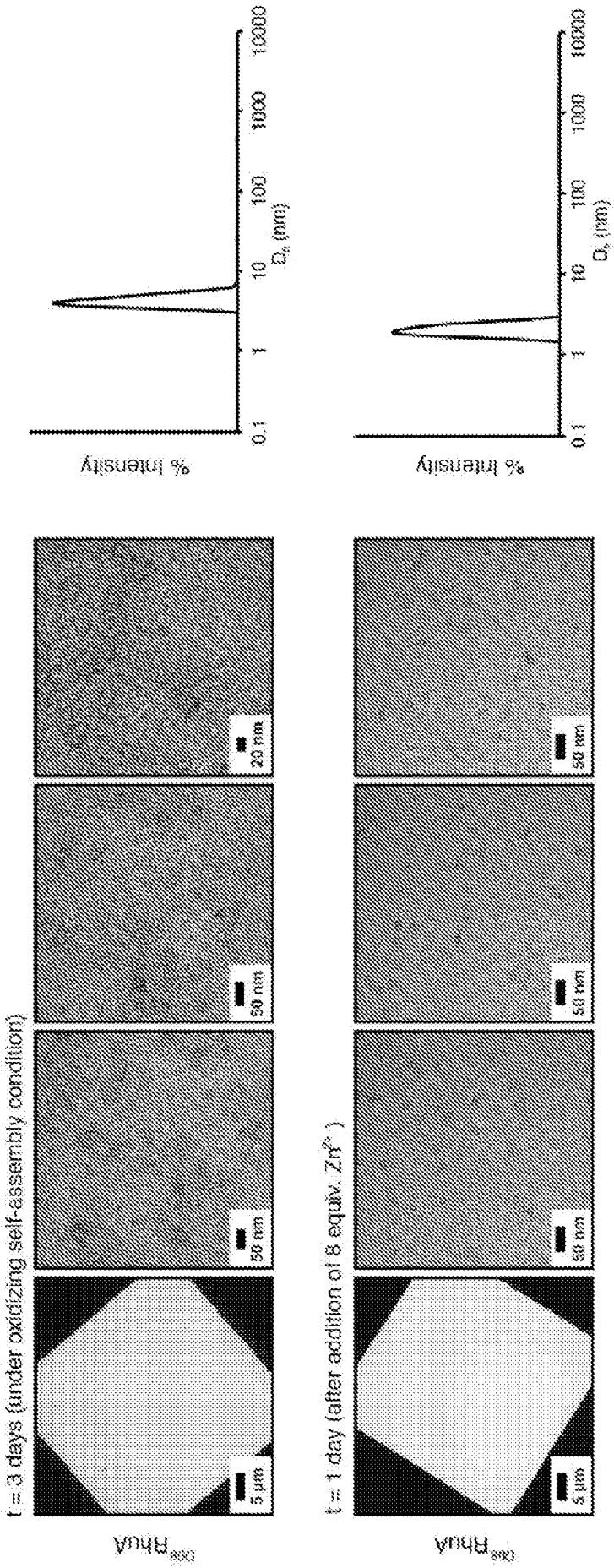


FIG. 60A


t = 3 days (under oxidizing self-assembly condition)
t = 1 day (after addition of 8 equiv. Zn2+)
5 μm
50 nm
20 nm
% Intensity
0.1
1
10
100
1000
10000
Dh (nm)

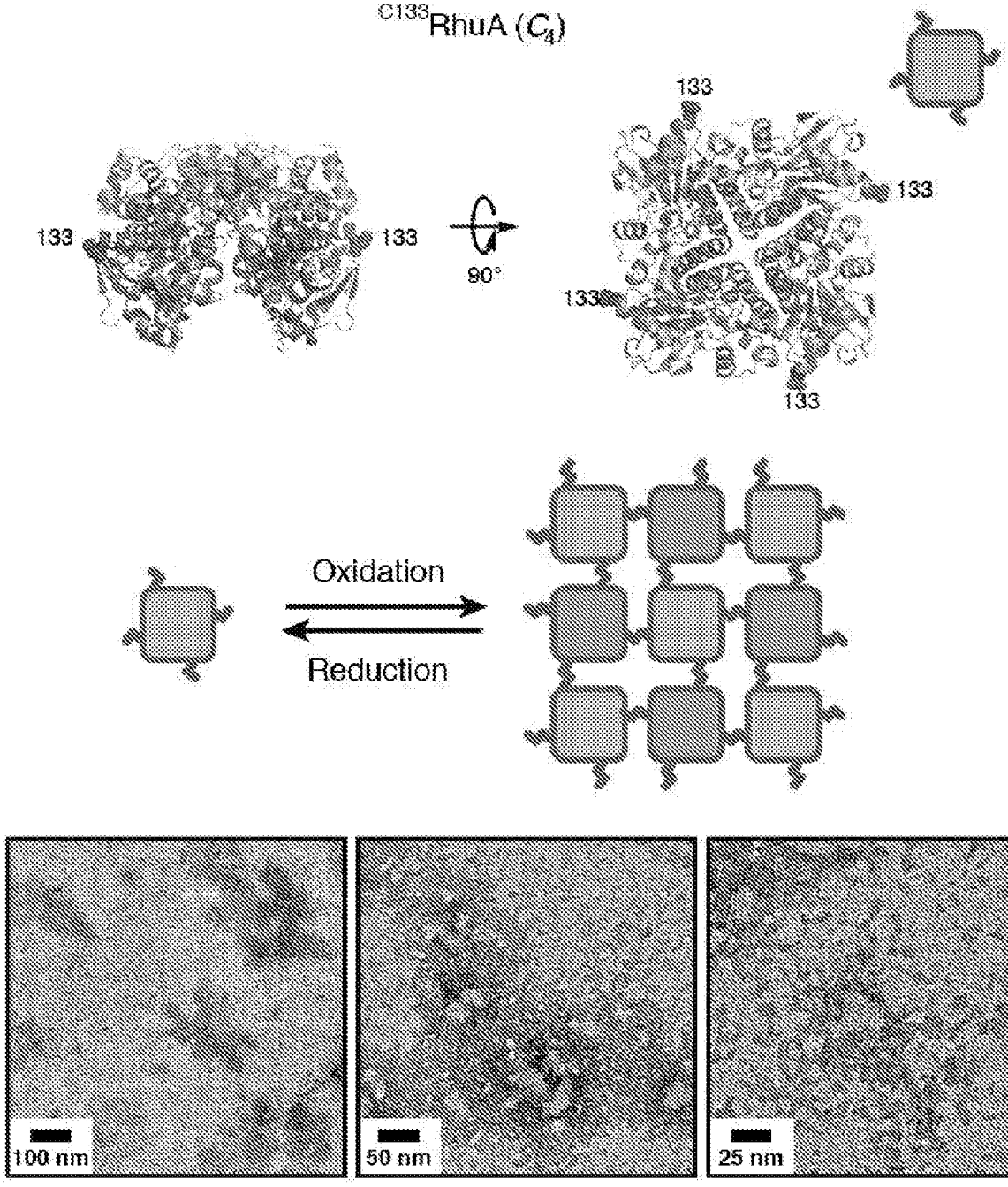

C133RhuA (C4)
133
133
90°
133
133
133
133
Oxidation
Reduction
100 nm
50 nm
25 nm

FIG. 60B

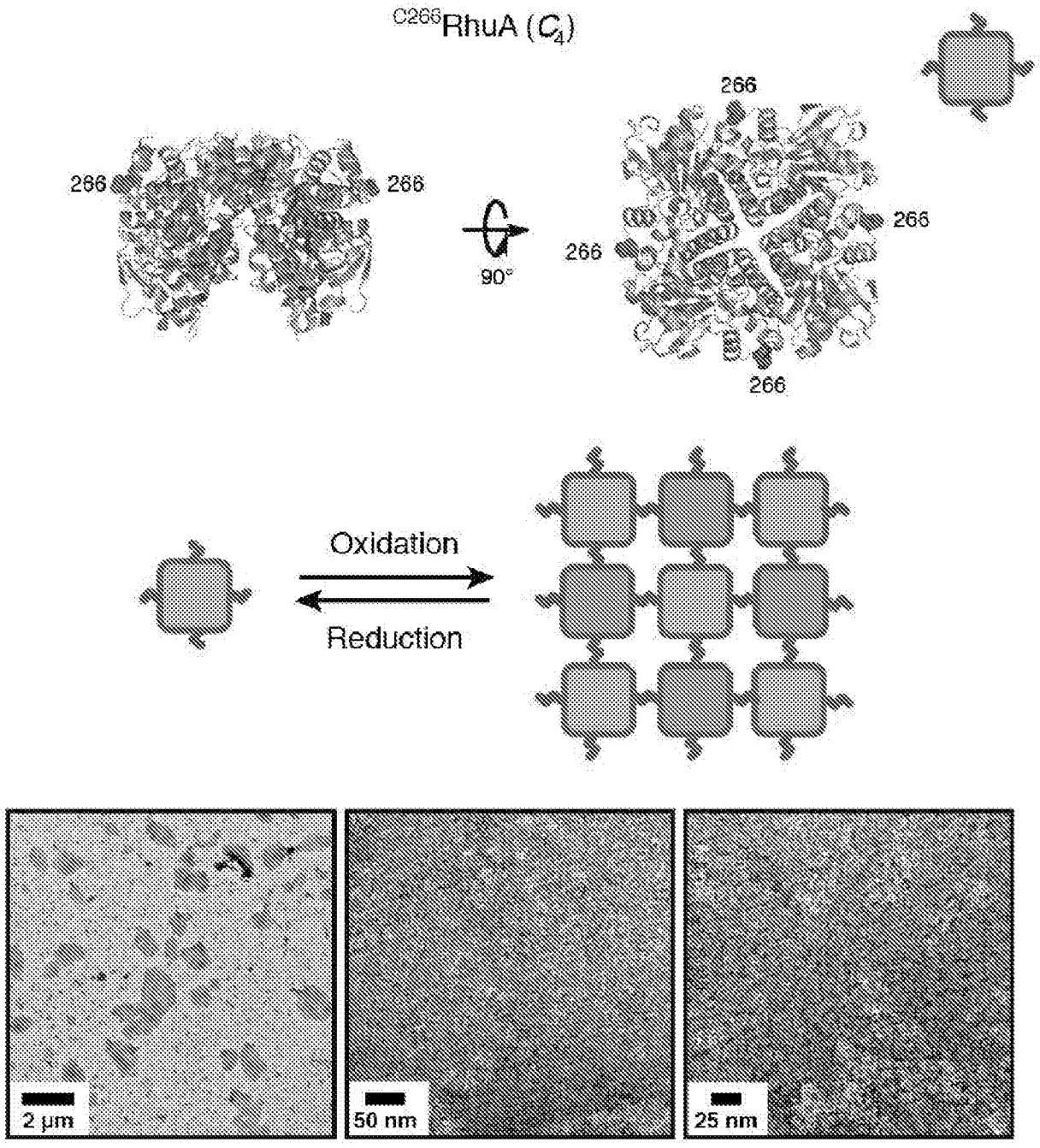

C266RhuA (C_4)
266
266
90°
266
266
266
Oxidation
Reduction
2 µm
50 nm
25 nm

FIG. 60C

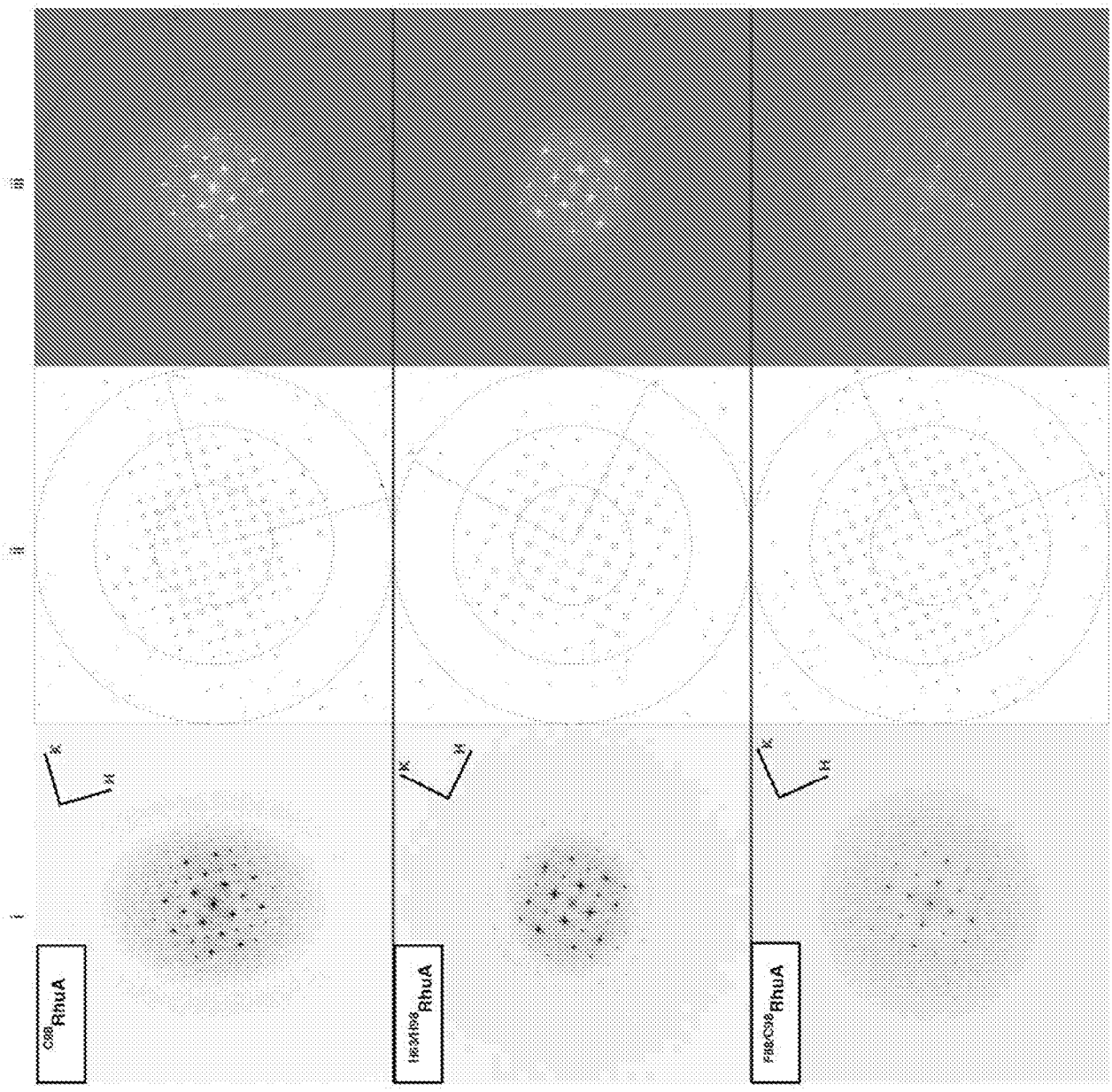


FIG. 61A

FIG. 61B

	C96 RhuA	H63A/H98 RhuA	F68/C96 RhuA
No. of images used for analysis	43 (12)	50 (44)	33 (13)
Unit cell dimensions			
a = b (Å)	114 ± 3	91 ± 3	115 ± 1
γ (°)	90	90	90
Plane-group symmetry	p42,2	p4	p42,2

FIG. 61C

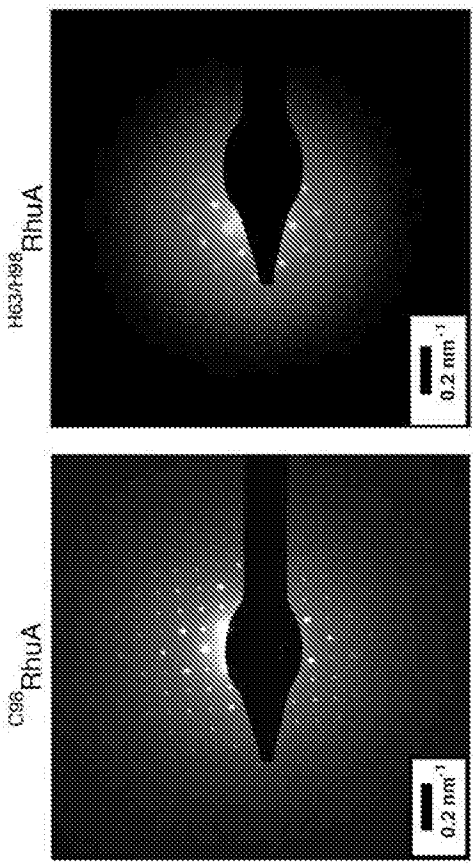


FIG. 62A

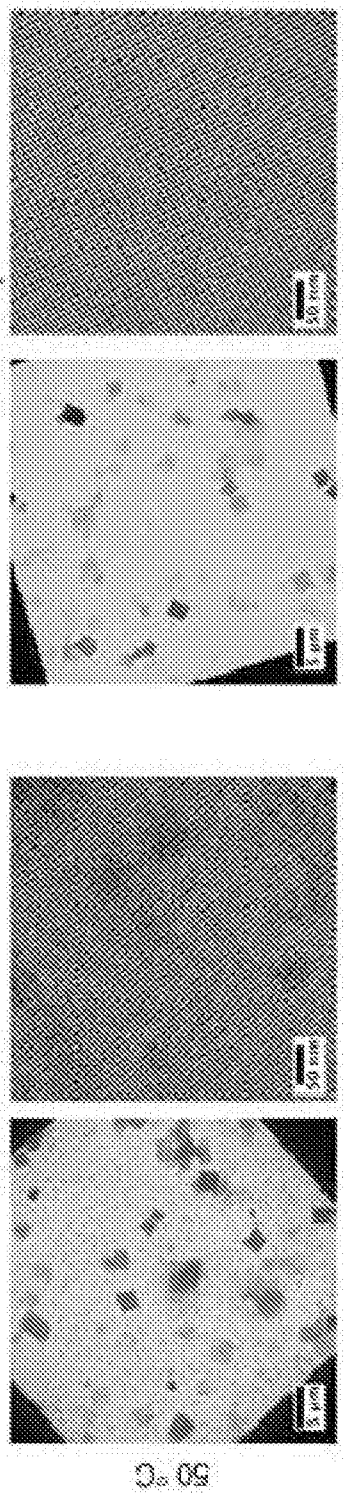
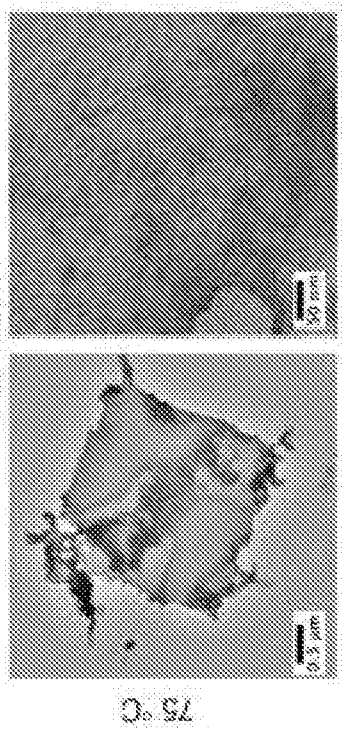


FIG. 62B



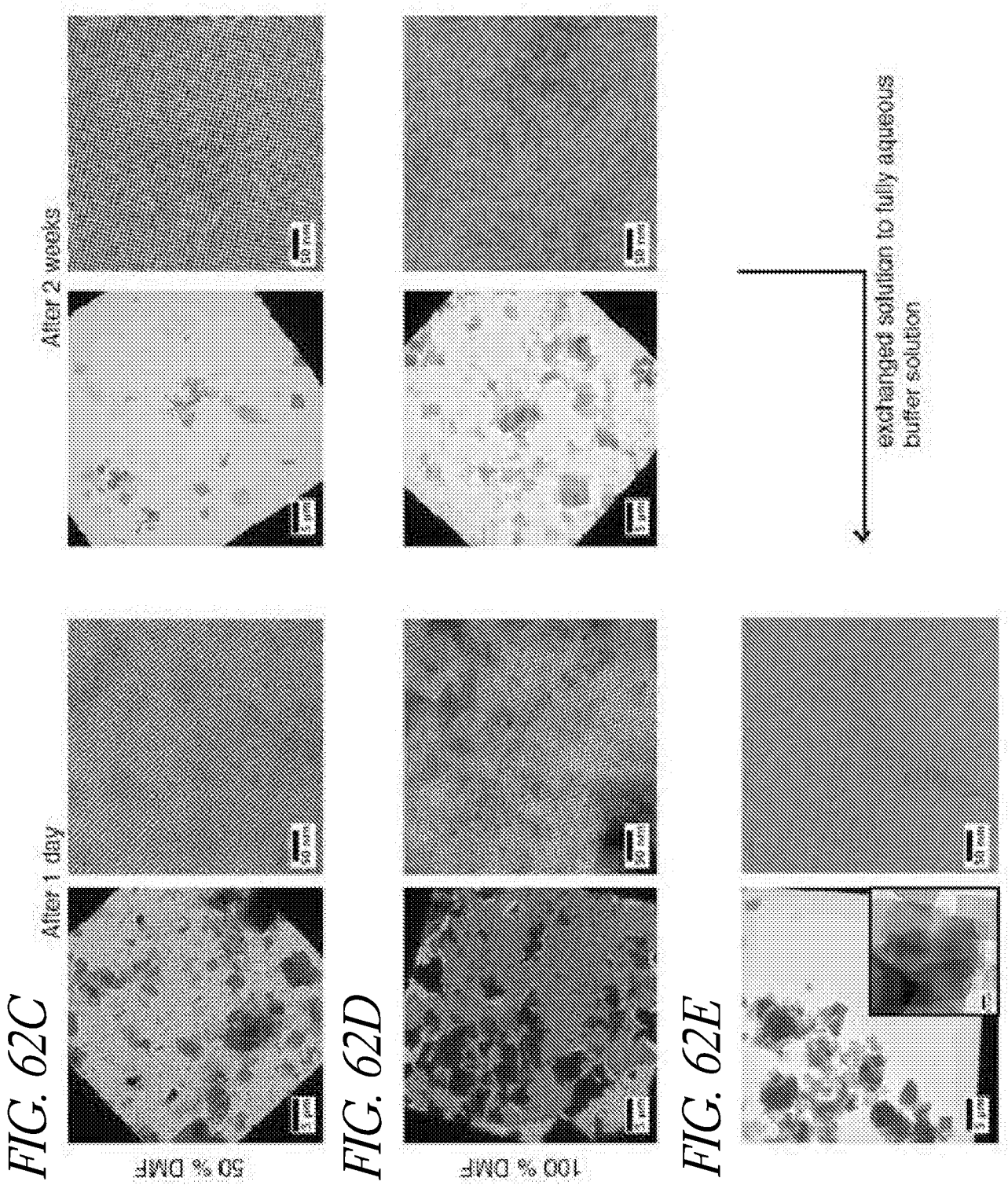
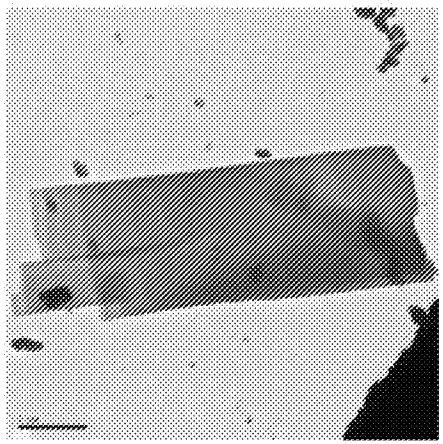

FIG. 62C
After 1 day
After 2 weeks
50 % DMF
FIG. 62D
100 % DMF
exchanged solution to fully aqueous buffer solution
FIG. 62E

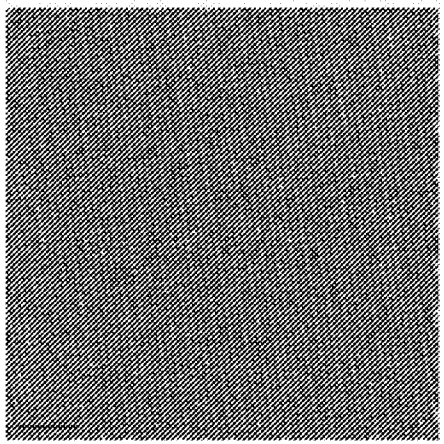
FIG. 63

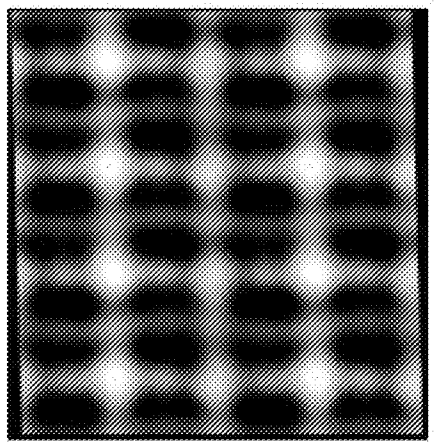
RhuA-C98-iphen (100 μM) with 2eq $NiSO_4$ in 20 mM Mes at pH5.5 after 1day

Sheet observed



2dx





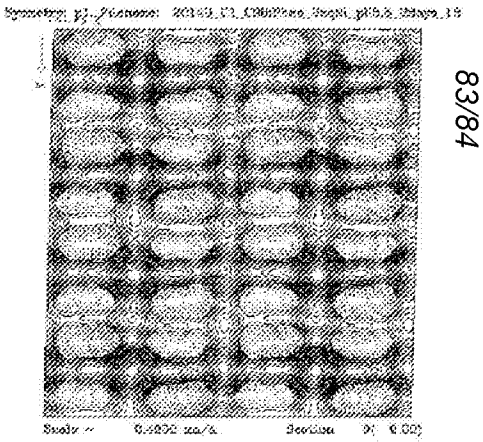
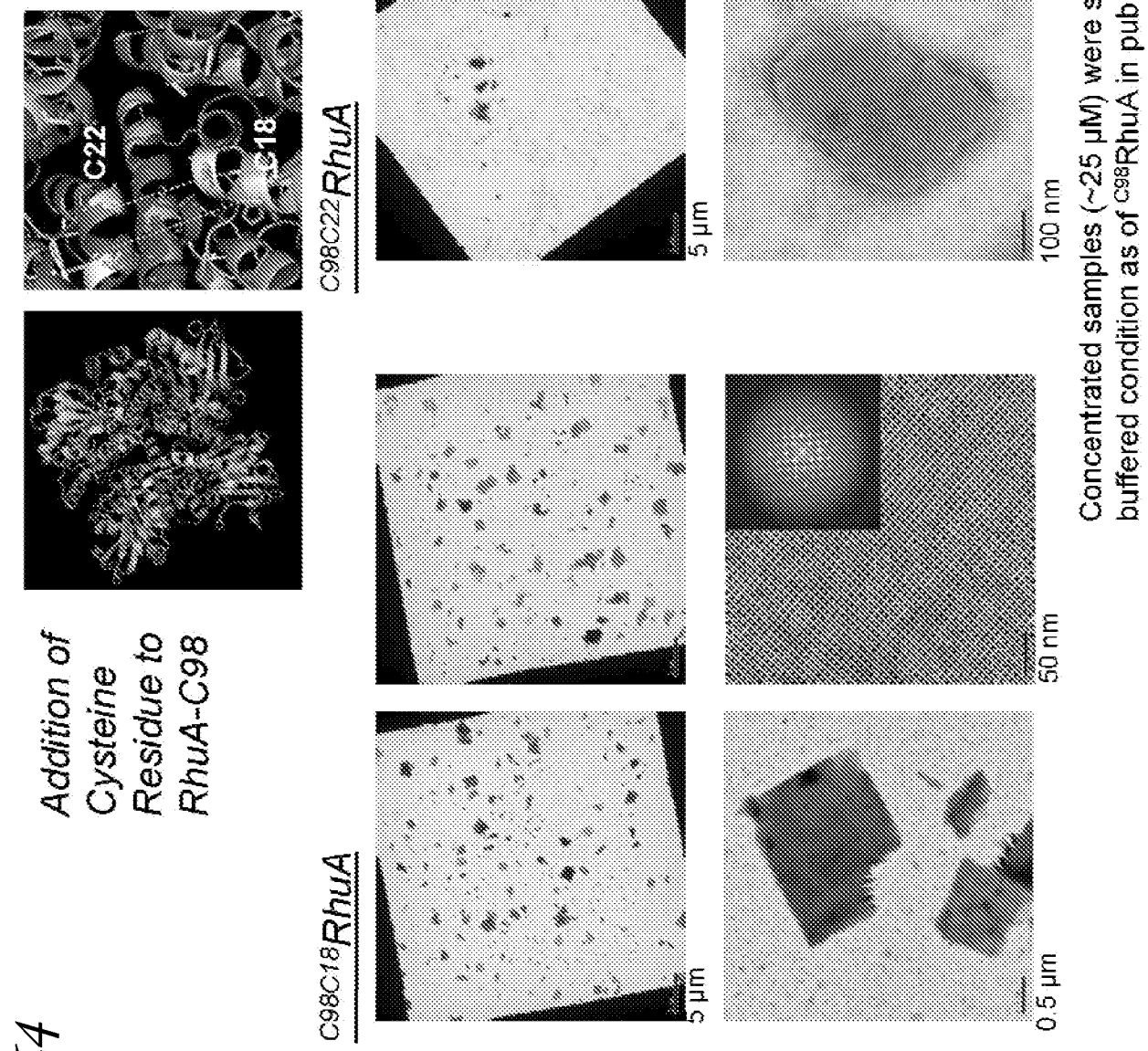


FIG. 64


Addition of Cysteine Residue to RhuA-C98
C22
C18
C98C18RhuA
C98C22RhuA
5 µm
5 µm
100 nm
100 nm
50 nm
50 nm
0.5 µm
Concentrated samples (~25 µM) were shaked for 1 day under same buffered condition as of C98RhuA in published paper

INTERNATIONAL SEARCH REPORT

International application No.
PCT/US 16/42361

A. CLASSIFICATION OF SUBJECT MATTER
IPC(8) - C07K 14/00 (2016.01)
CPC - C07K 2319/00, B82Y 5/00, C07K 14/001
According to International Patent Classification (IPC) or to both national classification and IPC

B. FIELDS SEARCHED

Minimum documentation searched (classification system followed by classification symbols)
IPC(8): C07K 14/00 (2016.01)
CPC: C07K 2319/00, B82Y 5/00, C07K 14/001

Documentation searched other than minimum documentation to the extent that such documents are included in the fields searched
USPC: 530/408, 530/350, 977/705, 430/320

Electronic data base consulted during the international search (name of data base and, where practicable, search terms used)
PatBase, Google Patents, Google Scholar, Google Web, search terms: symmetrical polypeptide, building block, cysteine residues, disulfide bonds, 2D crystals, surface cysteine residues, C3, C4, C6, D3, D4, D6 symmetry, crystals, histidine residues, recombinant, coordination, surface histidine, corner positions

C. DOCUMENTS CONSIDERED TO BE RELEVANT

Category*	Citation of document, with indication, where appropriate, of the relevant passages	Relevant to claim No.
X — Y	Ringler et al. Self-Assembly of Proteins into Designed Networks. Science (03 October 2003) Vol. 302, Issue 5642, pp. 106-109) by abstract, pg 106, col 2, para 2, col 3, para 1-2, pg 107, col 1, para 3 - col 2, para 1, Figs 1,2	48-50 ----- 1-3
Y	Banatao et al. An approach to crystallizing proteins by synthetic symmetrization. PNAS (31 October 2006) vol. 103 no. 44, pp 16230-16235, pg 16230, col 1 para 3 - col 2 para 1	1-3

☐ Further documents are listed in the continuation of Box C. ☐

* Special categories of cited documents:
"A" document defining the general state of the art which is not considered to be of particular relevance
"E" earlier application or patent but published on or after the international filing date
"L" document which may throw doubts on priority claim(s) or which is cited to establish the publication date of another citation or other special reason (as specified)
"O" document referring to an oral disclosure, use, exhibition or other means
"P" document published prior to the international filing date but later than the priority date claimed
"T" later document published after the international filing date or priority date and not in conflict with the application but cited to understand the principle or theory underlying the invention
"X" document of particular relevance; the claimed invention cannot be considered novel or cannot be considered to involve an inventive step when the document is taken alone
"Y" document of particular relevance; the claimed invention cannot be considered to involve an inventive step when the document is combined with one or more other such documents, such combination being obvious to a person skilled in the art
"&" document member of the same patent family

Date of the actual completion of the international search	Date of mailing of the international search report
22 November 2016	16 DEC 2016
Name and mailing address of the ISA/US Mail Stop PCT, Attn: ISA/US, Commissioner for Patents P.O. Box 1450, Alexandria, Virginia 22313-1450 Facsimile No. 571-273-8300	Authorized officer: Lee W. Young PCT Helpdesk: 571-272-4300 PCT OSP: 571-272-7774

Form PCT/ISA/210 (second sheet) (January 2015)

INTERNATIONAL SEARCH REPORT

International application No.
PCT/US 16/42361

Box No. II Observations where certain claims were found unsearchable (Continuation of item 2 of first sheet)

This international search report has not been established in respect of certain claims under Article 17(2)(a) for the following reasons:

1. ☐ Claims Nos.:
because they relate to subject matter not required to be searched by this Authority, namely:

2. ☐ Claims Nos.:
because they relate to parts of the international application that do not comply with the prescribed requirements to such an extent that no meaningful international search can be carried out, specifically:

3. ☒ Claims Nos.: 4-47, 51-94, 107-120, 133-147
because they are dependent claims and are not drafted in accordance with the second and third sentences of Rule 6.4(a).

Box No. III Observations where unity of invention is lacking (Continuation of item 3 of first sheet)

This International Searching Authority found multiple inventions in this international application, as follows:

---------- see extra sheet ----------

1. ☐ As all required additional search fees were timely paid by the applicant, this international search report covers all searchable claims.

2. ☐ As all searchable claims could be searched without effort justifying additional fees, this Authority did not invite payment of additional fees.

3. ☐ As only some of the required additional search fees were timely paid by the applicant, this international search report covers only those claims for which fees were paid, specifically claims Nos.:

4. ☒ No required additional search fees were timely paid by the applicant. Consequently, this international search report is restricted to the invention first mentioned in the claims; it is covered by claims Nos.:
1-3, 48-50

Remark on Protest

☐ The additional search fees were accompanied by the applicant's protest and, where applicable, the payment of a protest fee.

☐ The additional search fees were accompanied by the applicant's protest but the applicable protest fee was not paid within the time limit specified in the invitation.

☐ No protest accompanied the payment of additional search fees.

INTERNATIONAL SEARCH REPORT

International application No.
PCT/US 16/42361

Continuation of Box No. III, Observations where unity of invention is lacking:

This application contains the following inventions or groups of inventions which are not so linked as to form a single general inventive concept under PCT Rule 13.1. In order for all inventions to be examined, the appropriate additional examination fees must be paid.

Group I: Claims 1-3 and 48-50, directed to a non-natural symmetrical polypeptide building block, comprising corner residues positioned to facilitate formation of 2D crystals.

Group II+: Claims 95-106 and 121-132 (in part), directed to a polypeptide comprising an additional modification [Note, SEQ ID NOs: 3, 4, 5, 2, 19, 20, 21, and 24 are variants of L-rhamnulose-1-phosphate aldolase, RhuA, see instant specification, pg 99, Table 6, para [0155], [0251]]. Group II+ will be searched upon payment of additional fees. The polypeptide may be searched, for example, to encompass SEQ ID NO: 3 modified with a His tag of SEQ ID NO: 22 for an additional fee and election as such. It is believed that claims 95-100, (105-106)(in part) read on this exemplary invention. Additional polypeptides and tags will be searched upon the payment of additional fees. Applicants must specify the claims that encompass any additionally elected polypeptides and tags. Failure to clearly identify how any paid additional invention fees are to be applied to the"+" group(s) will result in only the first claimed invention to be searched. Another exemplary election would be a polypeptide SEQ ID NO: 2 modified with a Pd4 tag of SEQ ID NO: 23 (claims 121-124, 127-128, (131-132)(in part).

The inventions listed as Groups I and II+ do not relate to a single general inventive concept under PCT Rule 13.1 because, under PCT Rule 13.2, they lack the same or corresponding special technical features for the following reasons:

Special Technical Features

Group II+ does not require a non-natural symmetrical polypeptide building block, comprising corner residues positioned to facilitate formation of 2D crystals, wherein said polypeptide has inherent C3, C4, C6, D3, D4 or D6 symmetry, as required by Group I.

Group I does not require a specific polypeptide (L-rhamnulose-1-phosphate aldolase variant) comprising an additional modifications, as required by Group II+.

The technical feature of each of the inventions listed as Group II+ is the specific RhuA polypeptide sequence and modification recited therein. Each invention of Group II+ requires an RhuA variant amino acid sequence and an additional modification, not required by any of the other inventions. In addition, UniProtKB entry C5A070 (RHAD_ECOBW) [retrieved on 22 September 2016 from http://www.uniprot.org/uniprot/C5A070.txt] discloses Rhamnulose-1-phosphate aldolase amino acid sequence.

Common Technical Features

The inventions of Groups I and II+ share the technical feature of a polypeptide. The inventions of Group II+ share the technical feature of a L-rhamnulose-1-phosphate aldolase variant polypeptide having an additional modification [e.g. a His -tag]. However, this shared technical feature does not represent a contribution over prior art, because the shared technical feature is anticipated by the article entitled "Self-Assembly of Proteins into Designed Networks" (Science (3 Oct 2003) Vol. 302, Issue 5642, pp. 106-109) by Ringler et al (hereinafter 'Ringler'), (pg 106, col 2, para 2, col 3, para 1 "We chose the structurally characterized proteins L-rhamnulose-1-phosphate aldolase (RhuA) and strepavidin as building blocks. RhuA is a C4-symmetric tetramer ... RhuA was fused with a His6 tag at each of the four C termini").

As the technical features was known in the art at the time of the invention, they cannot be considered special technical features that would otherwise unify the inventions.

Groups I and II+ therefore lack unity under PCT Rule 13 because they do not share the same or corresponding special technical feature.

Note, continuation of item 4: claims 4-47, 51-94, 107-120, 133-147 are not not drafted in accordance with the second and third sentences of Rule 6.4(a) regarding multiply dependent claims.